Controls on upper Viséan (Carboniferous) depositional environments in Ireland

Volume I (of II)

Text

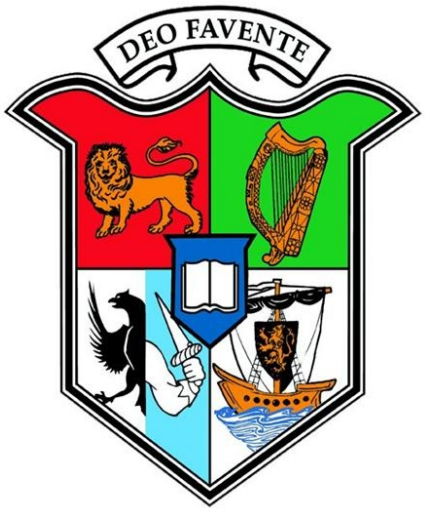

Milo Barham

Supervisors: Dr. John Murray and Prof. D. Michael Williams

A thesis submitted for the degree of Doctor of Philosophy

Earth and Ocean Sciences
School of Natural Sciences
National University of Ireland, Galway

November 2010

TABLE OF CONTENTS

CONTENTS

Volume II of this thesis contains all the Figures and Appendices referenced in the main text. A separate table of figures is provided at the beginning of Volume II.

ABSTRACT

The lithostratigraphy and fauna of Carboniferous sedimentary sequences in northwest and southwest Ireland were investigated to reconstruct how and why palaeoenvironments were changing throughout the upper Viséan and Serpukhovian time interval. Spectral analysis of a sequence in northwest Ireland indicates an influence of the precession and obliquity Milankovitch cycles on sedimentation in the early Asbian. The development of palaeokarsts in southwest Ireland, and high-frequency lithological variation in the northwest, indicate rapid sea-level fluctuations in the late Asbian and Brigantian, which are attributed to glacioeustasy. Stable isotopic analyses of biogenic apatite indicate cooling of local sea-surfaces by ~6ºC from the basal Asbian to the mid-Brigantian. Isotopic curves are compatible with the 3rd order sea-level curve identified in this work, suggesting that global climate and glaciation was the primary driving force of palaeoenvironmental change in Ireland during this time. It is proposed that the climate began deteriorating (heralding the onset of an episode of the Carboniferous glaciation) at the base of the Asbian before stabilising (in a glaciated state) in the mid- to late-Brigantian.

Comparative, optical and Laser Raman investigations of (tandem) ichthyolith and conodont apatite samples suggest that ichthyoliths are prone to diagenetic lowering of their $\delta^{18}O$ values. However, discrepancies between the values of conodonts and altered ichthyoliths appear relatively consistent, and therefore are potentially correctable within regions.

A suite of conodont species was recovered and their biostratigraphical and palaeoenvironmental significances are discussed. An evolutionary lineage of the genus *Lochriea* was identified in northwest Ireland that is compatible with published work, although the recognition of irregular and transitional forms suggests some reconsideration of the taxonomy is necessary. The first appearance of *L. ziegleri* and *L. cruciformis* suggest that the base of the *L. ziegleri* Biozone (proposed base of the Serpukhovian) correlates with the late Brigantian P_{2a} ammonoid Biozone in Ireland.

ACKNOWLEDGEMENTS

I gratefully acknowledge the financing of this project with an IRCSET (Irish Research Council for Science, Engineering and Technology) postgraduate scholarship. Additional funding from the Thomas Crawford Hayes trust fund was also invaluable.

Although the sole author of this work, without the assistance and guidance provided by innumerable academics, friends, family and even strangers, I doubt I ever could have accomplished this task. To the many I am indebted yet have accidently omitted, I apologise wholeheartedly.

First and foremost I would like to express my thanks to my supervisors John Murray and Mike Williams. Mike for his wisdom, calm and sensibility (which kept me on the level) and John for his ceaseless energy and interest in the project, especially on the numerous occasions when his dedication came at the detriment of his own interests.

I am especially indebted to Prof. Michael Joachimski for the use of the stable isotope laboratory at the GeoZentrum Nordbayern, Erlangen, Germany, without which this project quite simply would not have been possible. The time, knowledge and kindness shown by everyone at the facility, but most particularly by Michael Joachimski and Daniele Lutz, were fundamental to this work and will never be forgotten.

I would like to express my thanks to Prof. George Sevastopulo, whose incessant curiosity and boundless knowledge were both an inspiration and an invaluable resource, and Dr. Margaret Duncan for affording me time to discuss all things phosphatic, small and weird.

Thanks to everyone in the department at NUIG, from the postgrads and postdocs to the support staff and lecturers; you all contributed in some way. I am especially grateful to Martin Feely, Tiernan Henry and Martin White for their time and discussion regarding a variety of topics. Fellow students J. P. O'Donnell and Edward Lynch were very generous in affording their own precious time to introduce me to, and assist me with, digital spectral analysis and Laser Raman techniques. Special thanks also go to Mr. Pierce Lalor in Anatomy, whose technical assistance was a breath of fresh air.

I must acknowledge the help of the farmers and other landowners who facilitated me parking, working and even camping on their land. Particular thanks goes to Mr. Padraig Brady who generously gave me the use of a cottage with no wish for any means of compensation, your generosity was much appreciated.

I am extremely appreciative for all the support of my family, not only during the course of this work but throughout my education and life. My parents have always been especially helpful, encouraging my decisions and providing for me whenever in need. To Anne, my grandmother, I will always be indebted for supporting my education. I can only hope to someday emulate your patronage.

Last, but certainly not least, many thanks to Catherine for sharing the burden with me every step of the long, long way.

Finally, I apologise to everyone, particularly Catherine, my friends and family, for whom I haven't been around as much as I probably should have…… I am back.

CHAPTER 1 - INTRODUCTION

This project concerns the fossil fauna, sedimentary facies and palaeoenvironments of Viséan to early-Serpukhovian (Carboniferous) strata in southwestern and northwestern [NW] Ireland. Sedimentary successions in counties Sligo and Leitrim (NW Ireland) were examined at outcrop, to elucidate information on their nature and origin. These results were combined with those from lab-based analyses of the stable isotopes of oxygen contained in fossilised biogenic apatite, to synthesise a more complete understanding of the palaeoenvironmental conditions and their links with palaeoclimate. Two short stratigraphic sections in County Clare were investigated in a similar manner to act as a control on the data obtained from NW Ireland. The primary aim of this study is to determine to what degree both the sedimentation style and oxygen isotope ratios, preserved in the Carboniferous lithological sequences examined in Ireland, were controlled by local conditions, and to what extent (if any) the Permo-Carboniferous glaciation was responsible. At present, the published literature contains significantly conflicting evidence concerning the magnitude and timing of this significant cooling episode. Important aspects of the biostratigraphy of the mid-Viséan to Serpukhovian period in Irish sequences are also addressed.

By way of introduction, this chapter will provide a background to some of the key concepts relevant to the later chapters of this thesis as well as detail the techniques and aims of the project. The chapter will conclude with a thesis map, describing the layout of information in the various volumes and chapters.

1.1 CONODONT BIOLOGY AND BIOFACIES

Conodonts range from the Cambrian to the late Triassic and are found in virtually all marine palaeoenvironments. For the majority of the history of conodont research, speculation about the conodont animal was restricted to the histology of the only mineralised tissue in the animal – the dental elements, or to the arrangement of multi-element associations (e.g. Lindström, 1973, 1974; Müller,

1981b). Since the discovery of fossilised conodont soft tissues, a greater understanding of the creature and its significance has been gained.

1.1.1 The conodont animal

Currently, only three sites, worldwide, have yielded unequivocal euconodont body fossils (Table 1.1.1).

Location and age	***Background, lithology and palaeoenvironment***	***Conodont fossil***	***Refs.***
Granton Shrimp Beds, Edinburgh, Scotland. ***Carboniferous***	Organic-rich silt and organic-poor dolomite, indicating a brackish lagoon or inter-distributary bay environment. The fauna is dominated by shrimps, with the fully marine fauna thought to represent brief marine incursions. The fauna is thought to have been killed by algal blooms.	Represents the most significant conodont lagerstätte. 10 specimens are preserved in fluorapatite and display features from the entire length of the organism, often in fine detail.	(Aldridge *et al.*, 1986; 1993; Briggs *et al.*, 1983)
Brandon Bridge Dolomite, Waukesha County, Wisconsin, USA. ***Silurian***	The lithology comprises finely laminated, argillaceous dolomite indicating a low-energy, anoxic tidal(?) environment. An abundance of other soft-bodied fossils and arthropods are also present.	Only a single, incomplete, poorly-preserved specimen exists, exhibiting a trunk and associated (coniform) dental apparatus.	(Mikulic *et al.*, 1985)
Soom Shale, Table Mountain Group, South Africa. ***Upper Ordovician***	The site is located ~150km north of Cape Town. The host rock consists of black, finely-laminated, argillaceous silt and mud which formed in an ice-proximal, >100m deep marine basin.	A single, incomplete specimen exists but it displays finely preserved features of the trunk, feeding apparatus and eyes. NB muscle fibres.	(Gabbot *et al.*, 1995)

Table 1.1.1 Current sites where conodont soft-part preservation is recorded.

Despite the taxonomic differences of the conodonts found within the three sites listed above, the soft-bodied anatomy (Aldridge *et al.*, 1993; Gabbot *et al.*, 1995; Mikulic *et al.*, 1985) appears very similar (Fig. 1.1.1). Conodonts were bilaterally symmetrical and elongate, with a general body width of 1-2mm and a general length of a little over 40mm. The conodonts preserved in the Soom Shale are exceptional and are believed to have been 10 times as large (by extrapolation of the

S-element length and trunk height). The body was mildly laterally compressed, particularly towards the tail region, and expanded slightly anteriorly towards the "head". V-shaped muscle blocks are particularly well preserved in some specimens in both the Granton and Soom Shale localities, where muscle fibres are visible. A pair of linear structures, representing a probable notochord, taper posteriorly and anteriorly and extend as far rostrally as the feeding apparatus. The tail of the animal is characterised by fin rays on both the dorsal and ventral margins. Two lobate sclerotic cartilages indicate the position of probable eyes, which are located anterior to the phosphatic feeding elements. Fossilised traces of extrinsic eye musculature may suggest that conodonts lived within the photic zone, since hagfishes, which are thought to be closely related to conodonts, and live at great depths, lack it (Lamb *et al.*, 2007). The probable traces of a notochord, myomeres, otic capsules, branchial structures and fibrous extrinsic eye muscles within the head region are all suggestive of a vertebrate affinity. The growing consensus (e.g. Aldridge & Purnell, 1996; Sweet & Donoghue, 2001) is that conodonts represent early predatory agnathan vertebrates.

1.1.2 Conodont elements

Conodont elements are small (generally 0.2–<2mm in length), denticulate, phosphatic microfossils. Elements are internally divisible into three broad units – a basal body, lamellar crown and white matter (Fig. 1.1.2a). Homologies have been identified between the various layers and other hard tissues in extant vertebrates, most significantly by Sansom *et al.* (1992; 1994), who recognised cellular bone in conodont elements, thus providing unequivocal evidence of their vertebrate affinities. Conodont dental elements (without the rarely preserved, organic-rich basal filling) are thought to be compositionally closest to francolite (Pietzner *et al.*, 1968), a carbonate apatite, given as:

$$Ca_5Na_{0.14}(PO_4)_{3.01}(CO_3)_{0.16}F_{0.73}(H_2O)_{0.85}$$

Conodont elements vary texturally and also in colour (from amber to black) with increasing temperature and time, reflecting increasing depths of burial and organic maturation (Epstein *et al.*, 1977; Harris, 1981; Nöth, 1998). During metamorphism,

organics, responsible for maturation-darkening, begin to volatilise and oxidise (Rejebian *et al.*, 1987), resulting in progressive lightening of the elements until they eventually become translucent.

There are three traditional shape categories into which conodont elements are classed (Table 1.1.2a).

Type	***Description***	***Example***
Coniform (S,M & P)	Simple, commonly gently curved conical bodies. Constitute the most primitive element apparatuses.	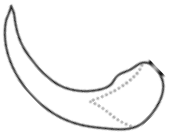
Ramiform (S & M)	Delicate, thin and blade-like with two or more processes or saw-like "teeth". Found in conjunction with Pectiniform elements.	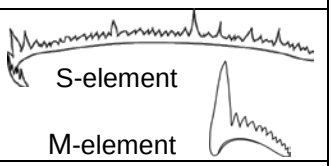 S-element M-element
Pectiniform (P)	Tend to be the most distinctive, diagnostic and common element due to their form and robustness. Consist of a free blade that is attached to and can continue into a platform.	 *Gnathodus homopunctatus*

Table 1.1.2a Basic conodont element forms.

Different arrangements of conodont elements are thought to have existed in the different major classes of the animals. Late Palaeozoic species generally follow the ozarkodinid body plan (Fig. 1.1.2b). Purnell *et al.* (2000) provided the most recent scheme for a universal orientation and anatomical notation system for elements, based on topology (Fig. 4.2a). In the scheme, conodont elements are designated specific letters with subscripts according to their positions with respect to the principal axes of the body. The designations are as follows, in a caudal to rostral (posterior to anterior of the body) sense:

- P – Single pairs of elements in contact, which lie caudally of the complex rostral feeding array and along the caudal-rostral axis. Subscripts 1, 2… etc. increase in value for each pair further towards the rostral end.
- S – Complex, rostrally positioned array of elements arranged symmetrically about the caudal-rostral axis. Subscript 0 refers to an unpaired element positioned on the symmetry plane. Subscripts 1, 2, 3… etc. apply to

symmetrical (but separated) paired elements and increase in value dorsally and rostrally.

- M – Single pair of elements that are symmetrical (but separated) and positioned both rostral and dorsal of the S-element array.

The function of conodont elements has been the subject of some significant debate, which, prior to the discovery of soft-part preservation, had strong implications for the taxonomy of the group. Two main models were proposed (Table 1.1.2b):

Model	***References***
Soft tissue supports. The conodont elements were permanently enclosed in soft tissue which acted as a filter feeding array or microphagous structure. S- and M-elements supported tissue which selectively directed fine organic matter towards the P-elements where they were gently bruised and crushed prior to digestion. This model has been compared (Nicoll, 1987) to the feeding strategy of the cephalochordate *Branchiostoma* (amphioxus).	(Hitchings & Ramsay, 1978; Lindström, 1973, 1974; Nicoll, 1987)
Exposed teeth array. Elements were exposed and functioned (cutting, slicing and piercing) as predatory teeth. S- and M-elements actively grasped prey which was then directly processed via the P-elements. This model has been proposed as being somewhat analogous to that employed by the lingual apparatus of myxinoids.	(Briggs *et al.*, 1983; Purnell & von Bitter, 1992; Purnell, 1993, 1994, 1995)

Table 1.1.2b Main hypotheses for conodont element array functions.

The main support for a microphagous model comes from the internal lamination patterns observed in conodont elements, which appear to have formed through centrifugal accretion (Fig. 1.1.2a). This requires the conodont element to have been covered in secretory tissue at least during discrete phases of growth. The microphagous model explains supposed cell impressions on conodont surfaces (Dzik, 2000) as well as examples where conodont elements appear to have regenerated portions or healed complete breaks (Dzik, 2010; Müller, 1981a). Despite the above interpretations, no evidence, in the form of mineral replacement, an impression, outline or halo, for any tissue covering conodont elements has been reported. The model is widely considered as incorrect because of this and also in light of and the details outlined for the second model below.

Several lines of evidence suggest that conodont elements were exposed (at least) for periods when they actively functioned as food processing structures. Donoghue & Purnell (1999) identified recurrent patterns of damage and growth which they interpreted as evidence for cyclical alternations of element use followed by re-envelopment and growth. Further evidence for a predatory or macrophagous function for conodont elements has been championed by Purnell (see also Purnell & von Bitter, 1992; 1993, 1994, 1995). Functional analyses, as well as corresponding wear patterns on elements, have identified cutting, crushing and shearing feeding designs in different element forms, proving unequivocal evidence for direct element-food and element-element contact. Analysis of skeletal ontogeny demonstrates that functional platform area increased at, or above, the rate required in order to maintain sufficient feeding efficiency as teeth. The length and effective area of S- and M-elements, on the other hand, did not increase at a rate sufficient to feed the growing conodont animal, if operating purely as a filter feeding array (Purnell, 1993, 1994). Based on the evidence discussed above, it is believed that elements maintained the same function throughout life and were retained and repaired, rather than replaced (Donoghue & Purnell, 1999; Purnell, 1994). Elements can therefore be broadly used as a proxy for conodont abundances, while P_1 (platform elements) can be used as a proxy for creature size.

1.1.3 Upper Viséan to Serpukhovian conodont biofacies

The relevant conodont biostratigraphy and biofacies models applicable to the rocks examined during this project have been established for Europe, Ireland and Britain by Austin (1974), Higgins (1975), Austin & Davies (1984), Varker & Sevastopulo (1985), Concil *et al.* (1990), Riley (1993), Jones & Somerville (1996), Somerville & Somerville (1998) and Somerville (1999). More detailed studies of conodont faunas from selected sections in the west of Ireland were carried out by Austin *et al.* (1970) and Skompski *et al.* (1995), whilst investigations of the faunas of NW Ireland were undertaken by Aldridge *et al.* (1968), Austin & Husri (1974), Austin & Mitchell (1975), Browne (1981) and Kelly (1989).

Despite conodonts being considered pelagic, certain ubiquitous taxa still display particular affinities for specific palaeoenvironments (for example *Mestognathus* is

often considered a shallow water genus, e.g. von Bitter *et al.*, 1986). The factors driving the choice of habitat are still poorly understood, and it should be noted that rarely are any species found to be wholly confined to any specific palaeoenvironmental niche. More generally, a biofacies is manifest in the numbers, or relative abundance of a particular species, rather than its presence or exclusion. Early over-simplified models (e.g. Druce, 1973) were constructed to explain recurrent conodont communities or biofacies groups (Fig. 1.1.3a). Continued study refined these early basic models to better explain the complexity of species distribution, particularly in the dynamic nearshore palaeoenvironment. The work of Somerville (1999) provides a good understanding of late Viséan conodont biofacies in Ireland and her models are reproduced here in Figs. 1.1.3b-c.

In general terms, for the Viséan of Ireland, nearshore palaeoenvironments tended to be dominated by *Cavusgnathus* and *Mestognathus* species. In further offshore palaeoenvironments, above wave base, *Synclydognathus* and *Kladognathus* species became more abundant. In deeper, open marine palaeoenvironments, conodonts belonging to the genera *Lochriea* and *Gnathodus* were more prevalent (Somerville & Somerville, 1998; Somerville, 1999; Varker & Sevastopulo, 1985).

1.2 CARBONIFEROUS STRATIGRAPHY

Research for this project was carried out on rocks of Carboniferous age. All the subdivisions referred to herein follow those ratified by the Subcommission on Carboniferous Stratigraphy, International Commission on Stratigraphy and the International Union of Geological Sciences (Heckel & Clayton, 2006), except where referring to intervals described in older texts (where the correct up to date equivalent will be provided immediately after in brackets). The ratified subdivisions for the Carboniferous are shown in Fig. 1.2. The Carboniferous Period (or System) is divided into the Mississippian and Pennsylvanian Subsystems. The Mississippian Subsystem is split into Lower, Middle and Upper Series, which correspond to the Tournaisian, Viséan and Serpukhovian Stages respectively. The Pennsylvanian Subsystem has a similar tripartite subdivision; however, the Lower and Middle Series correspond with the Bashkirian and Moscovian Stages (respectively) whilst the Upper Series is represented by both the Kasimovian and Gzhelian Stages. As well as the global Stage, Series, Subsystem and System terminology, most of the western European Substages of the Viséan are also utilised in this work (see below).

The Carboniferous Period represents some 60 million years [My] of time ranging from 359.2 ±2.5 to 299.0 ±0.8 million years ago [Ma] (Heckel, 2008). At present, the base and top of the period are defined by Global Boundary Stratotype Section and Points (GSSP's) in addition to two other internal sub-divisional boundaries:

(1) The base of the Carboniferous System (base of the Tournaisian Stage) is defined by the first appearance datum [FAD] of the conodont *Siphonodella sulcata* in Trench E at La Serre, France (Paproth *et al.*, 1991).

(2) The base of the Middle Mississippian Series (base of the Viséan Stage, dated as 345.3 ±2.1 Ma) is defined by the FAD of the benthic foraminifer *Eoparastaffella simplex* in the Penchong section, southern China (Devuyst *et al.*, 2003).

(3) The base of the Pennsylvanian Subsystem (base of the Bashkirian Stage, dated as 318.1 ±1.3 Ma) is defined by the FAD of the conodont *Declinognathodus noduliferous* in the Arrow Canyon Section, Nevada, USA (Lane *et al.*, 1999).

(4) The top of the Carboniferous System (base of the overlying Permian System) is defined by the FAD of isolated nodular morphotype of the conodont *Streptognathodus wabaunsensis* in Aidaralash Creek, Kazakhstan (Davydov *et al.*, 1998).

The other stage boundaries of the Carboniferous System are, at the time of writing, in various phases of examination, selection and ratification. Of particular relevance to this project is the selection of a GSSP and index fossil for the base of the Serpukhovian Stage (dated as 326.4 ±0.8 Ma). At present, the task group charged with establishing this GSSP close to the existing boundary (currently the FAD of the goniatite *Cravenoceras leion* in western Europe) agree that the FAD
"of the conodont Lochriea ziegleri …. presents the best of the known biostratigraphic events for definition of the boundary" (pg. 8, Richards & Group, 2008).
The *Lochriea* lineage will be discussed in greater detail in Chapter 4. The current candidates for a GSSP for this boundary are the Verkhnyaya Kardailovka Section in the southern Urals, Russia (Nikolaeva *et al.*, 2009b) and Nanshui in southern China (Heckel, 2008).

Fig. 1.2 also shows the relative positions of the older subdivisions, which were widely used in past reports for the Carboniferous in Western Europe. Although some designations have been accepted as global (Tournaisian and Viséan) the rest have now become virtually defunct (from an international perspective, e.g. Namurian). Since,

(i) a large proportion of historical mapping undertaken in the study areas utilised this "older" terminology
and
(ii) the divisions represent a finer temporal resolution,

- the traditional subdivisions of the Viséan erected by George *et al.* (1976) are retained herein. One modification is the renaming of the lowest Viséan Substage from Chadian to "*Lower Viséan*". This is necessary as the base of the Chadian does not actually correspond with the base of the Viséan (Sevastopulo & Wyse Jackson, 2009). Additionally, the Pendleian and Arnsbergian Substages of the Lower Namurian, as shown in Fig. 1.2, are also used where considered appropriate. The

subdivisions of the Viséan and Serpukhovian recognised herein are shown in Table 1.2.

Global Stage	*Substage used herein*	
Serpukhovian	Arnsbergian	
	Pendleian	**326Ma**
Viséan	Brigantian	
	Asbian	
	Holkerian	
	Arundian	
	Lower Viséan	**345Ma**

Table 1.2 Regional Substages utilised in this thesis.

1.2.1 Upper Viséan to Serpukhovian biostratigraphy

The conodont biostratigraphic zones for the Viséan to Bashkirian interval are shown in Fig. 1.2.1a, in addition to ammonoid, miospore and foraminiferal biozones. The number of conodont species reduced around the Tournaisian–Viséan boundary and consequently, the biozones are temporally broad until a proliferation of *Gnathodus* and *Lochriea* genera in the late Viséan, through into the early Serpukhovian. The detailed biostratigraphy for some late Viséan conodont species is shown in Fig. 1.2.1b.

Although the Brigantian is shown in Fig. 1.2.1a to be broadly split into three biozones, the recognition of these biozones in the sections examined is challenging. The conodont *Mestognathus bipluti* may not be confined to the Brigantian, since in NW Ireland it has been discovered in the Asbian-aged Meenymore Formation by Kelly (1989). However, the Meenymore Formation has, somewhat controversially, been reassessed as Brigantian in age by Cózar *et al.* (2005; 2006) and Somerville *et al.* (2009). The practice of separating species into temporally significant subspecies, such as in the case of the subspecies of *Gnathodus girtyi*, is also somewhat problematic and difficult to apply in practice (Austin, 1973; Somerville, 1999). The subtle differences used to characterise subspecies can be difficult to recognise in geographically distinct areas and also to discern from background population

variation and abnormality (Austin, 1972; 1973; Conway Morris, 1989; Müller, 1981a).

The *Lochriea* lineage is of particular significance to this project. *Lochriea nodosa*, and its probable ancestor *L. mononodosa*, are useful markers for the Brigantian substage, although the exact timing of their first appearance within the Brigantian is not uniformly or consistently defined. Although not ratified, studies (e.g. Belka & Lehmann, 1998; Nemirovskaya *et al.*, 1994; Nemyrovska, 2005; Nikolaeva *et al.*, 2009a; 2009b; Skompski *et al.*, 1995) based on the complex platforms of *L. ziegleri* and *L. cruciformis* have led to the former being the main candidate for defining the base of the Serpukhovian.

1.3 THE CARBONIFEROUS GLACIATION

The Carboniferous (or Permo-Carboniferous) glaciation is widely recognised as one of the most significant cold intervals in Earths history (Fig. 1.3). This glacial event was a particularly complex climate episode (Fielding *et al.*, 2008b), similar to the more fully understood Pleistocene glaciation, but with significantly less evidence preserved about its occurrence. Only through integrating the results of detailed studies (for example the combination of isotopic, digital spectral and sequence stratigraphical techniques) can the dynamics of this climatic episode be understood. The glaciation event can be broken down into the three main topics: timing, magnitude and causes. These are discussed in Sections 1.3.1, 1.3.2 and 1.3.3 below:

1.3.1 Timing

Fig. 1.3.1a compares several models of the Permo-Carboniferous glaciation event. Early publications, due to both a lack of data and limited chronological correlation/resolution, proposed relatively simple models of waxing and waning glacial centres throughout the Carboniferous and into the Permian (Frakes & Crowell, 1969). Caputo & Crowell (1985) examined glacial deposits from South America and considered the onset of the "*strong Late Paleozoic Ice Age*" to have taken place in early to early-mid Carboniferous (Tournaisian to Viséan) times. Veevers & Powell (1987) combined Euramerican cyclothem data with records of Gondwanan glaciogenic deposits and concluded that the lead-up to the glaciation was more complicated than had previously been appreciated. They suggested that two short, geographically confined episodes in the Famennian (latest Devonian) and Viséan were followed by an expansive, long-lived episode of glaciation beginning in the Namurian (Serpukhovian). In a more comprehensive synthesis of the available data, Isbell *et al.* (2003b) identified three non-overlapping glacial successions. Two periods of alpine glaciation, from the Frasnian (Upper Devonian) to possibly Tournaisian and the Serpukhovian to mid-Bashkirian, were thought to have been succeeded by large-scale ice-sheets in the Stephanian (Upper Pennsylvanian) to Sakmarian–Artinskian (Cisuralian Series, Permian). This trend of refinement has continued (Fielding *et al.*, 2008a; Jones & Fielding, 2004), with at least eight distinct phases (Fig. 1.3.1a) now recognised (Rygel *et al.*, 2008). This

dynamic of expanding and retreating ice-sheets may rectify the seemingly conflicting evidence for ice-free conditions (Isbell *et al.*, 2003a) reported during purported periods of glaciation. High latitude warming has been proposed from brachiopod diversity and migratory patterns between the middle and late Viséan (Kelley *et al.*, 1990), at a time which has also been postulated as having high latitude glaciation (Crowley & Baum, 1992; Frakes & Francis, 1988). Fossil flora from Argentina contained in non-glacial sediments, which are interbedded with glacially derived lithologies from this time (Balseiro *et al.*, 2009; Pujana & Cèsari, 2008), also suggests that periods of climate amelioration existed between ice advances. With refined dating, apparent contradictions in the evidence for glaciation may be reinterpreted as merely rapidly alternating cool and warm micro-intervals.

Significant difficulties are associated with traditional methods used to identify the onset of a glaciation. Proximal, glaciogenic lithologies are often undateable, or are eroded, or re-deposited during subsequent glacial advances (Frank *et al.*, 2008). Thus, the closer to the site of palaeoglaciation, the more likely it is that only the last glacial advance and retreat will be recorded sedimentologically with any degree of confidence. For this reason, distal proxies are often used to trace the initiation and subsequent waning of ice-sheets during palaeoglaciations. However, all the proxies used to infer the onset or increase in glacial activity must be treated with caution, as they generally do not have a direct genetic relationship to the ice-sheets. Most of the proxies used are controlled by multiple factors (for example, the ratio of the stable isotopes of O in a fossil is controlled by the organism, the temperature of the water, and the O ratio in the water mass, which is itself controlled by a number of extrinsic factors). The full proxy system must be understood before one can begin to interpret information about the exact nature and influence of glaciation. This has been demonstrated by a number of studies (Crowley & Baum, 1991; Horton & Poulsen, 2009; Isbell *et al.*, 2003a; 2003b) which raised questions about the long established idea that the Carboniferous Euramerican cyclothems are near wholly attributable to the waxing and waning of ice-sheets (Wanless & Shepard, 1936). Despite the dangers of using proxies to study past climates, there has been a recent proliferation in the use of stable isotopes, particularly of oxygen (^{18}O) and carbon (^{13}C), to identify palaeoenvironmental shifts.

The concept of using stable isotopes as palaeoclimate proxies will be discussed more fully in Chapter 5. Previous isotopic studies have identified various different isotopic excursions throughout the Carboniferous and Permian which have been interpreted as (somewhat temporally contradictory) climate shifts (Fig. 1.3.1b). Where alteration of the signal is excluded, the differences demonstrate the dangers of small scale studies on an essentially punctuated rock record, which is providing local, temporal and geographical, palaeoenvironmental information. At least six different positive excursions in $\delta^{18}O$, often in conjunction with similar shifts in $\delta^{13}C$, have been identified in the Carboniferous and postulated as periods of ice-volume increase (Table 1.3.1):

Timing	***References***
Middle Bashkirian	(Mii *et al.*, 1999)
Serpukhovian-Bashkirian	(Grossman *et al.*, 2002; Veizer *et al.*, 1999)
Viséan-Serpukhovian/Early Serpukhovian	(Buggisch *et al.*, 2008; Mii *et al.*, 1999; 2001; Saltzman, 2003; Smith & Read, 2000)
Early to Middle Viséan	(Bruckschen *et al.*, 1999; Mii *et al.*, 2001)
Tournaisian-Viséan	(Bruckschen *et al.*, 1999; Mii *et al.*, 1999)
Early to Middle Tournaisian	(Bruckschen *et al.*, 1999; Buggisch *et al.*, 2008; Mii *et al.*, 1999; Saltzman *et al.*, 2000; Saltzman, 2002)

Table 1.3.1 Isotopically identified glacial periods in the Carboniferous.

Although the picture is very complicated, one temporal interval stands out as being of particular interest in the development of the Carboniferous glaciation. A large proportion of published work (e.g. Bishop *et al.*, 2009; Buggisch *et al.*, 2008; Rygel *et al.*, 2008; Smith & Read, 2000; Wright & Vanstone, 2001) has identified the upper Viséan to Serpukhovian interval as marking either the onset of widespread glaciation or as a period of definite ice-sheet expansion (Figs. 1.3.1a-b).

1.3.2 Magnitude

The published magnitudes of Carboniferous and Permian glacial centres are as variable as the range of timings discussed in Section 1.3.1 above. This is unsurprising, given the problems in harmonising results derived from the many

methodologies used to decipher past glacial extents. The two basic methodologies of determining the overall size of the Carboniferous glaciation involve:

(1) Mapping the areal extent of directly influenced palaeosurfaces and lithologies, and therefore the likely areal extent of glacial centres.

Early attempts at quantifying the scale of the Permo-Carboniferous glaciation largely relied on collating information on glacial pavements and tillites and even the latitudinal extent of dropstones (Frakes & Francis, 1988) from the preserved basins scattered across former Gondwanaland.

(2) Quantifying changes in other systems which were affected by ice build-up (e.g. glacioeustatic sea-level changes and $\delta^{18}O$ variations).

Simple observations of facies juxtaposition, erosion depths and sequence cyclicity, purportedly caused by sea-level fluctuations associated with the waxing and waning of glaciers, has been widely used (Rygel *et al.*, 2008). More complex methods involve quantifying the recognised changes in $\delta^{18}O$ values, floral/faunal bands (Iannuzzi & Pfefferkorn, 2002; Kelley *et al.*, 1990) or interpreting shifts identified in the lithological indicators of climate (Scotese & Barret, 1990; Scotese *et al.*, 1999; Witzke, 1990) similar to those proposed by Cecil (1990).

Crowley & Baum (1991), building on the earlier work of Bambach *et al.* (1980), Parrish *et al.* (1986) and Veevers & Powell (1987), modelled three possible scenarios of ice-sheet cover (Table 1.3.2).

Model	*Ice area (Km^2)*	*Ice-volume (km^3)*	*Glacioeustatic capacity*
ICE I	17.9×10^6	39.8×10^6	45-75m
ICE II	27.2×10^6	63.9×10^6	90-120m
ICE III	40.0×10^6	108.4×10^6	150-190m

Table 1.3.2 Carboniferous glacial magnitude models of Crowley & Baum (1991). Note that glacioeustatic capacity refers to isostatically adjusted sea-level change.

Crowley & Baum (1991) decided that the ICE I model of 17.9×10^6 km^2 maximum ice cover during the Moscovian, more appropriately matched the available evidence than either ICE II or III. This implied a likely limit of 45-75m for glacioeustatic shifts at the peak of glaciation in the Carboniferous.

González-Bonorino & Eyles (1995) calculated a value of $21x10^6$ km^2 for the greatest extent of Gondwanan ice, which was in broad agreement with the ICE I model of Crowley & Baum (1991). However, the timing of the peak of glaciation did not agree between these two proposed models. González-Bonorino & Eyles (1995) suggested that an inverse relationship between ice-extent and the glacial record exists. It was argued that at peak glaciation, very meagre glacial deposits were preserved around the margins of large continental glaciers. González-Bonorino & Eyles (1995) proposed that the abundant glacial record around the Carboniferous–Permian boundary, which many workers attribute to peak glacial conditions (Bambach *et al.*, 1980; Isbell *et al.*, 2003b; Veevers & Powell, 1987), may instead be linked to extensional subsidence of intracratonic basins, which promoted marine flooding and fragmentation of the ice cover.

Isbell *et al.* (2003b) broadly agreed with the models of Crowley & Baum (1991) and González-Bonorino & Eyles (1995). Isbell *et al.* (2003b) suggested ice-sheets covered a maximum area of between 17.9 and 22.6 x 10^6 km^2 around the Carboniferous–Permian boundary, but argued that the previous estimates of overall ice-volume were exaggerated. They demonstrated that, for a given area covered by ice, there exists a large variation in the actual volume of the ice depending on the number of ice-sheets which cover the area. They calculated that the break up of a single ice-sheet into ten stable ice-sheets, covering an equal area, will result in an approximate 41% decrease in the volume of the ice and an identical decrease in the effect of isostatically adjusted sea-level change. Isbell *et al.* (2003b) went on to argue that it would take the ablation of an unrealistically extensively glaciated area to produce the sea-level fluctuations which are reported to have caused some of the Euramerican cyclothems. Isbell *et al.* (2003a), meanwhile, demonstrated that such an extensive area of glaciation was improbable, since a large area of Antarctica (required to be virtually covered in ice-sheets for the extensive glaciation model) was largely ice-free and never actually near a glacial spreading centre during the late Palaeozoic.

Other attempts to model the Carboniferous glaciation have had mixed success. Hyde *et al.* (1999) succeeded in modelling a significant ice-sheet of ~$150x10^6$ km^3

(~$44x10^6$ km^2), theoretically capable of isostatically adjusted sea-level fluctuations of ~260m. Although the model failed to achieve complete deglaciation without CO_2 changes, the Milankovitch-induced fluctuations in ice-sheet volume were comparable to Pleistocene glacial/interglacial signals. Horton & Poulsen (2009) successfully replicated a realistic ice-sheet of ~$79x10^6$ km^3 (~$26x10^6$ km^2) which, with complete ablation, could increase sea-levels by ~139m (isostatically adjusted). However, Milankovitch cyclicity in this model was only capable of producing ~25m of sea-level change, which is insufficient to drive the larger sea-level fluctuations observed (Heckel, 1995) in Euramerican cyclothems. Additionally, it required CO_2 concentrations of >2240ppm (compared to ~390ppm today) to cause collapse and complete ablation of the modelled ice-sheet.

Adlis *et al.* (1988) analysed the $\delta^{13}C$ and $\delta^{18}O$ values of well-preserved brachiopod shells and predicted a minimum sea-level fluctuation of 70m for the Pennsylvanian cyclothem concerned, which they attributed to glacioeustasy. Joachimski *et al.* (2006) analysed $\delta^{18}O$ of conodonts and demonstrated that the Pennsylvanian north American cyclothems preserved comparable isotopic shifts to those observed in Pleistocene foraminifera. They concluded that Carboniferous glacioeustatic sea-level fluctuations must also have been comparable to the ~120m oscillations observed in the Pleistocene (Fairbanks, 1989; Pillans *et al.*, 1998). Since the glacial maxima are represented by terrestrial sediments, or erosive levels, and analysable fossil materials are not available from these levels, both the values of 70m and 120m do not represent the full sea-level change recorded in the cyclothems studied by Adlis *et al.* (1988) and Joachimski *et al.* (2006).

Although some workers doubt that the cyclothems of Euramerica are wholly attributed to glacioeustatic sea-level change (e.g. Isbell *et al.*, 2003b), the vast bulk of evidence supports the theory. The speed with which the sea-level changes are calculated to have occurred vary between 0.1 and 0.5Myr (Miller & Eriksson, 2000; Rygel *et al.*, 2008). This precludes the influence of more gradual tectonic controls, such as ridge spreading rates, the average age of oceanic crust (Cogné & Humler, 2008) or mantle-convection driven topography changes (Muller *et al.*, 2008). The magnitude and ability to correlate both within a basin and between basins (Miller & Eriksson, 2000; Ross & Ross, 1985) both:

(1) discounts local sedimentary or rapid tectonic controls on sea-level, such as delta lobe switching or basin margin faulting.

and

(2) provides a more compelling argument in favour of an extrinsic influence on sedimentation.

Miller & Eriksson (2000) demonstrated that discrete thrust loading events were unlikely to be responsible for cyclicity observed in the central Appalachians, since the cyclicity could be correlated with those in the intracratonic Illinois Basin, where the effect of these tectonic events would not be felt. Work by Haq & Schutter (2008) has also highlighted the link between the Carboniferous glaciation and sea-level fluctuations. There is an obvious correlation between enhanced, rapid, high-order sea-level change and the postulated onset of glaciation (towards the upper Viséan), as well as a marked low in the global sea-level curve in the Bashkirian, during a time of possible maximum glaciation. The use of cyclothems to proxy the magnitude of ice-volume changes appears reasonable, as at present such a control is the only one known to be capable of producing the cyclic sedimentary sequences recorded.

Glacioeustatic sea-level fluctuations of 100-120m (Heckel, 1977; Joachimski *et al.*, 2006; Rygel *et al.*, 2008; Soreghan & Giles, 1999), ice-sheet coverage of between 17.9 and 22.6x10^6 km^2 (Isbell *et al.*, 2003a) and $\delta^{18}O$ shifts of between 1.0 and 1.7‰ around the time of the peak Carboniferous glaciation all compare favourably with equivalent features of the Pleistocene glaciation. It thus appears that, although there is a variation in understanding regarding its magnitude, the Carboniferous glaciation may be considered comparable in most general aspects to the younger and more fully understood Pleistocene glaciation.

Wright & Vanstone (2001) suggested that the late Viséan marked the build-up to full-scale glaciation as significant magnitudes in sea-level change become apparent in the sedimentary record from this time. Calculations of glacioeustatic fluctuations for this interval are given as 20-95m by Smith & Read (2000) and 25-60m during the Asbian through to the mid Brigantian and 60-120m from the mid Brigantian onwards by Rygel *et al.* (2008).

1.3.3 Causes

The combination of factors likely to be responsible for the scale of climate change observed during the Carboniferous glaciation are numerous and complex. Milankovitch cycles were certainly responsible for the waxing and waning of established glacial centres during this time, as demonstrated by computer models (Crowley & Baum, 1992; Crowley *et al.*, 1993; Hyde *et al.*, 1999) and the ~400,000yr (eccentricity) periodicities recognised in cyclical sedimentary deposits (Miller & Eriksson, 2000; Schwarzacher, 1964, 1989; Smith & Read, 2000; Veevers & Powell, 1987; Weedon & Read, 1995). Milankovitch cycles are repetitive and are, in fact, probably quantifiable (to a degree) for at least the last 500My (Berger *et al.*, 1989). Since alternating greenhouse and icehouse conditions existed during this timeframe, orbital cycles cannot have been solely responsible for initiation of an icehouse period. It could also be argued that Milankovitch cycles with periodicities all <400ka could not also be independently responsible for initiating and sustaining Permo-Carboniferous glacial intervals which lasted for up to 8My (Fielding *et al.*, 2008a) at a time.

Isotopic analyses of Carboniferous and Permian brachiopods and conodonts indicate that strong positive shifts in $\delta^{13}C$ occurred in conjunction with positive shifts in $\delta^{18}O$ values and increases in predicted ice-volumes (Bruckschen *et al.*, 1999; Buggisch *et al.*, 2008; Grossman *et al.*, 2002; Mii *et al.*, 1999; 2001; Popp *et al.*, 1986; Saltzman *et al.*, 2000; Saltzman, 2003). These shifts are interpreted as representing enhanced burial of organic ^{12}C and therefore effective drawdown of atmospheric CO_2. There are several possible reasons as to why significant amounts of $^{12}C_{org}$ became trapped during this time:

(i) It is possible that the burial of $^{12}C_{org}$ can be attributed to the expansion of terrestrial flora (Cleal & Thomas, 2005), in particular the spread of early forests.

(ii) Saltzman *et al.* (2000) has highlighted the effect orogenic events had on the development of restricted water masses in isolated basins in which organic material could accumulate.

(iii) Stagnation of bottom waters due to eustatic, non-glacial, sea-level change or variations in global oceanic circulation patterns (Saltzman, 2003; Smith &

Pickering, 2003) could also have been responsible for increased $^{12}C_{org}$ storage.

Research on Palaeozoic CO_2 levels has focused on modelling the global feedback mechanisms (Berner, 1990), undertaking direct stomatal counts on fossil plants and analysing the $\delta^{13}C$ values of soil carbonate, fossil soil organic matter and shallow water brachiopods (Beerling, 2002; Montañez *et al.*, 2007; Mora *et al.*, 1996; Royer *et al.*, 2004). These studies indicate that atmospheric CO_2 levels for the Carboniferous and Permian are strongly linked to global temperature and glacial intervals. However, intervals where:

(i) $\delta^{13}C$ shifts lag behind those of $\delta^{18}O$ and therefore glacial expansion (Buggisch *et al.*, 2008)

(ii) CO_2 levels remained low whilst global climate began ameliorating and glaciation waned (Beerling, 2002)

and

(iii) comparative modelling of CO_2 levels from strontium isotope records displays no systematic correspondence with the geological record of climatic variations at tectonic timescales (Rothman, 2002)

- indicate that atmospheric CO_2 concentrations could not feasibly be considered as the primary driver of climate change for every event during the Palaeozoic. Shaviv & Veizer (2003) argued that celestial drivers, such as the modelled cosmic ray flux (a forcing that is considered largely insignificant in modern times; Forster *et al.*, 2007), more accurately match and therefore are more likely to have controlled global climate conditions during the Phanerozoic.

An important factor in the development of ice-sheets, on the scale of those observed in the late Palaeozoic, relates to the geographical location of the landmasses at the time. Caputo & Crowell (1985) noted that the extreme continentality of the landmasses and their proximity to the palaeo-southpole probably facilitated and catalysed the Permo-Carboniferous glaciation. Other tectonic factors have also been considered as influential in triggering the onset of glaciation. The closing of equatorial seaways is postulated to have led to weakened circum-equatorial deepwater currents, altered oceanic distributions of nutrients and the enhanced poleward transport of heat and moisture necessary for the accumulation of large ice-

sheets (Saltzman, 2003; Smith & Read, 2000). Isotopic evidence (Mii *et al.*, 1999; Saltzman, 2003) supports the theory of the closing of the seaway between Laurussia and Gondwana at the onset of glaciation (Smith & Read, 2000; Smith & Pickering, 2003). Though not considered primary controls, the uplift of mountain areas can also provide nucleation points for glaciers (Powell & Veevers, 1987) and cause disruption of atmospheric circulation patterns (Smith & Read, 2000). A more significant effect of mountain building events is in the associated drawdown of CO_2 due to increased weathering rates. Uplift of the Allegheny plateau (Smith & Read, 2000), the Antler (Saltzman *et al.*, 2000) and Variscan (Bruckschen *et al.*, 1999) orogenies, as well as other South American and Australian events, principally in the Andes, the Amadeus Transverse Zone and the Tasman Fold Belt (Powell & Veevers, 1987), have all been proposed as having an effect on global CO_2 concentrations during the Carboniferous.

It is clear that a combination of a number of factors is necessary to fully explain the timing, duration and extent of the Permo-Carboniferous glaciation. However, certain controls appear to have been more dominant than others and although models (Crowley & Baum, 1992; Horton & Poulsen, 2009; Hyde *et al.*, 1999) obtained mixed results when attempting to quantify the main components of the Carboniferous glacial system, the inputs of geography, solar luminosity and CO_2 appear to have been most significant.

In summary, the Permo-Carboniferous glaciation was not a single cold climatic event, as had been previously thought, but was actually a series of discrete events, of varying magnitude. The expansion of terrestrial flora, in combination with enhanced weathering and burial of organic matter may have led to a significant drawdown of CO_2. Lower atmospheric CO_2 concentrations in combination with weakened solar output and enhanced cosmic ray flux would also have provided ideal conditions for the nucleation of glaciers (from the newly configured moisture laden atmospheric and oceanic currents) on the continentalised palaeo-southpole and uplifted regions.

Very significant climate cooling (in advance of the main body of maximum glaciation) began in late Viséan to Serpukhovian times. This period is crucial to our understanding of the dynamics of the main glaciation and represents the time interval examined in this project. Glacioeustatic sea-level fluctuations recorded in Euramerica of at least 20 to 60m indicate that ice-sheets may have been expanding aerially to ~5.5–13.3x10^6 km^2 and attaining volumes of ~11.4–34.2x10^6 km^3 during this time. The glaciation appears to have peaked (~23x10^6 km^2, ~67x10^6 km^3, ~117m isostatic sea-level change) in the Moscovian (Pennsylvanian) and was at least comparable in size to glacial maximums observed during the Pleistocene.

1.4 THE VISÉAN TO SERPUKHOVIAN OF IRELAND

During the Mississippian, Ireland was situated just south of the palaeoequator (Scotese & McKerrow, 1990; Witzke, 1990) and deposition, for the most part, occurred in a warm, shallow, epeiric sea (Fig. 1.4a). As Ireland slowly drifted north during the Tournaisian and Viséan, the sea began to transgress northwards (Fig. 1.4b) due to crustal extension and tectonic subsidence (Sevastopulo & Wyse Jackson, 2009). In Serpukhovian and Pennsylvanian times, carbonate deposition virtually ceased and siliciclastic sedimentation began to dominate, with environments ultimately becoming deltaic and terrestrial (Sevastopulo, 2009). This abrupt cessation of carbonate deposition is not restricted to Ireland (Guion *et al.*, 2000), although it is not contemporaneous everywhere. The mechanisms are still poorly understood, but Variscan flexure, resulting in drowning of the carbonate factory (Wignall & Best, 2000), or the development of large river systems (Sevastopulo, 2009) due to either a change in climate, through northward continental drift, or more likely uplift in the source region, have all been noted as potential causative factors.

The general deepening, followed by shallowing of palaeoenvironments is punctuated and interrupted by an overprint of more localised events, such as delta progradation and reactivation of faults. The large Laurussian continent to the northwest and west of Ireland was an influential presence and small, terrestrial areas such as the Leinster-Welsh massif (Wales-Brabant High) and the Southern Uplands High were present to the east (Fig. 1.4c, Guion *et al.*, 2000). The Galway High (Sevastopulo, 2009; Sevastopulo & Wyse Jackson, 2009) may also have influenced conditions, particularly in the Shannon Basin region.

During the Viséan and early Serpukhovian, many of the sediments of NW Ireland were deposited in relatively shallow water (Brandon & Hodson, 1984), making the sequences sensitive to minor sea-level fluctuations, such as those potentially caused by the waxing and waning of ice-sheets (Schwarzacher, 1964, 1989). Meanwhile, broadly contemporaneous sediments in County Clare, located further south, in the west of Ireland, were deposited in generally deeper water associated with the Shannon Basin, which had an axis roughly similar to that of the modern River

Shannon (Hodson & Lewarne, 1961). Although eustatic sea-level fluctuations are harder to identify in these more southerly sections, their supposed setting in a deeper and more open water mass, further from a palaeo-shoreline should be more representative of open marine conditions and chemistry.

1.5 THE PROJECT

1.5.1 Background

Ireland was located near the equator during the Carboniferous, and does not appear to have been directly affected by the progressing glaciation and, so, its rock sequences were not disturbed by the localised effects of successive glacial advances and retreats. Instead, the stratigraphic successions would be expected to record the influence of waxing and waning glacial centres through related changes in climate, sea-level and ocean chemistry. Glacioeustatic fluctuations of significant magnitude are recognised throughout Ireland and Britain from the Asbian onwards (Vanstone, 1996; Wright & Vanstone, 2001). In Ireland, cyclicity associated with eustatic sea-level changes is reported widely during the Asbian and Brigantian (Table 1.5.1).

Formation(s)	***Location***	***Age***	***No. cycles***	***Ref.***
Burren	County Clare, southwestern Ireland	Late Asbian	9	(Gallagher, 1996; Gallagher *et al.*, 2006)
Ballyclogh	North Cork area, southern Ireland	Late Asbian	7?	(Gallagher, 1996; Gallagher & Somerville, 1997)
Ballyadams	Southeast Ireland, predominantly the Carlow area	Late Asbian	At least 6	(Cózar & Somerville, 2005; Gallagher, 1996)
Clashavodig	Cork Syncline, southern Ireland	Asbian	9	(Heselden, 1991; Sevastopulo & Wyse Jackson, 2009)
Benbulben, Glencar and Dartry	NW Ireland, most notably the Dartry Mountains	Holkerian and early Asbian	Ten's of high frequency	(Schwarzacher, 1964, 1989)

Table. 1.5.1 Late Viséan cyclicity in Ireland.

Rocks of upper Viséan (Asbian and Brigantian) through to Serpukhovian age in NW Ireland (Counties Leitrim and Sligo) were selected for investigation (Fig. 1.4c and 1.5.1a) due to their suitable age, lithology, outcrop, palaeogeographical setting and reported sedimentological expression of glacioeustatic cyclicity (e.g. Schwarzacher, 1989). Fig. 1.5.1b illustrates the composite, regional stratigraphy relating to the sections shown in Fig. 1.5.1a. The geology and stratigraphy of these

sequences is discussed in detail in Chapter 2. Two contemporaneous sections in County Clare, located ~100km further south (Fig. 1.4c and 1.5.1c) were also examined. By comparing and contrasting the sedimentary and isotopic records across the Viséan–Serpukhovian boundaries in these two regional study areas it should be possible to identify and correct for any local effects on the systems examined. The stratigraphy of the Clare region, which will be discussed in greater detail in Chapter 3, is shown in Fig. 1.5.1d.

Substantial disagreement still exists about the timing of the individual climatic episodes which comprise the Carboniferous glaciation. The bulk of the disagreements are probably attributable to problems with correlation and the inevitably temporally discontinuous sedimentary rock record. In order to precisely correlate glacial episodes it is vital that the time zones used are well defined and internationally correlateable. Two stratigraphic boundaries are of particular interest to this work:

(1) The Asbian–Brigantian boundary

In NW Ireland, some disagreement exists concerning the placement of this particular boundary. It was generally accepted that the transition was located in the Drummangarvagh or Doobally Sandstone Members of the Bellavally Formation (Fig. 2.1.7), due to the presence of B_{2b} goniatites in the Lugasnaghta Shale and P_{1b} goniatites in the Glenkeel Member (Legg *et al.*, 1998, see Fig. 1.2.1a for goniatite biozones). Substantial work has been published on the ammonoids of the Leitrim Group (e.g. Brandon, 1973, 1977; Brandon & Hodson, 1984; Caldwell, 1959; Dixon, 1972; Hodson, 1958; Korn, 1990; Legg *et al.*, 1998; Moore & Hodson, 1958; Padget, 1953; Smith, 1980) which have the finest biostratigraphical resolution for this particular time interval (Fig. 1.2.1a). Miospore data (Higgs, 1984) is consistent with the ammonoid scheme, placing the Asbian–Brigantian boundary between the Glenkeel and Sraduffy Members of the Bellavally Formation. However, recent work by Cózar *et al.* (2005; 2006) has argued that the boundary should be moved down (stratigraphically) to the Dartry Limestone–Meenymore contact, which agrees with Brunton & Mason (1979 - fig. 2), who appear to place it in conjunction with the regressive phase of Cycle 5 (Ramsbottom, 1973). Using the occurrences of foraminifera,

calcareous algae and (rare) conodonts Cózar *et al.* (2005; 2006) suggested that the Asbian–Brigantian boundary in NW Ireland correlates to both the ammonoid and miospore schemes differently in Ireland than elsewhere and that its true position should be based on a new integrated biostratigraphical scheme. This discrepancy between biostratigraphical schemes is not seen in England, where the Substage stratotypes are geographically located (Sevastopulo & Wyse Jackson, 2009). In all figures (relating to NW Ireland) in this thesis, both the proposed Asbian-Brigantian boundary recognitions are shown with question marks used to demonstrate the current uncertainty.

(2) The Viséan–Serpukhovian boundary

Currently the Viséan–Serpukhovian boundary is defined by the first appearance of Namurian (Serpukhovian) index ammonoids at the base of the Dergvone Shale Formation. This is consistent with miospore data, which confines the boundary to above the lower portions of the Carraun Shale Formation (Higgs, 1984). To-date, no significant studies have been undertaken in Ireland or Britain on the occurrence and range of *Lochriea* conodont species, which may provide an alternative index fossil for the base of the Serpukhovian (Richards & Group, 2008).

1.5.2 Aims

This project will deal with several important issues relating to the biostratigraphy, biofacies, micropalaeontology and $\delta^{18}O$ record of Viséan to Serpukhovian rocks in Ireland. The findings will have a substantial bearing on our understanding of the Carboniferous glaciation and also the placement of significant stratigraphic boundaries.

The main goals of this project are to:

(1) Examine the middle Viséan to Serpukhovian stratigraphy of NW Ireland to determine the likely controls on depositional environments. In particular it is hoped to assess the true extent of any climatic influence or signal in the succession.

(2) Collect and process rock samples from the northwest sections to create a record of microfossil material, in particular, catalogue the phosphatic remains of fish and conodonts.

(3) Analyse the $\delta^{18}O$ values of fish and conodont apatite throughout the sections studied.

(4) Undertake similar lithological, microfaunal and isotopic investigations of two additional, temporally relevant, sections in western Ireland to constrain the effects of local events on the record of environmental change observed, further north, in the Sligo and Leitrim sections.

The steps listed above will also enable the following key biostratigraphic, chemostratigraphic and palaeoenvironmental questions to be addressed:

(a) How is the *Lochriea* (conodont) lineage developed in the Viséan-Serpukhovian rocks of Ireland and does the FAD of *L. ziegleri,* or any of its relatives, appear suitable for redefining the base of the Serpukhovian?

(b) Are there significant occurrences of any age-specific conodont species in the Meenymore or Bellavally Formations and thus, where is the correct placement of the Asbian–Brigantian boundary in NW Ireland?

(c) How comparable are apatite $\delta^{18}O$ analyses between (i) Ireland and international sites, (ii) west and northwest Ireland study areas, (iii) sections within a study area, (iv) conodont and fish analyses in the same section, (v) different conodont species and (vi) different fish species?

(d) Did significant cooling associated with the Carboniferous glaciation begin in the Viséan and, if so, when did it begin and how severe was it?

1.5.3 Methods

This project was based on both field and lab-based investigative techniques. The lithological, palaeontological and sedimentological features (of the rock sections examined) were recorded through detailed, cm-scale logging, and/or, m-scale mapping, depending on both the structural complexity of the sequence and the nature and condition of outcrop. The precise methodology employed for each of the sections studied is noted in the relevant section of text.

Lithological descriptions herein follow standard schemes (Stow, 2005; Tucker, 2001; Tucker & Wright, 2008). Often, several classification systems were used in order to more accurately describe a rock. The Grabau and Dunham classification schemes are used in this work to describe carbonates in terms of grain-size and texture, although the Folk scheme occasionally appears where a description has been taken from a referenced work. The following lithological terms are used with the following meaning throughout:

- The term "shale" is used to refer to very fine-grained, sedimentary units which are distinctly fissile. The exact nature of its grain-size or degree of cleavage development, along with any other notable characteristics will be given as a prefix descriptor if deemed relevant, e.g. "*finely cleaved, silty, calcareous shale"*.
- The term "mudstone" is used herein, purely in terms of a limestone bed with lime mud supporting larger grains, which constitute less than 10% of the whole rock, i.e. in the sense of the Dunham scheme.
- Where the term "mudstone" is used with a prefix describing the carbonate content of the rock i.e. *non-calcareous, poorly-calcareous* or *calcareous,* the term refers to a lithified, competent (non-fissile), mud-grade (<63μm) sediment.
- The term "laminite" is used exclusively for calcilutite grade mudstones which characteristically exhibit fine laminations associated with shallow-marine hypersaline conditions.

Macrofossils recovered in the field from outcrops were photographed in-situ (where necessary) and their stratigraphic position carefully recorded before removal to the laboratory for further preparation. Fossils were cleaned by gently washing in hot water and, in some instances, mild bleach (to remove recent encrusting organic material) or acid solutions (to better expose silicified structures). Physically robust fossils which had a covering of argillaceous sediment obscuring fine external details were cleaned for an appropriate length of time in an ultrasonic bath. The fossils were then photographed on a matt black cardboard background, under low angle light with a mounted standard digital camera.

Carbonate and shale samples were removed from sections in the field and processed using standard techniques to liberate microfossils (primarily conodont and ichthyolith elements). A detailed overview of the exact methodology employed for disaggregating each lithological type, as well as sorting and picking the resultant residues, is provided in Appendix A.

Microscopic materials, predominantly conodont and ichthyolith elements, were imaged (generally at 10.0Kv) using the Scanning Electron Microscope of the Department of Anatomy, National University of Ireland, Galway. Specimens were attached to 15mm diameter, aluminium SEM stubs using an adhesive carbon pad and were gold coated using a sputter coater (a small number were carbon coated, but no discernable differences in the images obtained were apparent).

All fossil images were contrast normalised before being digitally cut, cleaned and finally placed on a white background using the photo-editing software Adobe Photoshop CS3. Fossil plates were constructed by compiling the cleaned images in the graphical program Adobe Illustrator CS2 and giving each specimen a number and scale.

The sedimentary sequence in the Tievebaun Section (Section 2.2.1) was investigated for depositional cyclicity using the freeware program REDFIT v3.8 (Schulz & Mudelsee, 2002). Details of the methodology employed for this analysis is provided in Section 2.5, and in significant detail in Appendix B.

Conodont and ichthyolith biogenic apatite samples were transported for analysis to the Stable Isotope Laboratory managed by Prof. Michael Joachimski in the Geo-centre of northern Bavaria, at the Friedrich-Alexander University of Erlangen-Nuremberg, Germany. Fossil phosphate samples were chemically purified and analysed in multiplicate, in conjunction with regular in-house and international standards, in a high temperature-conversion elemental-analyser (TCEA) connected online to a ThermoFinnigan Delta Plus mass spectrometer. Full details on the chemical preparation and analytical techniques are given in Appendix C.

Finally, Laser Raman spectroscopy was undertaken to determine the molecular composition of certain materials identified during this study. A LABRAM HR, with a beam width of 2μm and a wavelength of 532μm, based in the Martin Ryan Institute, NUI Galway was used for the analyses.

1.5.4 Thesis plan

This thesis is divided into two volumes. **Volume I** contains the main text and tables and is divided into six chapters as follows:

- **Chapter 1** provides an introduction and background to the project.
- **Chapter 2** gives a detailed account of the lithostratigraphy and palaeoenvironments of the rock sequences investigated in the NW Ireland study area.
- **Chapter 3** contains a description of the lithostratigraphy and evolution of the Shannon Basin region, focusing particularly on the Burren Platform area located to the north of the basin structure.
- **Chapter 4** presents all of the microfossil data from the sections in NW Ireland and Co. Clare and discusses their stratigraphic and palaeoenvironmental significances.
- **Chapter 5** is perhaps the central chapter of the thesis and details and discusses all of the results from the stable isotope analyses of biogenic apatite recovered from the various sections examined.
- **Chapter 6** synthesises all of the observations from the previous chapters and integrates them into a palaeoenvironmental model for Ireland in the late Viséan and early Serpukhovian. Emphasis is put on the dominance of global controls (in particular the Carboniferous glaciation) on sedimentation during the interval. Recommendations for the direction of future work are also provided.

Volume II comprises all of the figures referenced in Volume I. In addition, seven appendices are provided towards the very end:

- **Appendix A** provides a description of the methodologies employed during rock disaggregation as well as tables of sample weights and chemicals used.

- **Appendix B** contains a detailed account of how digital spectral analysis was undertaken on the Tievebaun Section.
- **Appendix C** comprises the step-by-step methodology utilised for the stable isotopic analysis of biogenic apatite.
- **Appendix D** details the exact positioning of microfossil samples removed from sections investigated in NW Ireland.
- **Appendix E** details the exact positioning of microfossil samples removed from sections examined in the Burren Platform.
- **Appendix F** describes the invertebrate microfossil material recovered during the course of rock-processing.
- **Appendix G** is a repository for tabulated information relating to the phosphatic samples subjected to stable isotope analysis.
- **Appendix H** provides maps to the SEM stubs onto which all figured specimens are attached. All stubs are lodged in the James Mitchell Museum at the National University of Ireland, Galway.

All tables and figures are numbered so that each refers to the text section to which they relate (generally in their first instance), e.g. Table 1.3.1, and Fig. 1.3.1a relate to the timing of the Carboniferous glaciation, discussed in Section 1.3.1. Where more than one table or figure relate to a section, the first is given the suffix letter “a”, the second “b” and so forth e.g. Fig. 1.3.1a is the first figure relating to Section 1.3.1.

References cited in the text, appendices or in figure captions are listed at the end of Volume I.

CHAPTER 2 - THE GEOLOGY OF NW IRELAND: SUCCESSIONS IN COUNTIES SLIGO AND LEITRIM

This chapter will begin by introducing important aspects of the lithostratigraphy of the northwest study area before describing the results of fieldwork (on a section by section basis) and concluding with a discussion on the sedimentological and lithostratigraphical findings of the work.

2.1 STRATIGRAPHY OF THE NW IRELAND SUCCESSIONS STUDIED

Rocks of Carboniferous age in NW Ireland outcrop in a series of related shallow basins which extend, approximately, from the Carrick Basin to the Donegal Syncline on the northwest coast of Ireland (Fig. 2.1a). The thickest successions are found in the Lough Allen Basin, but many of the established formation names are derived from the Sligo Syncline. Philcox *et al.* (1992) suggested from subsurface data that some of the thickness variations, exhibited across the basins, were a result of facies changes, but along with Kelly (1996), Legg *et al.* (1998) and Mitchell (2004), concluded that, during the Asbian, local tectonics controlled subsidence, the development of carbonate platforms, and therefore deposition.

Although major facies variations are evident between these basins, lithostratigraphic and biostratigraphic similarities are sufficient to enable inter-basin correlation (Brunton & Mason, 1979). This suggests that the forces controlling sedimentation in the region over operating over a wide area. The relationships and depositional similarities between the northwest successions and Carboniferous basins abroad have also been demonstrated (Mitchell, 1992). Smith (1980) suggested that the Lough Allen Basin and part of the Ballymote Syncline can be considered the south-westerly extension of the Midland Valley of Scotland. This correlation is based on the fact that this area lies to the south of the inferred line of the Highland Boundary Fault (locally the Ox Mountains, Castle Archdale and

Omagh Faults) and north of the inferred continuation of the Southern Uplands Fault (Figs. 2.1a-b). Brunton & Mason (1979) concluded that there was sufficient depositional similarity between Irish, British, eastern Canadian and Svalbard successions to allow correlation of the overall lithological sequences.

The stratigraphical sequence examined in this work (uppermost Holkerian to lower Serpukhovian) is shown in Fig. 1.5.1b, and described in detail in the subsections below. Variation in stratigraphic terminology for the region can be confusing; work by Brandon (for example) has variously used the terms Sligo Group (1968), Dartry Limestone Group (1972b) and Tyrone Group (1977; Brandon & Hodson, 1984) to refer to the division of Viséan rocks comprising the Dartry Limestone Formation and the older limestones of Oswald (1955). The term Sligo Group has been (somewhat) replaced by the term Tyrone Group (Brandon, 1972b, 1977; Legg *et al.*, 1998; Mitchell, 2004; Sevastopulo & Wyse Jackson, 2009); however, it will be retained here since the relevant stratigraphic interval was actually examined in the Sligo Syncline. Fig. 2.1c demonstrates some of the origins and equivalence of lithostratigraphic terms, as well as the biostratigraphy, for the northwest region.

The lithological and geological descriptions in this chapter will focus on the Sligo Syncline and Lough Allen Basin successions.

2.1.1 The Mullaghmore Sandstone Formation

This particular formation was not directly observed during this study but, according to Oswald (1955), it directly underlies the oldest formation investigated. The Mullaghmore Sandstone Formation is ~200m thick in its type area, on the coast west of the Drownes River at Mullaghmore Head, Co. Sligo (MacDermot *et al.*, 1996). The base of the formation is variable in development, being occasionally erosive, pebbly or calcareous, but can essentially be defined by the appearance of the first major sandstone body (Graham, 1996). Thinning and progradation into more fully marine conditions further south, along with palaeocurrent flow data, indicate a north or northwest source for the sediments of this formation (MacDermot *et al.*, 1996). Higgs (1984) identified TS miospores, indicating an Arundian-Holkerian age.

The Mullaghmore Sandstone Formation is characterised by deltaic (Sheridan, 1972) and fluviatile sandstones with some minor palaeosol developments (Graham, 1996). The top of the formation is oolitic with calcareous sandstones and thin limestones in places, which have been attributed to reworking during a rapid sea-level rise (Graham, 1996).

2.1.2 The Benbulben Shale Formation

The boundary between the Mullaghmore Sandstone and Benbulben Shale Formations has been defined by the disappearance of sand-grade clastics (MacDermot *et al.*, 1983). The relatively abrupt change from the underlying Mullaghmore Sandstone Formation represents a major flooding event which is likely isochronous (Brunton & Mason, 1979), and eustatic rather than tectonic in origin. The Benbulben Shale Formation is late Holkerian to early Asbian in age based on foraminifera (Kelly, 1989) and miospores (Higgs, 1984).

A complete 99m long stratigraphic section is exposed on Tievebaun at grid reference [GR] 17680 35090 (MacDermot *et al.*, 1996). The formation is defined by fully marine, fossiliferous (typically dominated by crinoids, brachiopods, solitary corals and bryozoans), dark grey calcareous shale with subordinate thin-medium impure limestone beds (MacDermot *et al.*, 1983).

2.1.3 The Glencar Limestone Formation

The base of this formation is marked by an increase in the thickness and proportion of limestone beds, in conjunction with a reduction in shale content (Oswald, 1955). The boundary between the Benbulben Shale and Glencar Limestone Formations is very difficult to identify precisely outside of the type area (as originally identified by Oswald, 1955) and its (likely) diachronous nature has led to the grouping of the formations in some areas (Sevastopulo & Wyse Jackson, 2009). The coral/brachiopod fauna of the Glencar Limestone Formation indicates an Asbian age (Oswald, 1955). A complete section of the Glencar Limestone Formation

(150m), including its contacts, is exposed in a stream on the north side of Tievebaun Mountain, Co. Sligo (Section 2.2.1).

This formation is characterised by rhythmic alternations of limestone and shale. The shale is calcareous and fossiliferous, whilst limestone beds commonly possess upper and lower, parallel-laminated, dolomitic margins enclosing a central wackestone/packstone in which bioclasts are orientated parallel to bedding (MacDermot *et al.*, 1996).

2.1.4 The Dartry Limestone Formation

The transition from the underlying Glencar Limestone Formation is highly variable, depending on the nature of the Dartry Limestone which is developed locally. Hubbard & Sheridan (1965) stated that the boundary between the Glencar and Dartry Limestone Formations could be placed at the first appearance of dark chert. A more widely applicable diagnosis for this boundary is an overall reduction in shale content and increase in nodular and bedded chert. The Dartry Limestone Formation contains a microfauna and coral horizons which indicate an Asbian age (Cózar *et al.*, 2005; 2006).

The Dartry Limestone Formation has been divided into several different members (Fig. 2.1.4), principally by Kelly (1989, 1996) and Legg *et al.* (1998) in Co. Fermanagh. The thickness of the formation varies considerably from ~120-360m (Kelly, 1996) depending on the presence or absence of the mudmound facies described below. Many of the members are geographically restricted (particularly in the western Fermanagh highlands) and only the following two are regionally recognised:

(1) **Dartry Limestone** (Oswald, 1955), a.k.a. Glenboy Limestone Member (Brandon, 1968) – Consists of medium to thickly-bedded, cherty, dark grey, bituminous limestone. It is usually fine-grained and sparsely crinoidal with interbedded, thin, shaly limestone and subordinate calcareous shale and siltstone. Bluish-black to brown, and occasionally cream coloured chert occurs in variously shaped nodules, but more commonly in layers parallel to

bedding and can comprise up to 50% of the rock. Bioclasts, where present, are frequently silicified and weather proud of the surface.

(2) **Mudbank Limestone** (MacDermot *et al.*, 1996), a.k.a. Knockmore Limestone Member (Legg *et al.*, 1998), a.k.a. Kilmakerrill Limestone Member (Brandon, 1968), a.k.a. Facies B (Kelly, 1989) – Identified as massive mudmounds, 9-150m thick and several km in aerial extent, with significant palaeotopographies of up to 122m, and steep flanks of 25-40° (Kelly, 1989; Oswald, 1955; Schwarzacher, 1961). A structural control for the development of the mudmounds has been discussed by several workers (Brandon, 1968; Caldwell & Charlesworth, 1961; Sevastopulo & Wyse Jackson, 2009) who noted an association of mudmounds with the palaeo-highs of the Ox and Curlew Mountains. Sevastopulo & Wyse Jackson (2009) concluded, however, that substantial developments of mudbank limestone cannot be directly correlated with any known faults.

2.1.5 The Meenymore Formation

The base of this unit was placed (West *et al.*, 1968) above the last fossiliferous marine limestone of the Dartry Limestone Formation at its type section in the Aghagrania River (Section 2.3.1). This level falls slightly below the occurrence of the first laminite, which is a characteristic feature of the formation. Foraminifera (Kelly, 1996) and B_2 goniatites (Fig. 1.2.1a) from this and overlying units (Brandon, 1977; Brandon & Hodson, 1984) indicate an Asbian age. Recently, however, Cózar *et al.* (2005) and Cózar & Somerville (2006) suggested that the Meenymore Formation is actually Brigantian in age based on conodonts, calcareous algae and foraminifera. The formation rests both conformably and disconformably on the top of the Dartry Limestone (Kelly, 1989; Legg *et al.*, 1998; Somerville *et al.*, 2009). In places, where a residual palaeotopography was created by underlying mudbank limestone, the Meenymore Formation is seen to onlap the flanks of the mounds and becomes thin or absent across the top of the mounds (Brunton & Mason, 1979), Fig. 2.1.4 and Fig. 2.1.5a. Although uncommonly developed, localised fossil horizons do occur in which macrofossils are often micritised, coated and rolled, probably indicating shallow water conditions (Brandon, 1977).

The Meenymore Formation displays rapid lateral and vertical variation and lacks distinct mappable horizons, making it difficult to readily subdivide. This variation has been attributed to the irregular surface of the underlying Dartry Limestone Formation mudmounds (Brandon, 1977) and local differences in subsidence rates (Brandon & Hodson, 1984). On Slieve Rushen, in Counties Cavan and Fermanagh, where the formation is anomalously thick (~244m, cf. 30-45m thickness around Cuilcagh Mountain, Co. Fermanagh), thin sandstones have been interpreted as turbidites (Brandon, 1977) generated during rapid, localised, fault-controlled subsidence.

This formation comprises predominantly unfossiliferous grey shale with subordinate, thin, massive mudstones and laminites and at its type section it has been divided into three members (Smith, 1980; West *et al.*, 1968), which are shown in Fig. 2.1.5b and described below in Table 2.1.5 in ascending stratigraphical order:

	Member	***Details***
Meenymore Formation	**Corloughlin** ~25m	Unfossiliferous shale with interbedded, thin laminated and massive carbonates.
	Dorrusawillin ~1.5m	Fossiliferous, calcareous shale with thin limestone interbeds (West *et al.*, 1968).
	Drumcroman ~12m	Unfossiliferous shale and often laminated limestone and dolomite. Cherty, unlaminated carbonates and breccias are notable.

Table 2.1.5 Members of the Meenymore Formation in the Aghagrania Section.

2.1.6 The Glenade Sandstone Formation

The base of this formation is defined by the first thick unit of a (nearly continuous) sequence of predominantly unfossiliferous, thick-bedded sandstones (MacDermot *et al.*, 1983). Angular argillaceous clasts suggest that the base may be locally erosive (Brandon & Hodson, 1984; Brunton & Mason, 1979). The formation forms a southerly thinning wedge (Fig. 2.1.5a), ranging from an estimated 300-350m in the Fermanagh highlands (Legg *et al.*, 1998) to less than 4m at the southern end of Lough Allen (Smith, 1980; West *et al.*, 1968). This pronounced thickness variation

has been attributed to both gentle synsedimentary subsidence in the north (Brandon & Hodson, 1984), as well as deposition in a half-graben (Mitchell, 1992).

The southward thinning, presence of small metamorphic clasts and minor palaeocurrent indicators (Brunton & Mason, 1979) developed in this formation suggests a provenance in the north, most likely the Donegal Mountains.

2.1.7 The Bellavally Formation

The Bellavally Formation does not have a designated type section, but is most completely exposed in the Aghagrania River, Co. Leitrim, where it is ~33m thick (MacDermot *et al.*, 1983). The Asbian–Brigantian boundary is located within this particular formation, based on both miospore (Higgs, 1984) and ammonoid (Legg *et al.*, 1998) biostratigraphy. The members of the formation are quite consistent in both thickness and lithological character across the various basins (Brandon & Hodson, 1984), suggesting that deposition occurred across a relatively uniform surface. The base of the formation is taken at the first appearance of calcareous mudstone, marine shale or algal laminite above the Glenade Sandstone Formation (MacDermot *et al.*, 1996). Unlike the Meenymore Formation, which it otherwise generally resembles, fossiliferous horizons are more common in the Bellavally Formation, possibly due to the presence of marine waters of more normal salinity or oxygen level (Smith, 1995).

Nine mappable members are present within the Bellavally Formation; however, minor irregularities do exist and the lowest two members are not well developed or are entirely absent in the south (Fig. 2.1.5a). The members seen in the Carraun Section of Brandon (1968) are shown in Fig. 2.1.7, whilst all the known members are described below in Table 2.1.7 in ascending stratigraphic order:

	Member	Details
Bellavally Formation	**Corry**	Typified by upper and lower units of predominantly finely-laminated, dolomitic micrite and macrocells separated by a unit of dominantly fissile, grey, unfossiliferous, dolomitic shale (Brandon & Hodson, 1984). Subordinate amounts of each of the units are found in the other.
	Sheena Shale	Lithologically similar to the Lugasnaghta Shale below (Brandon, 1968). Several traceable faunal bands are present, including (Brigantian) P_{1b} goniatite horizons (Brandon & Hodson, 1984; Legg *et al.*, 1998).
	Glenkeel	Variable in development and lithology from unfossiliferous calcareous mudstone (Legg *et al.*, 1998) to micaceous silty shale and laminated algal micrites (Brandon & Hodson, 1984). A P_{1b} ammonoid fauna has been recovered, placing it within the lowermost Brigantian (Legg *et al.*, 1998).
	Doobally Sandstone	Commonly micaceous pale brown, medium-grained massive sandstones with subordinate siltstone and shale (Brandon & Hodson, 1984). Desiccation cracks are common. Dated as lowermost Brigantian (miospore VF) by Higgs (1984). Variable in thickness, but laterally persistent throughout the region (Fig. 2.1.5a).
	Drumman-garvagh	Fine laminites, unfossiliferous poorly-calcareous mudstones and fissile shale, as well as laminated sandstones (Brandon, 1968). Impersistent in its occurrence (Fig. 2.1.5a).
	Lugasnaghta Shale	Fossiliferous, medium grey, calcareous mudstones and shale with thin, occasionally bioturbated, wackestone and mudstone interbeds (Brandon, 1968).
	Sraduffy	Series of green-grey calcareous mudstones with flaggy, impersistent, fine-medium grained, rippled and desiccated sandstones, bound by thinner laminite units (Brandon & Hodson, 1984).
	Larkfield Shale	Compact micritic beds in calcareous mudstone and shale with a marine fauna of B_2 age (Brandon, 1968). Macrofossils are rolled and micritised (Brandon & Hodson, 1984).
	Tullyskeherny	Finely laminated stromatolitic carbonates and, in parts, a macrocell horizon (Brandon & Hodson, 1984).

Table 2.1.7 Members of the Bellavally Formation found in the Connaught Coalfield.

2.1.8 The Carraun Shale Formation

The Carraun Shale Formation has its type section in the stream between the townlands of Carraun and Lugasnaghta on the northeast side of Dough Mountain, Co. Leitrim (see Section 2.3.2). The formation is Brigantian in age and is thought to span the P_{1b}/P_{1c} to P_{2c} ammonoid biozone interval (Brandon & Hodson, 1984; Legg *et al.*, 1998). It is ~54m thick at its type section, but reaches a maximum thickness

of 160m in the Fermanagh Highlands (MacDermot *et al.*, 1996). The base is defined by the first fossiliferous shale above the Corry Member of the underlying Bellavally Formation (Brandon, 1968). There is a marked reduction in the abundance of thick-shelled, benthic organisms such as corals, gastropods and brachiopods up through the formation (Brandon & Hodson, 1984).

The Carraun Shale Formation (Fig. 2.1.8) is predominantly composed of dark grey, pyritic, often fossiliferous, calcareous shale. Five limestone members have been identified and are described in Table 2.1.8 in ascending stratigraphic order.

	Member	***Details***
Carraun Shale Formation		Poorly fossiliferous, dark grey shale, containing four, probable, K-bentonite horizons (Legg *et al.*, 1998).
	Camderry Dolomite	Two shaly, dolomitic carbonates, separated by thin fossiliferous shale (Brandon, 1968). Large lenticular bullions are occasionally developed, yielding well-preserved basal P_{2c} (Brigantian) ammonoids (Brandon & Hodson, 1984).
		Poorly fossiliferous, dark grey to bluish-black shale with three, possible, K-bentonite clay horizons (Legg *et al.*, 1998).
	Sranagross Dolomite	Dark grey, argillaceous, dolomitic limestone, 15-61cm thick, with crushed fossils of P_{2b} age (Brandon & Hodson, 1984).
		Fossiliferous (P_{2a} & P_{2b}), dark grey, calcareous shale (Brandon & Hodson, 1984).
	Ardvarney Limestone	A single bed (~30cm thick) of brittle, medium-dark grey, slightly argillaceous, bioclastic micrite (Brandon, 1968) with fine shale laminae (Legg *et al.*, 1998). Fragments of brachiopods and crushed goniatites are found, particularly on the bed surface, which indicate a Brigantian, basal P_{2a} age (Legg *et al.*, 1998).
		Fossiliferous, poorly-calcareous mudstones (Legg *et al.*, 1998).
	Tawny-unshinagh Limestone	Lithologically, palynologically and environmentally similar to the Meenymore and Bellavally Formations (Smith, 1995). Consists of two stromatolitic, laminated carbonates separated by a unit of unlaminated carbonate and shale (Brandon, 1968). Stromatolitic clast lags, calcareous sandstones, oncolites and algal structures are developed (Brandon & Hodson, 1984).
		Medium grey, calcareous mudstone and shale with thin limestone beds and P_{1c} to P_{1d} (Brigantian) fossils (Brandon & Hodson, 1984; Legg *et al.*, 1998).
	Derreens Limestone	A series (usually nine) of fossiliferous, argillaceous limestone and calcareous mudstone and shale (Brandon & Hodson, 1984). Its upper contact is rather arbitrarily placed where the limestone beds become thinner and the interbedded shales become thicker (Brandon, 1968). The third limestone in this member is the distinct Derrybofin Bed, a hard, compact micrite containing a rich marine fauna (Brandon & Hodson, 1984).

Table 2.1.8 Members of the Carraun Shale Formation in NW Ireland.

2.1.9 The Dergvone Shale Formation

The base of the Dergvone Shale Formation is taken at the FAD of the *Cravenoceras leion* marine band (MacDermot *et al.*, 1983), which marks the boundary between the Viséan and the Pendleian (Serpukhovian). There is no indication of a break in the sequence at this level (Sevastopulo, 2009) as seen elsewhere, particularly in the Shannon Basin area (Chapter 3). The formation is ~150m thick at its type section in the townland of Dergvone, Co. Leitrim, GR 19550 33175 (MacDermot *et al.*, 1996), but varies (Fig. 2.1.9a) from ~118m on Slieve Anierin, Co. Leitrim to ~168m on Thur Mountain, Co. Leitrim, to the north.

The formation mostly comprises dark grey and bluish-black ferruginous shale, thin calcareous mudstone, sideritic nodules and beds as well as rare thin (possibly turbiditic) sandstones (Legg *et al.*, 1998). Several members have been identified in the formation (Fig. 2.1.9b) and are described in Table 2.1.9 in ascending stratigraphic order.

	Member	Details
Dergvone Shale		Silty shales and thin siltstones, eventually grading into the overlying Briscloonagh Sandstone Formation (Brandon & Hodson, 1984).
	Lacoon Sandstone	Interbedded brown-grey sandstones, micaceous siltstones and grey, poorly-fissile shale (Brandon, 1968). Sandstones can contain convolute bedding, cross-lamination and sole structures, which indicate palaeocurrents flowed from the northeast (Legg *et al.*, 1998).
		Dark-grey unfossiliferous shale and occasional thin sandstone/ siltstone (Legg *et al.*, 1998). Sole marks indicate transport from the north-northeast (Brandon, 1968).
	Kilooman Shale	Fossiliferous (E_{1c}), hard, dark grey, calcareous mudstone and shale with large, poorly-fossiliferous bullions frequently developed basally (Brandon & Hodson, 1984; Legg *et al.*, 1998).
		Unfossiliferous, fissile, blue grey shale and sideritic ironstone.
	Tonlegee Shale	Lithologically similar to the Tullyclevaun Shale Member and contains the E_{1a}–E_{1b} boundary near its base (Brandon, 1968; Brandon & Hodson, 1984; Legg *et al.*, 1998).
		Unfossiliferous, fissile, blue grey shale and sideritic ironstone.
	Tully-clevaun Shale	Blocky, fossiliferous (E_{1a}), blue-grey calcareous mudstone, with large bullions (some fossiliferous) common in parts of Co. Leitrim (Brandon & Hodson, 1984).
	Black Mountain Shale	Homogenous dark shale with a sparse fauna and rare, small bullions (Brandon, 1968). A distinct sandstone (The Loughaphonta Sandstone) is developed impersistently at its base.
	Gubaveeny Shale	Represents an E_{1a} (Serpukhovian) marine band, comprising grey-blue, calcareous shale (Brandon, 1968).

Table 2.1.9 Members of the Dergvone Shale Formation in NW Ireland.

2.1.10 The Briscloonagh Sandstone Formation

The basal contact of this Formation with the underlying Dergvone Shale (the youngest stratigraphic unit examined herein) is transitional and the base is subjectively placed directly beneath where substantial sandstone beds become developed (Brandon, 1968). The Briscloonagh Sandstone Formation grades from distal to proximal facies upwards, representing a sandstone/siltstone dominated, southerly prograding delta system and basin filling episode (MacDermot *et al.*, 1996). It is petrographically comparable to the Glenade sandstone and most likely derived from a similar source (Brandon, 1968).

2.2 SLIGO GROUP SECTIONS IN NW IRELAND

Six separate river and cliff sections were investigated in order to establish those which best represented the upper portions of the Sligo Group (Table 2.2a). A deliberate effort was made to select sections which avoided areas where the Mudbank Limestone Member of the Dartry Limestone Formation is developed (with resultant "non-standard" stratigraphy). These sections are found in a ~90km^2 area around Truskmore, Glencar Lough and Glenade Lough in Counties Sligo and Leitrim.

Section	*Location*	*Reference*	*Description*
GL01	N Copes Mtn., Co. Sligo. G7300 4146	MacDermot *et al.* (1996)	Cliffs exposing a gradational Glencar Limestone-Dartry Limestone contact.
GL02	N Tievebaun Mtn., Counties Sligo and Leitrim. G77395 50754	MacDermot *et al.* (1996)	Poorly exposed stream cut of the central Glencar Limestone. Downhill, numerous stream cuts expose the upper Benbulben Shale.
GL03, GLTV	N Tievebaun Mtn., Co. Sligo. G76742 51001	Higgs (1984)	The western tributary of a prominent stream exposes the Glencar Limestone Formation and its contacts.
DA01, DAGL	N of L. Glencar, Co. Leitrim. G74919 44334	Schwarzacher (1964) and Browne (1981)	Stream in hanging valley exposes the lower Dartry Limestone Formation and its basal contact.
DAGL2	N L. Glencar, Co. Sligo. G74024 44171	Personal reconnaissance	Composite section follows stream and cliff exposure covering the Glencar-Dartry Limestone contact.
DA02, DAGN	SE of L. Glenade, Co. Leitrim. G85010 45897	MacDermot *et al.* (1983)	Higher, easily accessed portion of more extensive river section exposing the upper Dartry Limestone Formation.

Table 2.2a Sligo Group Sections investigated in NW Ireland.

White rows represent sections which were fully logged and sampled, while grey rows equate to sections which were deemed unsuitable for further investigation.

Three of the six sections around the Dartry Mountains were selected for more detailed investigation and sampling (Fig. 2.2), and are described in the following sub-sections of this chapter:

- 2.2.1 – the Tievebaun Section (GL03, GLTV)
- 2.2.2 – the Glencar Section (DA01, DAGL)
- 2.2.3 – the Glenade Section (Leckanarainey stream, DA02, DAGN)

The remaining rock sections, GL01, GL02 and DAGL2 were deemed unsuitable for detailed analysis.

2.2.1 Tievebaun Section (GL03, GLTV)

Tievebaun Mountain is the most northerly projection of the Truskmore plateau in the Dartry Mountain range, which straddles the border between Counties Sligo and Leitrim. A stream on the north face of the mountainside (Fig. 2.2) exposes a near continuous succession from the mid/upper Benbulben Shale Formation, through the Glencar Limestone Formation, to the lower portions of the overlying Dartry Limestone Formation.

The section is exposed in the most westerly of three tributaries and begins at the first significant (and continuous) bedrock exposure at GR G76742 51001 ±8m, 232m elevation (Figs. 2.2.1a-c). The bulk of the section is tracked by switching between the eastern and western banks, while the upper portions, leading to the top of the section (GR G76600 50791 ±8m, 441m elevation) are only exposed on the large knoll to the west of the stream.

Just over 216m of stratigraphic section (Fig. 2.2.1d, key to logs in Fig. 2.2.1e) was logged and 32 2kg limestone beds (taken at approximately 7m intervals), in addition to three smaller nodular horizons, were sampled for microfossil processing. Detailed logs and exact details of sample locations can be found in Appendix D. A brief account of the main aspects of the section is provided below.

2.2.1.1 The Benbulben Shale Formation

The section begins in typical Benbulben Shale Formation facies comprising fossiliferous, calcareous shale with subordinate, thin limestone (wackestone) interbeds. A diverse fauna, including ramose and fenestrate bryozoans, various brachiopods, trilobites and echinoids, but dominated by crinoid and coral material, is contained in both lithologies (Figs. 2.2.1f(i) & 2.2.1g-h). Fossils are particularly well-preserved in the shale units, but tend to be more disarticulated in the thin interbedded wackestones. Autochthonous brachiopods with partial spine attachments and crinoid stems up to 10cm in length are preserved in the shale. A substantial variety of crinoid stems were recovered from the shale, with notable amounts of cirri on most pluricolumnals.

Thicker limestone beds occur where notable and relatively persistent fasiculate coral horizons are developed and these act as useful stratigraphic markers locally. Isolated coral colonies are also found in irregular limestone bodies within shale units.

Subordinate thin, crinoidal packstone beds typically contain size-sorted and disarticulated fossil material and tend to be laterally impersistent over distances greater than a few metres. Thicker carbonate beds often display preferential concentration and horizontal alignment of fossils in the bed core. Fenestrate bryozoan colonies are largest on the surfaces of the limestones.

2.2.1.2 The Glencar Limestone Formation

The contact between the Benbulben Shale and the Glencar Limestone was taken at 49.4m above the section base (ASB), where an increase in the proportion and thickness of limestone beds is identified. Though obviously more limestone-rich, the various facies of the Glencar Limestone Formation are otherwise very similar to those seen in the Benbulben Shale Formation. Fossil material is initially less abundant (particularly corals), except where the lithological development more closely resembles that of the Benbulben Shale Formation. Some vertical (in limestones) and horizontal (on muddier surfaces) bioturbation is apparent within the formation.

Just over 50m stratigraphically above the base of the formation (~107m ASB), gaps in exposure precede a return to a shale-dominated lithology. Thin subordinate limestones with gradational contacts and common dolomitisation become progressively thinner and more argillaceous upwards. Between ~107m and ~187m ASB, large portions of the succession become fossil poor and difficult to divide into clearly defined lithological units. At these levels the silty calcareous mudstones are more competent whilst limestones are more cleaved and argillaceous with gradational contacts.

Thin limestone beds slowly become more frequently developed approaching ~187m ASB where limestones again become the dominant lithology. At this level the limestone beds become purer and more fossiliferous (wackestones, Fig. 2.2.1f(ii & iii)). Stringers and amorphous bodies of pyrite become commonly developed in the limestone beds. Echinoderms are particularly well represented in the upper portions of this formation by cladid crinoid and *Monoschizoblastus* blastoid calyxes, as well as rare disarticulated echinoid plate and spine accumulations (Fig. 2.2.1h).

2.2.1.3 The Dartry Limestone Formation

The Glencar–Dartry Limestone contact is located at 197.525m ASB, where the limestone becomes virtually devoid of fossils (possible horizontal bioturbation is expressed on fresh bed surfaces) and large nodules and beds of banded silicification occur. Small dispersed, irregular chert nodules are evident in the fossiliferous carbonates immediately preceding this contact. The chert/silicification is incompletely developed and is grey and grainy in appearance. Stylolites are developed in some of the carbonate beds and are best displayed where silicification has occurred up to the level of the dissolution horizon, creating a strong contrast across the contact (Fig. 2.2.1f(v)). The carbonate beds up through the sequence become increasingly silicified. Some purer limestone pockets exist in the centre of the chert nodules and horizons. A poorly-preserved, 6.5cm long orthoconic nautiloid represents the only fossil identified in the Dartry Limestone Formation in this section (Fig. 2.2.1f(iv)). Large, cm-sized, crystallised vugs occur towards the top of the succession.

2.2.2 Glencar Section (DA01, DAGL)

Spectacular cliff exposures of the Glencar and Dartry Limestone Formations are found to the north of Lough Glencar. A stream in a deeply cut hanging valley, north of the Swiss Valley (Fig. 2.2.2a) was selected as the section which best exposes the lower and middle portions of the Dartry Limestone (without intersecting any mudmound limestone facies), whilst also exhibiting the contact with, and upper portions of, the Glencar Limestone Formation. The section begins at a large, reasonably level platform below a significant waterfall, but above a second waterfall which is heavily vegetated (Fig. 2.2.2b). The base of the log (and first sample taken) lies at GR G74919 44334 ±7m, 210m elevation (Fig. 2.2.2c). Almost continuous exposure can be followed until GR G75089 44508 ±6m, 287m elevation. A final one-off exposure of Dartry Limestone was sampled at GR G75106 44556 ±6m, 297m elevation.

Detailed logging was only possible for the lower portions of the section (Fig. 2.2.2d), above this, the quality of exposure diminishes whilst lithological lateral variability increased (Fig. 2.2.2e). Fifteen 2kg microfossil samples were taken at roughly 7m intervals from the exposed succession. A more precise record of where samples were removed can be found in Appendix D. A description of the lithologies as well as notable characteristics of the section is provided below.

2.2.2.1 The Glencar Limestone Formation

The section begins in relatively typical, but shale-rich, Glencar Limestone facies, comprising fossiliferous, calcareous, variably cleaved silty shale with thin, irregular, argillaceous, crinoidal wackestone interbeds. The fauna of the Glencar Limestone in the Glencar Section is essentially indistinguishable from that preserved in the Tievebaun Section. A large, flattened orthoconic nautiloid (Fig. 2.2.2f(i)) was the only non-typical fossil discovered.

2.2.2.2 The Dartry Limestone Formation

The contact between the Glencar Limestone and Dartry Limestone Formations is placed at 23.25m ASB, where well-developed silicified nodules and horizons become ubiquitously developed. Minor amounts of chert are found below this level, but not in significant concentrations. Limestone beds within the Dartry Limestone Formation in this section are typically quite undulatory and hummocky, particularly where silicified nodules are large and well-developed, causing bedding "blisters" (Fig. 2.2.2f (ii & vii)).

Limestones units in this formation are typically medium or thickly bedded and separated by thin muddy horizons. Fossils are generally silicified and weather proud; however, fenestrate bryozoans almost invariably weather preferentially to form "trains" of solution holes marking out the frond structure. Although large portions of the sequence are texturally mudstones, wackestone horizons, with brachiopods, crinoid plates as well as bryozoans and corals, are locally significant. Many of the brachiopods are articulated and crinoid stems appear to be of a single variety, and bear insignificant concentrations of cirri. Certain stratigraphic levels within this formation are particularly rich in pluricolumnals, with many attaining lengths of over 20cm (Fig. 2.2.2f(iv)). One (slightly disturbed) specimen measured 45.5cm in length. Orientation analysis of the crinoid stems was carried out on several horizons (Fig. 2.2.2g), indicating that currents were approximately north-south orientated (see Section 2.4). Crinoid stems and (rarely) partial crowns are best preserved where a thicker mud drape separates two limestone beds. On these surfaces delicate brachiopods (Fig. 2.2.2f(v)), fenestrate bryozoan sheets, *Cladochonus* colonies (Fig. 2.2.2f(vii)), fine bioturbation (Fig. 2.2.2f(vi)) and rare solitary zaphrentid corals are often preserved.

Towards the top of the section, the amount of chert decreases and the limestones become more argillaceous. *Monoschizoblastus* blastoid crowns become a conspicuous constituent of the fauna towards the top of the section, although the fossil content in general appears reduced, possibly related to a decrease or lack of silicification.

Continuous exposure of the section ends at a small step, downstream of a bend at GR G75089 44508 ±6m, 287m elevation. The stream continues uphill from here, however only a single outcrop at GR G75106 44556 ±6m, 297m elevation, is exposed on the west side of the channel (Fig. 2.2.2c & h).

2.2.3 Glenade Section (Leckanarainey stream, DA02, DAGN)

A near complete sequence of non-reef Dartry Limestone is found in a deeply cut stream section in the townland of Leckanarainey, east of Glenade Lough. Although the basal contact with the Glencar Limestone Formation is not exposed, the upper contact with the Meenymore Formation can be constrained to a gap in exposure which represents ~12m of stratigraphy. The section is mostly cliffy and bound by steep gulley walls and, therefore, is only workable at very low river flows. Where the section levels out, for short intervals between waterfalls, the overall valley is deep and heavily overgrown, making accurate geographic positioning challenging.

Due to the difficulties associated with accessing the lower portions of this section, and the considerable stratigraphic overlap with the Glencar Section, only the upper levels of the Glenade Section, near the contact with the Meenymore Formation, were examined.

2.2.3.1 The Dartry Limestone Formation

The stratigraphically lowest sample was taken from the southeastern bank at GR G85010 45897, 217m elevation, where the stream opens up between two narrow gorges (Fig. 2.2.3a). The ravine downstream of the sample site is ~10m deep and virtually unworkable. The outcrop at GR G85010 45897 consists of relatively horizontal, laterally persistent, thickly bedded, light to medium grey cherty limestone. Flattened nodules and impersistent beds of chert become progressively less common stratigraphically upwards. Microfossil sample DAGN2 was taken from a prominent step formed by an echinoderm rich, calcarenite wackestone bed, ~50cm below the top of the exposure (Fig. 2.2.3b). Upstream, the river has cut a ~4m deep gorge exposing cherty, medium bedded, pale grey wackestones, dominated by brachiopods, corals (Fig. 2.2.3c(ii)) and crinoids.

Outcrop continues upstream (with only minor breaks) to GR G84994 46045, 230m elevation, where the highest exposure of the Dartry Limestone was sampled (DAGN1). The sampled unit, a medium-dark grey calcarenite wackestone, constitutes an extensive ~30m long bedding plane (Fig. 2.2.3d). This bedding

surface displays an abundance of silicified macrofauna which weather proud. Dendroid, fasiculate colonial corals are very common but large productid brachiopods (hinges >10cm long), zaphrentid and cylindrical solitary corals, crinoid pluricolumnals and ossicles are also well preserved. In cross-section it is obvious that some of the large coral colonies are in life position (Fig. 2.2.3c(i)); however, several of the smaller colonies appear disturbed (Fig. 2.2.3c(iii)) and overturned (Fig. 2.2.3c (iv-v)).

2.2.3.2 The Meenymore Formation

Upstream of DAGN1 bedrock is completely obscured by cobbles and boulders until an isolated (~90cm high and ~6m long) bank exposure of shale and carbonate, attributed to the Meenymore Formation, is encountered at GR G84952 46233, 242m elevation (Fig. 2.2.3a & e). The lower 40cm of the exposure is composed of blue-grey, poorly cleaved, calcareous mudstone. The upper 50cm comprises a couplet (upper unit is thicker) of deeply weathering, weakly lineated, argillaceous dolomite beds separated by silty shale. The highest strata in the outcrop contain crinoid ossicles.

2.3 LEITRIM GROUP SECTIONS IN NW IRELAND

The lower (shale-dominated) units within the Leitrim Group (Meenymore, Bellavally, Carraun Shale and Dergvone Shale Formations) tend to be poorly exposed and restricted to deep stream-cut sections in the Lough Allen Basin. Three sections were visited in order to establish which would be most appropriate for a full investigation of the lithology and stratigraphy of the Leitrim Group in NW Ireland (Fig. 2.3). Ultimately the Aghagrania and Carraun/Lugasnaghta (Lugasnaghta Section of Brandon & Hodson, 1984) Sections were chosen as being the most representative of the stratigraphic interval concerned and they are discussed in Sections 2.3.1 and 2.3.2 below.

2.3.1 Aghagrania Section (AGHA)

This section is located in the Aghagrania River, which flows off the slopes of Slieve Anierin towards the town of Drumshanbo, Co. Leitrim (Fig. 2.3.1a). Approximately 2.5km east-northeast of Drumshanbo, towards the small village of Aghacashel, the road bends and passes over the Aghagrania River Section. The outcrop north of the bridge is easily accessed from the bridge, while the section downstream is best accessed from the farmhouse adjacent to the river (Fig. 2.3.1b).

This section exposes the complete stratigraphic sequence (with only small gaps) from the upper Dartry Limestone Formation to the base of the Carraun Shale Formation and represents the most complete exposure of both the Meenymore and Bellavally Formations. A non-typical, severely thinned representative of the Glenade Sandstone Formation separates the Meenymore and Bellavally Formations. The Dartry-Meenymore and Bellavally-Carraun formational contacts are exposed in this section whilst those of the Glenade Sandstone Formation are only well constrained.

The quality of the current level of exposure in this stream section was thought inadequate to improve upon the earlier logging of West *et al.* (1968) and Smith (1980). Instead, the section was mapped in detail at a scale of 1:2000 (Fig. 2.3.1b-c). Minor amendments to the stratigraphy of the section are shown in Fig. 2.3.1d

and a single detailed log across the Dartry-Meenymore contact was completed at a scale of 1:20 (Fig. 2.3.1e).

In total, 17 microfossil samples were taken from the Aghagrania Section (Fig. 2.3.1c-d), comprising; two from the Dartry Limestone Formation, nine from the Meenymore Formation, five from the Bellavally Formation and one from the Carraun Shale Formation. An account of the section is given below, whilst the exact location of microfossil samples is provided in Appendix D.

2.3.1.1 Dartry Limestone Formation

Continuous mapping of the section began ~300m south of the bridge at GR: G99593 11970 (where bedrock of cherty limestone becomes distinct). The watercourse downstream of this point is littered with boulders and cobbles of cherty limestone, characteristic of the Dartry Limestone Formation. The chert in these rocks tends to be a milky grey colour and is consistently paler than that described previously in Sections 2.2.1-3. The degree of silicification varies significantly (from essentially nothing, to almost 80% of the rock) over short lateral and vertical distances. The development of chert often appears random, and fails to demonstrate the bedding as clearly as the chert horizons found in the Dartry Mountain sections.

The first (definite) outcrop consists of massive, cherty calcarenite/siltite wackestone (microfossil sample AGHA.CAV1). The Dartry Limestone Formation is then exposed for ~45m upstream to a ~2m high waterfall at GR G99612 11987 (Figs. 2.3.1e-f) where its contact with the overlying Meenymore Formation is exposed. The lower 5.25m of stratigraphy (dominantly tabular, crinoidal wackestones) in the short waterfall section are attributed to the Dartry Limestone Formation. A crinoidal packstone bed (AGHA.A2) ~4m below the top of the formation was sampled for microfossils.

2.3.1.2 Meenymore Formation

(a) Drumcroman Member

The Meenymore Formation (and Drumcroman Member) begins at the base of bed AGHA.A7, a 7cm thick laminite (first in the sequence). The stratigraphically highest unit in the logged outcrop (microfossil sample and bed AGHA.A11), ~1.5m stratigraphically above the members base, is a calcilutite/siltite mudstone with irregular chert occurrences at intermittent intervals. The top surface of the unit comprises a subrounded to subangular calcilutite pebble-conglomerate (Fig. 2.3.1g(i)). The clasts attain a maximum size of 6cm.

Patchy exposure of dolomitised and cherty carbonates continues upstream. At GR G99635 12006 a distinctive 25cm thick carbonate horizon can be traced (striking ~090º) across the stream bed. A distinctive thin, deeply weathered, argillaceous, fine calcarenite wackestone layer defines the top of the bed, appearing to fill an irregular (possibly scoured) surface. Microfossil sample AGHA1 was removed from the top ~5cm of this bed (~4m stratigraphically above the member's base). The coarser upper portion of the bed contains calcilutite clasts and common fossils, including crinoid pluricolumnals, echinoderm plates and coiled cephalopods. Thick (~1cm), simple, roughly vertical (~4-5cm long) burrows are found just below, and are infilled by, the overlying fossiliferous sediment (Fig. 2.3.1g(ii)). The thicker lower unit of the bed is heavily bioturbated, but is dominated by thinner (mostly ~1mm wide, some up to 4mm wide), more uniform and persistent (at least 12cm long), sub-horizontal and sub-vertical burrows (Fig. 2.3.1g(ii)). Bioturbation becomes less intense towards the bottom of the bed.

Impersistent exposures of argillaceous (occasionally cherty) limestones and dolomites as well as laminites, calcareous mudstones, siltstones, shale and also a single horizon of limeclast breccio-conglomerate are encountered upstream to GR G99668 12042. At this point (~8m stratigraphically above the members base) a 32-37cm thick, undulating/hummocky, cherty, calcilutite mudstone was sampled (AGHA2) from the core of a small anticline on the east bank. A ~1m high waterfall consisting predominantly of laminated and massive mudstones is exposed a few metres upstream. Small, sub-cm, crystalline filled cracks, interpreted as possible

syneresis structures, are found on a bedding plane at the top of the small waterfall (Fig. 2.3.1g(iii)). Exposure deteriorates rapidly upstream from the waterfall and only isolated outcrops of laminated dolomites and limestones are visible near the stream banks. At GR G99691 12060 a small, weathered outcrop exposes a limeclast conglomerate bed in the core of a small anticline.

Upstream, at GR G99695 12064, a prominent, thick (at least 1m) limestone unit is exposed on the northwest bank which, further upstream, forms a spine of rock along the riverbed for ~65m. The unit generally consists of medium grey calcisiltite mudstones, with only minor amounts of fine echinoderm fragments. Roughly one-third of the way upstream from where this unit is first encountered, the lateral equivalent of the lower to middle levels of the unit becomes a clast-supported breccio-conglomerate. The generally angular (occasionally sub-rounded) clasts range from a few mm, to >10cm, in size and are apparently randomly orientated, but generally fitted. The unit becomes more fully brecciated further upstream; the lateral transition from competent beds to breccia is shown in Fig. 2.3.1h. In parts isolated pockets of breccia are developed within otherwise competent beds (Fig. 2.3.1i). At GR G99747 12074, a matrix-supported floatbreccia is partially exposed, underlying the clast-supported breccia described above. The clasts within this chaotic floatbreccia are similar to the limestone of the overlying unit. Microfossil samples AGHA3.1 and 3.2 were extracted from the limestone bed overlying the first downstream appearance of breccia. This limestone unit represents the top of the (~14m thick) Drumcroman Member of the Meenymore Formation (Fig. 2.3.1d).

(b) Dorrusawillin Member

Overlying the distinctive carbonate unit (described above) is a ~1.5-2m thick series of fossiliferous, silty, calcareous mudstones and shales. Impersistent, thin beds of argillaceous, calcilutite mudstone and nodular wackestones and mudstones are also developed within this unit. Nodular horizons are sometimes associated with solitary horn corals and orthoconic nautiloids.

(c) Corloughlin Member

This member directly overlies the Dorrusawillin Member and the contact between the two is exposed at GR G99768 12085. The lower portions of the Corloughlin Member are completely exposed and comprise unfossiliferous, shaly, calcareous mudstone with units of siltstone and thin, argillaceous, pyritic mudstone. At GR G99768 12098 a small step in the streambed exposes three thin (2-5cm) carbonate beds. The lowest is a dark laminated mudstone whilst the upper is a foetid, argillaceous limestone. The middle bed is 4.5cm thick and was sampled as AGHA4 (~4m stratigraphically above the member's base). The sampled bed has a calcarenite wackestone centre enclosed by dark grey calcisiltite mudstone. Approximately 0.5m stratigraphically higher than AGHA4, a 9cm thick macrocell (sensu West, 1965) bed is exposed (Fig. 2.3.1g(iv)). This unit consists of a basal undulating shale horizon (<1cm thick) with a very irregular contact with an overlying "mush" of 1-2mm sized, crystalline structures dispersed throughout a medium to light grey calcareous mud/silt matrix.

At GR G99780 12109 a series of calcarenite and calcisiltite beds are exposed. Overlying these, the sequence becomes dominated by light grey shaly, calcareous mudstone and thin, 1-6cm thick, intercalations of laminated and massive siltstones. Microfossil sample AGHA5 was taken from a mudstone with poorly developed laminations at GR G99788 12130, ~12m stratigraphically above the member's base.

An individual horizon exhibiting desiccation structures was identified within a series of thin laminites, calcilutite mudstones and medium-grey, shaly, calcareous mudstones at GR G99795 12145, ~19m stratigraphically above the members base (Fig. 2.3.1g(v)). Microfossil sample AGHA6 was taken from an 8cm thick, calcilutite mudstone bed located 18cm stratigraphically above the desiccated horizon. Brittle, synsedimentary reorganisation of the sediment is identified by localised lamination disturbance within beds. Exposure degrades and becomes restricted to the banks further upstream. A single, almost completely submerged outcrop at GR G99803 12168 marks the highest (exposed) stratigraphical unit in this member (and the Meenymore Formation, Fig. 2.3.1d). Microfossil sample AGHA7 was taken from the upper calcisiltite mudstone bed exposed here, ~23m

stratigraphically above the members base (the member is extrapolated to be ~27m thick in total).

2.3.1.3 Glenade Sandstone Formation

The lowest exposure of this formation consists of a >1m thick, weakly calcareous, medium-grained sandstone which outcrops at GR G99807 12182, directly beneath Aghagrania Bridge (Fig. 2.3.1b). Large, steeply inclined cross-laminations are evident in the bed. A small outcrop comprising 17cm (minimum) of micaceous, non-calcareous, dark green, fine-grained sandstone represents the stratigraphically highest (and only other) exposure of the formation ~12m upstream from the bridge. The formation is estimated to be slightly less than 4m in total thickness.

2.3.1.4 Bellavally Formation

(a) Sraduffy Member

At GR G99810 12201, ~18.5m upstream from Aghagrania Bridge, the first outcrop of this particular member (and formation) is exposed, although it is submerged. The sequence exposed here comprises shale and calcareous siltstones with subordinate calcilutite mudstone. At GR G99806 12209, ~4m stratigraphically above the members (and formations) base, a prominent 53cm thick calcilutite mudstone was sampled for microfossils (AGHA8). A thin (5cm) horizon within the sampled bed exhibits cross laminations, which indicate a palaeotransport direction towards the ESE (114.5º). The remainder of this member consists of calcareous mudstones and siltstones with subordinate calci- and dololutite mudstones, as well as rare laminated mudstones. The upper levels of the member are poorly exposed and its upper contact is constrained by the first exposure of the overlying Lugasnaghta Shale (see below). Many of the submerged bedding surfaces of this member display excellent examples of desiccation cracks (Fig. 2.3.1g(vi & vii)). This member is estimated to be ~11m thick in total.

(b) Lugasnaghta Shale Member

The lowest exposed bed (a 30-33cm thick, bioturbated, fossiliferous calcisiltite wackestone) of this member occurs at GR G99794 12234, and the top 15cm of this

unit was sampled for microfossils (AGHA9). Burrows within this bed attain a maximum width of ~1cm and are generally sub-horizontal to sub-vertical in orientation. Fossils include goniatites, brachiopods, orthocones, spine fragments and echinoderm plates. Exposure, although often poor, is virtually continuous for the next ~90m upstream towards the Aghagrania Weir (Fig. 2.3.1b). The Lugasnaghta Shale Member is almost continuously exposed for 22m upstream to GR G99792 12254. This member dominantly comprises pale to dark grey calcareous siltstone, fossiliferous (small colonial corals, orthocones brachiopods and crinoids) silty shale and argillaceous limestones. The Lugasnaghta Shale Member is thought to be ~7m thick.

(c) Drummangarvagh Member

The boundary of the Drummangarvagh Member with the underlying Lugasnaghta Shale Member was stratigraphically lowered during this work by ~78cm to include poorly-laminated mudstones. The Drummangarvagh Member is considered herein to be ~85cm thick, in contrast to the ~18cm originally estimated by Smith (1980) and it is exposed in the stream at GR G99786 12256 (Fig. 2.3.1c). It consists of unfossiliferous shale, poorly-calcareous mudstone as well as laminated mudstones. Many of these laminations are contorted or show evidence of brittle deformation.

(d) Doobally Sandstone Member

The Doobally Sandstone Member directly overlies the Drummangarvagh Member and is ~2m thick. Exposed portions of this member are composed of thin and (rarely) medium-bedded, micaceous, fine-grained, weakly calcareous, sandstones and siltstones. The beds occasionally display small-scale cross-lamination.

(e) Sheena Shale Member

At GR G99782 12265 a 5cm thick, calcilutite mudstone (overlying micaceous, shaly siltstone at the top of the Doobally Sandstone Member) marks the base of the Sheena Shale Member. Microfossil sample AGHA10 was taken from a 15cm thick, bioturbated, calcilutite/siltite wackestone, 0.5m stratigraphically above the base of the member. Goniatites, orthocones, crinoid ossicles and brachiopod valves were identified in the sampled unit. Calcareous, fossiliferous shales with thin to medium-

bedded (occasionally fossiliferous) calcilutites comprise the remainder of the Sheena Shale Member, which totals ~5m in stratigraphical thickness.

(f) Corry Member

The basal bed of this member is a 16cm thick, rubbly macrocell horizon encountered at GR G99776 12279. The shaly laminites overlying this unit display good examples of synsedimentary deformation (Fig. 2.3.1j). A second, 20cm-thick macrocell horizon is exposed at GR G99772 12289 and is composed of a recessed lower 5cm thick laminite which gives way to a central dispersed crystalline horizon which is, in turn, overlain by an upper, 5-7cm thick laminite punctuated by isolated macrocells. The succession continues upstream through calcareous shale and hard calcilutite mudstones and in parts displays notable synsedimentary, brittle deformation structures (Fig. 2.3.1k).

A relatively fossiliferous, calcareous mudstone was sampled for microfossils (AGHA11) at GR G99766 12304, 1m stratigraphically below the top of the member (and formation). Microfossil sample AGHA12 meanwhile was taken from an 8-9cm thick, hard, calcilutite/siltite mudstone, 40cm stratigraphically below the top of the this member. An 18cm thick poorly laminated mudstone, at GR G99764 12308, represents the highest unit of the Corry Member in this section and is directly overlain by fossiliferous beds attributed to the Derreens Limestone Member of the younger Carraun Shale Formation (Fig. 2.3.1l). The Corry Member is calculated to be ~8m in stratigraphic thickness.

2.3.1.5 Carraun Shale Formation

(a) Derreens Limestone Member

The basal unit of this member (and formation) consists of a 16cm thick, argillaceous, conglomeratic wackestone, dominated by orthocones, goniatites, crinoid ossicles, brachiopods and fenestrate bryozoans and was sampled as AGHA13. Limestone clasts are particularly common in basal portions of the bed. Continuous exposure in the streambed ends at this point, ~4m downstream of the weir; however, a side channel eroded into the eastern bank exposes fossiliferous limestones belonging to this member. Mapping of the Aghagrania Section ended at

the weir, ~150m north of the bridge at GR G99761 12316 (Figs. 2.3.1b-c & l), exposures upstream of this point are infrequent but consist of siltstones, shales and carbonates of the Carraun Shale Formation.

2.3.2 Carraun/Lugasnaghta Section (CNLG)

This section is located between the townlands of Carraun and Lugasnaghta in a small tributary of the Sraduffy River which flows northeast from Dough Mountain, Co. Leitrim (Fig. 2.3.2a). It is the type section for the Carraun Shale Formation but also exposes the majority of the underlying Bellavally Formation and a significant portion of the overlying Dergvone Shale Formation. It was first examined by Brandon (1968), who established the general succession and geology of the stream.

Due to gaps in exposure and the presence of numerous small folds it was not feasible to re-log the entire sequence. Continuous mapping at a scale of 1:2000 was undertaken in the stream from the lowest point on Brandon's (1968) log, at G95578 43058, for ~1km to G94886 42510 (Figs. 2.3.2b-c). Exposures are very isolated upstream from the latter GR, allowing only spot sampling. The stratigraphy of the entire section is shown in Fig. 2.3.2d. Four logs at well-exposed or particularly important stratigraphic intervals were completed at a scale of 1:20 (Figs. 2.3.2e-h).

A total of 22 microfossil samples were taken from the Carraun/Lugasnaghta Section (Figs. 2.3.2c-d). Nineteen were taken from carbonate beds while a further three were collected from fossil-rich shale horizons in the Bellavally and Carraun Shale Formations. Seven samples were extracted from the Bellavally Formation, 12 were taken from the Carraun Shale Formation and three were obtained from the Dergvone Shale Formation. An account of the section is provided below, whilst figures and tables indicating the exact location of microfossil samples taken can be found in Appendix D.

2.3.2.1 Bellavally Formation

(a) Sraduffy Member

The lowest observed exposure, comprising alternations of thin to medium bedded laminites and shale within thicker calcareous shale units, is located directly beneath the bridge at GR G95628 43091. Isolated outcrops of shale, siltstone, poorly-calcareous mudstone and rare mudstone beds are apparent in the steep banks further upstream.

The Carraun/Lugasnaghta Section, as recognised originally by Brandon (1968) begins at GR G95578 43058 (Fig. 2.3.2i). The first 2.25m of stratigraphy exposes the contact between the Sraduffy and Lugasnaghta Shale Members (Fig. 2.3.2e). Only the top 15cm the lowest bed examined - a limeclast breccia, CNLG.A.1, is exposed. The clasts are sub-rounded to sub-angular and reach up to 2cm in length. The matrix is an argillaceous, calcisiltite mudstone. Microfossil sample CNLG1 was taken from a wackestone horizon (CNLG.A.3), ~1.4m stratigraphically below the top of the member (Fig. 2.3.2e). Fossils are common throughout the sampled bed and include ramose bryozoans, small brachiopods, crinoid ossicles, goniatites and solitary corals. A distinctive macrocell horizon (CNLG.A.5) is located ~0.5m stratigraphically above the sampled bed and can be subdivided into three fairly distinct units:

(1) The lowest level is generally 5cm thick, relatively laterally consistent, but with an undulatory upper surface. Laminations become more prevalent upwards.

(2) The central unit (9-15cm thick) is separated from the underlying horizon by a muddy lamination (several mm thick) and, in parts, a thin vuggy-weathering macrocell horizon. The main macrocell interval consists of ~0.7cm wide, white, irregular crystalline bodies in a mottled medium to pale grey carbonate matrix.

(3) The upper level (5-8cm thick) is similar in appearance to unit (1). It is separated from the macrocell interval by a weakly laminated portion and an isolated, thin, poorly-developed macrocell horizon. Possible thin micrite rafts are apparent in the top few cm of the bed.

Units (1) and (2) were sampled as a composite unit (CNLG2), whilst the upper unit was sampled separately (CNLG3) for microfossils (Fig. 2.3.2i). A further 62cm of stratigraphy belonging to the Sraduffy Member is exposed in this outcrop and comprises thin calcilutite mudstones and calcareous mudstone.

(b) Lugasnaghta Shale Member

At the location described above, the Sraduffy Member is overlain by fossiliferous, occasionally nodular or silty shale attributed to the Lugasnaghta Shale Member.

Microfossil sample D.K. CNLG.A was extracted from a marine band exposed on the northwest stream bank, 0.5m stratigraphically above the base of the Lugasnaghta Shale Member. Goniatites, orthocones, corals and gastropods are commonly found at this level, and many appear coated and/or partially crushed.

This member is exposed upstream to GR G95541 43032 as a series of medium grey, shaly, calcareous mudstones with common carbonate nodule horizons. Many of the nodules have a distinctive honeycomb texture (Fig. 2.3.2k(ii)) which Brandon (1968) erroneously identified as the coral "*Michelinia* sp." This member is believed to be ~5.5m thick in total.

(c) Drummangarvagh Member

A small, poorly-exposed outcrop of interbedded laminites and shale, ~110m upstream from the bridge, represents the lowest exposed beds of the Drummangarvagh Member. More complete exposure of the upper levels of this member is found at GR G95538 43020, where the contact with the overlying Doobally Sandstone Member is exposed, as well as its contact with the succeeding Glenkeel Member (Fig. 2.3.2f). Towards the top of the Drummangarvagh Member, the sequence becomes more carbonate dominated. Microfossil sample CNLG4 was taken from relatively poorly laminated carbonates which lie 18.5-30.5cm stratigraphically below the contact with the overlying Doobally Sandstone Member. The Drummangarvagh Member is estimated to be ~1.5m thick.

(d) Doobally Sandstone Member

This member consists of unfossiliferous, calcareous siltstone with medium to thickly-bedded, medium and fine-grained sandstone beds with horizons of conspicuous desiccation cracks. The sandstone beds of this member are gently folded and repeated in the stream bed. Higher up the eastern bank are exposures displaying more extensive folding, as well as minor faulting (Fig. 2.3.2k(i)). The Doobally Sandstone Member is exactly 142cm thick (Fig. 2.3.2f).

(e) Glenkeel Member

The highest bed of the Doobally Sandstone Member (CNLG.B.6 - Fig. 2.3.2f) is eventually overlain by pale grey shaly siltstones and poorly-calcareous mudstones

of the Glenkeel Member (Fig. 2.3.2f) at GR G95519 42996. The Glenkeel Member outcrops for a further ~20m upstream and is ~3m thick in total. The lower portions of this member are dominated by pale grey micaceous shales and shaly siltstones, whilst the upper portions comprise alternations of thinly bedded laminites and silty shales.

(f) Sheena Shale Member

The first bed of this member is a fossiliferous marine limestone, which is encountered at GR G95501 42985. Slightly silty, medium to dark blue-grey shale overlies the basal limestone and rich fossil concentrations are observed ~30cm stratigraphically above the base of the shale. Microfossil sample D.K. SHEENA was removed from the faunal band ~75cm stratigraphically above the basal limestone bed. The Sheena Shale Member is believed to measure ~3m in total thickness.

(g) Corry Member

This member is initially exposed at GR G95493 42977, with the strata over the next 20m (upstream), though clearly folded and faulted, exposing it and its contact with the Derreens Limestone Member of the overlying Carraun Shale Formation (Fig. 2.3.2g). The lowest 12cm of the Corry Member (microfossil sample CNLG5 - Fig. 2.3.2j) is a poorly laminated dolosiltite mudstone with minor macrocell development. The succeeding 38cm of the member consists of thinly-bedded laminites. The Corry Member is at least ~50cm thick as its upper contact with the overlying stratigraphical unit is faulted.

2.3.2.2 Carraun Shale Formation

(a) Derreens Limestone Member and directly overlying strata

The Derreens Limestone Member comprises a basal (minimum) 30cm of unfossiliferous, silty shale underlying three argillaceous limestones which have gradational contacts with intervening units of calcareous shale. The third limestone, a 20cm thick, argillaceous, calcilutite mudstone with wackestone intervals, probably represents the Derrybofin Bed and was sampled for microfossils

(CNLG6). Goniatites, orthoconic nautiloids, crinoid ossicles, brachiopods and echinoderm plates are all identifiable in and above the Derrybofin Bed.

The sequence above the Derreens Limestone Member consists predominantly of shale with isolated (occasionally fossiliferous) limestones. Microfossil sample CNLG7 was taken from a ~15cm thick, poorly fossiliferous calcilutite mudstone, ~4m stratigraphically above the base of the formation at GR G95468 42959. Microfossil sample D.K. ABV. DERREENS was recovered slightly higher in the section, from a ~14m long bank exposure of fossiliferous, slightly silty, calcareous shale, ~6m stratigraphically above the base of the formation at GR G95440 42937.

A calcilutite mudstone with a hummocky and uneven surface was sampled (CNLG8) at GR G95421 42923 (~9m stratigraphically above the base of the formation). Relatively continuous exposure of grey calcareous mudstone, shale and siltstone with thin limestone interbeds outcrops for the next >120m upstream. Limestone beds are rare, argillaceous and tend to be laterally irregular. Orthocones and goniatites are found associated with some carbonate horizons as well as in more concentrated marine bands. Microfossil sample CNLG9 was taken from the top 15cm of a fossiliferous, 23-27cm thick, calcisiltite mudstone exposed in the southeast bank of the stream at GR G95289 42864 (~20m stratigraphically above the base of the formation). The sampled bed is a dark grey colour with orthocones (>3cm) and brachiopod shells orientated parallel to bedding. Stratigraphically higher in the section, microfossil sample CNLG10 was taken from the top 15cm of a 40cm thick, roughly tabular, medium grey, calcisiltite mudstone (CNLG.D.3 - Fig. 2.3.2h), developed ~1m below the base of the overlying Tawnyunshinagh Member at GR G95271 42856.

(b) Tawnyunshinagh Member and succeeding strata

The basal bed (CNLG.D.7 - Fig. 2.3.2h) of the Tawnyunshinagh Limestone Member is a laterally variable, 35-62cm thick stromatolitic carbonate with possible algal or beekite structures (see Section 2.4) and is exposed in a ~4m tall waterfall at GR G95262 42852. A concentrated, 2cm thick band of small, ~0.5cm wide, often articulated, partially pyritised shelly fossils occurs approximately 2cm up from the base of the bed, but is only obvious on fresh faces. Microfossil sample CNLG11

was taken from the bottom 6cm of this bed. Laminations weather proud and are planar across most of the outcrop, except where the bed changes thickness dramatically and laminations are folded and broken as a consequence. Thin, tightly-spaced laminations tend to be a dark grey colour, whilst thicker, more dispersed and laterally impersistent bands are a deep red/brown colour and have a botryoidal texture.

A second distinctive stromatolitic carbonate (CNLG.D.11) occurs above CNLG.D.7 after an intervening ~117cm of shale with irregular, massive and laminated mudstone beds and nodules. CNLG.D.11 varies from 37-54cm in thickness. The bed is laminated except for the top ~10cm which is more massive and contains broken, impersistent bands (~1cm thick) of possible beekite or algal structures which weather proud and exhibit generally smooth or gently wrinkled upper surfaces and bulbous, bubbly lower surfaces (Figs. 2.3.2k(iii) & 2.3.2l). No single band is traceable unbroken for >30cm, but many horizons are laterally consistent. The top surface of the member is brecciated, with clasts dominantly consisting of reworked structures similar to those described above. Limestone clasts are also evident on the upper surface.

Microfossil sample CNLG12 was taken from a ~25cm thick calcilutite mudstone bed which succeeds the Tawnyunshinagh Limestone Member via a thin shale parting. A sequence of occasionally fossiliferous, finely-cleaved, calcareous shales with medium interbeds of argillaceous mudstone, outcrops further upstream. *Posidonia* (Fig. 2.3.2k(iv)), orthocones and (occasionally pyritised) goniatites can be found in certain shale horizons.

(c) Ardvarney Limestone Member and succeeding strata

The Ardvarney Limestone Member outcrops at GR G95209 42818, ~39m stratigraphically above the base of the formation. The top 15cm of the ~34cm thick, gently undulatory calcisiltite mudstone was sampled for microfossils (CNLG13). Numerous orthocones, goniatites and other shelly fossils appear restricted to the surface of the sampled bed.

The Ardvarney Limestone Member is directly overlain by moderately calcareous, fossiliferous (goniatites and *Dunbarella*-like bivalves) shales. Large bullions found in the stream bed occasionally display (possible) exceptionally large, partially crushed orthocone tests (Fig. 2.3.2k(v)). A horizon of calcareous bullions is exposed in the streambed ~4.5m stratigraphically below the overlying Sranagross Dolomite Member at GR G95175 42785 (Fig. 2.3.2c). The bullions (sampled as CNLG14) reach up to 40cm in length, ~17cm in thickness and are generally a flattened spheroidal shape. Fragments of orthocones (up to 6cm long) as well as goniatites and other shelly material were observed within the bullions.

(d) Sranagross Dolomite Member and succeeding strata

A small step in the stream exposes the Sranagross Dolomite Member at GR G95163 42774, ~45m stratigraphically above the formations base. The 31-33cm thick dolo/calcisiltite mudstone member is weakly lineated, roughly tabular and contains a sparse shelly fauna at certain levels. Microfossil sample CNLG15 was taken from the top ~15cm of the bed. Poorly cleaved, calcareous mudstone and shale dominate the continuous exposure above this member. Fissile intervals and more fossiliferous horizons, exposing crushed and flattened goniatites, orthocones as well as imprints of *Posidonia*, are also exposed.

(e) Camderry dolomite Member and succeeding strata

The Camderry Dolomite Member is exposed at the top of a ~4m high waterfall at GR G95137 42737 ~50m stratigraphically above the formations base and is composed of a 27cm thick, fossiliferous calcilutite mudstone bullion. The bullion horizon, which passes laterally (upstream) to a heavily veined dolomite bed, was sampled for microfossils (CNLG16).

The upper portions of the Carraun Shale Formation are composed of predominantly poorly cleaved, moderately calcareous shale with a sparse fauna and small isolated bullions. The Carraun Shale Formation is estimated to be ~56m thick in total.

2.3.2.3 Dergvone Shale Formation

(a) Gubaveeny Shale Member

The basal contact of this member (and formation) was taken at GR G95105 42710 where the shale becomes darker, more competent and seemingly devoid of fossils. A fossiliferous, 5cm thick, relatively calcareous mudstone horizon was sampled for microfossils (CNLG17) from the top of the waterfall near to the base of this member. The sampled horizon contains flattened shelly fragments in addition to possible plant fragments that measure 0.5-2cm long. This member is believed to equal ~6.5m in total thickness.

(b) Loughaphonta Sandstone Member

The Loughaphonta Sandstone Member (elsewhere recognised only as a Bed within the Black Mountain Shale Member) is exposed in a ~5m high waterfall, ~6.5m stratigraphically above the transitional Carraun Shale-Dergvone Shale contact at GR G95100 42708. This member is composed of two distinct sandstone beds separated by 60-65cm of fissile, dark grey shale. The lower, slightly flaggy, sandstone varies from 40-51cm in thickness over 4m of outcrop and appears to have an erosive contact with the underlying Gubaveeny Shale Member. The bed is a pale grey, fine to medium grained, non-calcareous sandstone with common (abundant near the base) rip-up, dark grey shale flakes which are generally ≤ 0.5cm in length and ≤ 1mm in thickness. Muscovite is common on bedding surfaces with individual flakes measuring up to 3mm x 2mm. The upper sandstone is similar in appearance to the lower but it contains only rare shale clasts and it becomes more massive in appearance upwards. This member is estimated to be ~6m thick in total.

(c) Black Mountain Shale Member

Silty shale assigned to this member is first exposed ~8m upstream of the Loughaphonta Sandstone Member at GR G95088 42690. Carbonised plant fragments up to 6cm in length are found in subordinate, more fissile shale horizons. Homogenous, unfossiliferous (occasionally silty) shales of this member are exposed in a discontinuous manner for ~300m upstream to the last significant waterfall in the section at GR G94888 42510.

At GR G95038 42648, where a tributary joins the main stream, at least six thin sandstone dykes are exposed cutting irregularly through the shale. The dykes are composed of non-calcareous, medium-grained, micaceous sandstone and are occasionally weakly banded or have pyrite accumulations along the margins. Small shale clasts appear to have become incorporated into the outer margins of one of the structures. The dykes range from 1-40cm in thickness (average ~12cm) and occur in various sub-horizontal to vertical orientations. They rapidly change direction and split in parts, although the persistence of dyke branches is difficult to trace (Fig. 2.3.2k(vi)). The thickest unit is in a near horizontal orientation and possibly represents an original, highly disturbed bed and thus local source of sand for the dykes.

Sandstone dykes were also identified at several other localities upstream (Fig. 2.3.2c):

(1) At GR G94988 42583, two (approximately parallel) sandstone dykes cut sub-vertically through blue-grey shales on the southeast bank. The more northerly dyke is poorly preserved but appears to be ~1m thick while the second is ~54cm thick.

(2) At GR G94924 42548, at least two thin sandstone dykes are exposed in the tall, scree covered, northwest bank.

(3) A single, sandstone dyke is exposed in the southeast bank at GR G94910 42528. The dyke measures 12cm in thickness at the bottom of the bank exposure and pinches out entirely at the top.

A single, prominent 16-19cm thick, non-calcareous, fine-grained sandstone bed is exposed ~2.3m stratigraphically below the Black Mountain Shale Members contact with the overlying Tullyclevaun Shale. This member is thought to be ~35m thick (in total).

(d) Tullyclevaun Shale Member

A ~4.5m high waterfall (GR G94888 42510) exposes large bullions which mark the base of the Tullyclevaun Shale Member. Microfossil sample CNLG18 was taken from the horizon and although none of the bullions were fully exposed, some are estimated to reach 1m in diameter and 30-40cm in thickness. The sampled bullion is

a dark grey, argillaceous calcilutite mudstone. Small pyrite flecks and common fossil fragments are distributed throughout. The transition to the Tullyclevaun Shale Member is also exposed in pockets of outcrop at the very top of the stream cut on the northwest bank at GR G94924 42548 (sandstone dyke location (2) above). At this outcrop no bullion horizon was observed, instead the transition is marked by a change to lighter grey, calcareous, fossiliferous shale. This member is very poorly exposed above its base, but is thought to be ~11m thick.

(e) Tonlegee Shale Member

A recent detachment of soil and vegetation in the streambed (GR G94811 42469) exposed a carbonate bullion horizon which was taken as the base of the Tonlegee Shale Member, and was sampled for microfossils (CNLG19). The hard, medium to dark grey calcilutite mudstone/wackestone horizon is ~25cm thick and overlies ~90cm of shale. Goniatites, orthocones and shelly fragments are preserved in 3d.

The highest exposure in the Carraun/Lugasnaghta Section is located just over 1km upstream of the bridge at GR G94787 42469. At this location, shale is overlain by 60cm of laminated, fine-grained, micaceous, shale clast bearing flaggy sandstone. Approximately 15m upstream of this outcrop the grassy stream flattens out completely and the section ends.

2.4 INTERPRETATION AND ANALYSIS OF FIELD DATA

The significant thicknesses of shale and the detailed preservation of fossils in the Benbulben Shale and Glencar Limestone Formations indicate very low energy levels, and deposition below mean storm wave base. The occurrence of in-situ collapsed echinoid plates and spines (Fig. 2.2.1h) signify that rates of deposition were not rapid, although the presence of articulated blastoid crowns, crinoid crowns, pluricolumnals and brachiopods (Fig. 2.2.1g), occasionally with spines, also precludes prolonged exposure on the seafloor. A particularly dense pocket of articulated trilobite material (one specimen appearing complete and partially coiled - Fig. 2.2.1h), may suggest the influence of occasional obrution events. Rapid burial may also account for the sudden termination of laterally extensive but stratigraphically well-defined *Siphonodendron* colonies. Often, the development of limestone beds and large nodules appears controlled by coral colonies, forming as a result of either, the baffling of carbonate material, or the local nucleation of carbonate during diagenesis.

Thin wackestone and packstone interbeds in the Benbulben Shale and Glencar Limestone Formations contain generally aligned but disarticulated fossil material and their bases (sometimes) appear to scour weakly into the underlying shale. The thin limestone interbeds clearly represent an increase in energy levels and could be the result of storm events or minor debrite/turbidite flows. Any of these mechanisms may account for the apparently rapid burial of fossils discussed above. Since many of the thin limestone beds are characteristically discontinuous and no significant palaeoslopes were believed to have been developed at the time, a tempestite origin is more likely. Other limestones which are demonstrably laterally persistent over significant distances (Section 2.5) are less likely to have a tempestite origin. At several levels a striking regularity in the pattern of limestone bed development is identified. This patterned development suggests some regularity in depositional controls (investigated in more detail in Section 2.5).

A significant variety of crinoid pluricolumnals, and therefore probable variety of species, was recovered from the Benbulben Shale and Glencar Limestone Formations (Fig. 2.2.1g). Virtually all the specimens recovered, regardless of their form, exhibited large concentrations of cirri along their length. It is likely that the abundance of the cirri can be attributed, at least in part, to the requirement of additional support and attachment on a soft, muddy bottomed environment. Specimens where cirri are concentrated purely along one side of the stem (Fig. 2.2.1g - 12) may have lain recumbent on the sea-bed with only the crown and uppermost stem raised off the seafloor (Clarkson, 1979).

Increased ambient energy levels (in the local palaeoenvironment) are indicated in the Dartry Limestone Formation, most obviously by a notable reduction in the development of shale. Delicate fossil species, in particular bryozoans, are also reduced in numbers relative to the underlying Benbulben Shale and Glencar Limestone Formations. Where fossils are found they tend to be more robust and are dominantly strongly ridged brachiopods or more simple crinoid stems. Crinoid stem orientation analyses (Fig. 2.2.2g) all plot with mean trends of between NW-SE and NNE-SSW. A bimodal distribution of data (approximately at 90º) is commonly displayed and may represent two populations, one aligned with current-flow and the second a “rolling”-group. An important bedding plane in the Glenade Section, near the top of the Dartry Limestone Formation, indicates the occurrence of episodic and very strong water currents. Several significant (up to ~50cm) *Siphonodendron* coral colonies are observed in overturned or recumbent positions (Fig. 2.2.3c). A larger coral colony in the same bed was undisturbed. Since the colonies are all relatively intact and the remaining fossils are well preserved and of various sizes, it is likely that the fossils were not transported far and were essentially disturbed in-situ by a sudden current event of unusually high strength. Common episodes of much lower energy within the Dartry Limestone Formation are indicated by shale horizons with delicate fossils preserved intact, such as coral colonies of *Cladochonus* (Fig. 2.2.2f).

The Meenymore and Bellavally Formations contain a very similar range of lithologies representative of similarly diverse palaeoenvironments which existed close to sea-level.

(1) Marine conditions are indicated by limestones and shales containing bioturbation and a normal, diverse fauna, including corals, echinoderms, cephalopods, brachiopods and gastropods.

(2) Barren, occasionally cross-bedded sandstones and siltstones which often display desiccation horizons are indicative of sub-aerial exposure and are most likely representative of fluviatile environments.

(3) Barren or faunally restricted (gastropods, cephalopods and rare corals) calcareous mudstones and shales which are interbedded with the other lithologies, most likely represent a lagoonal facies.

(4) Evidence for shallow-marine, high-salinity deposition in both formations is common. In addition to laminites, a lack of bioturbation or any macrofossils, are structures interpreted as syneresis cracks (Fig. 2.3.1g). These characteristic trilete and diamond-shaped cracks are typical of sub-aqueous, salinity induced, water-removal from sediment (Stow, 2005). Further evidence for evaporite minerals is discussed below.

Several pieces of evidence suggest that a significant limeclast breccia discovered in the Meenymore Formation (Figs. 2.3.1h-i) was formed through solution (possibly of evaporite minerals) and collapse. West *et al.* (1968) considered a solution and collapse origin for breccias in the Aghagrania Section, but concluded that a syndepositional tectonic origin was most likely to have caused in-situ brecciation and localised syn-sedimentary folding. Tectonism whether syn- or post-depositional is discounted herein for the formation of the main, sub-Dorrusawillin breccio-conglomerate. Not only is it difficult to conceive a means by which tectonism could form discrete pockets of brecciation in a single bed, in an otherwise competent sequence (Fig. 2.3.1i), but no evidence for faulting was observed in this or bounding units (locally). The angularity and relatively fitted (crackle or mosaic structure) nature of the mono-lithological clasts implies both some degree of lithification prior to brecciation and very little transport or movement of material. Clasts appear, infact, to be lithologically identical to the laterally equivalent competent limestone bed. Although the underlying units were not identified specifically during this work, Smith (1980) records a "*cavernous residue of a gypsum deposit*". Such a horizon could be dissolved by fluids of lesser salinity, creating a void into which the overlying limestone bed would have eventually

collapsed. In Fig. 2.3.1h it is possible to make out a portion of relatively competent strata towards the bottom right of the picture which is deflected downwards as if partially collapsed. Directly underlying the possible solution/collapse breccia is a matrix-supported breccia, with clasts apparently lithologically identical to the overlying limestone, this is interpreted as the main fill of the solution void.

Further evidence for the former presence of evaporite minerals is taken from the occurrence of mm- and cm-scale faulting and folding in the Meenymore and Bellavally Formations. Tectonically induced faulting and folding is also evident in the sections, however it is possible to distinguish this from horizons which were clearly deformed during sedimentation. Sediment slumping can probably be discounted, since no preferred direction of overturned folds exist according to West *et al.* (1968). In the identified cases (e.g. Figs. 2.3.1j-k), disruption is on a relatively small-scale and is stratigraphically restricted, with enclosing units completely undeformed. Tectonic shocks during sedimentation cannot be discounted as a causative agent; however, since deformation was found to be near wholly restricted to laminite and macrocell horizons, it is suggested that the particular characteristics of these layers may be linked to the mode of deformation. It is possible for example that the folding and faulting in the laminated beds occurred due to space problems created by the in-situ growth and subsequent replacement of various evaporite minerals. The fact that the beds are laminated and thus would more clearly demonstrate small-scale disruption to bedding is not believed to explain the "apparent" lithological restriction of deformation since thin mudstone horizons are more commonly developed but are not similarly affected.

Macrocell layers have previously been interpreted as evaporitic in origin (West *et al.*, 1968). In order to test this idea, the mineralogy of the crystals, which comprised macrocell level CNLG3 (CNLG.A.05.3 – Fig. 2.3.2e) in the Bellavally Formation, was analysed. Crystalline bodies were examined under a binocular microscope and SEM and three different mineral structures were identified. The most abundant mineral is colourless, orthorhombic (Fig. 2.4a), has a hardness of ~3.5 and is compositionally celestine. This diagnosis was supported by Laser Raman spectroscopy (Fig. 2.4a). The other two minerals were confined to open cavities in the centre of the macrocells. The first mineral, identified as strontianite by Laser

Raman spectroscopy (Fig. 2.4a), is colourless to white and generally forms radiating needle like projections. The second colourless mineral (which lacks a defined crystal form) was identified as calcite by Laser Raman spectroscopy (Fig. 2.4a). Celestine may have formed as a replacement of gypsum (West *et al.*, 1968), or by primary precipitation associated with high evaporation rates (Deer *et al.*, 1992). Calcite and strontianite, meanwhile, are common later alteration products of celestine (Deer *et al.*, 1992). Therefore it is very likely that macrocell horizons represent primary sites of evaporite mineral deposition.

The Carraun Shale Formation begins with the Derreens Limestone Member, a sequence of calcareous shale and limestones with a normal marine fauna. Overlying shales (in general) become less calcareous and more organic-rich up through the formation (only after the Tawnyunshinagh Limestone Member) and into the overlying Dergvone Shale Formation. The fauna of the shale also becomes almost entirely composed of goniatites, orthocones and *Posidonia* and *Dunbarella*-like bivalves, with a loss of all benthic creatures. This transition is interpreted as indicating increasingly stagnant and low-oxygen bottom conditions. A lack of bioturbation and preservation of carbonised plant material in shale horizons within the Dergvone Shale Formation supports increasingly dysoxic bottom conditions up through the sequence.

The Tawnyunshinagh Limestone Member (Carraun Shale Formation) is lithologically similar to hypersaline horizons in the Meenymore and Bellavally Formations and is interpreted as such for the following reasons:

(1) The limestones of the member are virtually devoid of fossils (except for a concentrated monospecific shell layer near its base), whereas the other limestones in the Carraun Shale are commonly fossiliferous.

(2) The limestones are generally laminated in an almost identical way to those interpreted as stromatolitic in the stratigraphically lower Meenymore and Bellavally Formations. The laminites even display similar syn-sedimentary deformation structures.

(3) Structures interpreted as the remnants of algal mats are also preserved in the two main limestone units. Such mats are usually only preserved where the

environment is too harsh (e.g. high salinity) for burrowing and grazing animals. The nature of these structures is discussed further below.

(4) The top limestone unit displays evidence of the desiccation of possible algal mat structures, demonstrating that net water loss was occurring from the very shallow and occasionally exposed system at times.

Proud weathering wrinkled disc-like bodies in the Tawnyunshinagh Member bear resemblances to both beekite structures (a typically concentrically layered form of silica replacement) and laminations produced by modern algal mats. Distinguishing between the two interpretations is difficult. The structures always occur as either thin, isolated flakes or thin horizons or mats. The coherency of the mats is shown in Fig. 2.4b where partially detached bodies appear to have curled and separated in a similar manner to modern exposed and desiccating algal mats/crusts. Beekite structures are predominantly associated with the replacement of fossil material; however, in this case it would require the replacement of compositionally different, coherent layers, a likely source of which would be an organic algal mat. Regardless of whether primarily or secondarily textured, it is believed that the original structures preserved were indeed algal in origin, since no other explanation for the mats is apparent.

A significant number of sandstone dykes were mapped during the course of this work. In the past these have been thought as being sourced from the Loughaphonta Sandstone Member (e.g. Brandon, 1972a). However, the Loughaphonta Sandstone is thought not to have been the sole source for the following reasons:

(1) No disturbance of the Loughaphonta sandstone was observed or has been reported in the literature.

(2) An intervening sandstone separates the Loughaphonta Sandstone from the lowest sandstone dyke exposed in the Carraun/Lugasnaghta Section.

(3) The thickest sandstone dyke discovered (~1m) is located >20m stratigraphically above the top of the Loughaphonta Sandstone. The sheer volume of sand represented by such a thick dyke makes such a distance of transport extremely unlikely. Additionally you would expect the thickest dykes to occur closest to the source.

(4) The highest dykes outcrop ~35m stratigraphically higher than the Loughaphonta Sandstone.

Although not certain, it is believed that multiple beds must have acted as local sources for the dykes. Inadequate exposure and severe disruption of the source beds may account for their lack of recognition. The relatively consistent composition of the dykes and similarity to the Loughaphonta Sandstone is not seen as being diagnostic.

In summary (Fig. 2.4c), deposition is thought to have occurred across a relatively stable carbonate platform during the early Asbian (Benbulben Shale and Glencar Limestone Formations). The depth of deposition slowly shallowed throughout the Asbian and conditions became more energetic in the Dartry Limestone Formation. A relatively rapid sea-level fall occurred at the base of the Meenymore Formation and conditions proceeded to rapidly oscillate from shallow marine to hypersaline (and even terrestrial) palaeoenvironments throughout the Meenymore, Glenade Sandstone and Bellavally Formations. Conditions deepened slightly at the base of the Carraun Shale Formation in the early Brigantian but dramatically shallowed during the deposition of the Tawnyunshinagh Limestone Member. Palaeoenvironments later rapidly deepened and became progressively less oxygenated throughout the upper Carraun Shale and into the Dergvone Shale Formation.

2.5 CYCLICITY AND DIGITAL SPECTRAL ANALYSIS OF THE TIEVEBAUN SECTION

Cyclicity in bed thickness, lithology and limestone percentage content has previously been reported for the Benbulben Shale, Glencar Limestone and Dartry Limestone Formations by Schwarzacher (1964, 1989). Digital spectral analysis of the Tievebaun Section was undertaken due to the apparent cyclical nature of limestone bundles. Despite the seemingly impersistent and irregular nature of some of the limestone units exposed in the section, it was discovered that it is possible to identify and correlate some horizons ~690m along strike (Fig. 2.5a). The fact that thin beds are correlateable over such distances suggests that the depositional environment was relatively uniform and that the driving force behind lithological development was operating over quite a wide area. This may imply that the control on the variation in deposition was not local, but rather extrinsic or external.

Milankovitch cycles have been proposed as the driving forces behind many examples of Carboniferous sedimentary cyclicity (Section 1.3). The three main parameters of Milankovitch cycles (Schwarzacher, 2000) are shown in Table 2.5a.

Parameter	***Effect***	***Periodicity***
Eccentricity	Determines how elliptical the Earth's orbit is around the Sun and therefore the distance between the Earth and the Sun during a year.	Dominantly 400ka, other periodicities simplified to 100ka.
Obliquity	Defines the angle between the rotational axis of the Earth and the plane of its orbit around the Sun.	Dominantly 50ka & 40ka.
Precession	Defines a "wobble" of the Earth's rotational axis relative to its plane of orbit around the Sun.	23ka & 19ka, simplified to 21ka.

Table 2.5a Milankovitch cycles influencing Earths climate.

The eccentricity of the Earths orbit is controlled, predominantly, by the interaction of the gravitational pulls of the Sun, Saturn and Jupiter and this has been essentially stable for at least the last 400My (Collier *et al.*, 1990). However, the precession and obliquity Milankovitch cycles are the result of Sun-Earth-Moon interactions (Schwarzacher, 2000) and have changed through time as the Earths rotation has

slowed and the Moon has drifted further away (Barnett *et al.*, 2002; Berger *et al.*, 1989; Collier *et al.*, 1990; House, 1995; Schwarzacher, 1993, 2000). It has been argued that orbital parameters cannot be accurately calculated in the Palaeozoic due to increasing uncertainties (Laskar, 1999; Laskar *et al.*, 2004). However, several attempts have been made to simplify orbital system models and make estimations of Carboniferous Milankovitch cycle periodicities. According to Berger *et al.* (1989) mid-Carboniferous obliquity cycles were probably reduced to 42ka and 33.9ka (average 38ka) periodicities, whilst the precession cycles may have been reduced to 20.5ka and 17.2ka (average 18.9ka) periodicities. Collier *et al.* (1990) calculated an obliquity periodicity of 31.1ka for the Carboniferous and precessional periodicities of 20ka, 19.1ka, 16.5ka and 16.7ka (averaging 18.1ka).

In an attempt to identify any potential cyclicity in the Tievebaun Section, and (if present) the periodicities of, the depositional patterns observed, the logged succession was digitised and analysed for dominant spectra using the program REDFIT, version 3.8 (Schulz & Mudelsee, 2002).

A range of estimates were made for the length of time over which the section was deposited to enable the conversion of sediment thickness into time (Table 2.5b).

	Holkerian (My)	***Asbian (My)***	***Total (My)***	***Accumulation rate (m/My)***
Total Substage duration	7.0	6 ± 0.8	13 ± 0.8	*NA*
Likely minimum in GLTV	0	1.7	1.7	~125
Likely maximum in GLTV	1.0	3.4	4.4	~49
Probable value for GLTV	0.5	2.5	3.0	~72

Table 2.5b Estimation of time represented by the Tievebaun Section.

The total Substage duration is derived from Sevastopulo & Wyse Jackson (2009) and references therein. Likely minimum and maximum values are derived from estimates of the amount of each of the stages exposed in the section.

The rates of sedimentation determined in Table 2.5b fall within the accumulation rates published for early Carboniferous carbonate platforms of between ~75 and ~175m/My (Bosscher & Schlager, 1993). The rates are also very consistent with those published for both carbonate platform and terrigenous shelf environments in a

compilation of sediment accumulation rates by Sadler (1981). In both environments, the mean and slower rates of deposition (derived above) are closest to the densest data groupings within the ranges published. Relatively non-compacted shelf sediments in the Gulf of Mexico, at a broadly equivalent distance from the shoreline as is thought to have been the case for the Tievebaun Section, accumulated at a comparable rate of ~150m/My during the Palaeogene (Galloway & Williams, 1991).

The stratigraphic sequence was divided into 5cm intervals and classified as either limestone or shale. This simple "end-member" approach can be readily applied to the lithological succession in the Tievebaun Section and it has been demonstrated (Weedon & Read, 1995) that a two-coded approach to analyses can yield very similar results to those conducted using a greater number of lithological categories. Published vitrinite reflectance work (Philcox *et al.*, 1992) was combined with conodont C.A.I. determinations to estimate the depth of burial for the sequence, in order to calculate the degree of compaction of the shale and limestone units. Due to the assumptions inherent in the calculations, three decompaction models were used and the results of their spectral analyses were compared to test the validity of any periodicities detected:

1. all the rock decompacted equally = Tievebaun_Original.
2. shale units decompacted approximately three times more than the limestone = Tievebaun_Decompact_1.
3. shale units decompacted approximately twice as much as the limestone = Tievebaun_Decompact_2.

The methodology of preparing the data and undertaking the digital spectral analysis on the Tievebaun Section is provided in detail in Appendix B.

In order to simplify the computational requirements of the spectral analysis, Welch-Overlapped-Segment-Averaging (WOSA) was applied to the Tievebaun Section. For standard analyses, the section was broken into five overlapping (50%) segments, each approximately 1My in duration (minimum 577ka, maximum 1.47My). In an attempt to identify the controls of cycles >100ka, models of Tievebaun_Decompact_1 were also run with WOSA, set at 1, 29, 50 and 70 (3My, ~200ka, ~118ka and ~85ka respectively). Cycles with periodicities greater than the

length of time represented in each of the overlapping segments should not thus be detected.

The spectra of the three models of the Tievebaun Section are shown in Fig. 2.5b. The spectra derived for the various WOSA conditions applied to Tievebaun_Decompact_1 are displayed in Fig. 2.5c. Spectra below a cycle length of 10ka are not shown in order to give a higher resolution view of significant peaks. Schwarzacher (1989) found no consistent indications for such short periodicities in the same formations from a different geographic area.

In all the analyses, a strong peak is identified for a cycle periodicity of ~15-19ka and in all but one (WOSA_1 - Fig. 2.5c) a period around 30ka is also significant. The detection of these cycles across all the models as single spikes, or very closely spaced peaks, indicates that the periodicities observed are remarkably stable and similar throughout the section. The ~30ka periodicities correlate with the 2-3m thick cycles identified by Schwarzacher (1964, 1989) in sections of the Benbulben Shale, Glencar Limestone and Dartry Limestone Formations around Lough Glencar, Co. Sligo. The occurrence of dominant cycles as a series of excursions instead of a single peak is most likely due to the effects of spectral leakage and differential compaction.

The estimated minimum lengths of the identified periodicities are 9.6ka and 17ka, whilst the estimated maximum durations are 24.9ka and 44ka respectively. Although there is scope for variation in the periodicity of the main cycles identified in the Tievebaun Section, the significant peaks, of (probable) 17ka and 30ka length, are remarkably similar to the periodicities proposed for the obliquity and precessional cycles during the Carboniferous. Given the rapidity of the cycles and environment of deposition, the obliquity and precession Milankovitch forcings must therefore be seriously considered as the most likely control of these sedimentary cycles.

No 100ka (eccentricity) periodicity was identified in the spectral analyses of the Tievebaun Section. Several long wavelength cycles were identified, but these were of periodicities which are not readily explained by orbital cycles alone. Fig. 2.5b

displays a (somewhat) defined peak at 200ka, adjacent to a statistically significant gentle peak from ~250ka towards 1My. It is thought that this represents long-term facies change, probably reflecting basin or long-term climatic controls, possibly with some degree of contribution from the eccentricity Milankovitch cycle. Tievebaun_Decompact_1 WOSA_1 (Fig. 2.5c) shows the most differentiation of the long periodicity peaks, with significant cycles of ~300ka, ~500ka, ~750ka and 3My. The latter is not shown for plotting reasons.

In summary, strong cyclicity, with estimated wavelengths of 17ka and 30ka, has been identified in the Benbulben Shale, Glencar Limestone and Dartry Limestone Formations in the Tievebaun Section. The periodicities of the short cycles are very similar to published estimates for the frequency of Carboniferous precession and obliquity Milankovitch cycles. Evidence for the effects of the longer period eccentricity cycles is however, more cryptic. Wright and Vanstone (2001) and Barnett *et al.* (2002) have both suggested that during the early Asbian, cycle periodicities were shorter than those in the late Asbian and Brigantian and were possibly controlled by the obliquity orbital cycle. This is analogous to the Pleistocene glaciation, where it has been demonstrated (Lisiecki & Raymo, 2005; Pillans *et al.*, 1998) that the obliquity cycle was dominant for an extended period prior to the eccentricity cycle becoming more prominent approximately 700,000 years ago. Since glaciation was probably only in its early stages in the Asbian (see Section 1.3), it is conceivable that, similar to the more recent glaciation, the short-term Milankovitch cycles initially dictated ice-volumes, sea-levels and thus sediment cycles, before some threshold was reached, whereby the longer term eccentricity cycle became dominant in the late Asbian and Brigantian. This particular time is outside of the stratigraphic coverage of the Tievebaun Section.

2.6 DISCUSSION

The Carboniferous sedimentary rocks examined in NW Ireland are a product of an evolving shoreline and watershed (located further north from the study area), superimposed on the effects of relative sea-level fluctuations and also basin/platform development.

The Benbulben Shale and Glencar Limestone Formations were deposited during a time of gradual change in depositional setting. The shale-dominated Benbulben Shale Formation retained a significant argillaceous component, most probably supplied by river and delta systems located to the north which had earlier formed the Mullaghmore Sandstone (Section 2.1.1). Fluctuations in the limestone to shale ratio throughout the Benbulben Shale and Glencar Limestone Formations can probably be explained by two controls:

(1) The waxing and waning influence of the river delta complexes in the north. Whenever the shoreline retreated further north and/or large delta lobes switched, argillaceous input to the south decreased and bottom conditions cleared sufficiently to allow extensive coral biostromes or thicker limestones to develop.

(2) Orbital cyclicity. A cyclical control on deposition was identified in this study in the Tievebaun Section (Section 2.5) and has also been reported from the Benbulben Shale, Glencar Limestone and Dartry Limestone Formations (Schwarzacher, 1964, 1989). Significant periodicities are apparent throughout the section examined, regardless of lithology (i.e. whether limestone or shale dominated), and may represent the precession and obliquity Milankovitch cycles. The exact manner in which short periodicity Milankovitch cycles influenced sedimentation over such an area is difficult to determine. Two possibilities are considered most probable:

(a) Orbital variations influenced the waxing and waning of ice-sheets and thus eustatic sea-level which in-turn caused periodic alteration of sedimentation in the sequences examined.

or

(b) Orbital variations caused climatic disturbance in the immediate area and directly effected sedimentation through any number of pathways; e.g. changing rainfall and thus river output, disruption of currents (both atmospheric and oceanic) etc.

Deposition of the Dartry Limestone Formation marked a significant reduction in the supply of argillaceous material to the area. Shale is generally reduced to thin intervals between thicker, more laterally persistent limestones. There are a number of factors which could have affected this change:

(1) Increased palaeocurrent activity identified during the course of this investigation in both the Glencar and Glenade Sections (Section 2.4) could have prevented the deposition of fine argillaceous material, as suggested by Caldwell & Charlesworth (1961). Evidence for both significant current events and increased ambient (north-northwest to south-southeast) currents identified herein, are in agreement with both the work of Somerville *et al.* (2009) and Schwarzacher (1961) respectively.

(2) An increase in local tectonic activity, which has been recorded by a number of workers (Kelly, 1996; Legg *et al.*, 1998; Mitchell, 2004; Philcox *et al.*, 1992; Somerville *et al.*, 2009), may have resulted in reorganisation of the platform and greater isolation of the water mass from the northerly source of argillaceous material.

(3) Variations in the glaciated condition of the planet (suggested by the influence of probable Milankovitch cyclicity on sedimentation) may have caused a reduction of argillaceous material in a similar fashion as is postulated as being responsible for the rapid limestone-shale variation discussed above.

Lithologically, the Benbulben Shale and Glencar Limestone Formations are laterally consistent (within the area studied), which is in agreement with them having been deposited during a period of relative tectonic quiescence and uniform subsidence which ultimately gave rise to carbonate platforms and ramps (Mitchell, 1992; Philcox *et al.*, 1992). In contrast, the development of pronounced lateral facies changes in the overlying Dartry Limestone Formation (Section 2.1.4) may signify increased tectonic activity and the development of intra-basinal ramps and

platforms (Kelly, 1996; Mitchell, 1992). This proposition is in agreement with the model of Bridges *et al.* (1995) for the environmental setting and development of Viséan mudmounds in Ireland and Britain (Fig. 2.6). Bridges *et al.* (1995) suggested that in the Asbian and Brigantian, the occurrence of carbonate mudmounds was fundamentally controlled by the development of fault-bounded shelf platforms and intra-shelf ramps. Due to faulting (and associated rapid depth changes and increasing supplies of siliciclastic material), carbonate mudbanks would have become restricted to clearer-water, photic zones (Bridges *et al.*, 1995). In NW Ireland Asbian carbonate mudbanks are extensively developed in the Dartry Limestone Formation (Schwarzacher, 1961) and their distribution has been linked to the presence of local faults, although such correlation cannot be made for all mounds (Sevastopulo & Wyse Jackson, 2009). Kelly (1989, 1996) and Mitchell (2004) suggested that north–south compression during the Asbian caused reactivation of Caledonian structures to form local pull-apart basins on the ramp.

Localised fault movements may have continued during the deposition of the overlying Meenymore Formation as large thickness variations occur and it is difficult to track members across the basin (Brandon, 1977; Legg *et al.*, 1998). The Meenymore Formation marks a significant change in palaeoenvironment in NW Ireland. The transition from platform limestones (Dartry Limestone Formation) to very shallow water deposits (Meenymore Formation) has been attributed to an episode of uplift (Somerville *et al.*, 2009). However, the relatively sudden nature of the palaeoenvironmental change may discount a long term tectonic control on the observed relative sea-level fall, while the widespread nature of the shift indicates that rapid local fault movement is also unlikely to be entirely responsible. It is considered possible herein that a eustatic sea-level fall can account for the relatively abrupt transition from the Sligo Group to the Leitrim Group. It is *tentatively* suggested that, due to Milankovitch forcings, an increase in icevolume could have caused such a eustatic fall.

The exact nature and placement of the Dartry–Meenymore contact in the Aghagrania Section has varied in the past, and reconciling the boundary of West *et al.* (1968) or Kelly (1989) with the observations of this study proved difficult. West *et al.* (1968) appeared to place the contact at the base of the first carbonate bed,

which is above the last fossiliferous marine limestone of the Dartry Limestone. Kelly (1989) followed this definition but revised the description of the basal limestone, significantly stating that the basal Meenymore bed rests disconformably upon the Dartry Limestone with a relief of 10-20cm. From plate 2.3.18 (Kelly, 1989) it is possible to correlate Kelly's placement of the boundary with the plane separating beds 6.1 and 6.2 in the sequence logged herein (Fig. 2.3.1e-f). No evidence for an erosive or irregular base for the Meenymore Formation was found during this study or, infact, has been reported by any other workers (MacDermot *et al.*, 1983; Smith, 1980; West *et al.*, 1968) in the Aghagrania Section.

The Meenymore and Bellavally Formations, as studied in the Aghagrania and Carraun/Lugasnaghta sections, represent several, relatively rapid palaeoenvironmental shifts which tend, however, not to deviate too far from base sea-level (Section 2.4). Given the frequency of these shifts, particularly those above sea-level, it may be expected that the sequence from the Meenymore Formation through to the Carraun Shale Formation would contain hiatuses or even erosional levels, thus leading to an incomplete temporal record. However, it is believed that the actual sea-level shifts observed were relatively small and transient, and it is a nature of deposition occurring near base-sea-level that such dramatic lithological characters were developed. Although, admittedly, the available exposure was limited, no significant erosional levels were encountered in either the Aghagrania or Carraun/Lugasnaghta Sections. Evidence for minor erosion was observed in the form of reworked calcilutites in both the Meenymore and Bellavally Formations and, most significantly, a probable in-situ solution/erosion, collapse and fill structure in the Meenymore Formation. In addition to the lack of substantial eroded/reworked horizons in the Meenymore or Bellavally Formations, no significant gaps appear to be developed in the goniatite (Brandon & Hodson, 1984) or conodont (see Section 4.4) faunal sequences. The complete stratigraphic sequence was therefore taken to be essentially continuous and reasonably reliable for the construction of isotopic trends (Chapter 5).

The correlation of thin (characteristic) lithological horizons (members) in both the Aghagrania and Carraun/Lugasnaghta Sections (~30km apart) suggests that deposition of the Bellavally Formation occurred over a relatively uniform area

which was not effected by local, differential fault movements. This tectonic stability was attributed to regional thermal subsidence by Mitchell (1992). The Carraun and Dergvone Shale Formations represent a return to deeper and stable marine conditions, as indicated by common faunal bands and the absence of rapid palaeoenvironmental fluctuations.

Increasing sedimentation rates, dysoxic conditions and water depth are generally recorded up through the Carraun and Dergvone Shale Formations (see Section 2.5). However, initially this phase of deepening may actually be attributable to fault movement, since palynofacies do not indicate a more distal depositional setting (Smith, 1995). A persistence of the lowstand of cycle five (Ramsbottom, 1973 - see Section 6.1) into the lower Carraun Shale Formation, is suggested by the shallow-water, hypersaline Tawnyunshinagh Member and palynological evidence for some degree of restriction in lower portions of the formation Smith (1995). Isolated limestone beds in the Carraun Shale Formation probably represent the reduction of argillaceous material in the water column, due perhaps to eustatic change, a temporary shift in climate in the source region to the north, or a large-scale change in the delta systems which supplied the terrigenous material. The appearance of possible turbiditic sandstones in the Dergvone Shale is compatible with continued deepening and may also demonstrate greater proximity to the source delta front.

Since deposition, the NW region has experienced uplift and both conodont colour alteration index (C.A.I.) values (Chapter 4) and vitrinite reflectance values (Philcox *et al.*, 1992) indicate that a significant thickness of post-Bashkirian cover has been removed from the district. Despite this uplift, the sequence has been left relatively undisturbed by tectonic events and dips rarely exceed 30º (away from faults).

CHAPTER 3 - THE SHANNON BASIN AREA

This chapter will describe the lithostratigraphy and geological history of parts of the Burren Platform, an area located north of the Shannon Basin in Co. Clare. The results of fieldwork undertaken on two short sections will be described and the significance of their lithological development discussed.

3.1 STRATIGRAPHY OF THE SHANNON BASIN AREA

The post-Viséan siliciclastic rocks of the Shannon Basin have been extensively researched, particularly due to their relevance to hydrocarbon reservoirs and basin fill dynamics (e.g. Elliot *et al.*, 2000; Goodhue & Clayton, 1999; Martinsen & Collinson, 2002; Rider, 1974; Wignall & Best, 2000). The contributions of some of the more important studies undertaken in the region are discussed here.

The Tournaisian and Viséan limestones of County Clare were first mapped and investigated in detail by Douglas (1909), who utilised the biostratigraphical scheme established by Vaughan (1905) in the Bristol district of England. Douglas (1909) was the first to note a break in the rock record at the junction of the limestone and shale in the region (between the Magowna and Clare Shale Formations, Fig. 1.5.1d), although it was then noted only as "*slight*".

The Viséan limestones of the Burren region have recently been examined and described by Gallagher *et al.* (2006), building upon the earlier work of Gallagher (1996). These studies constructed detailed biostratigraphical and micro-facies correlations for the area and demonstrated the frequent and widespread nature of eustatic sea-level fluctuations, which are apparent in the Asbian and Brigantian-aged portions of the succession.

Hodson (1953) conducted the first thorough examination and division of the Serpukhovian and Bashkirian rocks which overlie the Viséan carbonates in northwest Co. Clare. The work revised and subdivided regional lithological unit boundaries and, most importantly, erected many of the goniatite biostratigraphical

divisions within the sequence. It became apparent, from biostratigraphical correlation, that the shale sequence was condensed in its lower portions and that a considerable non-sequence existed between the shale and the underlying limestone (determined as D_2; Brigantian). Hodson (1953) was the first to propose the positioning of a deeper basin in southern Co. Clare, with basin sediments and goniatite zones onlapping upslope northwards. Kelk (1960) demonstrated that sediments preserved at Ballybunion (northwest Co. Kerry) were deposited in the axial region of the basin. Hodson & Lewarne (1961) refined and extended, further to the south, the goniatite zones of Hodson (1953). With some local exceptions (interpreted as upstanding ridges), Hodson & Lewarne (1961) demonstrated that a Carboniferous trough of sedimentation developed with an axis roughly coincident with that of the present River Shannon (Fig. 3.1). The basin was deepest, and developed the thickest sediment accumulation, around the Shannon region and shallowed both to the north and to the south (Fig. 3.1). The basal beds of the Clare Shale Formation (Section 3.1.4), were shown by Hodson & Lewarne (1961) to range in age from E_1 (basal Serpukhovian, see Fig. 1.2.1a) immediately north of the Shannon estuary to H (Bashkirian) at the northern (and also probably the southern) limits of the basin. Kelk (1960) had previously reported P_2 (Brigantian) ammonoids from the Clare Shale at Ballybunion. Thus the base of the Clare Shale Formation has been shown to be very diachronous, with a clearly condensed Viséan–Namurian (Serpukhovian/Bashkirian) sequence away from the basin depocentre.

Rider's (1974) revision of the stratigraphy overlying the Viséan limestones remains relatively unchanged today. From this work it was accepted that the Namurian (Serpukhovian/Bashkirian) sequence lies disconformably, rather than unconformably, on top of the Viséan carbonates. Rider (1974) proposed that the Serpukhovian to Bashkirian succession, preserved in the Shannon Basin, formed due to basin filling from the west, and the stratigraphy was divided into the Shannon [Ross Sandstone, Clare Shale and Gull Island Formations] and Central Clare [Cyclothem] Groups.

The lithostratigraphy of the units examined to the north of the Shannon Basin (Figs. 1.4c & 1.5.1c), as well as their local stratigraphical equivalents and adjacent

formations, are shown in Fig. 1.5.1d, and described in ascending stratigraphic order in the subsections below:

3.1.1 The Burren Formation

This formation was not encountered in either of the sections examined, but directly underlies the Slievenaglasha Formation (Gallagher *et al.*, 2006) which was the lowest formation examined herein. The Burren Formation is ~365-385m thick and ranges in age from Holkerian to late Asbian (Gallagher *et al.*, 2006). It consists of pale grey packstones and wackestones, with intervals of darker cherty limestones associated with oolitic grainstones (Sleeman & Pracht, 1999). The upper part of the formation is cyclical, with periods of emergence marked by palaeokarst surfaces and clay way-boards, which are thought to represent palaeosols (Sevastopulo & Wyse Jackson, 2009).

3.1.2 The Slievenaglasha Formation

The base of this formation often rests directly on a pronounced palaeokarstic surface, at the very top of the underlying Burren Formation (Gallagher *et al.*, 2006). The upper boundary of the Slievenaglasha Formation is placed at the top of the limestone which is stratigraphically below the phosphate and chert of the overlying Magowna Formation (Pracht *et al.*, 2004). A composite ~94m thick type-section has been proposed at Slievenaglasha, GR R3094 9796 and Clooncoose, GR R2802 9526 (Pracht *et al.*, 2004).

The Slievenaglasha Formation is Brigantian in age (Sleeman & Pracht, 1999) and was divided into four members (described in Table 3.1.2 below, in stratigraphic order) in the Burren region by Gallagher *et al.* (2006):

	Member	Details
Slievenaglasha Formation	**Lissylisheen** 1-2m	Thick bioturbated limestone with solitary rugose corals and vertical pedotubules.
	Ballyelly ~31m	Consists of thickly bedded crinoidal limestone arranged in five cycles, each of which is capped by a thin interval of crinoid-poor limestone. It is thus, very similar to the Balliny Member, except for the presence of chert horizons in the thick-bedded crinoidal limestone portions.
	Fahee North ~25m	Characterised by intraclastic, well-bedded, dark grey, bioturbated limestone with chert horizons.
	Balliny ~36m	Typified by five cycles, each of which comprises alternations of thickly bedded crinoidal limestone and thinner units of crinoid-poor limestone.

Table 3.1.3 Members of the Slievenaglasha Formation in southwest Ireland.

The surface of the uppermost bed in the Slievenaglasha Formation is reportedly a palaeokarst in some areas and may represent a sudden and significant shallowing event (Gallagher, 1996; Gallagher *et al.*, 2006).

3.1.3 The Magowna Formation

This formation is only 3m thick at its type section at Magowna, Co. Clare (GR R2890 8220) and it thins progressively to the north before passing laterally into the Cahermacon Member of the Clare Shale (Pracht *et al.*, 2004). The Magowna Formation lies disconformably on the (sometimes undulose) palaeokarstic top surface of the underlying Slievenaglasha Formation (Lissylisheen Member). This formation represents the youngest Viséan limestone in its type area and has yielded fossils of both late Brigantian and early Namurian (Serpukhovian) age (Sleeman & Pracht, 1999). It is generally composed of interbedded dark micritic limestone and black calcareous shale and is known to contain solitary rugose corals and cephalopods (Pracht *et al.*, 2004).

3.1.4 The Clare Shale Formation

This formation is commonly poorly exposed due to susceptibility to weathering, but its development marks a significant change in facies in the Shannon Basin. The age of its base is highly variable, with the magnitude of the underlying non-sequence increasing away from the basin depocentre (Fig. 3.1). In the south, at Ballybunion

and immediately north of the Shannon, goniatites of late Brigantian (P_2) age have been discovered (Kelk, 1960), whereas in the north, on Slieve Elva, Co. Clare, the lowest goniatite horizon is of lower Bashkirian (H_{2a}) age (Pracht *et al.*, 2004). The thickness of the formation varies from approximately 180m around the basin axis to roughly 10m in North Clare (Elliot *et al.*, 2000). It thins in a similar manner to the south. Three members are generally recognisable (Pracht *et al.*, 2004) and are described in Table 3.1.4 below in stratigraphical order (thicknesses quoted are for northern Clare):

	Member	***Details***
Clare Shale Formation	**Goniatite Shale** ~12m	Comprises black shale with discrete thin bands of flattened goniatites. Goniatites in carbonate bullions are often preserved in three-dimensions. Coaly plant fragments and bivalves are also found, particularly towards the top.
	Phosphate Shale 0-4m	Represented by black non-calcareous mudstones and shale with occasional laminae and bands of pyritic phosphate. Thins northwards.
	Cahermacon 0-5m	Consists of highly siliceous, typically non-calcareous mudstones and shales with numerous phosphatic nodules and chert. The proportion of chert decreases from the south to the north.

Table 3.1.4 Members of the Clare Shale Formation in southwest Ireland.

3.1.5 The Ross Sandstone and Gull Island Formations

The Ross Sandstone Formation can be correlated, using goniatite biozones, with parts of the Clare Shale Formation (Rider, 1974). Three goniatite bands within the Ross Sandstone Formation are all lower Bashkirian in age (Sevastopulo, 2009). At Loop Head, County Clare, the Ross Sandstone Formation is at least 300m thick, with the base unseen (Rider, 1974). The formation consists of fine-grained sandstones with interbedded siltstones and shales, which represent deposition in a deep marine environment with regular turbiditic incursions (Sleeman & Pracht, 1999). Slumping is a notable feature of the formation and significant dewatering events have given rise to well-developed sand volcanoes (Gill, 1979). A controversial, alternative interpretation for the Ross Sandstone has been proposed by Higgs (2004, 2009), who suggested that the formation actually represents lacustrine, river-fed and wave modified turbidites.

Overlying the Clare Shale (in the north) and Ross Sandstone (in the south) Formations, is the Gull Island Formation, which varies significantly in thickness from ~130m in the north to ~550m in the south (Sevastopulo, 2009). The lower portions of the Gull Island Formation consist of fine turbiditic sandstones and siltstones (which are commonly disturbed), whilst upper portions tend to be less disturbed and contain minor amounts of shale and channel structures (Rider, 1974). The upper part of the formation is not as variable in thickness as the lower part, perhaps suggesting that the basin had almost become sediment filled by the time of its deposition (Sevastopulo, 2009). Analysis of slumps and turbiditic sandstone sedimentary structures indicate that they formed on a southeast facing palaeoslope (Martinsen & Collinson, 2002). The Gull Island Formation is overlain by the cyclothems of the Central Clare Group (Pracht *et al.*, 2004).

3.2 GEOLOGY OF THE SECTIONS EXAMINED ON THE BURREN PLATFORM

Two sections which expose strata spanning the Viséan–Serpukhovian boundary were examined in Co. Clare. Such sections are comparatively rare in the area, since the end of the Viséan is, commonly, marked by the onset of widespread shale development, which tends to weather easily, and thus the actual contact is generally very poorly exposed.

3.2.1 Kilnamona Section (KMONA)

The small village of Kilnamona is located to the north of the N85, approximately 8.5km west-north-west from Ennis, Co. Clare. The section is exposed approximately 0.5km to the east of Kilnamona at GR R27745 80395. It is traced in a small stream running alongside a driveway which leads to a farmhouse (Fig. 3.2.1a). Details of the exact location and stratigraphical height of microfossil samples taken from this section is provided in Appendix E.

The section was first described by Hodson & Lewarne (1961); however, very little detail was provided and their thickness measurements appear somewhat inaccurate. The section was later visited, sketched (Fig. 3.2.1b) and logged by D. Meischner (Skompski *et al.*, 1995).

A sequence of alternating limestones and shales, typical of the Magowna Formation, are exposed in the section (Fig. 3.2.1c), as well as (possibly) the contacts with the Slievenaglasha and Clare Shale Formations. The section is dominantly limestone at its base (Fig. 3.2.1d) but shale becomes prevalent towards the top of the section. Since the area of the outcrop is limited, it is difficult to determine whether the limestone near the base of the section represents the upper portion of the Slievenaglasha Formation or, alternatively, part of the Magowna Formation. Similarly, establishing whether the shale at the very top of the section relates to the Magowna or Clare Shale Formation is equally problematic. It is likely that the contact between the Slievenaglasha and Magowna Formations can be

placed 113cm ASB, at the junction between units KMONA6 and KMONA7A. At this point, shale overlies a crinoidal calcarenite, more typical of the Slievenaglasha Formation, and the section stratigraphically below this level dominantly comprises limestone comparable to that of the youngest, Lissylisheen Member of the same formation. The top of the Magowna Formation may be placed at 180cm ASB (above the calcareous horizon of KMONA11B), giving a total stratigraphical thickness of 67cm. Above the Magowna Formation the section is composed entirely of fissile, dark and non-calcareous shale, which is assigned herein to the Clare Shale Formation.

The stratigraphically lowest bed in the section (KMONA1) is incompletely exposed but comprises a limeclast bearing crinoidal wackestone. Limeclasts are generally rounded and flattened. The fauna is generally dominated by crinoidal material; however, solitary corals and brachiopods are also common. The upper surface of the bed appears irregular and pitted. A 9-11cm-thick interval of recessed, poorly-calcareous shale overlies KMONA1. Irregular, calcilutite wackestone nodules are exposed within the shale interval. Above the shale, another limeclast bearing, thickly-bedded crinoidal wackestone is developed (KMONA3), although the full extent of the clasts was not observed. Small (1cm x 5cm), slightly proud-weathering vertical structures are thought to represent *Skolithos*-type bioturbation. The boundary between KMONA3 and the overlying KMONA4 is somewhat irregular.

Limestone beds KMONA4, 5 and 6 are all similar crinoidal wackestones (though they vary in thickness). Solitary corals, brachiopods and even an isolated, poorly-preserved goniatite were identified, but were found to be numerically subordinate to echinoderm plates and ossicles. KMONA6 appears to contain rare limeclasts, up to 1.5cm in width, and its upper surface is irregular on a fine scale and may possibly represent a very poorly developed palaeokarstic surface.

A 17cm thick, composite non-calcareous shale unit (KMONA7) overlies KMONA6, separating it from two ~9cm thick, more argillaceous wackestones (KMONA8 and 9). An 18.5cm thick, dominantly non-calcareous shale interval succeeds KMONA9 and is overlain by a couplet of organic-rich, fossiliferous calcareous mudstones. Fossils, dominated by brachiopods, but also including an

orthocone, trilobite pygidia and *Posidonia*, are generally slightly flattened and partially pyritised. Organic-rich, non-calcareous fissile shale overlies KMONA11B and constitutes the remainder of the exposed section.

Just over 2m of section was logged (Fig. 3.2.1b) and 11, ~2kg microfossil samples were taken from the section, representing nearly every exposed unit.

3.2.2 St. Brendan's Well Section (BW)

This section is located at GR R14550 98440, 1km to the east of Lisdoonvarna village, Co. Clare (Fig. 3.2.2a). The outcrop is restricted to a channel, cut by the Gowlaun River, a tributary of the Aille River. Horizontal Viséan limestone is exposed in the broad river bed, while overlying Serpukhovian and Bashkirian phosphates and shale are restricted to a bank cutting (Fig. 3.2.2b). The exact locations and stratigraphical heights of microfossil samples removed from this section are provided in Appendix E.

Similar to the Kilnamona Section, the St. Brendan's Well Section (Fig. 3.2.2c) exposes the Magowna Formation, along with its contacts with the underlying Slievenaglasha Formation and the overlying Clare Shale Formation. The lowest 40cm of bioturbated, crinoidal wackestone (BW1) in the section is assigned herein to the Slievenaglasha Formation. The upper surface of the Slievenaglasha Formation (in this particular section) is generally flat, but pock-marked and irregular on quite a fine scale. These irregularities can be traced under the overlying unit (Fig. 3.2.2d) and therefore, since it is an original feature, the surface probably represents a weakly developed palaeokarst. The Magowna Formation (at the site) comprises a thin, recessed shale interval, overlain by a thick limestone, which appears partially phosphatised on top (Fig. 3.2.2d). The Magowna Formation extends to 95cm ASB (Top of BW4) and is 55cm thick in total. It is directly overlain by a phosphatic conglomerate lag, which represents the base of the Phosphate Shale Member of the overlying Clare Shale Formation. Fissile, non-calcareous shale extends from the top of the phosphatic conglomerate for over 10m up the steep sides of the bank (Fig. 3.2.2e). The transition from the Phosphate Shale Member to the overlying Goniatite Shale Member of the Clare Shale Formation was

not directly identified during this work; however, the boundary must lie below the goniatite bearing bullion (BW10) encountered at 325cm ASB (Fig. 3.2.2e).

The lowest unit in the St. Brendan's Well Section (BW1) is not fully exposed but was examined in a prominent, dissolution-widened joint which cuts across the stream bed. Simple, granular *Skolithos*-type burrows (~4mm wide and 1-2cm long) are present in the crinoidal wackestone. A 2-4cm thick, deeply recessed shale horizon, with an impersistent, highly argillaceous wackestone unit, overlies the irregular surface of BW1 (Fig. 3.2.2d). A ~52cm thick, bioturbated crinoidal wackestone (BW3 & 4) succeeds the shale interval and forms a prominent step in the stream bed. The upper 6-12cm of the bed appears slightly coarser and is characterised by a very irregular alteration "front" or horizon, above which the rock is darker and less reactive to HCl. This horizon is interpreted as having been partially phosphatised.

A phosphatic conglomerate horizon rests directly on BW4 and is represented by two thin beds (BW5 & BW5B), which are commonly almost entirely concealed by scree derived from the overlying Clare Shale Formation (Fig. 3.2.2e). The lower bed (BW5) averages 6cm in thickness, whilst the upper bed measures 3-4cm in thickness. The beds appear compositionally similar, although the upper surface of BW5B is rougher and more irregular. Both units are a mottled medium grey colour on fresh faces, with dark, granule to pebble-sized phosphatic clasts. Portions of the matrix are weakly calcareous and strings and fine flecks of pyrite occur in somewhat dispersed horizons.

A thick succession of non-calcareous, occasionally pyritic shale overlies the phosphatic lag horizon and comprises the remainder of the exposed section. Impersistent, often 3d goniatite-bearing, foetid calcilutite bullions are found at several levels within the shale. Flattened goniatites, bivalves (*Posidonia* and *Dunbarella*) and wood fragments are also common on many of the shale surfaces.

Eight 2kg microfossil samples were removed from carbonate horizons in the section, another two samples were taken from the phosphatic conglomerate

horizons (BW5 and 5B) whilst a single sample was extracted from the shale almost directly overlying the phosphatic lag horizon (Fig. 3.2.2c).

3.3 EVOLUTION OF THE SHANNON BASIN AND BURREN REGION

The rocks examined in the west of Ireland are exposed on what was the northern platform bordering the Shannon Basin, also variously referred to as the Shannon Trough (e.g. Strogen, 1988) and the Western Irish Namurian Basin (e.g. Braithwaite, 1994; Martinsen & Collinson, 2002; Wignall & Best, 2000). It is thought that the basin developed in latest Devonian to early Carboniferous times through reactivation of the Iapetus suture (Martinsen & Collinson, 2002), although onset of significant subsidence and creation of accommodation space did not occur until the late Tournaisian to early Viséan (Strogen, 1988).

In the early Asbian, sediment deposition in southern Ireland occurred on a southerly dipping carbonate ramp (Gallagher, 1996). Widespread sea-level fluctuations initiated in late Asbian times, with sediments of the Ballyadams (Carlow, Kilkenny), Ballyclogh (north Cork), Burren (north Clare) and Clashavodig (east Cork) Formations all exhibiting well-developed shallowing upward cycles across the platforms which had developed in southern and central Ireland (Sevastopulo & Wyse Jackson, 2009). Similar cyclicity is widespread throughout Britain and Ireland at this interval and it has been suggested that glacioeustasy was the main driving force (Wright & Vanstone, 2001).

Widespread deepening occurred during the early Brigantian, resulting in the deposition of deeper-shelf, sub-tidal, chert-rich limestones over much of southern Ireland (Gallagher *et al.*, 2006). Eustatic sea-level fluctuations continued, but water depth changes were insufficient to cause much emergence in most areas (Gallagher, 1996; Gallagher *et al.*, 2006; Sevastopulo & Wyse Jackson, 2009). Apart from a reported rapid shallowing event at the top of the Slievenaglasha Formation (see Section 3.1.2), the Brigantian, in southwest Ireland, is thought to have predominantly been an interval of subsidence and gentle, continued deepening (Pracht *et al.*, 2004).

An abrupt, but diachronous, shift from carbonate to argillaceous/siliciclastic sedimentation is observed around the Viséan-Serpukhovian boundary. Deposition of the Clare Shale in the basin axis, where subsidence was greatest (Hodson & Lewarne, 1961), was initially coeval with continued carbonate deposition at the basin margins. In latest Brigantian times, areas further away from the Shannon Basin axis became sediment starved, resulting in highly condensed phosphates and shales (Hodson, 1953). Over time the Clare Shale Formation onlapped upslope (northwards and southwards), away from the centre of the basin and became developed more ubiquitously (Martinsen & Collinson, 2002). In early Bashkirian times, while deposition of the Clare Shale Formation was reaching the margins of the Shannon Basin, a thick sequence of turbiditic siltstones and sandstones (The Ross Sandstone Formation) began to be deposited in the deeper water axis of the basin (Rider, 1974).

The sediments of the Shannon Basin became progressively shallower from early- to mid-Bashkirian times. This is reflected in the successively younger stratigraphic units, which filled the basin, advancing from a broadly westerly direction (recorded by the Gull Island Formation and overlying Central Clare Group - Sevastopulo, 2009).

An alternative to the traditional view of the Shannon Basin was proposed by Wignall & Best (2000), who suggested that:

(1) Sediments were not sourced from the west and northwest, but actually from the southwest. It was argued by the workers that the majority of palaeocurrent directions from the Ross Sandstone and Gull Island Formations were more consistent with this.

(2) The rocks of northern Clare do not represent the shallower margin of the basin but actually deeper areas, more distal from a northeast facing slope, located further to the south. They proposed that, after deposition of Viséan limestone, the northern limb of the Shannon Basin began to subside, such that while the southern, more proximal portions of the basin began to fill, northern parts became sediment-starved. It was suggested that the non-sequence between Viséan and Namurian strata allows sufficient time for this part of the basin to deepen significantly. The phosphatic lag that is developed between the

limestone and shale was argued to contain both evidence of shallow and deep water deposition and that aspects of the Clare Shale in the north are more characteristic of deep-water accumulation.

The Wignall & Best (2000) model of basin development, although more consistent with some of the palaeocurrent data, is incompatible with the majority of available evidence and is not followed herein. Martinsen & Collinson (2002) provided several strong counter-arguments in support of the more "*traditional"* basin model and stated that Wignall & Best (2000) had ignored evidence from key localities as well as the broader region.

Higgs (2004) proposed another (more disparate) alternative evolutionary history for the Shannon Basin, which he considered developing as a foreland basin of the Variscan front. In the model, Higgs (2004) argues that the phosphatic conglomerate (at the base of the Clare Shale Formation) represents a "*transgressive ravinement lag"* resting unconformably on the eroded top of the Viséan limestone. It was proposed that subsidence in north Clare was outpaced by eustatic sea-level fall, causing emergence. Higgs (2004) suggests that impingement of the Variscan front may then have caused a severing of open ocean connections and thus, the gradual development of freshwater conditions in southern Ireland and England. Into this relatively deep-water lake, the sediments of the Clare Shale Formation and younger lithologies developed. During significant transgressions and highstands, sea-levels overtopped the "*sill"* and normal marine conditions returned to the lake, thus developing widespread, correlateable marine faunal bands. Higgs (2004) model, though interesting in its addressing of certain aspects of the Clare area, appears somewhat over-simplistic, and its supporting evidence is often equivocal.

Since deposition, uplift has occurred resulting in 2-4km of middle to late Carboniferous sediments being eroded and removed from the region (Goodhue & Clayton, 1999). Elevated thermal gradients (Goodhue & Clayton, 1999), during burial and prior to uplift and unroofing, resulted in vitrinite reflectance values in excess of 4% and conodont colour alteration indices (C.A.I) > 5 (Clayton *et al.*, 1989). Despite this high thermal history, the rocks in north Co. Clare are relatively

undisturbed and were only very gently folded by the northward-weakening Variscan front (Graham, 2009).

3.4 SIGNIFICANCE OF THE SITES INVESTIGATED

Although the two Co. Clare sections examined herein (Kilnamona and St. Brendan's Well) are only 22km apart and thought to expose broadly the same stratigraphic interval, their palaeogeographic positions at varying distances to the Shannon Basin axis have resulted in appreciable sedimentological differences. The most important disparity between the sections is the relative completeness of the temporal record in each.

The Kilnamona Section is located further south than the St. Brendan's Well Section and was positioned closer to the actual axis of the Shannon Basin (Fig. 3.1). A more continuous trace of sedimentation, with few or no obvious breaks in deposition is preserved in the Kilnamona Section, thus providing a more complete temporal record of events. The top of the Slievenaglasha Formation in the Kilnamona Section (KMONA6) was noted as *possibly* representing a poorly developed palaeokarstic surface, a feature noted elsewhere by Gallagher *et al.* (2006). It must be noted, however, that other horizons (lower in the Kilnamona Section) were also recorded as also being slightly irregular (KMONA1 & KMONA3). Karst surfaces have distinctive solution and erosive features (Summerfield, 1993) and although not a direct proxy for karst maturity (the presence, position and type of overlying vegetation has a pronounced effect), generally the irregularity of a limestone surface becomes more exaggerated with prolonged exposure (Briggs *et al.*, 1997). If the surface of KMONA6 in the Kilnamona Section does truly represent a minor palaeokarst, or karren horizon (Summerfield, 1993), then it may be of relatively small magnitude, since no large-scale erosive topography was observed, although the scale of the outcrop was admittedly very limited. Hodson & Lewarne (1961) also suggested the presence of "*cryptic non-sequences*" above and below the *Cravenoceras leion* beds (KMONA8 & KMONA9), although no specific evidence was provided. No faunal turnover or gap has been documented (Hodson & Lewarne, 1961; Skompski *et al.*, 1995) in the section, which might indicate a depositional or temporal hiatus. In this work, the Kilnamona Section was taken as representing an essentially continuous record of deposition at the resolution of the timescale available from the documented conodont fauna (see Section 4.4).

In contrast to the Kilnamona Section, the St. Brendan's Well Section appears more likely to contain a considerably condensed chronostratigraphic record, since sediment bypassing was more exaggerated above the Viséan limestones, further away from the Shannon Basin axis (Fig. 3.1). The probable palaeokarstic surface developed at the top of the Slievenaglasha Formation (BW1) is more irregular and therefore *possibly* more evolved than the corresponding surface in the Kilnamona Section. However, it is probably still of minimal significance since no substantial palaeokarstic features were observed, despite over $100m^2$ of the horizon being exposed and available for examination (Fig. 3.4). The most important depositional irregularity in the St. Brendan's Well Section is the phosphatic conglomeratic lag, which, although very thin, appears to represent the entire Serpukhovian (see Section 4.4). The lowest goniatite-bearing shale and bullion horizon, ~2m above the phosphate, contains H_{1b}, Chokierian (Bashkirian) *Homoceras beyrichianum* and possibly H_{1a}-aged *H. subglobosum* goniatites (Hodson, 1953). Whilst the Slievenaglasha Formation, 55cm below the phosphate horizon, has been dated using foraminifera as late Brigantian (Gallagher *et al.*, 2006). The phosphatic lag most likely represents a significant period of sediment by-passing, localised re-working and chemical erosion resulting in the concentration of chemically stable material (Braithwaite, 1994). Due to depositional retardation and concentration in the St. Brendan's Well Section, the use of the faunal (Chapter 4) or isotopic (Chapter 5) trends identified must be considered with respect to its irregular temporal record.

Despite the differences between the Kilnamona and St. Brendan's Well Sections, a number of features are actually highly comparable and have important implications for the evolution of palaeoenvironments in the region. The Slievenaglasha Formation in both sections can be identified by the development of common S*kolithos*-type burrows, the dominance of crinoid fossils, the relative purity of the limestone, and the presence of a (possible) weakly-developed palaeokarstic upper surface. The features of the Slievenaglasha Formation therefore indicate sedimentation in a shallow, energetic palaeoenvironment in which deposition was probably terminated by a relative drop in sea-level, exposure of the limestone and subsequent minor erosion. The identification of this possible palaeokarstic surface at the top of the Slievenaglasha Formation in both sections agrees with the assertion

of Gallagher *et al.* (2006) that a widespread shallowing event occurred across the region at the end of the Brigantian.

Given the poorly developed nature of the palaeokarstic horizon and similar fauna in the overlying Magowna Formation, the relative sea-level fall (responsible for its development) was probably relatively short-lived. The Magowna Formation in both sections is characterised by an increase in the shale content and the development of limestones which are more argillaceous and less fossiliferous, probably indicating a transition to slightly deeper water deposition.

Due to condensing of the section at St. Brendan's Well it is difficult to draw comparisons in the development of the Clare Shale between the two sections studied. However, given the foetid, non-calcareous, fine nature of the formation and its lack of benthic creatures, it is likely to have been deposited in a stagnant, hypoxic and significantly deep palaeoenvironment. It is notable that such a dramatic switch in sedimentation styles occurred across both the basin and its limbs, demonstrating that control was basin-scale and not local. The short stratigraphic (and probably temporal) interval over which the palaeoenvironments shifted, from shallow marine to karstic and subsequently back to deeper water, may suggest that these high-frequency relative sea-level changes can be attributed to glacioeustatic fluctuations.

CHAPTER 4 – MICROFAUNAL ANALYSIS

This chapter will present the results of extensive microfossil investigations undertaken on the sections in both NW Ireland and Co. Clare. Section 4.1 will initially provide a brief overview of some results from each lithostratigraphical section studied before the taxonomy, form and biostratigraphy of the conodonts recovered is discussed (Sections 4.2-4.4). Section 4.5 describes the morphological and taxonomic groups of the ichthyoliths identified, whilst Section 4.6 deals with the preservation of the microfossils themselves, focussing particularly on the ichthyoliths. The chapter closes (Section 4.7) with a discussion of the palaeoenvironmental significance of the microfauna. Information concerning the (predominantly non-phosphatic) invertebrate micro-material recovered during this work is located in Appendix F. It is important to note that the stratigraphic ranges of the various species and genera described in this chapter, purely refers to their range within the chronostratigraphic interval examined in this work (and thus does not necessarily constitute their total range).

4.1 MICROFOSSIL SAMPLES AND RESIDUES

Rock samples were carefully and systematically recovered from every stratigraphic section investigated in NW Ireland and Co. Clare in order to study the characteristics and general composition of the microfaunal assemblages. Samples were processed back in the laboratory using various methodologies, as detailed in Appendix A. In general, carbonates were digested using dilute formic acid, whilst shale samples were alternately wetted and dried, with occasional immersion in very dilute formic acid or, alternatively, an oxidising agent, depending on the precise composition of each sample.

4.1.1 Tievebaun Section

Ichthyolith and, in particular, conodont remains were recovered in low abundances and were generally greatly subordinate to the rich variety of silicified and occasionally partially or wholly pyritised microfossil material. The fidelity of

replacement varied through the section, but was generally good. Samples from the Glencar Limestone Formation were commonly argillaceous and produced large volumes of residue. Dartry Limestone samples were extensively silicified and proved difficult to digest. Incompletely digested rock fragments commonly exhibited fossil moulds. Pyrite, often framboidal, was relatively common throughout the section. Encrusting fossils, bored brachiopods and a variety of bryozoan material were also of note. Fossils became very rare in the Dartry Limestone samples. Samples GLTV31 and GLTV41 (in the Glencar and Dartry Limestone Formations respectively) were entirely barren.

4.1.2 Glencar Section

Samples from this section were generally difficult to dissolve completely, due to a large degree of silicification. Microfossil residues were generally small from the Dartry Limestone and typically more volumetric and argillaceous from the underlying Glencar Limestone. The fidelity of the surface detail of silicified fossils is (in general) reduced relative to the Tievebaun Section, although the Dartry Limestone samples from this particular section proved more productive than their Tievebaun counterparts. Again, ichthyolith and conodont material was found in very low abundances or was even entirely absent. Mouldic impressions and sediment infills of fossils (predominantly bryozoans, brachiopods and echinoderm plates and ossicles) were common on larger restite grains. Incomplete (often coarse) pyritisation of silicified fossils was also common, whilst framboidal pyrite was often found within finer residue fractions. A distinct reduction in the amount of microfossil material was apparent in the middle part of the section, in the lower Dartry Limestone Formation.

4.1.3 Glenade Section

The two samples recovered from the Glenade Section were relatively pure carbonates and yielded only small amounts of insoluble residue. Substantial quantities of (generally poorly-detailed) silicified microfossils, as well as some ichthyoliths and conodonts were obtained from DAGN1, whilst DAGN2 was found to be barren.

4.1.4 Aghagrania Section

Microfossil samples from this section were taken from a diverse range of lithologies. Silicified fossils were found to be significantly reduced relative to previous sections; however, conodonts and ichthyoliths were more common and, in places, ichthyoliths were exceptionally abundant e.g. AGHA4 Meenymore Fm. (Corloughlin Mbr.) = 100's/kg. Several samples (AGHA2, 5, 7, 8 & 12) were found to be virtually barren. Ichthyolith material recovered from sample AGHA13 was particularly degraded (oxidised) and, in many cases, partially pyritised.

4.1.5 Carraun/Lugasnaghta Section

Samples were again taken from diverse lithologies in this section and, as a result, yielded variable microfossil residues, both in terms of concentration and composition. Silicification of fossils was virtually absent throughout, with pyritisation the main means by which calcitic fossils were preserved. The pyritisation has, on occasion, resulted in quite detailed fossil replication. Residues tended to be somewhat micaceous and volumetrically small, except for the shale horizons sampled (samples prefixed with D.K.). Since limited volumes of acid were used in processing these shales, some calcitic shelly fossils were also recovered. Phosphatic fossils were relatively more common throughout the section. Several horizons were, however, completely barren of any microfossils, despite complete disaggregation (CNLG3, 4, 5, Bellavally Formation). Ichthyoliths in several horizons were partially pyritised (CNLG10, 13, 15 & 16, Carraun Shale Formation).

4.1.6 Kilnamona Section

In general, samples from this short stratigraphic section yielded very small volumes of insoluble residue and contained very few silicified or pyritised fossils. The fidelity of silicified and pyritised preservation becomes more detailed up through the sequence and into the more argillaceous units of the Magowna Formation. Conodonts and ichthyoliths were abundant in samples KMONA4-6 (Slievenaglasha Formation) and KMONA8 (Magowna Formation), common in KMONA1-3 (Slievenaglasha Formation) and KMONA9 (Magowna Formation), but were not

recovered from (the difficult to disaggregate) KMONA10, 11A and 11B (Magowna Formation). Many ichthyoliths and conodonts appeared matt-black in colour (rather than dark and lustrous) and were possibly not well-preserved.

4.1.7 St. Brendan's Well Section

In general, the residues obtained from this section were volumetrically small but proved especially rich (100's/kg) in conodont, and to an extent ichthyolith, material (BW2 was an exception to this and produced a lot of argillaceous residue, with few microvertebrate remains). Carbonate samples BW1 (Slievenaglasha Formation) and BW2-4 (Magowna Formation) reacted well with acid and broke down rapidly, whilst samples BW6-10 (Clare Shale Formation) were slower to digest and BW5 and 5B (Clare Shale Formation) were essentially unreactive. Silicified or pyritised fossils were uncommon throughout the section, being most abundant in BW2 and 4 (Magowna Formation). Conodonts in BW1, 3 and (in particular) BW4 were often encrusted or bound in small silica masses.

4.2 CONODONT FAUNA

Conodont elements (recovered from digested residues) were generally identifiable to species level; however, in some cases elements were recorded only at a generic level due to a combination of:

- the general complexity of the apparatus
- the poor state of preservation.

  or

- a lack of specimens.

Most species were only conclusively determinable via their P_1-elements, with P_2-, S- and M-elements used predominantly for generic designations. A total of 11 genera and 15 species were identified. No attempts at sub-species identifications were made, although typical examples of these were recognised in certain samples. In all the element descriptions below, the topological terminology of Purnell *et al*. (2000) is followed (Fig. 4.2a), whilst morphological terminology broadly follows that given in Sweet (1981).

Cavusgnathus (Harris & Hollingsworth, 1933)

Only P_1-elements were considered diagnostic of this genus, with the short free-blade of the platform being used to distinguish different species. However, this particular feature is prone to damage and thus, only one P_1-element was determined. P_1-elements comprise an elongate platform with a central trough (deepest ventrally) and a short free blade attached to, and continuing into a lateral parapet at the ventral margin. Parapets are transversely ridged. A short, thin and poorly-defined carina is visible at the dorsal, tapered termination of the platform, but this breaks into fine, isolated nodes and disappears completely approximately ⅓ of the way up the central trough. The basal cavity is flared, (relatively) symmetrical and is located ventrally of the dorsal platform termination.

C. naviculus (Hinde, 1900)

(Fig. 4.2b – 1)

Description:

P_1-platforms are slightly deflected downwards at the ventral and dorsal margins. The blade characteristically decreases in height ventrally and is composed (typically) of six relatively poorly-defined denticles. Denticles become more distinct approaching the cusp, which is significantly raised above the parapet from which it emerges.

Age, location and lithology of samples:

Found in samples ranging from the late Asbian (upper Viséan) to (possibly) the basal Serpukhovian, in only the Aghagrania and Kilnamona Sections. Productive samples were all argillaceous, fossiliferous marine limestones.

AGHA4, KMONA2 and possibly KMONA8

Unassigned *Cavusgnathus* P_1-element

Platforms in which the free blade was broken or obscured by sediment could not be determined to species level, but they were found in samples ranging from basal Asbian (upper Viséan) to the uppermost Brigantian (uppermost Viséan). Rare, unassigned P_1-elements were recovered from fossiliferous marine limestones in the Tievebaun, Carraun/Lugasnaghta, Kilnamona and St. Brendan's Well Sections.

GLTV18, CNLG10, KMONA5, BW4

Declinognathodus (Ellison & Graves, 1941)

(Fig. 4.2c – 1-6)

This genus was identifiable by P_1-element morphology only. Platforms are slightly asymmetric, lanceolate (taper dorsally) in shape, with two lateral noded or ridged parapets. A denticulate free blade extends ventrally approximately the same length as the platform itself. The blade has a median junction with, and continues onto, the platform as a carina, which characteristically merges with the rostral parapet. The base begins at the dorsal margin of the element and broadly follows the platform

shape, although it is flared asymmetrically, with the rostral side more inflated and the caudal side extending further ventrally.

D. lateralis (Higgins & Bouckaert, 1968)

(Fig. 4.2c – 1 & 2)

Description:

Parapets are transversely ridged and separated by a shallow groove. The carina comprises a short ridge which has no defined nodes. The rostral parapet is (at the ventral end) composed of a ridge running parallel to the carina, with occasionally poorly-defined transverse ridges developed. A characteristic feature of the species is the merging of the carina and parapet a short distance from the ventral margin of the platform. The merged carinal-parapet structure is composed of isolated, distinct transverse ridges, with occasionally a very fine ridge or series of fine nodes defining the internal edge of the parapet.

Age, location and lithology of samples:

Specimens were restricted to Bashkirian carbonate bullions in the St. Brendan's Well Section.

BW10, BW8

D. noduliferous (Ellison & Graves, 1941)

(Fig. 4.2c – 3-6)

Description:

Parapets are composed of more bulbous nodes or node-like transverse ridges (in comparison to *D. lateralis*). The short carina consists of a poorly defined noded ridge. Isolated nodes of the rostral parapet lie rostral and distinct from the carina at the ventral end of the platform. The merged carina and rostral parapet occurs as a series of distinct or slightly transversely elongate nodes, which are occasionally joined by a very fine indistinct ridge.

Age, location and lithology of samples:

Specimens were restricted to Bashkirian carbonate bullions in the St. Brendan's Well Section.

BW10, BW8

Gnathodus (Pander, 1856)

(Fig. 4.2d – 1-10, Fig. 4.2e – 2 & 6)

P_1-elements were used exclusively to determine species within this particular genus; however, some M- and P_2-elements were also recognised at a generic level. Although significant morphological variation exists between the various species identified during this work, all P_1-elements have a denticulate free-blade which extends ventrally from the platform for approximately the same distance as the entire platform length. Blades form a continuation of a denticulate or noded carina, which runs the entire length of the platform.

Some P_1-element forms which appeared transitional between *G. bilineatus* and *G. girtyi* were also recovered during this study and are shown in Fig. 4.2d (7 & 9).

G. bilineatus (Roundy, 1926)

(Fig. 4.2d – 2,4 & 8)

Description:

The species has a highly asymmetric platform. The caudal parapet is tall and composed of numerous transverse ridges, which grade into nodes towards the dorsal platform termination. The low rostral parapet is much wider and is ornamented by numerous irregular nodes, rows of nodes or even noded ridges. The carinal ornament becomes wider dorsally. A distinct "kink" of variable severity occurs in the carina approximately ⅔ of its length from the dorsal margin (see Fig. 4.2d – 8 for a particularly well-developed example of this feature).

Age, location and lithology of samples:

This species was relatively common and was found in marine limestone samples ranging from the upper Asbian (upper Viséan) to the lower Serpukhovian in the majority of sections (except the Dartry Mountain Sections).

AGHA3.1, AGHA3.2, AGHA9, AGHA10, AGHA13, CNLG1, CNLG6, CNLG9, CNLG13, CNLG14, CNLG15, CNLG17, CNLG19, KMONA1, KMONA2, KMONA3, KMONA4, KMONA5, KMONA6, KMONA8, KMONA9, KMONA10, BW1, BW2, BW3, BW4

G. girtyi (Hass, 1953)

(Fig. 4.2d – 1,3 & 10)

Description:

P_1-elements of this species have an asymmetric lanceolate outline with raised lateral parapets separated from the carina by shallow grooves. The caudal parapet extends further ventrally along the carina, and is typically wider, than the rostral parapet. Both parapets are typically composed of a row of individual nodes at their dorsal ends, but these evolve into transverse ridges ventrally. The base flares slightly on both the rostral and dorsal margin of the platform.

Age, location and lithology of samples:

G. girtyi was the most common species encountered in this study. Elements were recovered from various lithological samples ranging from the upper Holkerian (middle Viséan) to the lower Serpukhovian and from virtually every section investigated (except the Glenade Section).

GLTV13, GLTV14, GLTV15, GLTV16, GLTV23, GLTV26, GLTV27, DAGL13, DAGL14, DAGL15, AGHA1, AGHA3.1, AGHA3.2, AGHA4, AGHA9, AGHA10, CNLG1, CNLG2, D.K. CNLG.A, CNLG6, CNLG7, CNLG8, CNLG9, CNLG10, CNLG11, CNLG14, CNLG15, CNLG16, CNLG17, CNLG18, CNLG19, KMONA1, KMONA2, KMONA3, KMONA4, KMONA5, KMONA6, KMONA8, KMONA9, KMONA10, BW1, BW2, BW3, BW4

G. homopunctatus (Ziegler, 1960)

(Fig. 4.2d – 5 & 6)

Description:

P_1-elements have an approximately symmetrical platform with a lanceolate outline. Parapets comprise individual low, fine ridges or rows of fine, dispersed nodes, which run approximately halfway between the carina and the outer margin of the platform in a crescentic manner. Occasionally, parapets are very poorly developed with only one or two conspicuous nodes following a subtle change in slope in the platform.

Age, location and lithology of samples:

The species was found in generally low numbers (except the conodont-rich St. Brendan's Well Section) in samples ranging from the lower Asbian to the uppermost Brigantian (upper Viséan). Elements were recovered from fossiliferous marine limestones from all sections except the Glencar and Glenade Sections.

GLTV27, AGHA3.1, CNLG1, CNLG7, CNLG8, CNLG10, CNLG13, KMONA1, KMONA3, KMONA4, KMONA5, KMONA6, BW1, BW2, BW3, BW4

Gnathodus P_2

(Fig. 4.2e – 2)

Description:

P_2-elements attributed to the genus *Gnathodus* comprise a long slender blade with numerous (slightly) dorsally directed denticles. In rostral or caudal view the elements are gently curved (convex in the direction of the oral cavity). Some elements show some degree of (possibly) original torsion. Basal cavities are almost centrally located, only very mildly inflated and pinch out approximately ⅓ of the way towards both the dorsal and ventral element tips.

Age, location and lithology of samples:

P_2-elements belonging to the genus *Gnathodus* were found in samples ranging from the late Asbian (upper Viséan) to the lower Serpukhovian, in all but the Dartry Mountain Sections and in a variety of marine limestones.

AGHA9, AGHA10, CNLG13, CNLG15, CNLG19, KMONA1, KMONA3, KMONA4, KMONA5, KMONA6, KMONA8, KMONA9, BW1, BW3, BW4

Gnathodus M-element

(Fig. 4.2e – 6)

Description:

M-elements attributed to the genus *Gnathodus* are delicate and generally recovered incomplete. Elements comprise an enlarged cusp with a very slightly inflated, relatively deep basal cavity. Blades with delicate denticles descend from the cusp to form a sharp overall V-shape pointing (broadly) rostrally. The dorsal or adaxial arm is slightly curved in rostral view and is more pronounced than the ventral arm.

Age, location and lithology of samples:

Identifiable M-elements belonging to this genus were observed in only two fossiliferous marine limestones spanning the upper Brigantian (upper Viséan) to early Serpukhovian interval in the Carraun/Lugasnaghta Section.

CNLG15, CNLG19

Hindeodus (Rexroad & Furnish, 1964)

(Fig. 4.2b – 2 & 7)

A limited number of elements attributable to this particular genus was recovered. It is possible that (at least) some of this material represents the species *H. cristula*; however, it was decided (due to a level of uncertainty) to retain determination at a generic level.

P_1-elements recovered (Fig. 4.2b - 7) are angulate in shape and taller ventrally with a concave base. There are (on average) 9 denticles, which are usually slightly dorsally directed. Bases are flared into a dorsally pointed lanceolate shape.

Morphologically distinctive S-elements belonging to this genus are bipennate in shape (Fig. 4.2b - 2). The cusp marks the point of deflection in the element and also typically the thinnest part of the ramiform blade. A small basal pit directly underlies the cusp. The unequal lateral processes become deeper towards their terminations and their denticles increase in size in parallel. Commonly, a thick band of fine lineations, which have been attributed to successive basal margin regressions by Sweet (1981), is visible towards the element base.

Age, location and lithology of samples:

Elements were only found in marine limestones of the Kilnamona and (possibly) Aghagrania Sections. Unambiguous elements belonging to this genus were recovered from uppermost Brigantian strata, whilst uncertain element fragments may extend the range of the genus down to the upper Asbian.

?AGHA3.2, ?KMONA1, KMONA4, KMONA5

Idiognathoides (Harris & Hollingsworth, 1933)

(Fig. 4.2c – 8 & 9)

P_1-elements were used to identify elements to genus level only, but with further study individual species may be discernable. P_1-elements have flat, asymmetric platforms with a denticulate free blade (approximately as long as the platform itself) attached to the ventral end of the rostral parapet of the platform. Platform areas comprise two transversely ridged parapets separated by a shallow groove and no carina exists. Platforms do not quite reach the dorsal margin of the elements, although a rounded ridge does descend from the platform to the flared base. Bases are wider on the rostral margin but longer on the caudal margin.

Age, location and lithology of samples:

This genus was restricted to Bashkirian carbonate bullions in the St. Brendan's Well Section.

BW10, BW8

Idioprioniodus (Gunnell, 1933)

(Fig. 4.2b – 3 & 8)

The exact topological positions occupied by elements of this genus are difficult to determine given its Prioniodinid skeletal architecture (Stone, 1994). This feature, coupled with the commonly incomplete nature of the elements recovered, prevented comprehensive species level determinations to be made during this study. P-elements are bipennate in shape, with the cusp underlain by a slightly flared basal cavity, which tapers along the base of the descending lateral processes. Denticles on lateral processes are long but decrease in size towards the caudal termination. The cusp and denticles are often thin, delicate, elongate and commonly curved.

Age, location and lithology of samples:

Idioprioniodus elements were identified in samples ranging in age from the upper Asbian (upper Viséan) to the Bashkirian. Specimens were recovered from a variety of lithologies and from all except the Dartry Mountain Sections.

AGHA1, AGHA3.1, AGHA3.2, AGHA9, AGHA10, CNLG1, D.K. CNLG.A, D.K. CNLG SHEENA, CNLG6, CNLG7, D.K. CNLG ABV. DERREENS, CNLG8, CNLG10, CNLG13, CNLG14, CNLG15, CNLG19, KMONA1, KMONA3, KMONA4, KMONA5, KMONA6, KMONA8, KMONA9, BW1, BW3, BW4, BW10, BW8

Kladognathus (Rexroad, 1958)

Due to the recognised complexity of its apparatus (e.g. Somerville, 1999), elements belonging to this genus were not identified to specific level.

- P-elements are thought to comprise commonly curved or angled blades/processes, with long slender denticles which are often curved or deflected. Fine, short denticles are commonly found between longer more pronounced denticles, giving a distinct two-tiered appearance. A conspicuous basal groove is usually visible running along the blades/processes.
- M-elements of the genus are conspicuous and are dolabrate in shape, with a pronounced cusp which descends into a significant aboral process. The dorsal/caudal process is elongate, aborally concave and bears ~12 discrete denticles which decrease in height away from the cusp. A slight basal pit is developed beneath the cusp and it extends partially along the underside of the dorsal/caudal process.

Age, location and lithology of samples:

Specimens of this genus were recovered from various marine limestones sampled from all sections examined herein. Productive samples ranged in age from the uppermost Holkerian/lowermost Asbian (middle Viséan/upper Viséan) to the lower Serpukhovian.

GLTV15, GLTV16, GLT27, GLTV33, DAGL13, DAGL14, ?DAGL15, DAGN1, ?AGHA.CAV1, AGHA1, AGHA3.1, AGHA3.2, ?AGHA4, AGHA9, AGHA10, CNLG1, CNLG7, CNLG15, CNLG19, KMONA1, KMONA2, KMONA3, KMONA4, KMONA5, KMONA6, KMONA8, KMONA9, BW1, BW2, BW3, BW4

Lochriea (Scott, 1942)

(Fig. 4.2f – 1-7, Fig. 4.2g – 1-9, Fig. 4.2e – 3-5)

The *Lochriea* genus becomes particularly common and morphologically diverse around the Viséan-Serpukhovian boundary. Particular M- and P_2-elements were identified to genus level; however, only P_1-elements were used to distinguish individual species. Transitional platform morphologies were commonly encountered during this research. All P_1-elements have a lanceolate or sub-circular shaped platform and base which is commonly sub-symmetrical. The more morphologically complex (evolved) species are, however, more often strongly asymmetric in outline. A denticulate blade extends ventrally from the platform for approximately the same length as its carinal equivalent, which effectively bisects the platform and extends to the dorsal termination. Carinal denticles generally become broader dorsally and may break into finely noded transverse ridges or large, pitted nodes. The carinal ornament is commonly connected by a fine median crest.

L. commutata (Branson & Mehl, 1941)

(Fig. 4.2f – 1)

Description:

This particular species exhibits the most long-ranging and morphologically "simple" P_1-element encountered within the *Lochriea* genus, with its basic body-plan being modified in different ways in later species. The platforms of P_1-elements are lanceolate to oval in outline, slope away from the carina and are entirely devoid of ornament. In rostral or caudal view the P_1-elements are essentially rectangular, with only a very slight downward deflection in the dorsal end of the carina. Blades (and even whole elements) are sometimes gently curved in oral view.

Age, location and lithology of samples:

P_1-elements of this genus were found in marine limestone samples ranging from the lower Asbian (upper Viséan) to the lower Serpukhovian, in all but the Glencar and Glenade Sections.

GLTV27, AGHA1, AGHA3.1, AGHA3.2, AGHA9, AGHA10, CNLG1, CNLG6, CNLG15, CNLG19, KMONA1, KMONA3, KMONA4, KMONA5, KMONA6, KMONA8, KMONA9, BW1, BW2, BW3, BW4

L. costata (Kulagina *et al.*, 1992)

(Fig. 4.2g – 2 & 4)

Description:

P_1-elements are similar in gross morphology to *L. commutata*, but are characterised by individual, simple, typically straight, ridges on both sides of the platform.

Age, location and lithology of samples:

Unequivocal P_1-elements of this species were found in marine limestone samples of uppermost Brigantian (uppermost Viséan) and lower Serpukhovian age in the Carraun/Lugasnaghta and Kilnamona Sections.

CNLG19, KMONA3, KMONA4, KMONA5, KMONA6

L. cruciformis (Clarke, 1960)

(Fig. 4.2g – 1,3 & 5)

Description:

P_1-elements of this species are similar to those of *L. commutata* but have a more asymmetric outline. This asymmetry is due to the development of complex individual raised ridges, formed from rows of fused nodes, on both sides of (and attached to) the carina towards the dorsal or middle part of the platform. The ridges occasionally bifurcate, are typically not straight and often attach to the carina at different points.

Age, location and lithology of samples:

The exact first appearance of this species is somewhat complicated by the presence of transitional precursor forms. The marine limestone samples from the Carraun/Lugasnaghta, Kilnamona and St. Brendan's Well Sections in which the species was found range from the upper Brigantian (upper Viséan) to the basal Serpukhovian.

?CNLG13, ?CNLG14, CNLG15, KMONA1, KMONA6, KMONA8, KMONA9, BW1, BW3, BW4

L. monocostata (Kulagina *et al.*, 1992)

(Fig. 4.2f – 2 & 6)

Description:

This species is morphologically similar to *L. costata*, but is taxonomically separated due to the fact that it exhibits a ridge on one side of its carina only.

Age, location and lithology of samples:

This species was found in fossiliferous marine limestone samples which range in age from the upper Brigantian (upper Viséan) to the lower Serpukhovian, in the Carraun/Lugasnaghta, Kilnamona and St. Brendan's Well Sections.

CNLG15, CNLG19, KMONA1, KMONA3, KMONA6, KMONA8, KMONA9, BW1, BW3, BW4

L. mononodosa (Rhodes *et al.*, 1969)

(Fig. 4.2f – 5 & 7)

Description:

P_1-elements of this species are morphologically similar to those belonging to *L. commutata*, but bear a single node (discrete of the carina) on one side of the platform, approximately half-way towards the outer margin.

Age, location and lithology of samples:

Found in fossiliferous marine limestone samples ranging from the upper Brigantian (upper Viséan) to lower Serpukhovian in the Carraun/Lugasnaghta, Kilnamona and St. Brendan's Well Sections.

?CNLG13, CNLG15, CNLG19, KMONA1, KMONA3, KMONA4, KMONA5, KMONA6, KMONA8, KMONA9, BW1, BW2, BW3, BW4

L. nodosa (Bischoff, 1957)

(Fig. 4.2f – 3 & 4)

Description:

P_1-elements are morphologically similar to those of *L. mononodosa* differing only in the occurrence of a discrete node on both sides of the platform.

Age, location and lithology of samples:

L. nodosa was found in fossiliferous marine limestones from the Carraun/Lugasnaghta, Kilnamona and St. Brendan's Well Sections and these ranged from the upper Brigantian (upper Viséan) to lower Serpukhovian in age.

CNLG13, CNLG14, CNLG15, CNLG19, KMONA1, KMONA3, KMONA4, KMONA5, KMONA6, KMONA8, KMONA9, BW1, BW3, BW4

L. senckenbergica (Nemirovskaya *et al.*, 1994)

Description:

P_1-elements of this species are morphologically similar to *L. cruciformis,* but they exhibit a ridge-like ornament on both sides of the carina which is composed of adjacent (but discrete) thick, steep nodes which run approximately perpendicular to the carina from the centre or ventral half of the platform. Importantly, this row of projecting nodes does not adjoin or fuse with the carina. Nodes are not always aligned in a simple row.

Age, location and lithology of samples:

Elements attributable to this particular species were somewhat difficult to determine due to morphologically transitional forms and their similarity with other proposed *Lochriea* species. Unequivocal specimens were recovered from late Brigantian fossiliferous marine limestone samples in the Carraun/Lugasnaghta, Kilnamona and St. Brendan's Well Sections.

CNLG15, KMONA3, BW1

L. ziegleri (Nemirovskaya *et al.*, 1994)

(Fig. 4.2g – 6-9)

Description:

P_1-elements are morphologically similar to both *L. cruciformis* and *L. senckenbergica*; however, in *L. ziegleri* the ornament consists of individual, distinctively noded, thick, high ridges located on either side of the carina (but not attached), in the dorsal half of the platform. The noded ridges typically follow the dorsal margin of the element and are approximately transverse to the carina. Occasionally the ridges curve or suddenly change direction and in some rare cases they bifurcate towards the outer margin (Fig. 4.2g - 6,8 & 9).

Age, location and lithology of samples:

Elements of this species were recovered from fossiliferous marine limestone samples which ranged in age from the upper Brigantian (upper Viséan) to the early Serpukhovian. Productive samples were taken from the Carraun/Lugasnaghta, Kilnamona and St. Brendan's Well Sections.

CNLG15, CNLG19, KMONA1, KMONA3, KMONA4, KMONA5, KMONA6, KMONA8, KMONA9, BW1, BW3, BW4

Lochriea P_2

(Fig. 4.2e – 5)

Description:

P_2-elements belonging to the genus *Lochriea* are angulate in shape with the base identified by a slight flaring (widest approximately ⅓ of the distance from the dorsal end) and an aboral groove in the dorsal ½ to ⅔ of the element. The cusp is positioned slightly ventral of the widest part of the base. Denticles are typically slightly deflected dorsally and decrease in size (rapidly) towards the terminations. The aboral surface in the ventral part of the element is more planar and straight than the typically concave dorsal portion, this gives the elements a characteristic fan-like appearance at their dorsal end.

Age, location and lithology of samples:

Productive fossiliferous marine limestone samples, from all but the Glenade and Glencar Sections, range in age from the lower Asbian (upper Viséan) to the lower Serpukhovian.

GLTV19, AGHA3.2, AGHA10, CNLG15, CNLG19, KMONA1, KMONA3, KMONA4, KMONA5, KMONA6, KMONA8, KMONA9, BW1, BW3, BW4

Lochriea M-element

(Fig. 4.2e – 3 & 4)

Description:

The M-elements of *Lochriea* are dolabrate with a conspicuously tall cusp, which is sharply pointed and continues downwards into a short, sharp aboral process. The dorsal/caudal process is sharply downturned (aborally concave) and bears a dense crest of pointed, elongate denticles on its oral surface. The denticles (~17 or 18)

decrease rapidly in size away from (with the largest denticle partially merged with) the cusp. In oral view the elements are curved with the caudal/ventral surface concave. A basal groove is widest under the cusp, but thins along the underside of the processes.

Age, location and lithology of samples:

Elements were recovered from fossiliferous, marine limestones in all but the Dartry Mountain Sections. Productive samples ranged in age from the upper Asbian (upper Viséan) to the lower Serpukhovian.

AGHA3.1, AGHA3.2, AGHA9, AGHA10, CNLG1, CNLG13, CNLG15, CNLG19, KMONA1, KMONA3, KMONA4, KMONA5, KMONA6, KMONA8, KMONA9, BW1, BW3, BW4

Mestognathus (Bischoff, 1957)

Mestognathids were identified solely from P_1-elements. Since the oral and ventral margins of the P_1-elements are used to differentiate species and (similar to *Cavusgnathus*) these surfaces are often broken or obscured, only a single species (*M. bipluti*) was recognised. Where the designation of the element as *bipluti* was somewhat uncertain, due to the above condition, the sample number is prefixed by a question mark. P_1-elements are carminiplanate in shape and non-symmetrical. The blade is short and attached to the rostral margin of the element. The platform surface is grooved (deepest ventrally) and roughly bisected by a weakly-developed carina. The aboral surface has a grooved keel and an approximately centrally located (distinct) basal pit.

M. bipluti (Higgins, 1961)

(Fig. 4.2b – 4 & 5)

Description:

The two lateral parapets of the P_1-elements of this species are transversely ridged and separated from the carina by a smooth shallow groove. The carina is composed of a row of discrete nodes dorsally, but develops ventrally into a low, rounded ridge. Ventrally (where the fixed blade develops) the carina shifts closer to the

caudal margin, leaving a deeper and wider groove on the rostral side of the carina. Characteristically, the ventral end of the caudal parapet is raised into three denticles. The blade comprises at least six denticles which decrease in size ventrally. A particularly pronounced groove separates the free blade from the caudal parapet ventral to the platform.

Age, location and lithology of samples:

P_1-elements were recovered from upper Asbian (see Section 4.4) and upper Brigantian (upper Viséan) calcareous lithologies in the Aghagrania, Carraun/Lugasnaghta and Kilnamona Sections.

AGHA3.2, ?AGHA11, CNLG7, CNLG8, KMONA4

Neognathodus (Dunn, 1970)

(Fig. 4.2c – 7)

A small number of P_1-elements belonging to this genus were recovered but were not assigned to a species. The P_1-elements have an elongate lanceolate platform, with a flared base which is wider on the rostral side but longer on the caudal side. A dentculate blade is medially attached to the platform and its carinal continuation is flanked by high lateral parapets. The carina comprises a ridge at the ventral end of the platform, but this feature tends to break into widely spaced discrete nodes towards the dorsal margin. The parapets extend to the dorsal margin of the platform, are sub-symmetrical and are separated from the carina by a shallow groove. The caudal parapet comprises transverse ridges and is slightly wider and more elongate than the rostral parapet, which is more noded.

Age, location and lithology of samples:

Elements of this genus were only recovered in a Bashkirian carbonate bullion in the St. Brendan's Well Section.

BW10

Synclydognathus (Rexroad & Varker, 1992)

(Fig. 4.2b – 6)

Due to the paucity of the remains recovered, elements were identified at generic level only. Distinctive S-elements, which are asymmetrically bipennate in form with the two bars diverging at ~20-30º, were typically used to distinguish the genus. Denticles on the S-elements are typically short and broad and slightly bent ventrally. A relatively small basal cavity underlies the cusp, which marks the point of element flexure.

Age, location and lithology of samples:

Elements belonging to the genus were found in marine limestone samples of upper Asbian and uppermost Brigantian (upper Viséan) age in the Aghagrania, Kilnamona and St. Brendan's Well Sections.

?AGHA3.2, AGHA4, KMONA1, BW1, BW3, BW4

Unassigned elements

(Fig. 4.2e – 1, 8-11, Fig. 4.2h – 1-5)

Unidentifiable conodont element fragments, or unassignable P_2-, S- and M-elements were recovered from virtually every productive sample taken from every section spanning the uppermost Holkerian (middle Viséan) to Bashkirian interval.

GLTV14, GLTV16, GLTV17, GLT18, GLTV19, GLTV20, GLTV21, GLTV22, GLTV23, GLTV25, GLTV27, DAGL13, DAGL14, DAGL15, DAGN1, AGHA1, AGHA.A2, AGHA1, AGHA3.1, AGHA3.2, AGHA4, AGHA9, AGHA10, AGHA12, CNLG1, D.K. CNLG.A, CNLG6, CNLG7, CNLG8, CNLG9, CNLG10, CNLG11, CNLG13, CNLG14, CNLG15, CNLG16, CNLG18, CNLG19, KMONA1, KMONA2, KMONA3, KMONA4, KMONA5, KMONA6, KMONA8, KMONA8, KMONA9, KMONA10, BW1, BW2, BW3, BW4, BW10, BW8

4.3 TRANSITIONAL CONODONT FORMS, NATURAL VARIATION AND ABNORMALITIES

Any rich fossil assemblage will typically contain an abundance of "*standard*" morphotypes of any particular species but also several unusual or "*irregular*" forms (ignoring sexual dimorphism and ontogeny), which may be attributable to:

- Diseased, malformed or possibly damaged and repaired specimens inevitably being occasionally recovered despite their relative rarity.
- All species showing some degree of natural (phenotypic) variation caused by their slightly different life history and genotype.
- Species are (typically) constantly evolving into new forms, and therefore must go through transitional morphologies regardless of whether changes are rapid (punctuated speciation) or very slow (phyletic gradualism). The rate and style of evolutionary change will solely affect the temporal and thus stratigraphic range over which intermediate forms would thus be occasionally encountered.

Deciding how conodont elements are categorised and partitioned into neat taxonomic designations can often be a difficult task (e.g. Austin, 1972; 1973).

Any differences between elements of the same species which do not deviate beyond the established morphological bounds of the basic element description were recognised herein as natural variations. In *G. bilineatus*, for example, natural variation in P_1-elements can be expressed in the degree of "kinking" in the ventral part of the carina, or in the lack, or irregular development of portions, of ornament on the rostral extension of the platform (Fig. 4.2d). The basic conditions of the elements are preserved but slightly differently expressed morphologically (i.e. likely phenotypic variation).

The occurrence of intermediate forms is common in all detailed palaeontological studies. This may imply that true transitional forms are present or, alternatively, that perhaps a new species designation is justified. However, if the established species designations are too restrictive, then what is actually a single species (with particularly pronounced natural variation) may have been incorrectly split according to pseudo-distinctive end-members.

If the specimens truly represent evolutionary transitional forms then *ideally* they should be relatively temporally (and therefore stratigraphically) restricted and occur before, and (preferably) not in conjunction with, the descendant form. In reality this is rarely the case, and in many instances numerous sister groups co-exist. Therefore, the FAD of each group is particularly important in order to resolve evolutionary lineages. Transitional forms of the genus *Lochriea* were commonly encountered in both the Carraun/Lugasnaghta (predominantly CNLG14, 15 & 19) and Clare Sections (Figs. 4.3a-b), whilst only rare examples of *G. girtyi-G. bilineatus* intermediates were discovered in the Carraun/Lugasnaghta and St. Brendan's Well Sections (Fig. 4.2d – 7 & 9).

Intermediate *G. girtyi – G. bilineatus* forms have a transitional caudal parapet and a poorly defined *G. girtyi* type rostral parapet, which expands into an elongate, partially ornamented *G. bilineatus* type platform.

Morphologically intermediate forms were identified within the genus *Lochriea* between several species (Table 4.3a):

Morphotype 1	Morphotype 2	Fig.
L. commutata	*L. mononodosa*	
L. commutata	*L. nodosa*	
L. commutata	*L. costata*	**4.3a(6)**
L. mononodosa	*L. monocostata*	**4.3a(1a-b)**
*L. mononodosa**	*L. cruciformis**	**4.3b(1)**
*L. mononodosa**	*L. ziegleri**	
*L. mononodosa**	*L. senckenbergica**	**4.3b(5 & 7)**
L. nodosa	*L. costata*	**4.3a(2a-b)**
L. nodosa	*L. cruciformis*	**4.3a(3a-b)**
L. nodosa	*L. ziegleri*	**4.3a(4 & 7, a-b)**
L. nodosa	*L. senckenbergica*	
L. ziegleri	*L. cruciformis*	**4.3a(5)**

Table 4.3a Transitional Lochriea forms encountered in this study.

Asterisks associated with certain transitional forms indicate that the "morphotypes" listed are unlikely to represent a real evolutionary lineage, but instead forms with intermediated morphology best described by the two end-member species.

Many of the intermediate forms bear extremely complex ornament typical for evolved forms of *Lochriea* on one side of the platform but because the other side is completely bare or only simply noded (Figs. 4.3a-b), elements (essentially) taxonomically regressed to the more morphologically conservative, stratigraphically older classifications due to the (possibly inadequate) current species definitions. These elements with asymmetric, obviously highly evolved, complex ornamentation were only encountered in the upper Brigantian and Serpukhovian, yet their current ambiguous definition will not recognise their biostratigraphical importance. The relevance of these asymmetrically evolved *Lochriea* species is in the fact that their occurrence is intimately linked with that of *L. ziegleri*, a species with significant implications for the Viséan-Serpukhovian boundary. It is therefore believed that the current species classifications for the evolved forms of the genus *Lochriea* may need slight adjustments to accommodate the currently poorly-defined forms, but also because:

- Intermediate and difficult to designate specimens are often very common, which would not be expected if the current taxonomic system was more robust.
- Occasionally, apparent evolutionary intermediate forms of a species demonstrate transitions from separate potential ancestral species (e.g. different specimens indicate that both *L. commutata* and *L. nodosa* evolved into *L. costata*).

Abnormal or deformed conodont elements were considered (herein) those which were easily diagnosable to species level but which exhibited additional (usually non-functional) morphological characters (Fig. 4.3c). Virtually all of these irregular specimens belonged to the genus *Lochriea* and were recovered from the Clare Sections. Although this is probably primarily due to the closer scrutiny (morphologically) *Lochriea* elements received due to the enhanced stratigraphic resolution of sampling as well as the sheer abundance of conodont elements recovered from these sections. Irregularities predominantly comprised unusual ornament, nodes and protuberances on areas away from the typical functioning surface (Fig. 4.3c - 1,2,5-7); however, a specimen with slight bifurcation of the ventral tip of the blade was also observed (Fig. 4.3c - 4). Abnormalities probably did not greatly effect the functioning of the elements given their mature size. In one

specimen, however, which exhibited an unusual concave oral surface (typically relatively flat) with the lateral parapets raised and curling inward over the poorly developed carina, it is difficult to conceive how the element could have continued to function properly in an occlusal fashion (Fig. 4.3c - 3). Determining the cause, whether teratological or pathological of these abnormalities remains speculative.

4.4 CONODONT BIOSTRATIGRAPHY, WITH AN EMPHASIS ON THE GENUS *LOCHRIEA*.

The stratigraphic ranges of diagnosed conodont genera and species for the NW Ireland region, spanning the *Lochriea commutata, Gnathodus bilineatus, Mestognathus bipluti, Lochriea nodosa and Lochriea ziegleri* Biozones, are shown in Fig. 4.4a. The stratigraphic ranges of conodonts recovered from the Kilnamona Section (which exposes strata within the *L. ziegleri* Biozone) are shown in Fig. 4.4b, whilst those from the St. Brendan's Well Section (from the *L. ziegleri* and *Declinognathodus noduliferous* Biozones) are shown in Fig. 4.4c.

As discussed in Chapter 1, and seen in various figures relating to Chapters 1, 2, 4 and 5, the precise placement of the Asbian-Brigantian boundary in NW Ireland is currently the subject of some debate. Traditionally, goniatites (P_{1a}/P_{1b} Biozone boundary - Brandon & Hodson, 1984; Legg *et al.*, 1998; Sevastopulo & Wyse Jackson, 2009), and to a lesser extent miospores (NM/VF Biozone boundary - Higgs, 1984), have constrained the Asbian-Brigantian boundary to within the lower part of the Doobally Sandstone Member, in the upper Bellavally Formation. Recently, (predominantly) microfaunal re-evaluation of the lower Leitrim Group has proposed that the boundary be shifted to the Dartry-Meenymore Formation boundary, lower in the sequence (Cózar *et al.*, 2005; 2006; Somerville *et al.*, 2009). The conodont work of Kelly (1989), *specifically* the identification of *L. nodosa* and *M.* aff. *bipluti* in the Meenymore Formation, was of some importance to this proposed stratigraphic revision. However, these species, typically taken as indicative of a Brigantian age, were recovered in notably low quantities (single specimens in a sample quoted as yielding 600+ elements/kg) and Kelly (1989) originally proposed that these isolated and impoverished occurrences were anomalous and therefore not unequivocally indicative of Brigantian strata.

Some of the sampled beds of Kelly (1989) were revisited during this work in an attempt to help resolve the Asbian-Brigantian boundary issue. Over 6.5kg of rock from two horizons (AGHA3.1 and AGHA3.2) within the limestone bed directly

underlying the Dorrusawillin Member (Meenymore Formation), were acid-etched in an attempt to replicate the conodont yield of sample AB7 (Kelly, 1989). This did not produce a positive result and the inability to replicate the reported yields can probably be attributed to variation between slightly different sub-horizons within the unit being processed (Kelly also obtained a barren sample from the same limestone unit). The conodont fauna recovered from AGHA3.1 & 3.2 (Fig. 4.4a) was similar to that reported by Kelly (1989) for AB7. However, there was one significant exception: no *L. nodosa* P_1-elements were recovered (despite the recovery of several *L. commutata* P_1-elements as well as other conodont species typical of the same biofacies). Some small inconsistencies in the work of Kelly (1989) may suggest that his findings relating to the Aghagrania Section should be treated with a degree of caution:

(1) It is stated on page 63 that "*the first laminated carbonates are found 2.5 metres above"* the base of the Meenymore Formation. However, in the photograph provided (page 86) the first laminites are shown to be only ~70cm higher in the sequence.

(2) Figures 2.3.11 and 2.3.12 in Kelly (1989) both contain minor inaccuracies relating the placement of geological boundaries or recent geographic features.

L. nodosa P_1-elements were first encountered in the Ardvarney Limestone Member of the Carraun Shale Formation (Fig. 4.4a), which is in agreement with previous work (Aldridge *et al.*, 1968; Austin & Husri, 1974). The figured specimen reported by Kelly (1989) is unequivocally a P_1-element of *L. nodosa*, thus there are three possible explanations:

(1) Given the seeming reliability of the species for identifying Brigantian age strata, the Asbian-Brigantian boundary should be lowered as suggested by Cózar *et al.* (2005) and the ammonoid and miospore biostratigraphy re-examined.

(2) The species may, perhaps, have occurred in low numbers in the late Asbian before becoming more ubiquitous in the Brigantian.

or

(3) It is possible that the reported occurrence of this species in the Meenymore Formation may (*perhaps*) reflect some sample contamination, given the

paucity of specimens reported and the failure (by this study) to replicate its occurrence.

The occurrence of *M. bipluti* P_1-elements in the Meenymore Formation was, however, confirmed by this study (although in low numbers - 3 elements/2kg). Traditionally (Higgins, 1985; Varker & Sevastopulo, 1985), this species was accepted as ranging from the lower Brigantian to the uppermost Pendleian (middle Serpukhovian). However, it is not interpreted (herein) as definitively indicating a Brigantian age for two principal reasons:

(1) It appears in relative isolation in the Meenymore Formation, and does not re-occur until the upper Bellavally and lower Carraun Shale Formations, despite several intervening lithologically similar and conodont-rich horizons.

(2) The genera is generally taken as being restricted to shallow, near-shore hypersaline palaeoenvironments (von Bitter *et al.*, 1986), and given its specific habitat requirement its recognised stratigraphic extent might be poorly resolved (i.e. it may be a facies fossil). There are however, numerous examples of *Mestognathus* inhabiting non-restricted palaeoenvironments (pers. comm. G. D. Sevastopulo, 2010).

and

(3) Significantly, *M. bipluti* has been reported from late Asbian strata elsewhere in Ireland (Somerville & Somerville, 1998; Somerville, 1999).

The first recognised appearance of *G. bilineatus* occurs in the Meenymore Formation, in the same unit as *M. bipluti*. *G. bilineatus* typically first appears in the middle Asbian (Varker & Sevastopulo, 1985) and ranges into the Serpukhovian (Higgins, 1985), and even Bashkirian (Nemyrovska, 1999). Given the ubiquitous occurrence of this particular species, particularly in the upper Viséan, its first appearance in the Meenymore is significant and probably indicative of the formation's (true) upper Asbian age.

Considering the merits of the work in favour of modifying the Asbian-Brigantian boundary (Cózar *et al.*, 2005; 2006; Kelly, 1989; Somerville *et al.*, 2009), but pending further evidence, it is thought sensible to demonstrate the current level of

biostratigraphical uncertainty by displaying both possibilities for the boundary (e.g. see Fig 4.4a).

As discussed in Sections 1.2 and 1.5.1 the first appearance of complex forms of *Lochriea*, in particular *L. ziegleri* (Nikolaeva *et al.*, 2009a; 2009b; Richards & Group, 2008) and in the past (but to a lesser extent) *L. cruciformis* (Belka & Lehmann, 1998), have been proposed as possible candidates for marking the basal-Serpukhovian boundary, despite commonly appearing earlier than current definitions (*C. leion*, Fig. 1.2.1a), in the upper Brigantian (Nemirovskaya *et al.*, 1994; Skompski *et al.*, 1995). In the Carraun/Lugasnaghta Section both *L. cruciformis* and *L. ziegleri* first appear in the bullion horizon (CNLG14) between the Ardvarney and Sranagross Members (Carraun Shale Formation, Fig. 4.4a). Other complex forms such as *L. costata*, *L. monocostata* and *L. senckenbergica* appear in the Sranagross Member, only slightly stratigraphically higher in the sequence. This suggests that, under the new definition, the Viséan-Serpukhovian boundary would be stratigraphically lowered by over 15m (in the Carraun/Lugasnaghta Section) to within the P_{2a} ammonoid biozone.

The appearance of complex *Lochriea* forms, only a short stratigraphic distance above the FAD of the preceding (*possibly* ancestral) species *L. nodosa* (CNLG13) and below the first definitive *L. mononodosa* (CNLG15), may suggest that greater investigation needs to be undertaken lower in the sequence to conclusively prove that the apparent FAD are infact real. A single, sediment encrusted, possible *L. mononodosa* P_1-element was also recovered from the CNLG13 sample. The approximate coincidence of the appearance of “evolved” *Lochriea* forms with the stabilisation of marine conditions over the area may also require further investigation to disprove any environmental bias in the apparent biostratigraphic range. Support for the FAD (identified herein) for the evolved *Lochriea* forms comes from:

(1) Specimens, though low in number, consistently appear in, and above, the FAD sample, despite differential overall conodont yields (even in relatively conodont-poor samples).

(2) No indication of complex forms was found in this or other studies (Aldridge *et al.*, 1968; Austin & Husri, 1974) despite several stratigraphically lower

horizons yielding rich conodont faunas (many of which are indicative of the same open-marine conodont Biofacies).

Due to the co-occurrence of well-preserved ammonoids and conodonts, the Carraun/Lugasnaghta Section may, thus, have a considerable impact on the acceptance or rejection of complex *Lochriea* forms for defining the Viséan-Serpukhovian boundary.

Unfortunately, in both the Co. Clare Sections investigated (Kilnamona and St. Brendan's Well) complex *Lochriea* forms had already evolved and were present in the stratigraphically lowest beds examined (Fig. 4.4b-c). The sections cannot therefore provide any information as to the timing of the FAD of *L. ziegleri* or *L. cruciformis*. All that is evident is that in both sections complex *Lochriea* forms, including *L. ziegleri* and *L. cruciformis*, appear below the traditionally recognised level of the Viséan-Serpukhovian boundary.

The conodont faunas from the Clare Sections do demonstrate the biostratigraphical (and thus temporal) similarities between the sections examined in this work, particularly between the Kilnamona and St. Brendan's Well Sections. Conodont biostratigraphy also reinforces the proposal that the temporal gaps represented by possible palaeokarsts in the Slievenaglasha and Magowna Formations (Co. Clare Sections) are not of significant magnitude. No major faunal changes are apparent at the Slievenaglasha-Magowna contact in either section, although *G. homopunctatus* and *L. costata* do disappear at the boundary in the Kilnamona Section. The disappearance of *L. costata* is not seen as significant, given its paucity in samples in general; however, the disappearance of *G. homopunctatus* is possibly indicative that the apparent palaeokarst is real but, given the continuation of all other fauna, not temporally significant. An abrupt faunal turnover is observed at the Magowna-Clare Shale contact in the St. Brendan's Well Section (Fig. 4.4c). Every conodont (Viséan and, according to possible definitions, Serpukhovian in age) identified below this contact disappears (except the genus *Idioprioniodus*) and in the first productive sampled bed above the contact (BW10, 2.3m stratigraphically higher), lower Bashkirian conodont forms are encountered. This result strongly agrees with

considerable condensing of the St. Brendan's Well Section at the base of the Clare Shale Formation (particularly in the phosphate lag, see Sections 3.2.2 & 3.4).

4.5 ICHTHYOLITH FAUNA

Ichthyoliths (recovered from sample residues) generally proved difficult to assign to specific (or even generic) level due to both a lack of published work on comparable material and the fact that many ichthyoliths are very morphologically conservative (e.g. Duncan, 1999). The ichthyolith material discussed below was identified (using the published literature and unpublished Ph.D. research referenced in the appropriate sections) to as fine a taxonomic level as possible. Where exact designations proved difficult, elements were grouped according to similar overall morphology and inferred similar function or origin.

Class Acanthodii (Owen, 1846)

Acanthodian scales

(Fig. 4.5a – 8-9, Fig. 4.6a – 3 & 5)

Description:

Comprises a (mushroom-like) dome-shaped base separated from a quadrilateral crown by a defined neck. The base varies from being almost symmetric and very shallowly domed, to being particularly asymmetric and vertically exaggerated into a rounded cone. Crowns are generally flat, simple and equivalent in size or slightly smaller than the base; however, some specimens are weakly ornamented or concentrically lineated, whilst other enameloid crowns are enlarged and are extended into thin (almost) tear-drop shaped plates. These scales are typically ~0.4mm in width and length and slightly smaller in height.

Scales of this type were identified through comparison with numerous studies (e.g. Burrow *et al.*, 2009; 2010; Duncan, 1999).

Age, location and lithology of samples:

Found in samples ranging from upper Holkerian (middle Viséan) to Bashkirian age, from virtually every section investigated (except the Glenade Section) and from a variety of lithologies.

GLTV12, ?GLTV13, GLTV14, GLTV16, GLTV19, GLTV23, GLTV27, GLTV32, DAGL13, AGHA1, AGHA4, AGHA9, AGHA10, AGHA11, AGHA12, AGHA13,

CNLG1, CNLG2, D.K. CNLG.A, CNLG7, D.K. CNLG ABV. DERREENS, CNLG8, CNLG9, CNLG10, CNLG13, CNLG14, CNLG15, CNLG16, CNLG17, CNLG19, KMONA1, KMONA2, KMONA3, KMONA4, KMONA5, KMONA6, KMONA8, BW3, BW4, BW10, BW8

Class Anaspida (Traquair, 1899)

***Conopiscius* sp.** (Briggs & Clarkson, 1987)

(Fig. 4.5b – 4 & 8)

Description:

Two elements of apparent *Conopiscius* affinity were identified via comparison with the work of Dzik (2009). The elements are hollow, broadly conical in shape and curved. They are teardrop-shaped in cross-sectional outline, with the point of the tear-drop defining the concave surface of the curved element. The sharp concave edge is ornamented with small projecting cusps, which give the concave edge a serrated appearance. The surface of the elements appears smooth, although portions of one specimen exhibited a fine reticulate pattern of delicate ridges. Elements are ~0.9mm in length and ~0.4mm in depth at their base.

Age, location and lithology of samples:

Only one sample in the Meenymore Formation, Aghagrania Section of upper Asbian (upper Viséan) age yielded specimens. The sampled bed was a muddy wackestone in a sequence associated with hypersaline conditions.

AGHA4

Class Chondrichthyes (Huxley, 1880)

Teeth

Cladodont morphotypes

(Fig. 4.5c – 1,3,4,6 & 8)

Description:

The term cladodont is used to classify any ichthyolith with multiple isolated cusps arranged along the entire anterior margin of (and almost perpendicularly to), a planar or slightly dorsally convex (broadly D-shaped) basal plate. The largest cusp is positioned closest to the axis of symmetry of the basal plate, whilst minor cusps are generally arranged symmetrically on either side. Cusps may be simple, but more often they are marked by defined (occasionally basally bifurcating) ridges with a particularly distinct ridge defining the edge separating the anterior and posterior faces. Cusps are often slightly posteriorly curved and in some cases show a preferential inclination towards one end of the plate. The basal plate is often marked by distinct foramen and articulating nodes on the posterior tip of the structure (dorsal surface) and also on the anterior (ventral) surface. Various morphotype deviations on this basic plan were discovered, with the number of cusps ranging from a minimum of 3 to a maximum of 17 and basal plates ranging from a rounded rectangular outline to a thin triangular shape respectively. The most common morphotype consisted of 5 cusps (with the central cusp averaging ~1mm in height) on a D-shaped hexagonal or pentagonal base (averaging ~0.2mm in thickness, ~1.3mm in length and ~0.75mm from the anterior to the posterior).

Age, location and lithology of samples:

Cladodonts were found in samples ranging from uppermost Holkerian/lowermost Asbian (middle/upper Viséan) to the Bashkirian, in all sections except the Glencar and Glenade Sections and in variety of calcareous lithologies.

GLTV14, GLTV16, GLTV17, GLTV27, GLTV28, GLTV30, GLTV32, GLTV33, GLTV35, GLTV36, GLTV39, AGHA1, AGHA3.1, AGHA3.2, AGHA4, AGHA10, AGHA11, AGHA13, CNLG1, CNLG6, CNLG7, CNLG8, CNLG9, CNLG10, CNLG13, CNLG14, CNLG16, CNLG19, KMONA1, KMONA2, KMONA3,

KMONA4, KMONA5, KMONA6, KMONA8, KMONA9, BW1, BW2, BW3, BW4, BW5B, BW10

Ginteria (Duffin & Ivanov, 2008) and ***Cooleyella*** (Gunnell, 1933)

(Fig. 4.5b – 1,2,5,7 & 10)

Description:

Both of these genera comprise a triangular-shaped crown separated from a broadly triangular-shaped base by a constricted neck. The two genera are typically easily distinguished, but a few somewhat intermediate morphologies (which are thought to be closer to *Cooleyella)* proved difficult to classify individually and so the two genera were considered together (Table 4.5a)

Genus	Description	Outline
Ginteria Fig. 4.5b(1,5 & 10) **Comparative work** Duffin & Ivanov (2008)	Crowns are sharply triangular in outline (both in dorsal and lateral view) with the anterior end pointed and the posterior raised into a sharp edge. The crown surface is smooth and weakly concave (dorsally). A sharply defined neck separates the crown from the base. The base is relatively flat and pointed at its anterior end but expands into a descending plate approximately as broad as the crown in its posterior. Distinct but small foramens are visible on both the anterior and posterior faces of the base. Crowns are typically ~0.5mm wide and ~0.4mm from anterior to posterior, whilst the denticles as a whole are ~0.35mm tall.	
Cooleyella Fig. 4.5b(2 & 7) **Comparative work** Ivanov (2005) and Duffin & Ivanov (2008)	Crowns are slightly convex (dorsally) and more rounded and elongate than those of *Ginteria*; however, they maintain a broadly triangular shape. The crown is pointed anteriorly and raised posteriorly into an edge with a poorly-defined, off-centre rounded peak. A short, relatively subtle neck separates the base from the crown. The anterior of the base is pointed and bears a pronounced ventral hollow. The base expands and descends beyond the posterior margin of the crown (when viewed dorsally). A distinct notch exists in the centre of the posterior edge of the base. Denticles are ~0.3mm tall and typically measure ~0.7mm long and ~0.45mm, ~0.25mm from the anterior to posterior of the base and crown respectively.	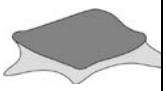

Table 4.5a Characteristics of the genera Ginteria and Cooleyella.

Age, location and lithology of samples:

Denticles of these two genera were found in samples ranging from the lower Asbian (upper Viséan) to the basal Serpukhovian, in nearly all sections (but not Glencar and Glenade), but generally only in particularly fossiliferous marine limestones.

?GLTV30 AGHA3.1, AGHA3.2, AGHA4, CNLG7, CNLG10, KMONA3, KMONA4, KMONA5, KMONA6, KMONA8, BW3, BW4

"Lissodus" (Brough, 1935) **morphotypes**

(Fig. 4.5d – 2-3)

Description:

These comprise teeth structures which are anteriorly-posteriorly compressed into ridge-like bodies formed from rounded, (very) poorly-defined, merging cusps atop a similarly shaped base. Cusps are always simple and the largest is almost always approximately centrally located. A thickened and slightly projecting "lip" very occasionally defines the base of the crown. More commonly, however, the transition from the crown to the base runs smoothly into a slight neck. Bases broadly mirror the same elongate shape as the crowns, but are slightly expanded aborally. Large foramina are commonly visible along the base. Teeth of this type were typically large, averaging ~2mm in length.

Teeth were ascribed as "Lissodus" morphotypes through consultation with Duncan (1999), Ivanov (1996) and Lebedev (1996).

Age, location and lithology of samples:

Found in samples from basal Asbian (upper Viséan) to basal Serpukhovian age, in all sections investigated but from only relatively fossil-rich marine limestone beds.

GLTV16, GLTV18, GLTV36, DAGL15, DAGN1, AGHA4, CNLG1, CNLG6, CNLG8, CNLG10, KMONA1, KMONA4, KMONA5, KMONA6, KMONA8, BW3, BW4

"Orodus" (Agassiz, 1838) **morphotypes**

(Fig. 4.5d – 1)

Description:

These consist of anteriorly-posteriorly compressed teeth which are broadly similar to those described as "Lissodus" above. Orodont-type teeth are, however, not as

compressed and exhibit very poorly-defined (virtually merged), smooth, rounded cusps. Generally three cusps are distinguishable, but occasionally only one (the central and always most prominent cusp) is apparent. The surface of the crown is typically covered by numerous very fine pits, which possibly define canal openings. The bases of the teeth are often poorly preserved. A particularly large specimen (~6mm long; "average" teeth are generally ~3mm) recovered from a hand sample of the Dorrusawillin Member (Meenymore Formation, Aghagrania Section) did, however, possess a base which was equal in height to the crown (~1.9mm each) and broadly convex dorsally, following the upper domed surface of the crown (Fig. 4.5d – 1).

Teeth of this type were termed "Orodus" morphotypes based on their similarity to teeth described and figured previously (e.g. Ginter, 2009; Lebedev, 1996).

Age, location and lithology of samples:

These teeth were found in samples ranging from the lower Asbian (upper Viséan) to the uppermost Brigantian (uppermost Viséan), in the Tievebaun, Aghagrania, Kilnamona and St. Brendan's Well Sections. This ichthyolith was dominantly found in fossiliferous marine limestones, but also occurred in calcareous, fossiliferous marine shale.

GLTV21, AGHA1, AGHA3.2, AGHA D1 (Dorrusawillin Mbr. handsample), KMONA5, BW3, BW4

"Protacrodus" (Jaekel, 1921) **morphotypes**

(Fig. 4.5d – 4-6)

Description:

"Protacrodus" morphotype teeth are broadly similar to those described as "Lissodus" (above) and comprise anteriorly-posteriorly compressed ridge-like structures formed from adjoining, distinct cusps atop a similarly shaped, but extended base. Cusps are typically joined by a central ridge separating the anterior and posterior crown faces. The number of cusps is variable, but the largest is characteristically positioned centrally or is only slightly offset (laterally) from the antero-postero central axis. A diagnostic feature of the group is the near vertical ridges which adorn the crown. In dorsal view the teeth are commonly very slightly V-shaped with the central cusp forming the central point of the "V", which is

directed anteriorly. The base displays numerous foramina and although following the broad shape of the crown, it is often significantly extended posteriorly. These teeth average ~1mm in length (though some specimens recovered are often much larger).

This group was termed "protacrodont" based on their similarities with morphologically similar teeth described and figured elsewhere (e.g. Duncan, 2006; Ginter, 2007; 2009).

Age, location and lithology of samples:

Found in samples from uppermost Holkerian/lowermost Asbian (middle/upper Viséan) to basal Serpukhovian age, in virtually every section (except Glencar) but only in commonly fossiliferous marine limestones.

GLTV16, GLTV18, GLTV22, DAGN1, AGHA1, AGHA3.1, AGHA3.2, AGHA4, AGHA10, AGHA13, CNLG10, KMONA4, KMONA5, KMONA6, KMONA8, BW3

***Thrinacodus* sp.** (St. John & Worthen, 1875)

(Fig. 4.5c – 2,5 & 7)

Description:

These very distinctive teeth comprise a tongue-shaped, posteriorly extended base with three enameloid cusps at the anterior end. One of the lateral cusps tends to be enlarged relative to the others, but all are posteriorly inclined or curved. The cusps are always approximately perpendicular to the base, but splay at various angles relative to one another, depending on the shape of the base and therefore probable position within the mouth array (see Duncan, 1999; 2003). Ridges can be traced from the tip of the cusps to the distinct termination of the enameloid crown tissue. Bases extend posteriorly 1-2 times the length of the cusps. The angle between cusps is smaller, and cusps are most equal in size on the smaller plates. Bases appear to be elongated on the side opposite the largest cusp, but appear thickest on the side of the largest cusp. Foramina are commonly visible on the base of the teeth, with the largest occurring in the swollen area on the side of the largest cusp. The teeth average ~0.6mm in length (but attain lengths of over 1mm), ~0.3mm in height (cusp length) and ~0.25mm in width, however these parameters are highly variable depending on the morphology of the base.

Thrinacodus sp. teeth were identified through comparison with Duncan (2003), Ginter (2009), Ginter & Sun (2007) and Ivanov (1996; 2005).

Age, location and lithology of samples:

Found in samples ranging in age from the upper Holkerian (middle Viséan) to basal Serpukhovian, in virtually every section investigated (except Glenade) and from a variety of marine limestones.

GLTV12, GLTV16, ?GLTV20, GLTV27, GLTV32, GLTV36, ?GLTV37, DAGL2, AGHA10, CNLG1, CNLG13, KMONA1, KMONA4, KMONA5, KMONA6, KMONA8, BW1, BW2, BW3, BW4

***Xenacanthus* sp.** (Beyrich, 1848)

(Fig. 4.5b – 6 & 9)

Description:

These comprise a domed, hemispherical base with three relatively large, slightly anteriorly inclined cusps. Enameloid cusps bear fine ridges which bifurcate basally and descend almost to the bottom of the tooth on the anterior face, but are simpler and restricted to the top of the cusp on the posterior face. A defined median ridge separates the anterior and posterior faces and runs across all three cusps. The central cusp is generally slightly smaller than the (equal in size) lateral cusps; however, since it originates higher up on the dome-like base, all cusps terminate at essentially the same height. Bases are covered in fine pits giving a somewhat "golfball-like" appearance. The posterior of the base on the dorsal and ventral surfaces bears a large foramen. An articulating node is located at the anterior side of the ventral surface of the base and is flanked by 2 more foramina. Teeth average ~0.6mm in height, ~0.5mm in basal width and ~0.75mm in lateral cusp tip-to-tip width.

Xenacanthus teeth were identified through comparison with Ivanov (1996) and Lebedev (1996).

Age, location and lithology of samples:

Xenacanthus sp. teeth were only found in upper Brigantian (uppermost Viséan) and basal Serpukhovian fossiliferous marine limestone samples from the Kilnamona and St. Brendan's Well Sections in Co. Clare.

KMONA1, KMONA3, KMONA4, KMONA5, KMONA6, KMONA8, BW3, BW4

Tooth whorls and families

(Fig. 4.5e – 1-6)

Description:

This grouping includes any associations of multiple teeth, whether whorls (curved plates with successively mature and enlarged teeth) or families (immature teeth found adjoined to [in readiness to replace] more mature teeth). Several different forms were recovered during this study, but most comprised units of anteriorly-posteriorly compressed teeth with an enlarged central cusp and reduced lateral cusps. Many examples were restricted to a single sample occurrence; however, one form was found in a number of samples and sections (Fig. 4.5e - 3,5 & 6). These teeth families consist of compressed teeth (comprising three or five cusps) with a median crest and a pronounced ridge, which runs posteriorly down from the base of the central (main) cusp and continues posteriorly out along the enlarged basal plate. In side profile the teeth are inclined anteriorly. The immature teeth are found in the concave underside of the anterior face of the teeth. A maximum of three teeth were discernable on any specimen.

Age, location and lithology of samples:

Teeth families or whorls were found in samples ranging from uppermost Holkerian/lowermost Asbian to uppermost Brigantian (middle/upper Viséan to upper Viséan), in the Tievebaun, Carraun/Lugasnaghta, Kilnamona and St. Brendan's Well Sections, but only in fossiliferous marine limestones.

GLTV16, GLTV22, ?CNLG6, ?CNLG13, KMONA3, KMONA4, KMONA5, BW3, BW4

Denticles

"Ctenacanth-type" scale morphotypes

(Fig. 4.5f – 1-3)

Description:

These consist of elongate denticles with posteriorly-directed, fan or wave-like dorsal cusp surfaces. Cusps may be smooth, with only shallow grooves, or they may be strongly ridged and partially separated into individual odontodes towards the

posterior termination. Cusps are separated from their (generally slightly flared, dorsally convex) bases by a neck of varying constriction. The antero-postero basal dimensions of the denticles are generally half the overall base lengths (up to ~1mm), whilst crown dimensions tend to be greater than those of the base.

The denticle forms outlined above are very similar to those described as "ctenacanth" in other studies (e.g. Duncan, 1999; Ginter, 2007; Ivanov, 1996). The term "ctenacanth-type" is thus utilised here in recognition of this morphological similarity.

Age, location and lithology of samples:

Found in samples ranging from the upper Holkerian (middle Viséan) to the Bashkirian, in virtually all sections (except the Glenade Section) and from a variety of lithologies. Denticles of this type were found to be quite common in certain samples.

GLTV12, GLTV15, GTLV16, GLTV19, GLTV22, GLTV28, GLTV32, GLTV35, DAGL3, AGHA1, AGHA3.1, AGHA4, AGHA9, AGHA10, AGHA11, AGHA13, CNLG1, D.K. CNLG.A, D.K. CNLG SHEENA, CNLG6, CNLG10, CNLG14, CNLG19, KMONA1, KMONA2, KMONA3, KMONA4, KMONA5, KMONA6, KMONA8, BW3, BW4, BW10

"Listracanthus-type" scale morphotypes

(Fig. 4.5f – 5)

Description:

"Listracanthus-type" denticles are similar in general appearance to the "ctenacanth-type" denticles described above, but they exhibit more distinguishing characters. Denticles are (comparatively) not as elongate, but are taller and only gently posteriorly curved. Crowns are ridged, have a broadly tri-cusped lanceolate shape (median peak being the largest) and are separated from the slightly flared base by a short neck. Ridges typically become adorned by small bulbous nodes towards the base. Denticle bases are typically convex upwards, ~0.4mm long and ~0.2mm in depth (antero-postero dimension) whilst crowns are 1.25-1.75 times the basal length.

Denticles of this type were determined as "listracanthus-type" based on similarities with material described by Ivanov (2005).

Age, location and lithology of samples:

"Listracanthus-type" scales were found in samples from the lower Asbian (upper Viséan) to the lower Serpukhovian (in all but the Glencar and Glenade Sections) and in typically fossiliferous marine limestones. These denticles were generally of low abundance.

GTLV17, AGHA4, AGHA9, AGHA10, CNLG14, CNLG19, KMONA5, KMONA6, BW3

"Mucous-membrane" morphotypes

(Fig. 4.5f – 4)

Description:

Denticles of this type comprise a series of posteriorly deflected, overlapping, broadly conical cusps which are arranged in a row. In cross-sectional profile cusps ranged from simple and almost circular, to ridged (occasionally bifurcating towards the base) with a curved D-shape (flatter side facing anteriorly). Cusps increase in size towards the posterior end and either coalesce or simply merge with the base. The base is generally slightly arched (convex upwards). Denticles average ~0.7mm in antero-postero length, ~0.35mm in width and ~0.5mm in height. Two basic forms were discovered, although some variation between the two exists:

(i) Cusps arranged in a single row

(ii) Cusps arranged in parallel adjacent rows

Denticles were determined as "mucous membrane-type" based on their close comparison to similar structures described by Duncan (1999).

Age, location and lithology of samples:

Found in samples ranging from upper Holkerian (middle Viséan) to uppermost Brigantian (uppermost Viséan) in all the sections studied (except the Glencar and Glenade Sections), but in only certain marine limestones and even then, in low concentrations.

GLTV13, GLTV950NOD, GTLV16, GLTV27, AGHA3.2, AGHA4, AGHA9, AGHA10, AGHA11, CNLG6, CNLG7, CNLG8, CNLG10, CNLG13, KMONA4, KMONA5, BW4

Hybodont placoid morphotypes

(Fig. 4.5g – 1-10)

Description:

A complex variety of small denticles were characterised as "hybodont-placoid" according to similarities with those figured and discussed in the literature (e.g. Delsate *et al.*, 2002; Derycke-Khatir *et al.*, 2005; Duncan, 1999). Three basic morphological categories were recognised herein (Table 4.5b):

Morphotype	Description	Outline
Button- or mushroom-like Fig. 4.5g(1-4)	Typified by a smooth, domed crown surface. Various shapes occur and the denticles can be either taller than wide (somewhat columnar) or low and flat-lying. Occasionally, small nodes or ribs are developed near the crown's basal termination. A short, slightly constricted neck separates the crown from a base that is generally smaller than, or equivalent in size to, the crown. The denticles range from ~1mm to ~0.25mm in size.	
Heart and lanceolate Fig. 4.5g(7-9)	Invariably comprise a tapering, posteriorly-deflected or antero-postero inclined crown. Crown outlines show very little gross variation in their tear-drop or lanceolate shape. Many specimens exhibit a central keel on the dorsal surface as well as definition of the lateral margins into weakly raised "wings". Others only demonstrate weakly defined grooves running parallel to the lateral margins, or subtle ridges near the crown base. Definition of all structures becomes less distinct towards the posterior tip. A defined neck separates the crown from a slightly flared base. Bases are typically cross shaped with four (approximately equal) projections defining the anterior, posterior and lateral points of the base. Lateral projections are commonly deflected slightly posteriorly. These denticles average ~0.5mm in height and ~0.3mm in width.	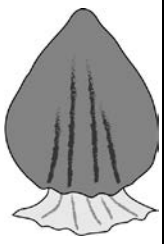
Thorn- and flame-like Fig. 4.5g(5,6 & 10)	No strict morphological definition was applied to this category. However, a basic morphological form is evident - All the denticles have a pointed dorsal termination to their (generally strongly) textured (almost invariably) singularly cusped crowns. Thorn-like denticles average ~0.5mm in height. Thorn-like forms are typically strongly ribbed (particularly towards the base of the crown), elongate along the antero-postero axis, and show some deflection posteriorly. Flame-like forms are tall, almost vertical in orientation and comprise a complex array of sub-vertical pronounced ribs (each ornamented with numerous nodes and processes), which merge into a central point. Flame-like denticles average ~0.9mm in height.	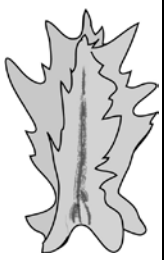

Table 4.5b Hybodont placoid morphotype descriptions.

Age, location and lithology of samples:

Hybodont placoid denticles were found in samples ranging from the upper Holkerian (middle Viséan) to the basal Serpukhovian, in all sections examined and in a variety of lithologies.

GLTV13, GLTV14, GLTV15, GLTV16, GLTV17, GLTV18, GLTV19, GLTV20, GLTV22, GLTV23, GLTV27, GLTV28, GLTV32, GLTV37, DAGL3, DAGL4, DAGL14, DAGN1, AGHA1, AGHA3.1, AGHA4, AGHA9, AGHA10, AGHA11, AGHA13, CNLG1, D.K. CNLG.A, D.K. CNLG SHEENA, CNLG7, CNLG10, CNLG12, CNLG14, CNLG16, CNL19, KMONA1, KMONA2, KMONA3, KMONA4, KMONA5, KMONA6, KMONA8, KMONA9, BW1, BW3, BW4

Nested morphotypes

(Fig. 4.5i – 3)

Description:

Represented by particularly morphologically distinctive denticles which comprise a series of “nested”, concave lanceolate odontodes which increase in size posteriorly, partially enveloping the preceding cusp. Weak vertical ridges are apparent on both the dorsal and ventral surfaces of the crown. A slight neck separates the mildly posteriorly-deflected crown “nest” from a (weakly) expanded base. The base broadly follows the outline of the crown and exhibits numerous small foramina. Denticles average ~0.7mm high and ~0.6mm in width and depth.

Age, location and lithology of samples:

Denticles of this type were recovered from only two samples, which range from the basal Asbian (upper Viséan) to the upper Asbian (upper Viséan). These productive marine limestone samples were removed from the Tievebaun and Aghagrania Sections.

GLTV18, AGHA3.2

Class Osteichthyes (Huxley, 1880)

Teeth

Palaeoniscid

(Fig. 4.5b – 3 & 11)

Description:

These teeth structures comprise simple, (generally) slightly curved, cones with a partially hollow base and a characteristic translucent, tapered acridine tip. Extremely fine, very impersistent vertical ridges are occasionally developed in dense networks on the tooth surface away from the acridine tip. Teeth are typically ~0.7mm tall and ~0.3mm wide at the base.

Age, location and lithology of samples:

Palaeoniscid teeth are extremely common microfossils, and were found in numerous samples from various lithologies, in every section investigated, ranging from the upper Holkerian (middle Viséan) to the Bashkirian. They were often found in considerable abundance.

GLTV12, GLTV13, GLTV14, GLTV15, GLTV16, GLTV17, GLTV18, GLTV19, GLTV20, GLTV21, GLTV22, GLTV23, GLTV24, GLTV25, GLTV27, GLTV28, GLTV29, GLTV30, GLTV32, GLTV33, GLTV34, GLTV35, GLTV36, GLTV37, GLTV38, GLTV39, GLTV40, DAGL1, DAGL2, DAGL3, DAGL13, DAGL14, DAGL15, DAGN1, AGHA.CAV1, AGHA1, AGHA3.1, AGHA3.2, AGHA4, AGHA6, AGHA9, AGHA10, AGHA11, AGHA13, CNLG1, CNLG2, D.K. CNLG.A, D.K. CNLG SHEENA, CNLG6, CNLG7, CNLG8, CNLG9, CNLG10, CNLG11, CNLG13, CNLG14, CNLG15, CNLG16, CNLG18, KMONA1, KMONA2, KMONA3, KMONA4, KMONA5, KMONA6, KMONA8, BW1, BW2, BW3, BW4, BW10

Scales

Actinopterygii (Klein, 1885)

(Fig. 4.5a – 1-7)

Description:

Scales belonging to this subclass are typically rhomboidal in shape, with a smooth, enameloid surface which is commonly ornamented by simple grooves and/or pits. On some particularly well-preserved examples, a short articulating process may be found along the margin of the scale. Scales are typically thin and flat, although, weakly concave or convex forms also occur (possibly reflecting their original position on the fish's body), along with significantly thickened forms and (very rarely) scales with translocated, elongate basal structures. Five main morphotypes (varying in long axis length from ~0.5mm to ~4mm) were identified, and are described in Table 4.5a, below:

Morphotype	Description	Outline
Beading Fig. 4.5a(7)	Elongate, thin enameloid surface defining the hinge line (convex side) of a tunnel or overturned gutter-shaped body.	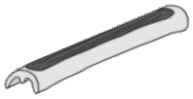
Elongate rectangular Fig. 4.5a(4)	Scale is rectangular and elongate (generally in a 3:1 or 4:1 ratio).	
Rhomb/Diamond Fig. 4.5a(1-3 & 6)	Characteristically rhomb or diamond shaped with curved lineations in the enameloid surfaces following the scale margins.	
Rounded rhomb/lanceolate	Typically comprise enameloid surfaces on a weakly convex rhomb or lanceolate shaped scale with gently rounded corners.	
Spear/Elongate rhomboid Fig. 4.5a(5)	Increased length:width ratios result in significant skewing of the rhomb shape.	

Table 4.5a Morphotypes of Actinopterygian scales.

Scales were identified as actinopterygian in origin through comparison with several studies (e.g. Burrow *et al.*, 2010; Duncan, 1999; Ginter, 2007; Long, 1990).

Age, location and lithology of samples:

Actinopterygian scales were found in samples ranging from the upper Holkerian (middle Viséan) to lower Serpukhovian, in every section investigated and from a variety of lithologies. They are relatively ubiquitous and are often found in significant concentrations.

GLTV12, GLTV13, GLTV14, GLTV15, GLTV16, GLTV18, GLTV19, GLTV20, GLTV21, GLTV22, GLTV23, GLTV24, GLTV25, GLTV26, GLTV27, GLTV28, GLTV30, GLTV32, GLTV33, GLTV34, GLTV35, GLTV36, GLTV37, GLTV38, GLTV39, GLTV43, DAGL1, DAGL3, DAGL13, DAGL14, DAGL15, DAGN1, AGHA1, AGHA3.1, AGHA3.2, AGHA4, AGHA5, AGHA6, AGHA7, AGHA9, AGHA10, AGHA11, AGHA12, AGHA13, CNLG1, CNLG2, D.K. CNLG.A, D.K. CNLG SHEENA, CNLG6, CNLG7, CNLG8, CNLG9, CNLG10, CNLG12, CNLG13, CNLG14, CNLG15, CNLG16, CNLG19, KMONA1, KMONA2, KMONA3, KMONA4, KMONA5, KMONA6, KMONA8, BW2, BW3, BW4

Other

"Gill-raker" or Actinopterygian quadrate bone morphotypes

(Fig. 4.5h – 1-2)

Description:

These structures are characterised by their thin, elongate, plate-like bodies with an oval outlined, concave, socket-like base. One long edge of the plate is deeply grooved whilst both flattened surfaces are marked by shallow grooves running parallel with the long axis of the structure. The structures range in size from ~2mm x ~0.5mm to ~3mm x ~1.5mm.

Similar structures have been interpreted as gill-rakers or Actinopterygian quadrate bones by Duncan (1999) and Delsate *et al.* (2002) respectively.

Age, location and lithology of samples:

These structures were found in samples ranging from uppermost Holkerian or lowermost Asbian (middle/upper Viséan) to the lower Serpukhovian, in all sections except the Glencar and Glenade Sections, but in only some marine limestones.

GLTV14, GLTV32, AGHA4, AGHA10, ?CNLG10, KMONA4, KMONA8, BW4

Incertae sedis

Denticles

Rooted cusp morphotypes

(Fig. 4.5i – 4-6)

Description:

These denticles comprise single or multiple cusps which are characterised by exaggerated (conspicuous), elongate porous root structures. The cusps are typically conical, posteriorly curved and vertically ridged. On specimens with multiple cusps they are arranged in a line, with cusp size increasing posteriorly. There seems to be no strict relationship between the number of cusps in the crown and the overall size of the element. The crown merges directly with the base and there is no intervening neck. Bases taper to a rounded point after attaining a length comparable to, or greater than (up to x2), that of the crown. On specimens with multiple cusps in the crown, bases are (sometimes) mildly swollen near the crown-base junction. Basal surfaces are covered in small canal openings. Elements average ~1.2mm in total length.

Age, location and lithology of samples:

These denticles were found in samples from uppermost Holkerian/lowermost Asbian (middle/upper Viséan) to basal Serpukhovian age, in most sections (all but Glencar and Glenade) but only in fossiliferous marine limestones.

GLTV16, AGHA3.2, AGHA4, AGHA10, CNLG1, CNLG6, CNLG10, CNLG16, KMONA1, KMONA3, KMONA4, KMONA5, KMONA6, KMONA8, BW3, BW4

"Skirted" cusp morphotypes

(Fig. 4.5i – 7-8)

Description:

These ichthyoliths comprise tall, narrow, straight simple cusps, which crown (perpendicularly) small, rapidly-flared bases. Commonly, a small cusp is merged with the main cusp (and is typically less than half the total height). Bases were generally poorly preserved but appear approximately circular in outline and

relatively small. Elements average ~1.5mm in height and ~0.3mm in width (at the base of the central cusp).

Age, location and lithology of samples:

Found in samples which range in age from the lower Asbian (upper Viséan) to the uppermost Brigantian (upper Viséan), in the majority of sections (except Glencar and Glenade), but only in particularly fossiliferous limestones.

GLTV27, AGHA10, CNLG1, CNLG14, KMONA3, KMONA4, KMONA5, KMONA6, BW2, BW3, BW4

"Thorn-like" morphotypes

(Fig. 4.5i – 1-2)

Description:

These structures comprise conical, posteriorly curved denticles somewhat reminiscent of "rose thorns". Crowns are ornamented by fine vertical ridges or, in some cases, four relatively defined vertical edges which can be traced down into the base where they project out into the main buttresses of the base. Samples devoid of edges have somewhat domed bases. Denticles average ~0.5mm in height.

Denticles of this morphotype are somewhat similar to the holocephalon clasper scales of Delsate *et al.* (2002).

Age, location and lithology of samples:

These denticles were recovered from samples which range in age from the upper Holkerian (middle Viséan) to the basal Serpukhovian, in most sections (all except Glencar, Glenade and St. Brendan's Well), but only in certain marine limestones.

GLTV12, GLTV13, AGHA4, ?CNLG1, CNLG9, CNLG15, KMONA6, KMONA8

Plates

Cusped plates

(Fig. 4.5j – 1-3)

Description:

Material assigned to this morphological group comprises any flat or slightly dorsally convex plate with numerous isolated cusps distributed across the entire surface. No complete plates were identified herein, but those recovered ranged in size from ~0.4mm x ~0.4mm to ~4.5mm x ~2mm. Two general end members are recognised (Table 4.5b):

Morphotype	Description	Outline
Simple Fig. 4.5j(1)	Relatively flat with cusps orientated vertically from the plate and distributed randomly (but densely) across the surface. Cusps are almost perfectly conical and are commonly entirely smooth or bear a band of numerous fine, impersistent, sub-vertical ridges below a slightly tapered smooth tip.	
Reclined Fig. 4.5j(2-3)	Bases are gently curved and cusps, which are broadly arranged into rows, are preferentially reclined or curved in one direction. Cusps are occasionally entirely smooth and circular in cross section, but more commonly exhibit prominent vertical ridges on a slightly flattened dorsal surface. Secondary flattening through apparent wear on these dorsal surfaces is notable. Cusps sometimes show an increase in size in the direction of inclination.	

Table 4.5b Cusped plate morphotypes.

Age, location and lithology of samples:

Cusped plates were found in samples ranging from the basal Asbian (upper Viséan) to the lower Serpukhovian, in all sections except the Glencar and Glenade Sections and from a variety of limestones.

GLTV18, GLTV22, GLTV23, AGHA4, AGHA6, AGHA10, CNLG1, CNLG6, CNLG10, CNLG13, CNLG14, CNLG15, CNLG19, KMONA1, KMONA2, KMONA3, KMONA4, KMONA5, KMONA6, KMONA8, BW3

Noded plates

(Fig. 4.5j – 4-5 & 7)

Description:

These comprise any flat or slightly dorsally convex plate structures with numerous isolated low domes or "nodes" distributed across the surface. Various shapes of plate and densities of nodes exist, probably reflecting various functions and origins. One specimen preserves remnants of a honeycomb-like texture which appears to have originally covered the entire plate, or at least the nodes (Fig. 4.5j - 5). This may represent fragments of a palatal plate. Plates are commonly greater than 1mm in size.

Age, location and lithology of samples:

Found in samples from upper Holkerian (middle Viséan) to uppermost Brigantian (upper Viséan), in all sections (except Glencar) and in several limestone beds.
GLTV13, GLTV23, DAGN1, AGHA4, AGHA13, CNLG8, CNLG10, CNLG13, KMONA1, KMONA3, KMONA4, KMONA5, KMONA6, BW3

"Stellar" plate morphotypes

(Fig. 4.5j – 6 & 8)

Description:

These phosphatic bodies comprise a slightly domed plate with rows of irregular nodes spreading out from a central point. Nodes increase in size away from the central point. Node bearing rows occasionally bifurcate and appear to control the development of "folds" in the plate surface. The very upper surfaces of the plates are often worn so that nodes are difficult to distinguish (in comparison to the detail preserved along the margins of the plate - areas which would be equally susceptible to post-mortem wear). It is thus inferred that these structures may have acted as palatal grinding plates in life. These denticles are commonly elongate in a particular direction and average ~1.5mm along their long axis.

Age, location and lithology of samples:

"Stellar" plate morphotypes were relatively uncommon and were found in only especially fossiliferous marine limestone beds in the Aghagrania, Kilnamona and

St. Brendan's Well Sections. Productive samples range in age from the upper Asbian to uppermost Brigantian (both upper Viséan).
AGHA10, KMONA4, KMONA5, BW4

Other

"Bar"-elements

(Fig. 4.5h – 3)

Description:

Consist of thin, straight, inverted (shallow) gutter structures with ridge like processes running almost perpendicular to the long axis of the element. Bars are predominantly found in isolation, although plates with bars running parallel to one another, but separated by smooth intervals, are also identified (Appendix F, Plate 3 (6)). Ridge-like "cusp" processes are sometimes weakly crenulated or exaggerated into asymmetric, fin-like forms. No full specimen was recovered and thus the original size of the phosphatic body remains unknown; individual bars attain widths of ~0.2mm and lengths of ~2mm whilst plates bearing the bars reach similar maximum dimensions.
Although still very poorly understood, bar-elements may actually be attributable to the conulariids (Duncan, 1999).

Age, location and lithology of samples:

Bar-elements were found in samples ranging in age from the upper Holkerian (middle Viséan) to the basal Serpukhovian and they occurred in every section investigated. These elements were recovered only from marine limestones.
GLTV12, GLTV14, GLTV16, GLTV18, GLTV23, GLTV27, GLTV36, DAGL7, DAGL15, DAGN1, AGHA4, AGHA9, CNLG1, CNLG10, CNLG13, CNLG15, KMONA4, KMONA5, KMONA6, KMONA8, BW1, BW2, BW4

"Catapult" structures

(Fig. 4.5h – 6-7)

Description:

These enigmatic microfossil structures consist of hollow biramous "catapult" shaped phosphatic structures. Removal of the outer layer has exposed evidence for canals on the surfaces of the structures, which are similar to those seen in other ichthyoliths. The structures are generally featureless, although sometimes weak grooves are evident below the point where the structures bifurcate. The hollow "arms" of the structures are typically oval in section. No complete specimens were recovered and their original full size is unknown, although specimens up to ~2.5mm in length were noted.

Age, location and lithology of samples:

These phosphatic structures were found in samples ranging from the lower Asbian (upper Viséan) to the basal Serpukhovian and were recovered from all sections (except the Glenade Section) but only in marine limestone residues. The structures were generally uncommon.

GLTV25, GLTV29, DAGL14, AGHA4, AGHA10, CNLG10, CNLG13, CNLG14, CNLG15, KMONA3, KMONA4, KMONA5, KMONA6, KMONA8, BW2, BW3, BW4

Serrated keel morphotypes

(Fig. 4.5h – 4-5)

Description:

Comprise morphologically distinct, thin enameloid serrated ridge structures. All specimens recovered were incomplete and so the full morphology is unknown. The two external surfaces of the ichthyoliths are relatively smooth and come together into a sharply defined jagged ridge. One specimen preserved original very porous phosphatic tissue within the ridge-like body, similar to that shown in Fig. 4.6a - 1a. Large fragmented specimens are up to ~3mm long.

Age, location and lithology of samples:

Found in low abundances in only a few samples which range in age from the uppermost Holkerian/lowermost Asbian (middle/upper Viséan) to the uppermost

Brigantian (upper Viséan). Specimens were recovered from fossiliferous marine limestones in the Tievebaun, Carraun/Lugasnaghta, Kilnamona and St. Brendan's Well Sections.

GLTV15, CNLG1, KMONA3, BW3, BW4

Other morphologies and unidentifiable fragments

(Fig. 4.5k – 1-7)

Description:

This grouping comprises any ichthyolith (whether complete or fragmentary) which was not identifiable, did not conform to any of the other categories discussed, or was not distinctive enough (individually) to define a morphological grouping. Many probable chondrichthyan denticles are included here. Only a selection has been figured.

Age, location and lithology of samples:

Unclassifiable elements were found in virtually every sample (which yielded any phosphatic microfossils) and every section spanning upper Holkerian (middle Viséan) to Bashkirian age.

GLTV12, GLTV13, GLTV14, GLTV15, GLTV16, GLTV17, GLTV19, GLTV20, GLTV21, GLTV22, GLTV23, GLTV24, GLTV25, GLTV27, GLTV28, GLTV30, GLTV32, GLTV33, GLTV34, GLTV35, GLTV36, GLTV37, GLTV40, DAGL2, DAGL3, DAGL7, DAGL11, DAGL13, DAGL14, DAGL15, DAGN1, AGHA1, AGHA3.1, AGHA3.2, AGHA4, AGHA5, AGHA6, AGHA9, AGHA10, AGHA13, CNLG1, CNLG2, CNLG6, CNLG7, CNLG10, CNLG11, CNLG13, CNLG14, CNLG15, CNLG16, CNLG19, KMONA1, KMONA2, KMONA3, KMONA4, KMONA5, KMONA6, KMONA8, KMONA9, BW2, BW3, BW4, BW5B, BW10, BW9, BW8

4.6 PRESERVATION OF VERTEBRATE REMAINS

Of primary importance to this project, given the aim of deducing stable isotopic trends for the upper Viséan stratigraphic sequence (Chapter 5), was assessing the quality of preservation of the phosphatic conodont and ichthyolith remains. This was principally done through (surficial) examination under a standard binocular microscope as well as using SEM. Unusual mineral structures and textures were also identified using Laser Raman Spectroscopy.

Conodonts and ichthyoliths were occasionally recovered which bore a fine dusting of white crystalline grains on their surfaces. Elements were otherwise identical to "non-encrusted" forms. These mineral coatings were found to comprise quartz and albite (feldspar). They formed only superficial overgrowths on the phosphatic elements and were generally easily removed using an ultrasonic bath. Since the phosphate was to be chemically purified (Appendix C) and no associated degradation of the phosphatic elements was evident, it was accepted that such mineral coatings were not a concern to (later) stable isotopic analysis.

In the sample CNLG19, sediment-bound associations of S-elements (one cluster also contains an M-element) whose long axes are parallel were recovered (Fig. 4.2h). Only one of five clusters exhibits an element which is in a conflicting orientation to its neighbours (Fig. 4.2h - 4) and it is believed that the associations are essentially representative of their original anatomical arrangement.

Some conodont elements from the Kilnamona and St. Brendan's Well Sections had a (somewhat) matted surface hue. Since it is the smooth surface of the dense lamellar crown tissue which gives conodonts their typical lustre, any reduction in shine may possibly indicate some degree of (at least surficial) element degradation. The restricted occurrence of matte conodont elements may relate to C.A.I. values, since they are significantly higher in Clare (~5.5) than in the NW Ireland sections (~3-4). In a similar fashion to the conodonts, some ichthyoliths exhibited clean, lustrous crown surfaces but rough and irregular basal bodies (Figs. 4.5f - 5, g - 9 & i - 2). Ichthyolith material with coarse basal surfaces occurred in all of the sections investigated. Since this coarseness is not a primary feature, and is predominantly

controlled by the irregular development of the apatite of the ichthyolith, rather than mineral overgrowths, it suggests that some degree of reorganisation (recrystallisation) or degradation had occurred. The restriction of the coarsened texture to the basal tissue may be as a result of its relatively greater porosity and therefore (possibly) greater susceptibility to alteration.

Ichthyoliths recovered from certain horizons (AGHA11 & 13 as well as CNLG10, 13, 15 & 16) in the Carraun Shale and upper Bellavally Formations were found to be partially pyritised. The pyrite replacement was faithful to the original form of the ichthyolith and was typically detailed. However, its presence is an unequivocal indicator that some apatite had been taken into solution and raises significant doubts over the reliability of the remaining apatite (in affected ichthyoliths) to faithfully represent the phosphatic bodies' original chemical composition.

Polygonal, columnar crystal growths were discovered (under SEM examination) on ichthyoliths recovered from both NW Ireland and Clare Sections (Figs. 4.5j - 8a-b & 4.6a); although, they are much rarer and more poorly developed in NW Ireland. The overgrowths are generally very difficult to identify under normal (reflected light) microscopic examination and affected ichthyoliths typically appear only slightly degraded or just superficially rough. The mineral has a vertically lineated, elongate/columnar, possibly hexagonal crystal form and tends to (initially) grow sub-parallel to the surface of the microfossil before becoming perpendicularly orientated towards its termination. The crystals appear to be intimately associated with (and form a continuation of) the host ichthyolith. Laser Raman Spectroscopy identified the mineral growths as apatite (Fig. 4.6b), which affects the reliability of the affected fish material for stable isotopic analysis, given that the apatite may represent phosphate precipitated purely from circulating diagenetic fluids. Alternatively, the apatite may have resulted from direct recrystallisation of the original ichthyolith, with only limited, or even no, elemental exchange with any circulating fluids (i.e. a closed system). The identification of pyrolitic carbon within the mineral growths (Fig. 4.6b) is significant, since it strongly implies that at least some contribution of material came from the original ichthyolith, since it is almost certainly the source of the matured carbon bound in the younger apatite crystals.

Fortunately, conodont elements were recovered in relatively pristine condition from all sections and although alteration of particular ichthyoliths was discovered during screening, the majority of material examined appeared much better preserved, in any case, efforts were made to select the most immaculate material (where possible) for isotopic analyses (see Section 5.2).

4.7 PALAEOENVIRONMENTAL SIGNIFICANCE OF MICROFOSSILS

The abundance and variety of silicified fossil groups (see Appendix F for full details and plates) in the Tievebaun, Glencar and (to a lesser extent) Glenade Sections is strongly indicative of oxygenated, normal salinity marine conditions. This is in agreement with the dominance of *G. girtyi,* typical of the *Gnathodus-Lochriea* open marine/basinal biofacies in conodont faunas (Figs. 1.1.3b-c). The articulation and level of surface detail preserved on silicified microfossils, as well as the range in size of the fauna recovered from the Sligo Group Sections, suggests that the bioclasts are unlikely to have been transported far or subjected to any hydrological size-sorting. The abundance and variety of epibiont fossils (Appendix F) likely indicates that limited hard grounds were available for organisms to stabilise themselves on and thus that the sea-floor was probably soft and muddy.

Sponge material (most obviously spicules) is most common in the Sligo Group Sections (and particularly in the Dartry Limestone Formation), and it is therefore likely that siliceous sponge material may have acted as a potential source of SiO_2 for fossil preservation and even chert development. Sponge material is almost completely absent higher in the stratigraphy (Leitrim Group) or in the Co. Clare Sections, in which chert development and in particular the silicification of microfossils is notably reduced. The pyritisation of microfossils tends to be much more common where silicification is absent, and *possibly* relates to the high salinity or stagnant, oxygen-poor water conditions identified in these areas.

The microfossil assemblages in the Aghagrania and Carraun/Lugasnaghta Sections are often relatively simple, comprising few phyla. Such depauperate faunas in the Leitrim Group formations are not thought to be a preservational artefact since gastropods were commonly recovered but were one of the least common and poorly preserved microfossils in the rich faunas of the Sligo Group Sections. The increased relative abundance of gastropods, which are commonly thought of as euryhaline (Raup & Stanley, 1978), and irregular faunas are interpreted to be a product of both

rapidly fluctuating and unfavourable (in biological terms) salinity conditions. Further support for environmentally restricted conditions (in the Meenymore Formation at least), comes from the discovery of *Conopiscius* elements which were (or at least their close relatives were) typically associated with near-shore, partially restricted palaeoenvironments (Briggs & Clarkson, 1987). The preferential occurrence of conodonts belonging to the *Cavusgnathus-Mestognathus* (restricted shallow marine with variable salinity and energy levels) and *Synclydognathus-Kladognathus* (shallow marine with normal salinity and moderate to high energy levels) Biofacies (Somerville, 1999) in the Aghagrania and Carraun/Lugasnaghta Sections (mainly the Meenymore and Bellavally Formations but also the lower Carraun Shale Formation) also indicates near-shore and eustatically-sensitive palaeoenvironments.

Whilst numerous indicators of shallow and irregular marine conditions were identified in this study in NW Ireland, microfossils recovered from several horizons in the sequences suggest that more open marine conditions were periodically developed also. Marginal marine conditions have been cited in the past for several members in the Meenymore and Bellavally Formations due to a failure to obtain fossils (e.g. Kelly, 1989). However, such gross palaeoenvironmental generalisations are not applicable to significant numbers of individual beds within the Meenymore and Bellavally Formations which contain abundant and diverse fish and conodont faunas (often attributable to the *Gnathodus-Lochriea* Biozone). This greater number of previously unrecognised, marine horizons within these particular formations indicates the rapid and common nature of base-level and therefore palaeoenvironmental fluctuations during the Asbian-Brigantian interval in NW Ireland, which can possibly be related to 4^{th} order cyclicity.

Microfossil material (predominantly ichthyoliths) recovered from the Meenymore and Bellavally Formations commonly exhibit a dense covering of fine, siliceous worm trails (Appendix F, Plate 3 - 6). The density of the trails, in conjunction with their occurrence on both sides of the host elements may indicate that the fossils lay exposed and were gently moved about (details preserved indicate no significant transport or energy levels) on the sea-floor for an extended period prior to burial.

The identification of woody tissue in the upper Carraun Shale Formation (and also the Clare Shale Formation) supports palaeoenvironmental reconstructions close to the palaeo-shoreline, or at least close to a source of terrigenous plant material (e.g. river mouth). Conodonts and ichthyoliths recovered from parts of the Carraun/Lugasnaghta Section were relatively small in size (~50% that of similar species in other formations), though morphologically well-formed. This may indicate some degree of size sorting or may, possibly, reflect some degree of restriction of the palaeoenvironment which led to a degree of growth retardation.

CHAPTER 5 - STABLE ISOTOPE ANALYSIS

This chapter will introduce the concepts of stable isotopes, particularly the use of oxygen in palaeoclimatic studies. The results of stable isotopic analyses undertaken on ichthyolith and conodont apatite are then presented and discussed.

5.1 INTRODUCTION TO STABLE ISOTOPES

Isotopes are variants of the same element (defined by atomic number) with differing numbers of neutrons in their nuclei. In general, the electronic structure of an element determines its chemical behaviour, while the composition of the nucleus is responsible for an atoms physical properties (Hoefs, 2009). Isotope ratios are controlled by the slight mass difference between atoms and how this affects the process by which they are selected for a product. Biasing is usually very slight, but given the amount of atoms and compounds processed in the trillions of global reactions everyday, these small differences become exaggerated and segregation of isotopes becomes apparent.

In isotope geochemistry, the isotopic composition of a compound is often expressed in terms of delta (δ) values. The δ value comparing isotopes of atomic mass X and X-1 of element E, in compound C, is given in per mil (‰) and calculated as follows:

Error! Bookmark not defined.

$$\delta^{X}E_{C} = \left(\frac{\left(\frac{\delta^{X}E}{\delta^{X-1}E}\right)_{Sample} - \left(\frac{\delta^{X}E}{\delta^{X-1}E}\right)_{Standard}}{\left(\frac{\delta^{X}E}{\delta^{X-1}E}\right)_{Standard}} \right) \times 10^{3}$$

The δ value of a substance is measured using a mass spectrometer. The analyte is volatilised and the resulting gas is charged and accelerated along a curved cylinder. Strong electric and magnetic fields cause the paths of the different massed isotopes to diverge. A detection plate monitors the various arrivals and masses of the

different isotopes, allowing a calculation to be made of the relative abundance of each.

5.1.1 Stable isotopes of Oxygen

Oxygen has three stable isotopes with the following relative abundances (Rosman & Taylor, 1998):

^{16}O = 99.757%

^{17}O = 0.038%

^{18}O = 0.205%

Since ^{18}O is more abundant and there is a greater mass difference between it and ^{16}O, it is preferred (relative to ^{17}O) for mass spectrometric analyses.

There are two different international standards to which $\delta^{18}O$ measurements are calibrated (Hoefs, 2009):

(1) **VPDB** (Vienna PeeDee Belemnite) refers to a belemnite from the Cretaceous PeeDee Formation in South Carolina, U.S.A. which was used in the 1950s during the construction of the carbonate palaeotemperature scale. Since the original sample was exhausted, a lab (based in Vienna) calibrated a new reference sample. VPDB is used in low temperature studies of carbonate for both O and C.

(2) **VSMOW** (Vienna Standard Mean Ocean Water) is a recalibration of the original SMOW, which is constructed by mixing distilled portions of seawater collected from different locations around the globe. All other O isotope analyses, on water, silicates, phosphates, sulphates and high-temperature carbonates, are given relative to VSMOW.

The O bound in the compound being examined is converted to CO or CO_2 for analysis, depending on the exact technique being used. The detailed methodology followed for all isotopic analyses undertaken for this project is provided in Appendix C.

5.1.2 Application to palaeoclimatology

The utilisation of the stable isotopes of O in palaeoclimatic research was established over 50 years ago (Epstein *et al.*, 1951; 1953). Carbonates and phosphates are the most intensively studied media for Palaeozoic climate research.

The δ value of a compound, which originally formed in isotopic equilibrium with seawater, is directly linked to the original isotopic composition and ambient temperature of the seawater. Since $H_2{}^{18}O$ is "heavier" than standard $H_2{}^{16}O$, it is preferentially left behind during evaporation and concentrated in the first precipitates as water vapour condenses. This continual process results in increasingly isotopically light water in the atmosphere from the site of original evaporation. Atmospheric circulation forces air masses away from the equator so that atmospheric precipitation at progressively higher latitudes is isotopically depleted in ^{18}O. Ice-masses at the poles and on continental mountains are formed from this "light" water and thus provide storage media during times of ice-sheet growth. Irregularities in the $\delta^{18}O$ values of water-bodies must be considered in terms of their evaporation (favours ^{18}O) - precipitation (favours ^{16}O) balance, in addition to the proximity to isotopically light meteoric inputs.

The biochemical reactions which incorporate O into biogenic CO_3^{-2} or PO_4^{-3} are controlled, in part, by temperature. If the palaeoenvironment is well understood, i.e. the controls on freshwater input, evaporation and approximate volume of ice on the planet are constrained, a value can be assumed for the original isotopic composition of the seawater and an isotopic measurement can then be used to calculate the palaeotemperature at the time of carbonate or phosphate formation as follows:

(1) For carbonate, (Erez & Luz, 1983):

$$T\ ^{o}C = 17.0 - 4.52(\delta^{18}O_c - \delta^{18}O_w) + 0.03(\delta^{18}O_c - \delta^{18}O_w)^2$$

Where $\delta^{18}O_c$ is the O-isotope composition of CO_2 derived from carbonate and $\delta^{18}O_w$ is the O-isotope composition of CO_2 in equilibrium with water at 25ºC.

(2) For phosphate, traditionally the equations derived by Longinelli & Nuti (1973):

$$T\ ^{o}C = 111.4 - 4.3(\delta^{18}O_p - \delta^{18}O_w)$$

and revised by Kolodny *et al.* (1983):

$$T\ ^{o}C = 113.3 - 4.38(\delta^{18}O_p - \delta^{18}O_w)$$

have been used. However, at the time of writing new work by Pucéat *et al.* (2010) has been published which calls for a major revision of the temperature equation used due to the significant evolution of analytical methodologies employed since the derivation of the original equation. The new equation has essentially the same slope as the originals, but results in substantially increased derived temperatures (~4-8ºC, depending on the techniques and standards used). The equation derived from the new data is given as:

$$T\ ^{o}C = 124.6 - 4.52(\delta^{18}O_p - \delta^{18}O_w)$$

Whilst that derived from combining the new data with corrected older data is:

$$T\ ^{o}C = 118.7 - 4.22((\delta^{18}O_p + (22.6 - \delta^{18}O_{NBS120c})) - \delta^{18}O_w)$$

Where T is the average growth temperature and $\delta^{18}O_p$ and $\delta^{18}O_w$ are the O-isotope values of phosphate and water respectively ($\delta^{18}O_w$ will be used in the sense of surface seawater from here unless otherwise stated). $\delta^{18}O_{NBS120c}$ reflects the value that analyses of the standard NBS120c have been normalised to.

Given the recent nature of the new equations outlined above, this work will retain the use of the original equations pending further investigation and analyses of the revised equation until its validity has been confirmed and internationally accepted.

Carbonate and phosphate compounds both commonly occur in ubiquitous, long-ranging fossil groups which act as storage media and are reportedly resistant to diagenetic alteration (e.g. Brand, 1989; 2004; Buggisch *et al.*, 2008; Joachimski & Buggisch, 2002; Joachimski *et al.*, 2003; 2004; 2006; 2009; Mii *et al.*, 1999; 2001; Trotter *et al.*, 2008; Veizer *et al.*, 1986; 1999).

The carbonate shells of many taxa are often easily replaced or recrystallised during diagenesis or may display a "vital effect" whereby metabolic processes (in life) prevented the precipitation of calcite in isotopic equilibrium with ambient seawater. Carbonate analyses (for the Palaeozoic) largely rely on low-Mg brachiopods, which are routinely tested for diagenetic alteration. Unaltered brachiopods are thought to display original shell microstructure, lack cathodoluminescence and have high Na, S and Sr, but low Mg, Fe and Mn concentrations (Adlis *et al.*, 1988; Brand, 1989; Bruckschen *et al.*, 1999; Grossman *et al.*, 2002; Mii *et al.*, 1999; 2001; Popp *et al.*, 1986; Rush & Chafetz, 1990; Veizer *et al.*, 1986; 1999), see Fig. 5.1.2a.

Isotopic analyses of phosphates are undertaken predominantly on the bio-apatite of ichthyoliths (generally fish teeth and scales) and conodonts. Ideally, analysis of fish material should be restricted to dense, resistant enamel; however, the combination of small denticles and reduced or absent enamel layers in Palaeozoic fish mean this is generally impossible (Sharp *et al.*, 2000). The isotopic analysis of biogenic phosphate was originally championed by Longinelli & Nuti (1968), followed by Kolodny *et al.* (1983), Luz *et al.* (1984) and Luz & Kolodny (1985). Conodont apatite analyses were originally hampered by the small size of the elements involved (platforms ~ 100μg). Studies required large amounts of rock and residue processing to obtain sufficient quantities of material to obtain a detectable signal (10-15mg in Luz *et al.*, 1984). Advances in purification (O'Neil *et al.*, 1992) and micro-analytical (0.5-1mg) techniques (Bassett *et al.*, 2007; Buggisch *et al.*, 2008; Joachimski & Buggisch, 2002; Joachimski *et al.*, 2003; 2004; 2006; 2009; Trotter *et al.*, 2008; Wenzel *et al.*, 2000) have established bio-apatite stable isotope analysis as widely applicable for the majority of Phanerozoic time.

Although the published trends of isotopic curves for carbonate (e.g. Veizer *et al.*, 1999) and phosphate (e.g. Buggisch *et al.*, 2008) are comparable in parts, the

magnitudes and timings of shifts are somewhat conflicting (Fig. 1.3.1b). Sampling resolution and imprecise correlation can clearly account for some of the discrepancies; however, apatite, and in particular conodont apatite, analyses are thought to represent the more accurate $\delta^{18}O$ dataset, for the reasons outlined below:

(1) The spread of individual data points in carbonate isotopic research is considerably larger than that of similar wide ranging conodont studies (Buggisch *et al.*, 2008; Joachimski *et al.*, 2009).

(2) Experimental work has demonstrated that, despite diagenetic variations in REE and trace elements (Trotter & Eggins, 2006), O exchange occurs extremely slowly in apatite. Alteration appears to be limited to biologically mediated reactions (Blake *et al.*, 1997; Zazzo *et al.*, 2004) or possibly through interaction with high temperature fluids (Pucéat *et al.*, 2004). However, factors such as recrystallisation (Pucéat *et al.*, 2004) and heating (up to stage 5 as measured with the Conodont Alteration Index [C.A.I.], Joachimski *et al.*, 2009) *appear* to have no direct effect on the preserved $\delta^{18}O$ values. Histological examinations have highlighted the density and relatively large crystal size of albid crown tissue in conodonts (Trotter *et al.*, 2007). The resistance of this particular tissue to any elemental exchange (Trotter & Eggins, 2006) likely offers a good deal of protection to the more porous and finely crystalline inner tissue. Since the PO_4^{-3} cation is quite robust, some reorganisation of the fossil element can transpire before any $\delta^{18}O$ value alteration occurs. Until an appropriate monitor of O isotope exchange in biogenic phosphate is discovered, it is proposed herein that detailed visual screening of samples (selected to the finest taxonomic level) and data interrogation represent the best option in obtaining accurate $\delta^{18}O$ records.

(3) Brachiopods are sessile, benthic organisms and as such (if producing their shell in isotopic equilibrium with ambient seawater) will be representative of the water depth it originally inhabited (James *et al.*, 1997). A good understanding of the palaeoenvironment and water depth of the extinct brachiopods being analysed must be obtained before any inferences can be made regarding changing conditions and temperatures through a lithological sequence (Carpenter & Lohmann, 1995). Conodonts, on the other hand, are

considered to have been nektic (see Section 1.1.1) and may be more representative of sea-surface conditions (Joachimski *et al.*, 2006).

(4) Carbonate analyses suggest a secular change in oceanic chemistry back through time, with older brachiopods being significantly depleted in ^{18}O relative to the Recent (Brand & Veizer, 1981; Brand, 1989; Popp *et al.*, 1986; Veizer *et al.*, 1986; 1999), see Fig. 5.1.2b. In order to explain the unrealistically high derived palaeotemperatures (>50ºC, above the thermal threshold for protein denaturation) and maintain the integrity of the data, workers argue that the $\delta^{18}O$ values of ancient oceans were variable. This suggestion is in conflict with the evidence from ophiolites and mudrocks, which argue for stable $\delta^{18}O$ oceanic values, buffered by weathering, hydrothermal and tectonic processes (Land & Lynch, 1996; Muehlenbachs, 1998; Muehlenbachs *et al.*, 2003). Results from studies on biogenic apatite have yielded $\delta^{18}O$ results which are comparable to modern values and can also be realistically interpreted in terms of palaeotemperature and palaeoenvironmental conditions (both locally and globally) if the older equations of Longinelli & Nuti (1973) and Kolodny *et al.* (1983) are utilised. However, if the equations in Pucéat *et al.* (2010) are followed then a secular change in seawater chemistry is suggested by the biogenic apatite record also.

The isotopic analysis of carbonates is extremely valuable for palaeoenvironmental and palaeoclimatological interpretation of the Phanerozoic; however, significant disadvantages are associated with their use (relative to biogenic apatite as discussed above). Thus, since biogenic apatite is considered more isotopically robust, is readily available in the form of ichthyoliths and conodonts, and conodont microfossils are extremely useful in biostratigraphical and biofacies determinations, all $\delta^{18}O$ data was derived from an apatitic source herein.

5.2 ANALYSIS OF BIO-APATITE FROM IRELAND

Only microscopic fish and conodont remains which were:

(1) of suitable quality

and

(2) recovered in sufficient quantities

- from samples removed and processed from sections examined in NW Ireland (Sections 2.2 & 2.3) and also the area north of the Shannon Basin (Section 3.2), were analysed for their $\delta^{18}O$ value. A single analysis (AGHA D1) was conducted on the outer layers of a large orodont ichthyolith element recovered from a shale hand-sample exhibiting an orthocone impression. The aim was not only to reconstruct an isotopic curve for the late Viséan and early Serpukhovian Stages, but also to examine whether any inter- or intra-species differences in $\delta^{18}O$ could be detected. Tables providing the details of the material analysed are contained in Appendix G. All the phosphatic microfossil material which was analysed was generally run in at least triplicate.

On the isotopic graphs plotted and presented in Figs. 5.2.1a-d and Figs. 5.2.2a-c each stratigraphic section (lithostratigraphy taken from the original diagrams relating to Chapters 2 and 3) is designated its own colour, with squares used to represent ichthyolith analyses and circles used for conodont analyses. The sample point is plotted at the average value of the triplicate analyses and error bars are used to represent one standard deviation (1σ) of the values:

■ = Ichthyolith ● = Conodont ⊢—⊣ = 1σ

5.2.1 $\delta^{18}O$ results from NW Ireland

Many of the sections in NW Ireland contained limited amounts of biogenic apatite. Phosphatic microfossil material in the Holkerian and lower Asbian sections generally comprised ichthyoliths, often of unknown affinity, while conodont elements were more common in the uppermost Asbian and Brigantian sections. In total, 48 analyses, representing 39 separate horizons, were conducted on samples from the northwest sections (Fig. 5.2.1a). A trend of increasing $\delta^{18}O$ is seen in the ichthyolith analyses from the uppermost Holkerian through the Asbian and possibly

into the early Brigantian. Values of both fish and conodont apatite are apparently relatively stable through the remainder of the Brigantian and into the early Serpukhovian. Where analyses from different sections overlap, values are found to be comparable. The results (on a section by section basis) are outlined below.

The results of 19 analyses undertaken on various fish material from the Tievebaun Section are shown in Fig. 5.2.1a, Fig. 5.2.1b and are also listed in Table 5.2.1a. Three horizons (GLTV14, GLTV16 & GLTV39) possessed a sufficient abundance of biogenic apatite material to enable two separate analyses to be made from them. Two samples from horizons GLTV30 and GLTV32, comprising actinopterygian scales, failed to react during sample preparation and did not yield analysable quantities of Ag_3PO_4.

		Sample No.	Analysis					$\delta^{18}O$	1σ
			1st	2nd	3rd	4th	5th		
Asbian	Glencar Limestone Fm.	GLTV39 OR1	17.84	18.24	18.00			18.03	0.20
		GLTV39 AN-2	17.62	17.59	17.62			17.61	0.02
		GLTV36 OR1	17.80	17.89	17.77			17.82	0.06
		GLTV30 AN-2	15.94	15.75	15.88			15.86	0.10
		GLTV28	17.05	16.99	17.18			17.07	0.10
		GLTV27 OR1	17.55	17.44	17.38			17.46	0.09
		GLTV22 OR1	16.81	16.64	16.91			16.79	0.14
		GLTV21 AN-1	17.30	17.41	16.89*	17.39	17.28	17.35	0.06
		GLTV20 OR1	16.19	16.23	16.12			16.18	0.06
?	Benbulben Shale Fm.	GLTV19 OR1	17.10	16.92	16.77			16.93	0.17
		GLTV18 OR1	15.91	16.00	16.10			16.00	0.10
		GLTV17 AN-1	16.72	16.85	17.28*	16.33*	16.74	16.77	0.07
		GLTV16 OR2	15.85	15.81	15.72			15.79	0.07
		GLTV16 OR1	16.71	16.76	16.60			16.69	0.08
		GLTV15	17.75	17.78	17.50			17.68	0.15
Holkerian		GLTV14 OR2	15.82	15.62	15.54			15.66	0.14
		GLTV14 OR1	16.24	16.27	16.31			16.27	0.04
		GLTV13 OR1	15.26	15.15	14.98			15.13	0.14
		GLTV12	18.15	18.07	18.07			18.10	0.05

Table 5.2.1a Results of isotopic analyses extracted from the Tievebaun Section.

All results are given in ‰ relative to VSMOW. Asterisks indicate statistically anomalous results which were excluded from calculating average values. All analyses represent ichthyoliths. Samples are listed with the stratigraphically youngest at the top.

The Tievebaun Section results demonstrate an erratic trend of increasing $\delta^{18}O$ values stratigraphically upwards through the section from an average value of ~16‰ at the base to ~18‰ at the top.

Isotopic determinations were only possible on the lowest and highest horizons of the 15 taken from the Glencar Section, all other horizons failed to yield sufficient biogenic apatite material. The results of the two analyses are shown in pink in Fig. 5.2.1a and listed below in Table 5.2.1b.

		Sample No.	Analysis					$\delta^{18}O$	1σ
			1st	2nd	3rd	4th	5th		
Asbian	Dartry Lmst. Fm.	DAGL15	17.88*	18.69	19.10	18.00*	19.07	**18.95**	**0.23**
	Glencar Lmst. Fm.	DAGL1 OR1	18.44	18.22	18.05			**18.24**	**0.20**

Table 5.2.1b Results of isotopic analyses extracted from the Glencar Section.

All results are given in ‰ relative to VSMOW. Asterisks indicate statistically anomalous results that were excluded from calculating average values. All analyses represent ichthyoliths. Samples are listed with the stratigraphically youngest at the top.

The Glencar data, though comprising only two points, appear to continue the increasing $\delta^{18}O$ trend (~18‰ to ~19‰) upwards through the stratigraphic sequence.

A single sample from the Glenade Section produced sufficient phosphatic microfossil material to enable separate analysis of two different ichthyoliths. The results of the analyses are shown in blue in Fig. 5.2.1a and listed in Table 5.2.1c. The two ichthyoliths produced two relatively different results, with a discrepancy of 1.3‰.

		Sample No.	Analysis					$\delta^{18}O$	1σ
			1st	2nd	3rd	4th	5th		
Asbian	Dartry Lmst. Fm.	DAGN1 AN-3	18.25	17.69	18.22	17.82	17.89	**17.97**	**0.25**
		DAGN1 OR1	16.79	16.53	16.69			**16.67**	**0.13**

Table 5.2.1c Results of isotopic analyses extracted from the Glenade Section.

All results are given in ‰ relative to VSMOW. All analyses represent ichthyoliths.

The limited stratigraphical extent of the Glenade Section reduces its use in elucidating a $\delta^{18}O$ trend for the northwest region. The results of the two analyses are similar to those of ichthyoliths from the Tievebaun Section (~17‰ & ~18‰) but appear too negative relative to the nearest analyses from adjacent sections (DAGL15 = 18.95‰ and AGHA1 = 18.56‰ and 18.94‰).

Fourteen samples were analysed from 10 separate horizons in the Aghagrania Section (Fig. 5.2.1a, Fig. 5.2.1c & Table 5.2.1d). Three analyses were based on conodonts, while the remaining 11 were conducted on various ichthyoliths.

		Sample No.	Analysis					$\delta^{18}O$	1σ
			1st	2nd	3rd	4th	5th		
Brigantian	Carraun Sh. Fm.	AGHA13 AN-2	18.41	18.73	18.07*	18.35		**18.50**	**0.20**
Asbian	Bellavally Fm.	AGHA11	18.54	18.46	18.63			**18.54**	**0.09**
		AGHA10 AN2-1	*20.98*	*20.90*	*19.93**			***20.94***	***0.06***
		AGHA10 AN1-2	18.29	18.38				**18.34**	**0.06**
		AGHA9 OR1	18.85	18.90	18.85			**18.87**	**0.03**
		AGHA9	18.17	18.02				**18.10**	**0.11**
	Glenade Sst. Fm.								
	Meenymore Fm.	AGHA6 OR1	18.69	18.33	18.54			**18.52**	**0.18**
		AGHA4 OR1	18.65	18.85	18.57			**18.69**	**0.14**
		AGHA4 AN-3	18.69	18.47	18.39			**18.52**	**0.16**
		AGHA D1	18.81	18.77	18.92			**18.83**	**0.08**
		AGHA3.2	*20.50*	*20.70*	*19.70**	*20.40*		***20.53***	***0.15***
		AGHA3.1	*19.66*^*	*20.31^*	*20.47^*	*20.50*	*20.49*	***20.44***	***0.09***
		AGHA1 OR1	18.87	18.99	18.97			**18.94**	**0.06**
		AGHA1	18.57	18.24	17.63*	18.53	18.88	**18.56**	**0.26**

Table 5.2.1d Results of isotopic analyses extracted from the Aghagrania Section.

All results are given in ‰ relative to VSMOW. Asterisks indicate statistically anomalous results which were excluded from calculating average values. Circumflexes denote samples that expressed possible N_2 contamination. Yellow italicised rows represent conodont analyses, other rows equate to ichthyolith analyses. Samples are listed with the stratigraphically youngest at the top.

The results of Aghagrania fish analyses are particularly stable (in comparison to stratigraphically lower sections), with all the results plotting between 18‰ and

19‰. The conodont $\delta^{18}O$ values also exhibit consistency, varying by only 0.5‰, although this is based on only three sample points.

Eleven phosphatic microfossil samples from 10 horizons were examined from the Carraun/Lugasnaghta Section. Nine analyses were conducted on conodont elements, and the remaining two were undertaken on ichthyoliths. Two samples of actinopterygian scales from horizons CNLG1 and CNLG13 failed to react completely or yield sufficient quantities of Ag_3PO_4 for analysis. The results are shown in Fig. 5.2.1a, Fig. 5.2.1d and listed in Table 5.2.1e.

		Sample No.	Analysis						$\delta^{18}O$	1σ
			1st	2nd	3rd	4th	5th	6th		
Pendleian	Dergvone Sh. Fm.	*CNLG19*	*20.31^*	*19.63^*	*19.44^*	*20.36*	*20.18*	*19.97*	***20.17***	***0.20***
Brignatian	Carraun Sh. Fm.	***CNLG15AN-1***	*20.24*	*20.27*	*19.94*	*19.64**	*20.33*		***20.20***	***0.17***
		CNLG14OR1	*20.33*	*20.27*	*20.27*				***20.29***	***0.03***
		CNLG14	18.89^	19.32^	19.07				**19.09**	**0.22**
		CNLG9 OR1	*21.02*	*21.00*	*20.90*				***20.97***	***0.06***
		CNLG8 OR1	*20.89*	*20.89*	*20.81*				***20.86***	***0.05***
		CNLG7AN-2	*21.05*	*20.85*	*20.93*				***20.94***	***0.10***
		CNLG6 OR1	*20.39*	*20.49*	*20.62*				***20.50***	***0.12***
Asbian	Bellavally Fm.	**CNLG A2**	17.92	18.16	17.89				**17.99**	**0.15**
		CNLG A1	*21.04*	*21.17*	*21.08*				***21.10***	***0.07***
		CNLG1AN2-1	*20.81^*	*21.21^*	*20.93^*	*21.10*	*21.08*	*21.01*	***21.06***	***0.05***

Table 5.2.1e Results of isotopic analyses from the Carraun/Lugasnaghta Section.

All results are given in ‰ relative to VSMOW. Asterisks indicate statistically anomalous results which were excluded from calculating average values. Circumflexes denote samples which expressed possible N_2 contamination. Yellow italicised rows represent conodont analyses, other rows equate to ichthyolith analyses. Samples are listed with the stratigraphically youngest at the top.

The $\delta^{18}O$ values obtained from the Carraun/Lugasnaghta Section appear reasonably stable and are very similar to those obtained from the Aghagrania Section. Fish analyses again range from ~18‰ to ~19‰, while the conodont analyses vary from ~20‰ to 21‰.

5.2.2 $\delta^{18}O$ results from the Burren Platform, western Ireland

Phosphatic microfossils were especially abundant in the majority of horizons sampled in the Slievenaglasha and Magowna Formations. In total 34 analyses were conducted on phosphatic remains recovered from 14 separate stratigraphic horizons in the two sections studied in the Burren area, north of the Shannon Basin. The results of these analyses are shown in Fig. 5.2.2a. The $\delta^{18}O$ values of conodont analyses from each section are highly comparable, although the results from St. Brendan's Well are consistently slightly lower. The results from each section are outlined below.

Twenty-four isotopic analyses were performed on fish and conodont material, recovered from nine horizons at Kilnamona (Table 5.2.2a). Five horizons (KMONA1, KMONA3 - KMONA6) yielded a substantial quantity and diversity of phosphatic microfossils, enabling multiple taxa-specific analyses to be performed. Thirteen isotopic determinations were carried out on conodont elements, while the remaining 11 analyses were performed on various ichthyoliths.

		Sample No.	Analysis					$\delta^{18}O$	1σ
			1st	2nd	3rd	4th	5th		
Pendleian	Magowna Fm.	*KMONA10 OR1*	*18.28*	*17.87*				***18.08***	***0.29***
		KMONA9 AN-1	*18.27*	*18.09*	*18.11*			***18.16***	***0.10***
		KMONA8 AN-3	*19.23*	*19.27*	*19.34*			***19.28***	***0.06***
Brigantian	Slievenaglasha Fm.	*KMONA6 AN5-2*	*17.96*	*18.24*	*18.16*			***18.12***	***0.14***
		KMONA6 AN4-1	*17.83*	*18.44*	*18.15*	*19.05**		***18.14***	***0.31***
		KMONA6 AN3-3	15.34	15.30	15.25			**15.30**	**0.05**
		KMONA6 AN2-3	15.64	15.50	15.40			**15.51**	**0.12**
		KMONA6 AN1-1	14.97	15.15	14.98			**15.03**	**0.10**
		KMONA5 AN7-2	15.08	15.04	15.11			**15.08**	**0.04**
		KMONA5 AN6-2	*18.02*	*17.87*	*17.97*			***17.95***	***0.08***
		KMONA5 AN5-3	*18.08*	*18.03*	*18.33*			***18.15***	***0.16***
		KMONA5 AN4-1	*18.94*	*18.07**	*18.62*	*18.72*		***18.76***	***0.16***
		KMONA5 AN3-3	15.63	15.60	16.01			**15.75**	**0.23**
		KMONA5 AN2	15.26	15.48	15.51			**15.42**	**0.14**
		KMONA5 AN1-3	15.38	15.26	15.01			**15.22**	**0.19**
		KMONA4 AN4-2	*18.49*	*18.02*	*18.25*			***18.25***	***0.24***
		KMONA4 AN3-3	*18.85*	*18.77*	*19.09*			***18.90***	***0.17***
		KMONA4 AN2-2	15.20	15.42	15.05			**15.22**	**0.19**
		KMONA4 AN1-3	15.69	16.04	15.72			**15.82**	**0.19**
		KMONA3 OR1	16.32	16.15	15.72*	16.37	16.50	**16.34**	**0.14**
		KMONA3 AN-1	*19.49*	*19.22*				***19.36***	***0.19***
		KMONA2 OR1	*18.96*	*19.00*	*18.97*			***18.98***	***0.02***
		KMONA1 OR1	16.23	15.98	16.32			**16.18**	**0.18**
		KMONA1 AN-2	*18.34*	*18.45*	*18.99**	*18.60*	*18.46*	***18.46***	***0.11***

Table 5.2.2a Results of isotopic analyses from the Kilnamona Section.

All results are given in ‰ relative to VSMOW. Asterisks indicate statistically anomalous results that were excluded from calculating average values. Yellow italicised rows represent conodont analyses, other rows equate to ichthyolith analyses. Samples are listed with the stratigraphically youngest at the top.

Both fish and conodont analyses in the Kilnamona Section exhibit an initial, minor increase of ~0.2‰ and 0.9‰ respectively, followed by a decline of ~1.1‰ and ~1.2‰ approaching the Viséan-Serpukhovian boundary (Fig. 5.2.2b). An isolated data point (KMONA8 AN-3, Table 5.2.2a) suggests a positive $\delta^{18}O$ excursion near the base of the Serpukhovian, but this relatively increased value is not maintained in stratigraphically higher analyses (Fig. 5.2.2b). The isolated nature of the excursion might indicate that it does not represent significant environmental change. A

discrepancy of ~3‰ is observed between the average values of ichthyolith and conodont analyses from the same horizon. A maximum spread of ~1‰ is observed between individual fish or conodont analyses (from the same horizon) within their respective result populations.

Ten isotopic determinations, (nine conodont, one ichthyolith), were performed on five separate horizons in the St. Brendan's Well Section (Table 5.2.2b). Multiple analyses were undertaken on four of the sampled horizons. Two additional fish samples (comprising a cladodont and actinopterygian scales) from the BW2 horizon failed to produce analysable quantities of Ag_3PO_4.

		Sample No.	Analysis			$\delta^{18}O$	1σ
			1st	2nd	3rd		
Bashkirian	Clare Sh. Fm.	*BW10 AN2-1*	*18.15*	*17.87*	*17.90*	***17.97***	***0.15***
		BW10 AN1-3	12.39	12.41	12.34	**12.38**	**0.04**
		BW8 AN-1	*17.80*	*18.11*	*17.93*	***17.95***	***0.16***
Serpu-khovian	PO_4 lag						
Viséan	Magowna Fm.	*BW4 AN3-3*	*17.36*	*17.42*	*17.30*	***17.36***	***0.06***
		BW4 AN2-1	*17.89*	*18.07*	*18.25*	***18.07***	***0.18***
		BW4 AN1	*18.09*	*18.24*	*18.26*	***18.20***	***0.09***
		BW3 AN2	*17.80*	*17.67*	*17.74*	***17.74***	***0.07***
		BW3 AN1-2	*18.51*	*18.97*	*18.75*	***18.74***	***0.23***
	Slievena-glasha Fm.	*BW1 AN2*	*18.57*	*18.17*	*18.26*	***18.33***	***0.21***
		BW1 AN1-3	*18.70*	*18.70*	*18.62*	***18.67***	***0.05***

Table 5.2.2b Results of isotopic analyses from the St. Brendan's Well Section.

All results are given in ‰ relative to VSMOW. Yellow italicised rows represent conodont analyses, the grey row equates to an ichthyolith analysis. Samples are listed with the stratigraphically youngest at the top.

Conodont apatite analyses from St. Brendan's Well demonstrate a mild decrease in $\delta^{18}O$ values (~0.5‰, from ~18.5‰ to just under 18‰) towards the top of the Magowna Formation (Fig. 5.2.2c). Two bullion analyses from the overlying Bashkirian Clare Shale Formation are almost identical in value (~18‰) relative to the highest horizons in the Magowna Formation below. A maximum spread of ~1‰ is recorded amongst conodont analyses from the same horizon, while a difference of

~5.5‰ is observed between conodont and fish analyses in the one bullion horizon where they were run in tandem.

5.3 DISCUSSION

5.3.1 Understanding the isotopic signal

Several key controls must be understood before attempting to interrogate (in greater detail) the $\delta^{18}O$ values obtained and consider their significance:

5.3.1.1 Global volume of water locked in ice at the time of deposition.

The presence and size of global ice reservoirs during the Viséan has already been dealt with in Section 1.3. In order to calculate the palaeotemperature of the water body in which the analysed fish or conodonts lived, it was necessary to assume a realistic value of oceanic $\delta^{18}O$ (on which the global volume of ice has a significant impact). Although not clear, many workers (e.g. Fielding *et al.*, 2008a; 2008b; Frakes *et al.*, 1992; Isbell *et al.*, 2003b; Rygel *et al.*, 2008) consider the early to middle Viséan as being not significantly glaciated. It therefore appears reasonable to assume the $\delta^{18}O$ value of Holkerian global ocean water to be broadly comparable to today. A value of 0 was substituted for $\delta^{18}O_w$ in the phosphate palaeotemperature equation provided in Section 5.1.2. Since $\delta^{18}O_w$ is in a constant state of gradual flux (due to changes in ice-volume), the substituted value would be expected to evolve towards a value appropriate for more extensively glaciated conditions which developed later in the Serpukhovian. Given that the magnitude of Serpukhovian ice development was most likely very similar to that in the last glacial maximum (Section 1.2.2) a $\delta^{18}O_w$ value of +1‰ (Schrag *et al.*, 2002) to +1.2‰ or even +1.3‰ (Fairbanks, 1989; Pillans *et al.*, 1998) would thus be expected.

5.3.1.2 Palaeoenvironment and palaeogeographical location of sedimentation.

The same evaporation-condensation balance which results in ^{16}O being preferentially removed from the oceans and stored in ice, also controls the localised $\delta^{18}O_w$ values of the worlds water bodies. In areas where the rate of evaporation is high and freshwater inputs are reduced, such as around much of the tropics, $\delta^{18}O_w$ values tend to be increased (Fig. 5.3.1.2). Since both the original $\delta^{18}O_w$ value and

the temperature of the water will affect the $\delta^{18}O$ value of the phosphate analysed, it is imperative to have a more complete understanding of the original palaeoenvironment and, in particular, palaeoceanographic set-up. The water depth, proximity to freshwater sources and palaeogeographical situation (palaeolatitudinal as well as the size and openness) of the water-body will all have a bearing on the possible biasing of the $\delta^{18}O$ value measured.

During the Viséan, Ireland was located just south of the equator in an epeiric sea (Fig. 1.4a). Modern surface waters around the equator exhibit relatively ^{18}O enriched compositions due to the atmospheric evaporation-precipitation balance (Fig. 5.3.1.2). It is therefore probable that the $\delta^{18}O$ value of the surface water in Ireland during the Carboniferous was slightly higher than the global average; however, it would be very difficult to calculate this offset. Since Ireland's palaeogeographic location was essentially static in the timeframe studied, no adjustments were deemed necessary to extract information about isotopic change through the sections.

Brand *et al.* (2009) argued that the use of isotopic data from epeiric seas for international correlation or the reconstruction of palaeoclimate was "*questionable*" due to local effects. Since the work of Brand *et al.* (2009) was based only on brachiopod calcite and, rather prematurely, discounted conodont apatite, the results are noteworthy, but of inflated significance. Even with the most rigorous screening methods, inter- and intra-section variations of brachiopod $\delta^{18}O$ tend to be significant and thus make it more difficult to identify local controls from random "noise". Sessile brachiopods are also more susceptible to being influenced by localised conditions, while nektic conodonts are thought to have been capable of recording much more of an averaged $\delta^{18}O_w$ value. Isotopic results, obtained from NW Ireland, are directly comparable to published $\delta^{18}O$ values of conodont apatite from elsewhere for the same time interval. The $\delta^{18}O$ values of late Viséan conodonts from NW Ireland (~20-21‰) are very similar to results from sections in the Cantabrian Mountains of Spain (~20-22‰, Buggisch *et al.*, 2008). The Cantabrian mountain sections were deposited as condensed carbonate sequences in a foreland basin setting (Keller *et al.*, 2007), which is distinct from the non-continuous carbonate platform setting of NW Ireland. Thus, since the NW Ireland

conodont results are compatible with those further south from Spain, it is likely that the NW Irish $\delta^{18}O$ values are reasonably representative of oceanic conditions, despite clear sedimentological evidence for periodic high evaporation rates.

5.3.1.3 Mode of life of the bearer of the phosphatic element analysed.

When analysing the chemistry of any fossil in order to elucidate information about the palaeoenvironment in which it lived, it is important that:

- **(a)** the relationship between the chemistry of the environment and that of the fossil organism is simple, with quantifiable controls and no significant "vital effect".
- **(b)** the life-cycle and life-strategy of the creature is well-understood. Structures which are shed repeatedly on short time-scales may record localised irregularities or perturbations, while elements which are maintained throughout life are more likely to represent an overall average of conditions recorded over the duration of the creature's life.
- **(c)** the palaeoenvironment of the creature being analysed is constrained, since, for example, the chemistry of deep marine and brackish estuary environments are obviously different.

Unfortunately Palaeozoic analyses must be undertaken on extinct creatures and so the degree to which it is possible to satisfy all the points above is quite variable.

Analyses in this work were restricted to fish remains (predominantly denticles) and conodont elements. Isotopic analyses of modern fish material (Kolodny *et al.*, 1983; Vennemann, 2001) have demonstrated that the biogenic apatite of fish is produced in isotopic equilibrium with the water they inhabit. Fossil fish remains, both by association with modern fish (Joachimski & Buggisch, 2002) and also due to the realistic $\delta^{18}O$ values they yield (Longinelli & Nuti, 1968), are also believed to have formed in equilibrium to the ambient water-body. Conodonts went extinct in the Triassic and it is, therefore, very difficult to prove conclusively that they too formed their phosphatic remains in equilibrium with the seawater in which they lived. Since conodont and fish analyses are often comparable (Joachimski & Buggisch, 2002) and conodont apatite appears to yield results which match palaeoenvironmental and temporal expectations (Joachimski *et al.*, 2003; Luz *et al.*, 1984), conodont apatite

is also generally accepted as accurately reflecting the $\delta^{18}O$ composition of palaeoseawater.

Although Palaeozoic fish have many extant relatives, understanding of their life-cycles is largely poor, as most fish denticles are highly morphologically conservative and it is difficult to identify Palaeozoic remains to a useful taxonomic level (Chapter 4). Nothing is really known about the life-cycles of conodonts, although the widespread distribution of environmentally restricted species may suggest that either, a wide-ranging planktonic stage existed, or conodonts were capable of travelling long distances. Due to the small size of the conodont animal, it is probably unlikely to have been capable of undertaking very large migrations in a single lifetime. Some of the larger elasmobranch remains analysed in this study probably belonged to a fish of sufficient size (probably up to 1m in length based on comparisons to extant, small sharks - Moss, 1972; Strasburg, 1963) to migrate reasonable distances.

Modern sharks replace their teeth at rates varying from several days to a few months, depending on the species and season (Luer *et al.*, 1990). Many of the ichthyoliths analysed here were also (probably) continuously replaced (although some Palaeozoic species did not shed their denticles - Williams, 2001) during animal growth and so may reflect the environmental conditions essentially of where they were found (unless they were transported or descended through a significant column of water post-mortem). Such shedding suggests that even if larger fish were migrating into compositionally different water masses, such chemical differences (e.g. $\delta^{18}O$ values) would not be reflected in the teeth analysed, since they most likely formed in the area in which the teeth were shed. As seen in Section 1.1.2, conodont elements were most likely retained throughout life; therefore analysis of an element will give an average of all the water in which the conodont lived. A bias will exist towards the water inhabited in later life, since the growth layers accreted during this stage will be volumetrically more significant. Since conodont animals were probably unable to migrate far, they too are likely to be representative of the water in which the host rocks were deposited (again, once transport and depth stratification have been considered).

The supposed palaeoenvironmental preferences of many of the conodonts found during this work have been discussed in Chapter 4 and in Section 1.1.3. Despite the existence of recognised conodont biofacies, isotopic analyses of conodonts in the past, from the same samples but supposedly different biofacies, have failed to show significant or consistent $\delta^{18}O$ differences (Joachimski *et al.*, 2003; 2006; 2009). These studies, in combination with the evidence of photic-zone adapted eyes, have been interpreted as an indication that all conodonts, and therefore conodont apatite, are essentially representative of both palaeosurface-water temperature and $\delta^{18}O$ values (Rigo & Joachimski, 2010). The palaeoenvironmental preferences of most of the fish in this work are harder to deduce, due to a lack of published work on the matter, as well as the difficulties associated with accurate identification of the material. Based on the variations amongst *and* between modern fish species, due to their preferred depth and habitat (Kolodny *et al.*, 1983; Vennemann, 2001), fossil fish material would be expected to display varying $\delta^{18}O$ values reflecting their palaeohabitat.

5.3.1.4 Fidelity of the phosphatic element being analysed.

The potential for alteration is an important consideration when interpreting any geochemical data. As discussed earlier, fish apatite has been shown to record the isotopic composition of the waters inhabited by the creature and that preservation of appropriately positive $\delta^{18}O$ values can be traced back into the fossil record and matched with similar realistic results from conodont apatite. Experimental work (Blake *et al.*, 1997; Zazzo *et al.*, 2004) has demonstrated that biogenic apatite is generally resistant, but that relatively rapid alteration of $\delta^{18}O$ values can occur during enzyme mediated microbiological action. It has also been suggested (Pucéat *et al.*, 2004) that some exchange of oxygen isotopes may occur between biogenic apatite and high-temperature crustal fluids. No clear cut-off temperature is proposed beyond which alteration will occur. However, the $\geq$ 5 C.A.I. values of the Co. Clare sections (equating to temperatures of ~350ºC), are significantly greater than the C.A.I values of 2-2.5 (and temperatures of 200ºC) suggested by Pucéat *et al.* (2004) where alteration might be expected. The work of Joachimski *et al.* (2009) contradicts the findings of Pucéat *et al.* (2004) and demonstrates virtually no change in conodont $\delta^{18}O$ values or trends up to at least C.A.I. 5.

Identifying strict criteria to determine when a biogenic apatitic element has undergone some degree of alteration is not straightforward. Rare Earth Element (REE), U, Th, Y and Sr concentrations, as well as crystallinity, have all been proposed as monitors of original isotopic signature (Brand *et al.*, 2009; Pucéat *et al.*, 2004; Trotter & Eggins, 2006; Zazzo *et al.*, 2004). Such monitors can indicate when samples are unquestionably pristine, but probably cannot be used to prove resetting of $\delta^{18}O$ values. Exchange of elements may occur in a biogenic apatite crystal without any reaction of O in the PO_4^{-3} cation and since only the O bound in the PO_4^{-3} is analysed, any other elemental alteration is meaningless with respect to the methodologies employed here (see Section 6.3 and Appendix C).

The density and crystal size of the biogenic apatite analysed is thought to be the dominant control on its susceptibility to O exchange. Chemical, histological and isotopic studies (Sharp *et al.*, 2000; Trotter & Eggins, 2006; Trotter *et al.*, 2007; Zazzo *et al.*, 2004) have shown that conodont albid crown tissue and tooth enamel (Fig. 1.1.2a) are the most resistant to isotopic exchange, whilst conodont hyaline crown and basal tissue (as well as bulk tooth and bone material) are more susceptible to change. Conodont albid crown, due to its densely packed arrangement of large crystals, has a reduced reactive surface area available for exchange. Conversely, bone and basal tooth crystals are more porous and traversed by extensive canal networks, effectively increasing the reactive surface area. Conodont albid crowns and fish enamel offer some degree of protection to their respective underlying, more susceptible dental material. Conodonts outer layers comprise dense apatite crystals (Trotter *et al.*, 2007), while Palaeozoic fish tended to have poorly developed enamel caps (Sharp *et al.*, 2000). The porosity of fish elements is therefore much greater than in conodonts. This means that conodonts should be the primary target for Palaeozoic isotopic studies based on biogenic apatite.

The fish material analysed herein is understood to have undergone some alteration and loss of ^{18}O for the following reasons:

(a) The variation in $\delta^{18}O$ values between fish analyses, taken from successive sampled horizons and also sometimes the same bed, tends to be significant

(e.g. Fig. 5.2.1b). This could, however, be real data, representing quite rapid climate oscillations, perhaps fitting the Milankovitch periodicities identified by the spectral analysis in Section 2.5.

(b) All fish analyses yielded $\delta^{18}O$ values systematically depleted in ^{18}O relative to broadly coeval conodont material. This depletion is a classic sign of interaction and O exchange with relatively ^{18}O-deficient fluids post deposition (Fig. 5.1.2a).

(c) The lower $\delta^{18}O$ values of fish analyses, if accepted at face value, represent palaeotemperatures (calculated using the equation in Section 5.1.2) which are not only implausible but are, in some cases, above the threshold of protein denaturation (commonly up to ~46ºC - Figs. 5.3.1.4a-b).

(d) A slightly larger disagreement between conodont and fish $\delta^{18}O$ values exists in the Burren Platform sections, compared to that observed in northwest sections. This may be attributable to greater alteration in the Shannon Basin region, where higher temperature fluids were probably circulating. The difference in the region specific conodont-fish discrepancy is discussed further in Section 5.3.3.

(e) Several horizons from both regions investigated yielded fish microfossils which had been partially or wholly replaced by pyrite, or were especially degraded and pale. Pyrite replacement indicates wholesale absorption of PO_4^{-3} and may indicate that significant isotopic exchange had occurred in the remaining apatite.

(f) Some fish material (from the northwest and Shannon Basin area) which appeared unaltered under initial microscopic examination (x10-x32), was found to have significant apatitic mineral overgrowths when viewed at higher magnifications under SEM (Section 4.6, Fig. 4.6a). The apatite overgrowths, if not formed in isotopic equilibrium/continuity with the original ichthyolith element, would offer a possible explanation for the lowered $\delta^{18}O$ values observed. The mineral overgrowths are probably the result of a combination of recrystallisation of the original biogenic apatite and precipitation of inorganic apatite from fluids onto the phosphatic nucleus. Recrystallisation may result in some degree of isotopic exchange with local fluids and initiate the formation of an in-growth “bud”. Any phosphate in the fluid system would then be attracted to precipitate upon

this “bud”. The inorganically formed apatite would most likely form in isotopic equilibrium with the parent fluid (diagenetic, crustal or meteoric etc.), and so should be significantly depleted relative to the original biogenic apatite.

Although the “cleanest” fish materials were selected for isotopic analysis, evidently some chemical alteration had already occurred which was not visually identified. Whether the alteration produced some identifiable indicator is not known, but nothing was apparent during several examinations under the microscope. Despite the alteration of the $\delta^{18}O$ values of the fish material analysed, it is believed that the resultant negative shift of the data may actually be compensated for (this is discussed further in Section 5.3.3 below).

5.3.2 Isotopic discrepancy between the study regions.

The trends and values of analyses from different sections within the same depositional area (i.e. *either* NW Ireland *or* the northern Shannon Basin area) are observed to be highly compatible (Figs. 5.2.1a & 5.2.2a), despite being up to ~30km apart (e.g. Aghagrania and Carraun/Lugasnaghta Sections). In contrast, a significant discrepancy in $\delta^{18}O$ values (of both fish and conodont material) is observed *between* the Co. Clare *and* NW Ireland sections.

The palaeotemperatures derived from conodonts extracted from the northwest appear realistic (using the original temperature derivation equations) and their isotopic values are highly comparable with those of temporally equivalent Spanish sections, some 1200km away (Buggisch *et al.*, 2008). The $\delta^{18}O$ values obtained from Co. Clare, on the other hand, appear to be recording some local perturbation in the $\delta^{18}O_w$ dynamic. Conodont analyses from the Burren region sections show a reduction in $\delta^{18}O$ values of between ~1‰ and 3‰ relative to those from the northwest region, whilst fish analyses exhibit an equivalent ~2‰ to 3.5‰ depletion. The discrepancy in the values between the two areas must be a product of one, or a combination, of the factors discussed below:

(a) Differing water mass palaeotemperatures

The isotopic offset between the two study areas, if attributed purely to temperature differences, requires an increase of ~4.3-12.9ºC (conodonts) or ~8.6-15.1ºC (fish) moving from the sections in the northwest to those located further south in Co. Clare. Such a seawater temperature gradient over a distance of just over 100km is difficult to envisage. To generate such a temperature increase, over a comparatively short distance, would probably require either some sort of strong palaeocurrent or some degree of watermass restriction.

There are no modern analogues for equatorial region currents developing strong temperature gradients in continental seas (Fig. 5.3.2a). It is very difficult to conceive a situation whereby a current could be responsible for significantly cooling only the northwestern area, particularly as deposition there, occurred in reasonably shallow water, which was probably insufficiently deep to sustain a large current system.

Viséan carbonates are preserved across the platform which existed between the Shannon Basin and the northwest study area. The Ox Mountains may have acted as a localised submerged high, but this would not have created the restriction necessary to increase the palaeotemperature of the Shannon Basin watermass. A probably emergent “Galway-high” existed in northern Clare and Galway during the early Serpukhovian (Sevastopulo, 2009). Although the “Galway-high” possibly interrupted direct watermass transport, it probably did not act as a complete barrier to water mass exchange between the Shannon Basin and NW Ireland. During pronounced lowstands associated with increases in global icevolume, temporary restriction of water masses may have occurred. However, Fig. 5.3.2a demonstrates that, essentially, complete isolation of a watermass is necessary to generate significant, localised temperature gradients and there is no evidence for this during the study interval in Ireland, especially the Viséan.

A water temperature difference, with the more equatorial northwestern sections considerably cooler than those in the Shannon Basin area is not thus considered feasible.

(b) Differing local conditions of evaporation and/or freshwater influx

The depositional palaeoenvironments of the northwest sections were described in Chapter 2, whilst those of the Shannon Basin were dealt with in Chapter 3. It was expected that since the northwest sections were located closer to a palaeoshoreline and were deposited in generally shallower water (particularly the Meenymore and Bellavally Formations), the isotopic results would be more likely to have been affected by the localised effects of meteoric run-off and/or high evaporation rates. Thus, the Burren Platform (north of the Shannon Basin), which was thought to have been located further offshore in deeper water, was expected to provide a more accurate (and stable) representation of the true $\delta^{18}O$ values of Viséan and Serpukhovian seawater. Being a larger water-mass it would be volumetrically greater and buffered against potential fluctuations. With widespread evidence of high evaporation rates (evaporites, desiccation cracks, hypersaline faunas, algal mats) in the northwest sections it could be that increased evaporation led to the concentration of ^{18}O in the nearshore waters and thus the increased $\delta^{18}O$ values relative to the Shannon Basin. However, since:

(1) results from macrocell horizons (i.e. horizons with mineral "pockets" which are thought to represent replacements of primary gypsum) and normal marine horizons within the Bellavally and Meenymore Formations are essentially the same

(2) $\delta^{18}O$ values from the Meenymore and Bellavally Formations are only slightly (~0.5‰) higher than those from the deeper marine, upper Carraun Shale and Dergvone Shale Formations

and

(3) isotopic results from the NW of Ireland are generally comparable to those obtained from deeper-water sections in northwest Spain,

- it is considered unlikely that increased evaporation can account for much, if any, of the large isotopic differences observed between the sections in the northwest and those in Co. Clare.

In order to locally decrease the $\delta^{18}O_w$ value in the Shannon Basin area, large freshwater inputs are required, most probably from a large river system. Since the northwest sections examined are not affected by the negative isotopic shift, the hypothetical river system which affected $\delta^{18}O_w$ values must not have flowed from

the northern landmass. No evidence for reduced salinity has been reported for the Viséan limestones which yielded the bulk of the samples taken from the Co. Clare Sections; however, some results from the post-Viséan sedimentary rocks may indicate more brackish conditions. Isotopic results from the late Viséan and Bashkirian in the St. Brendan's Well Section are virtually identical. This supports the idea that if a river system was developed in the Bashkirian, which affected the $\delta^{18}O_w$ values, then it *may* also possibly have been present in the late Viséan.

The post-Viséan sequence in the Shannon Basin contains concentrated fossil horizons or "marine bands" which have been interpreted elsewhere to represent fully marine conditions in an otherwise more brackish environment (Holdsworth & Collinson, 1988). During normal deposition the watermass would have been diluted to brackish conditions by freshwater influx, thus marine fossils tend to be reduced or absent. Fully marine conditions would have become established only during transgressions and highstands, leading to the development of widely correlateable beds bearing a marine fauna. Characteristic faunas were suggested by Holdsworth & Collinson (1988) for various salinity levels. Thick-shelled ammonoids were proposed as being typical of fully marine conditions, whilst thin-shelled ammonoids and bivalves were thought to represent more brackish conditions. The bivalves *Dunbarella* and *Posidonia* were found to be very common in the St. Brendan's Well Section. The magnitude of the suggested freshwater input between marine bands would have been sufficient to account for the isotopic discrepancy between study areas. Braithwaite (1994) refuted this fluctuating salinity and argued that conditions in the Shannon Basin never attained brackish or low salinity levels; however, there are several pieces of evidence which suggest a significant river system was present to the west of the Shannon Basin.

(1) In the Clare Shale Formation (particularly in the St. Brendan's Well Section) notable concentrations of flattened plant material are found within shale laminae. Some of the woody fragments attain lengths of ~50cm and widths of ~10cm or more. The presence of fossilised woody material and also a rare insect (Monaghan, 1995) suggests that a forested river basin existed nearby, whilst the high concentrations (observed at some stratigraphic levels) suggests that the volumes of freshwater being discharged may have been potentially large.

(2) The Ross Sandstone Formation (Serpukhovian to Bashkirian in age) is generally interpreted as comprising a deep sea turbiditic sequence (Section 3.1.5); however, Higgs (2004, 2009) has recently proposed a reinterpretation of the sequence as lacustrine, river-fed turbidites and wave modified turbidites. Much of the evidence provided by Higgs (2004, 2009) is ambiguous and numerous counter arguments to this alternative model have been made by Pyles (2009). Regardless of whether this new interpretation is valid, it is interesting that brackish or freshwater conditions have been proposed for much of the formation. Sedimentological evidence (e.g. hummocky cross-stratification and near symmetrical ripples) may indicate that deposition of the Ross Sandstone Formation occurred above storm wave-base (Higgs, 2004, 2009). It was also argued that the lack of fossils for large thicknesses of the formation, and in particular, the paucity of trace fossils was consistent with dominantly fresh or brackish conditions.

(3) Later, in Bashkirian times the Shannon Basin was filled with sediments from a broadly, westerly direction (Chapter 3). The basin filling was unequivocally strongly controlled by large river systems by this time. Initially this was manifest by probable turbidites, likely initiated due to the high output of river transported sediment onto an unstable slope. The probable turbidites of the Ross Sandstone and Gull Island Formations were then followed by the deltaic deposits of the Central Clare Group.

The presence of a landmass and river system to the west of the Shannon Basin later in the mid-Carboniferous is unquestionable, whether this river system was close enough and of sufficient magnitude to affect the $\delta^{18}O_w$ values of the basin earlier during the Viséan is equivocal, but plausible.

(c) Alteration on a regional scale

The sediments of the Shannon Basin have been subjected to significantly greater heat-flow than their northwestern counterparts (C.A.I >5 vs. C.A.I 3-4). A larger discrepancy between fish and conodont analyses in the Shannon Basin region (relative to northwest sections) could indicate that the higher metamorphic grade affected isotopic results from the Co. Clare sections. Studies (Joachimski *et al.*, 2003; 2009), which argue for no change in $\delta^{18}O$ values with increasing burial

temperature, make it more difficult to attribute these observed differences in conodont $\delta^{18}O$ values between the regions, purely to alteration. However, the studies cited above only worked on conodonts up to C.A.I 5, and other research (Pucéat *et al.*, 2004) has implicated increased temperature as effecting isotopic exchange between crustal fluids and biogenic apatite.

The similarity of the $\delta^{18}O$ between Kilnamona and St. Brendan's Well, separated by over 20km, argues against alteration of the isotopic signal, since it is unlikely that both sections would be affected to such a similar degree. If homogenous fluids and pervasive regional alteration accounted for the similarity of the isotopic signal between the sections, then the $\delta^{18}O$ values of conodont and ichthyolith analyses would be expected to flatline throughout the sections. This is clearly not the case in either the Kilnamona (Fig. 5.2.2b) or St. Brendan's Well sections (Fig. 5.2.2c). Alteration through isotopic exchange with circulating fluid would be expected to be strongly lithologically controlled, with samples from weaker, more permeable strata being significantly more affected. There is no indication of any lithological control on the $\delta^{18}O$ values obtained in either the Kilnamona or St. Brendan's Well sections.

(d) Different life habits of the analysed faunas

The faunas analysed in the northwest and Shannon Basin regions were largely identical and it is therefore implausible to suggest that different populations of the same species living in inter-connected water-masses possessed sufficiently different life strategies to affect their respective $\delta^{18}O$ values.

(e) Upwelling of a cold current in the Shannon Basin

Upwelling of ^{18}O-depleted cold currents can cause a lowering of $\delta^{18}O$ values in surface waters (See northwest coast of South America, Figs. 5.3.1.2 & 5.3.2a). The isolated nature of the Shannon Basin (Fig. 1.4c) in the Mississippian, with respect to other deeper water basins in the generally shallow epeiric sea, makes it improbable that a deepwater current could have been sustained in the area. However, the influence of upwelling along platforms in America have been suggested during highstands as a result of reconfigured palaeocurrents in the Carboniferous (Mii *et al.*, 2001).

(f) Effect of the Intertropical Convergence Zone (ITCZ)

The ITCZ refers to the near-equatorial low pressure belt where air is heated and rises (Fig. 5.3.2b). The heated air mass splits due to the Coriolis Effect and as the respective air masses travel north and south they begin to cool and descend, eventually re-converging towards the low pressure system, forming the trade winds (Garrison, 2007). The surface waters below the ITCZ tend to have lowered $\delta^{18}O$ values, relative to adjacent waters (Armstrong *et al.*, 2009), due to two main factors:

(i) As humid equatorial air rises, it expands and cools causing moisture to precipitate. As seen earlier, atmospheric water is relatively depleted in ^{18}O, therefore enhanced precipitation in the ITCZ (Fig. 5.3.2b) can cause negative isotopic shifting of $\delta^{18}O_W$ values.

(ii) The convergence of the trade winds in the ITCZ can cause the establishment of a weak wind blowing from east to west (Fig. 5.3.2b). This wind, though blowing from an easterly direction, causes a net flow of water to the north and south, away from the equator due to Ekman transport (Garrison, 2007). As the surface waters split, water from depth must rise to accommodate the space; thus causing upwelling of cooler ^{18}O-poor water (displayed clearly in the Pacific and South Atlantic in Fig. 5.3.1.2 and the Pacific in Fig. 5.3.2a).

The ITCZ does not exactly coincide with the geographical equator due to temperature irregularities; instead it coincides with the meteorological or thermal equator. The ITCZ is presently shifted slightly north of the equator due to the greater concentration of landmasses in the northern hemisphere (Garrison, 2007). Ireland was situated to the south of the equator in the Viséan along with the bulk of continental landmasses (Fig. 1.4a). The ITCZ was probably significantly deflected to the south of the palaeoequator during the Carboniferous, particularly during southern hemisphere summers, when Gondwana would probably have generated significant low-pressure systems (Falcon-Lang, 1999b). A seasonal monsoonal climate has been proposed for Ireland and Britain during the Asbian and Brigantian (Falcon-Lang, 1999a; Wright, 1990), with high rainfall amounts during the northern hemisphere summer, but low amounts during the southern hemisphere summer. It is possible that, since it would have been ~100km further to the south, and therefore closer to the southward-shifted humid belt, the Shannon Basin region received more rainfall than the northwest region. The relatively contemporaneous development

(during emergence) of palaeokarsts and palaeosols on the limbs of the Shannon Basin, whilst calcretes and evaporites dominated the northwest region, supports the idea of greater rainfall and therefore a possibly greater ITCZ influence on the Clare Sections, further south. However, more detailed work on the precise nature of emergent horizons in both the Shannon Basin region and northwestern study area is required.

On balance, it is very difficult to identify the exact reason for the significant isotopic offset between the Shannon Basin and NW Ireland regions. It is thought that despite the resilience of biogenic apatite, some alteration of the isotopic signature in the Shannon Basin region may have indeed occurred. Ichthyoliths from this area have almost certainly experienced some $\delta^{18}O$ alteration. Where probable alteration has occurred though, it seems to be relatively consistent and so has not affected the overall trends. The possibility of some degree of ^{18}O-poor water input, whether from the ITCZ or from a large river-system, is plausible, but admittedly equivocal based on the available evidence at present.

5.3.3 Inter- and intra-conodont and ichthyolith isotopic variations.

In an attempt to identify and quantify possible inter- and intra- conodont and fish $\delta^{18}O$ differences, which may reflect some intrinsic palaeobiological control, multiple apatite samples were analysed from several horizons. Conodont data were compared against other conodont analyses (Figs. 5.3.3a-b) as well as against fish (Figs. 5.3.3a, c-d). Less specific fish analyses were also compared (Fig. 5.3.3d).

Fig. 5.3.3a and Fig. 5.3.3b show the ten comparisons of conodont $\delta^{18}O$ values which were possible to run from the same stratigraphic horizons. Five of the points represent comparisons of *G. bilineatus* with other conodonts, four represent *Gnathodus* sp. (with a large proportion of *bilineatus*) vs. *Lochriea* sp. and a single point compares the results of large vs. small *G. bilineatus* platforms. All of the conodont comparisons fall in the positive field (i.e. *Gnathodus* sp. values were greater than those of the comparative conodont) with the magnitude of difference varying from 0.02‰ to 1‰.

Since conodont platform size can be used as a proxy for animal size, and therefore age (Donoghue & Purnell, 1999; Purnell, 1993, 1994), the $\delta^{18}O$ values of *G. bilineatus* platforms of considerably different sizes were compared. P_1-element width and length (sensu Purnell, 1994) of the small and large conodonts averaged 0.3mm:0.8mm and 0.7mm:1.6mm respectively:

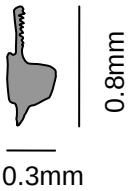

Juvenile *G. bilineatus*

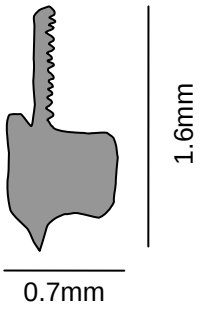

Mature *G. bilineatus*

The size difference between the platforms represents, approximately, a four-fold increase in platform area and therefore a significant increase in body mass. Despite the clear difference in age of the organisms there was virtually no difference between the $\delta^{18}O$ values observed (0.13‰ - essentially the same as the analytical reproducibility of analysis). This strongly suggests that, for *G. bilineatus* at least, young and old conodonts lived in the same palaeoenvironment and water level.

G. bilineatus elements were very common in many of the sections examined and due to their large platform size proved ideal for isotopic analysis. *G. bilineatus* was found to yield higher $\delta^{18}O$ values than other conodonts (*G. girtyi* – 0.61‰, *G. homopunctatus* – 0.34‰, 1.0‰, *Lochriea* – 0.02‰, 0.81‰ or mixed multi-element collections – 0.71‰, 0.84‰) on the five occasions where they were analysed together (Fig. 5.3.3b). Although there are not enough data to be certain, this would suggest that *G. bilineatus* elements are (relatively) very slightly enriched in ^{18}O. This suggestion is given support from additional *Gnathodus* vs. *Lochriea* analyses undertaken. In each of these comparisons the *Gnathodus* were found to be more positive (0.2‰, 0.65‰) than the *Lochriea* and it is proposed that the contribution from *G. bilineatus* is the reason. Preferential resistance to alteration cannot explain the differences observed in $\delta^{18}O$ values since

(1) the conodonts are essentially compositionally identical

and

(2) although the *G. bilineatus* platforms analysed tended to be larger and have a greater volume to reactive surface area than the other conodonts analysed, virtually no difference was observed between the larger and smaller *G. bilineatus* analyses, where there was a substantial differential in this particular ratio.

The higher $\delta^{18}O$ values found in *G. bilineatus* can be explained by the conodont living in either a slightly more saline (evaporation dominated) palaeoenvironment or, alternatively, in slightly cooler water. Since *G. bilineatus* is associated with deeper, open marine conditions (Somerville & Somerville, 1998; Somerville, 1999), the isotopic enrichment is possibly more likely a result of it inhabiting slightly deeper, cooler waters.

Apart from *G. bilineatus,* conodont analyses were found to be comparable and consistent with the concept (outlined in Section 1.1.1 and Section 5.1.2) that most conodont $\delta^{18}O$ values are likely representative of surface water conditions.

The discrepancy between fish and conodont analyses is clearly defined on Figs. 5.2.1c-d and 5.2.2a-c. Figs. 5.3.3a, c-d attempt to try and identify whether consistent offsets were present between conodont and fish elements throughout the sections studied. Insufficient species-specific analyses were undertaken to be able to make definite statements about the relationships between certain conodonts and certain fish. From 28 comparisons of conodont and fish $\delta^{18}O$ values, an average offset of 2.93‰ (fish material being relatively depleted) with a standard deviation of 0.72‰ was obtained. The bulk of the comparisons were made from the Kilnamona Section, whilst two comparisons were possible from the Carraun/Lugasnaghta Section and only single comparisons were possible from the Aghagrania and St. Brendan's Well Sections.

It appears that, apart from two discrete outliers (CNLG14 & BW10 AN1-3; extreme left and extreme right respectively on Figs. 5.3.3a & c), all of the fish and conodont data have an essentially stable offset of just under 3‰ regardless of location or isotopic value. This could imply that the difference between fish and conodont data may infact be original, since if it were diagenetic then varying degrees of alteration

may be expected. This would lead to larger offsets and decreased average $\delta^{18}O$ values (diagenetic alteration almost invariably lowers $\delta^{18}O$ values) being displayed by samples subjected to greater alteration. The most plausible explanation for a primary, and indeed consistent, isotopic offset between conodonts and fish (from the same stratigraphic horizon) would be to invoke some possible original bias in the incorporation of ^{18}O, but as discussed earlier there are strong arguments against this.

Upon closer inspection of the conodont-fish isotopic offset, it is clear that the discrepancy in $\delta^{18}O$ values is different in the northwest and Shannon Basin regions. The difference in the region specific conodont-fish offset is not clear from Fig. 5.3.3a or Fig. 5.3.3c, since not enough parallel analyses were possible in the northwest sections. The largest offset (3.11‰) between conodont and fish (acanthodian denticles) analyses in the northwest sections was found in sample CNLG.A. The offset appears to be very similar with those of the Shannon Basin region; however, when contrasted with the only conodont-acanthodian tandem analysis from the southerly area (BW10, producing a difference of 5.59‰), the analysis from CNLG.A is clearly less offset. In order to more fully understand the conodont-fish offset in the northwest sections, conodont and fish analyses from stratigraphically similar horizons (e.g. section overlaps) were compared. Once the abnormal acanthodian differences are excluded and conodont-fish comparisons from section overlap in the northwest (AGHA/CNLG) are included, the difference between conodont and fish $\delta^{18}O$ values in each region becomes much clearer (Fig. 5.3.3e).

The offsets between average conodont $\delta^{18}O$ and average fish $\delta^{18}O$ from the Kilnamona Section (taken as representative of the Shannon Basin region) in beds KMONA1 AND KMONA3-6 are 2.28‰, 3.02‰, 3.06‰, 2.92‰ and 2.85‰ respectively. These results suggest a relatively stable relationship between average fish and conodont $\delta^{18}O$ data (in the Kilnamona Section at least) with a mean offset of 2.82‰ and a standard deviation of 0.31‰ (the average offset of all the 24 individual Kilnamona comparisons is 2.9‰ with a standard deviation of 0.4‰). Conodont and fish $\delta^{18}O$ analyses in the Aghagrania and Carraun/Lugasnaghta Sections (taken as representative of the northwest study area) appear to differ by an

average of 2.0‰ (2 same horizon comparisons, 7 stratigraphically adjacent comparisons) with a standard deviation of 0.5‰.

The discrepancies in both the northwest and Co. Clare Sections are stable to within <1‰. The trends formed by fish data will be *tentatively* considered as "real" and may probably be returned to their original values by adding:

- 2‰ in the case of analyses from the northwest (Fig. 5.3.3f).
- 2.9‰ for analyses from the Shannon Basin region (Fig. 5.3.3g).

It is proposed here that the offset between conodonts and fish can almost wholly be attributed to slight alteration of the more porous and finely crystalline fish material. Thus the alteration in fish may possibly be relatable to the thermal maturation of a region and C.A.I. values. However, the relationship between the fish-conodont $\delta^{18}O$ offset and C.A.I. is not simple, since, a similar relatively stable offset of ~2‰ has recently been reported from the Silurian of Lithuania with a C.A.I. of no more than 1.5 (Žigaite *et al.*, 2010a).

The results of comparing $\delta^{18}O$ values from different fish materials are plotted in Fig. 5.3.3d. Insufficient multiple fish analyses were made to show any definitive trends. It appears that all fish material is essentially identical, with any variation tending to cluster around the 0-difference line, irrespective of average $\delta^{18}O$ values.

5.3.4 Palaeoclimatic interpretation

Once the fish $\delta^{18}O$ data in the northwest sections were adjusted for alteration they were combined with the conodont analyses and a 5-point moving average trendline was drawn to smooth any irregularities (Fig. 5.3.4). This trendline illustrates the overall variation in $\delta^{18}O$ values through the temporal interval studied; however, an adjustment must be made to convert this into sea surface temperature (SST) change. Significant cooling, sufficient to cause the formation of large-scale ice-sheets, is indicated from the northwest section data. The formation of large ice-sheets would have had the effect of increasing the $\delta^{18}O$ values of the seawater and thus give the impression of greater cooling than actually occurred (e.g. Buggisch *et al.*, 2008; Joachimski *et al.*, 2006). An increase in the $\delta^{18}O$ value of 1.2‰ in the

palaeoseawater is assumed herein to have occurred between the basal Asbian and the middle Brigantian (least and most positive results), as discussed in Section 5.3.1.1. The adjusted trendline, showing the change in temperature over the sections, is shown in red in Fig. 5.3.4. A maximum change of ~1.4‰ in the biogenic apatite analysed (taken as due to temperature only), represents a decrease in SST in the palaeoequatorial epeiric sea of ~5.9ºC. It is important to note that regardless of the equation used to determine palaeotemperatures from the $\delta^{18}O$ values of apatite, or even whether it is accurate to determine absolute temperatures through such methods, the calculation of the relative decrease in temperature identified in the temporally short dataset herein is valid. The value of 5.9ºC is compatible with that recorded for tropical SST change during the last glacial maximum (Beck *et al.*, 1997; Guilderson *et al.*, 1994). Cooling seems to have begun around the basal Asbian and attained its lowest values during the early Brigantian. Temperatures appear to have remained relatively stable during the middle and upper Brigantian substage before slightly warming in early Serpukhovian times.

Due to the relatively short stratigraphical coverage of the Co. Clare Sections, their use in studying the Carboniferous palaeoclimate is somewhat limited. Similar to the sections from NW Ireland, the Kilnamona Section demonstrates no apparent continued isotopic shift, and therefore no sustained cooling, across the Viséan–Serpukhovian boundary. No Serpukhovian samples were analysed from the St. Brendan's Well Section; however, two Bashkirian bullions yielded $\delta^{18}O$ values essentially identical to the uppermost Viséan carbonate values. This tentatively suggests that the glaciated climatic conditions which existed at the very end of the Viséan may have been similarly developed in the early Bashkirian.

CHAPTER 6 - DISCUSSION & CONCLUSIONS

This chapter will integrate the observations and results from Chapters 1-5, highlight the importance of the main findings of this work and make suggestions for the direction that future studies might take.

6.1 CARBONIFEROUS SEA-LEVELS AND SEQUENCE STRATIGRAPHY

Due to the close association of sea-level and sedimentation in a general sense, sea-level variations have had a significant impact on the recognition and correlation of stratigraphic sub-divisions. The link between sedimentation and fluctuating sea-levels in Carboniferous strata was identified as being particularly significant over 70 years ago (Wanless & Shepard, 1936). Since then, numerous studies (e.g. Cózar & Somerville, 2005; Gallagher, 1996; Gallagher & Somerville, 1997; Heckel, 1977, 1995, 2002; Schwarzacher, 1989; Wright & Vanstone, 2001) have strengthened the connection between high-frequency sea-level changes and (1) cyclical packages of sedimentary rocks *and* (2) numerous horizons of exposure within otherwise marine sequences, during Carboniferous times.

6.1.1 Global record of Carboniferous sea-levels

The Carboniferous was a period of relatively low global sea-levels (Haq & Schutter, 2008; Miller *et al.*, 2005) due to a combination of the effects of increased glaciation (see Section 1.3) and a relatively high state of continentality and (therefore) reduced volumes of young, buoyant oceanic lithosphere (Cogné & Humler, 2008). Superimposed on the long-term sea-level curve, are the effects of 3rd order (0.5-3My) and 4th order (0.1-0.5My) fluctuations. These 3rd and 4th order oscillations have been overwhelmingly attributed to glacioeustatic fluctuations since:

- They are demonstrably largely synchronous and internationally correlateable (e.g. Ross & Ross, 1985; 1987).
- They operated at much higher frequencies and magnitudes than large-scale tectonic and intrinsic sedimentological (e.g. delta-lobe switching) forces respectively (Miller & Eriksson, 2000).

and

- They initiated and increased in magnitude and frequency during glacial periods (Rygel *et al.*, 2008).

The absolute magnitude, or degree to which glacioeustasy could contribute to the (occasionally very significant) scale, of sea-level fluctuations is the only factor which has been questioned by some workers (e.g. Isbell *et al.*, 2003b).

Sequence stratigraphy and sea-level evolution have been particularly integral to the study of Tournaisian and Viséan stratigraphy since the pioneering work of Ramsbottom (1973), who proposed that six distinct cycles or "mesothems" (each with a distinct transgressive base and regressive top) were recognisable during this interval in Britain and Ireland. The exact expression of the transgression or regression on sedimentation was variable, depending on the local depositional setting. Basinal areas were less sensitive to sea-level fluctuation given the relative change in depth was minimal. Platform areas were, however, markedly affected by even minor sea-level fluctuations and developed rapid facies changes and were commonly exposed. Later, Ramsbottom (1979) refined and expanded his recognition of mesothems both geographically (NW Europe) and temporally (to include the whole of the Carboniferous).

Given the defined (both sedimentologically and biostratigraphically) nature of the emergent horizons which commonly mark the boundary between the regressive termination and the transgressive initiation of successive mesothems, it is not surprising that the regional sub-stage divisions (Fig. 1.2) erected by George *et al.* (1976) for the Tournaisian and Viséan, coincided with the mesothem boundaries of Ramsbottom (1973). The sequence boundary plots subsequently produced by Ross & Ross (1985; 1987) represented evolved forms of the original work of Ramsbottom (1973; 1979). The works of Ross & Ross (1985; 1987, 1988) have had a significant impact on late Palaeozoic studies in the fields of evolution, palaeoclimate and stratigraphy and have been widely cited and used as the basis for numerous theories (e.g. Alekseev *et al.*, 1996; Crowley & Baum, 1991; DiMichele *et al.*, 2001; Isbell *et al.*, 2003b; Mii *et al.*, 1999; Powell & Veevers, 1987). However, since the works of Ross & Ross are fundamentally based on privately held datasets their replicability (from published data) has been questioned, leading

to their accuracy being viewed with scepticism by some workers (e.g. Rygel *et al.*, 2008).

Overall, the sea-level curves produced by Ross & Ross (1987) suggested that (Fig. 6.1.1):

- the Arundian-Holkerian boundary was marked by the regression of mesothem D_3, whilst the transgression of mesothem D_4 should be traceable throughout the Holkerian.
- the Holkerian-Asbian boundary was coincident with a significant regression marking the end of mesothem D_4 and that the transgression of the subsequent mesothem (D_5) was broadly divisible into two parts (a & b), with the transgression more significant only after the mid-Asbian (D_{5b}).
- the Asbian-Brigantian boundary was defined by the regression of mesothem D_5 and that the transgression of mesothem D_6 was interrupted around the mid-Brigantian by another regression, which effectively divided mesothem D_6 in two (a & b). The transgression of D_{6b} occurred in a somewhat stepped fashion.
  and
- the Brigantian-Pendleian (Viséan-Serpukhovian) boundary was marked by the significant regression of mesothem D_{6b} and that Pendleian strata were deposited during part of the transgressive phase of mesothem N_1, which itself was punctuated by several short-term regressions.

6.1.2 Interpretation of upper Viséan and Serpukhovian sea-level variation in Ireland

Principally, sedimentology was used to reconstruct palaeoenvironments and constrain the depth of deposition for the sequences studied (see Sections 2.4, 2.6 & 3.4). This allowed basic 3rd order sea-level curves to be generated (Fig. 2.4c). Analyses of the taphonomy and palaeoenvironmental preferences of the macro- and microfauna recovered are in good agreement with the data described above (see Section 4.7).

The sea-level curve derived for the NW Ireland sequence is not clearly correlateable with the strict definitions of the mesothems of Ramsbottom (1973) e.g. Brigantian-Pendleian boundary. However, sufficient (broad) similarities allow comparisons between the curves to be made (Fig. 6.1.1). The correlation of mesothem boundaries herein contrasts with the work of Brunton & Mason (1979), whose correlations appear to indicate fewer mesothems in the Viséan (compare Figs. 2.1c & 6.1.1)

Although the Holkerian-Asbian boundary was not unequivocally identified during this study, no significant regression (mesothem D_4-D_5) was discerned in the appropriate stratigraphical sequence in the upper Benbulben Shale Formation (although it is *possible* that the actual boundary falls below the level investigated herein). The only shallowing identified around this interval was at the Benbulben Shale-Glencar Limestone contact in the lower Asbian, which *may* therefore represent the top of mesothem D_4. The magnitude of this regressive event (between the Benbulben Shale and Glencar Limestone Formations) may have been muted by the relative depth of deposition, with deeper regions showing almost no difference in sedimentation at this particular level (see Section 2.1.3).

A proposed slight deepening event is perhaps responsible for a return to more argillaceous conditions in the lower-mid Glencar Limestone Formation and *may* correlate with the more subtle transgression of mesothem D_{5a}. The slight (again possibly depth-muted) mid-Asbian shallowing that is identified in the upper-Glencar Limestone Formation and at the base of the Dartry Limestone Formation *may* relate to the subtle D_{5a}-D_{5b} boundary.

The significant sea-level fall identified at the contact between the Dartry Limestone and Meenymore Formations is almost certainly correlateable with the regression which supposedly marks the top of mesothem D_5. This lends further credence to the claims of Cózar *et al.* (2006) regarding the proposed (on biostratigraphical grounds) local lowering of the Asbian-Brigantian boundary.

Although (overall) the reconstructed sea-level remained low for the entire interval during which the Meenymore, Glenade Sandstone and Bellavally Formations were

deposited, intervening episodes of marine conditions (and therefore transgressions and deepening) were recognised. The deposition of the fluviatile and deltaic (Smith, 1996) Glenade Sandstone Formation is correlated herein with the regression marking the boundary between sub-mesothems D_{6a} and D_{6b}. The overall deepening of palaeoenvironments from the top of the Glenade Sandstone Formation to the base of the Tawnyunshinagh Member (Carraun Shale Formation) is interpreted as the transgressive phase of D_{6b}, whilst the Tawnyunshinagh Member is thought to *possibly* relate to the regressive termination of D_{6b}. Similar to Smith (1995) the deepening which occurred after the Tawnyunshinagh Member is seen as more pronounced and distinct from that which was interpreted for the lower part of the Carraun Shale Formation. Thus the deepening after the Tawnyunshinagh Member is interpreted as correlating with the transgression of the N_1 mesothem, despite occurring below the Brigantian-Pendleian boundary (as recognised biostratigraphically).

In a general sense, conditions in the early Asbian of NW Ireland were reconstructed herein as slowly shallowing, which is in contrast to the curves of Ross & Ross (1987) which propose that the Asbian was (overall) an interval of transgression. The Mullaghmore Sandstone and Benbulben Shale Formations are interpreted here as representing lowstand and transgressive systems tracts (LST and TST) whilst the overlying Glencar and Dartry Limestone Formations are thought to signify a highstand systems tract (HST). The palaeoenvironments of the Leitrim Group are complex and identifying sequence stratigraphic units is much more complicated. Despite this, the Glenade Sandstone Formation and Tawnyunshinagh Limestone Member (Carraun Shale Formation) are recognised here as representing probable LSTs, with the intervening stratigraphy representing a TST. The upper Carraun Shale Formation and portion of the Dergvone Shale Formation which was examined are taken to represent a TST evolving into a HST. Superimposed on all of the general sea-level variation (discussed above) are numerous examples of rapid sea-level fluctuations which are believed to relate to 4^{th} and 5^{th} order (~17ky and ~30ky cyclicity recognised in the Tievebaun Section, see Section 2.5) glacioeustasy.

The stratigraphically limited nature of sections examined in Co. Clare reduces their usefulness for deducing the evolution of base sea-level changes during the

Mississippian. However, the pronounced shallowing identified at the top of the Slievenaglasha Formation (see Section 3.2) in the upper Brigantian may indicate correlation with the regressive phase of D_{6b}, whilst deposition of the Clare Shale Formation is likely equivalent with the transgression of mesothem N_1.

6.2 CONTROLS ON NW IRELAND DEPOSITION – THE CARBONIFEROUS GLACIATION AND STABLE ISOTOPE RECORD

The primary goal of this project was to combine the palaeoenvironmental datasets obtained from sedimentological, palaeontological and geochemical (stable isotopic) analysis to produce a fuller understanding of the controls on deposition in the late Viséan to Serpukhovian of Ireland. This work (detailed in the previous chapters) has important global implications regarding the timing of the onset and severity of a significant episode of the Carboniferous glaciation.

The raw isotopic data for the NW regions is shown in Fig. 5.2.1a, whilst derived palaeotemperatures are plotted in Fig. 5.3.3f (with the fish adjusted for isotopic depletion) and again in Fig. 5.3.4 with a 5-point moving average and adjustment made for the glacially-induced evolution of $\delta^{18}O_{seawater}$. Although the data is spread (~1‰) and slightly erratic (possibly reflecting short-term glacial expansions and contractions), clear trends can be seen in both the raw and (more clearly) averaged $\delta^{18}O$ data.

$\delta^{18}O$ values (accounting for diagenetically corrected ichthyoliths and evolving $\delta^{18}O_{seawater}$ values - see Sections 5.3.3 and 5.3.4, respectively) increased from ~18.4‰ in the basal Asbian to ~19.5‰ at the base of the Meenymore Formation, with only minor perturbations (e.g. slightly sharper increase at the Glencar-Dartry contact) in the otherwise broadly linear trend. This increasing $\delta^{18}O$ trend translates into cooling of SSTs by ~4.7ºC (± only 0.2 ºC depending on the palaeotemperature equation used, see Section 5.1.2).

From the base of the Meenymore Formation to the lower-middle Carraun Shale Formation (mid-Brigantian) $\delta^{18}O$ values remained relatively stable (slight perturbations possibly reflect a combination of short-term climatic fluctuation as well as minor inputs from palaeoenvironmental variation), but overall values slightly increased to peak at ~19.7‰ (indicating a further ~1ºC of cooling). Subsequently $\delta^{18}O$ values decreased and the youngest data point (~19.3‰) in the

Pendleian (Serpukhovian) Dergvone Shale indicates slight warming of SSTs by ~1.5ºC.

Whilst localised faulting has been demonstrated to have controlled lithofacies variations between and within formations across the northwest study region (e.g. Kelly, 1996; Legg *et al.*, 1998; Mitchell, 2004; Philcox *et al.*, 1992; Somerville *et al.*, 2009), the close correlation (Fig. 6.2a) between sea-level (reconstructed from sedimentological and faunal data) and $\delta^{18}O$ curves (derived from conodont and ichthyolith apatite) suggests that climate and glacio-eustasy may have been the primary control on the larger-scale sedimentological (and thus, by proxy, palaeoenvironmental) evolution. It is believed, therefore, that glacioeustatic base level change (recorded in the $\delta^{18}O$) is largely responsible for the observed sea-level curve, as opposed to locally induced sea-level variations controlling the isotopic signature (via isolation etc. of the watermass) for several key reasons:

- $\delta^{18}O$ values remain relatively stable through the Meenymore and Bellavally Formations and even into the lower Carraun Shale Formation, despite the significantly different range of palaeoenvironmental conditions developed (see Section 2.4). The relative stability of the isotopic signature throughout the complex palaeoenvironments of the late Asbian and Brigantian demonstrates that variation in the connectivity of the watermass to open marine conditions (via sea-level change) was not a dominant control on $\delta^{18}O$ values.
- The $\delta^{18}O$ values of late Viséan conodonts recovered from the Aghagrania and Carraun/Lugasnaghta Sections in NW Ireland are almost identical to values reported from northern Spain (Buggisch *et al.*, 2008), despite the differences in palaeolatitude and palaeoenvironment between the study areas. Such comparisons strongly suggest that the values recorded are not solely a product of localised conditions and, by extension, local perturbations.
- The overall shallowing sequence preserved in NW Ireland can be correlated with other published evidence (Fig. 6.2b) for increasing global ice-volumes, especially the postulated influence of ice-sheet growth on sea-levels in palaeoequatorial Ireland and Britain (see Section 1.5.1 and also Wright & Vanstone, 2001, respectively). Of particular significance is the very close correlation between the evolution of the Carboniferous glaciation proposed

herein (developed predominantly from isotopic data), and the results of Rygel *et al.* (2008), who compiled the most comprehensive review of glacioeustasy based on over 60 published studies.

Despite the majority of the cooling trend being identified primarily from ichthyolith material (as insufficient conodont material was obtained from the lower part of the stratigraphy examined), alteration of the ichthyoliths $\delta^{18}O$ values is disregarded as producing the trend artificially for the following reasons:

1. The data is clearly non-random in two senses:
    a. Multiple analyses of the same ichthyolith or conodont sample demonstrate that the $\delta^{18}O$ values are highly reproducible (89% of samples had a standard deviation of $\leq 0.20‰$, whilst 100% had a standard deviation of $\leq 0.31‰$)
    b. The increasing $\delta^{18}O$ trends identified in both the Tievebaun and Glencar Sections have an approximately equal slope produced by a fairly systematic increase in $\delta^{18}O$ values. Such an almost linear trend would be unlikely to occur on a statistically "random walk".
2. If increasing depletion of ^{18}O through diagenesis was the reason for lower $\delta^{18}O$ values lower in the stratigraphy, then a similar slope would be expected higher in the sequence where the same increasing thermal (and therefore diagenetic) gradient with depth should have been developed.
3. The relative increases in thermal grade and potential increases in diagenesis in such stratigraphically short sections (maximum 216m) would be minor and extremely unlikely to induce such significant isotopic evolution.
4. The increasing $\delta^{18}O$ trend is not entirely uniform and minor inflections in the data argue against it being solely the result of a relatively stable, increasing diagenetic gradient.

Isotopic results, in combination with spectral analysis and the general sea-level reconstruction, strongly suggest that significant cooling and expansion of ice-sheets actually began at the base of the Asbian. Although the dataset obtained in this report is stratigraphically limited (in that it does not extend far below the Holkerian-Asbian boundary), average $\delta^{18}O$ values do not appear to start increasing (indicating decreasing temperatures and increased ice) until the uppermost portion of the

Benbulben Shale Formation. A basal Asbian onset for glaciation is in exact agreement with the relatively abrupt, marked increase of sedimentary cyclicity, particularly in palaeo-low latitudinal regions (Fig. 6.2b).

The Irish isotopic and climatic data is not, however, in agreement with all published isotopic work regarding the timing of the Carboniferous glaciation (Fig. 6.2c). No clearly defined temporal level can be identified or correlated which unequivocally marks the onset of the main episode of glaciation. This inability to correlate isotopic curves which were proposed as being fundamentally representative of global conditions can probably be explained by one, or a combination, of the following:

- Different bio- and litho-stratigraphic constraints and, therefore, inadequate correlation resolution between different studies undertaken in different areas. For example, the traditional ammonoid marker (*C. leion)* for the Viséan-Serpukhovian boundary was retained in this work, whilst the figures of Buggisch et al. (2008) plot *L. ziegleri* as their Serpukhovian biomarker (although no mention of this species was found in their description of the appropriate sections). The peak isotopic values obtained herein would shift (stratigraphically) more in line with those of Buggisch et al. (2008) if the Viséan-Serpukhovian boundary was lowered to the first appearance of *L. ziegleri.*
- Given the spatial and temporal complexity and waxing and waning nature of the Carboniferous glaciation, it is likely that no sampling frequency, or even stratigraphic sequence, will be sufficiently detailed to provide a complete record of every perturbation which occurred (particularly with respect to large-scale studies). Isotopic curves constructed from widely spaced sample points, retrieved from essentially incomplete temporal records, can only provide the broader picture of isotopic change through a sequence and thus should not be expected to match exactly. Relative periods of generally increasing or decreasing isotopic values are of significant importance though.
- As shown in Fig. 5.3.1.2, the $\delta^{18}O$ values of the world's oceans and seas are not homogenous, due to the local interaction of processes such as evaporation, precipitation etc. (Section 5.3.1.2). Changes in climate and ocean chemistry would occur at different rates, in different regions of the globe, during the onset

of a glaciation. Virtually all the datasets plotted in Fig. 6.1c were obtained from sequences deposited in epeiric seas, which are more prone to the effects of sea-level fluctuations. Studies based on samples recovered from epeiric seas are therefore probably more likely to preserve slightly different records of climate deterioration (according to the local conditions) than rarely-preserved open-ocean sediment sequences (Brand *et al.*, 2009). No epicontinental (epeiric) seas of any significant size are in existence today, although the Persian Gulf has been cited as a modern example (Brownfield & Weaver, 1992).

Given the more focussed nature of this study (in terms of scale - a relatively large number of horizons were sampled in a short stratigraphic interval), understanding of the local stratigraphy and the analysis of an originally mobile isotopic medium (conodonts and fish), the impact of the problems listed above are thought to have been minimised.

Previously, several sedimentological (Fig. 1.3.1a) and isotopic (principally, Buggisch *et al.*, 2008) studies had proposed the Viséan-Serpukhovian boundary as marking the onset of a significant phase of glacial expansion (see Section 1.3.1). Results obtained herein strongly suggest that cooling occurred earlier, at the basal Asbian, and no evidence was discovered which supports the recognition of pronounced cooling at the Viséan-Serpukhovian boundary (although admittedly only a few data points were recovered above this boundary). Only a single data point (CNLG19) was obtained from the Pendleian (Serpukhovian) in the NW region but its $\delta^{18}O$-value is consistent with the results obtained from the Brigantian (upper Viséan), even indicating slightly warmer conditions (Fig. 5.3.3f). More substantially, data from the Kilnamona and St. Brendan's Well Sections in Co. Clare indicate that $\delta^{18}O$ values in the early Serpukhovian and Bashkirian (respectively) were almost identical (differing by than ~0.5‰ on average) to those in the late Brigantian (Fig. 5.3.3g). A single datum (KMONA8) was found to be enriched by ~1‰ relative to its neighbouring bed analyses. This *possibly* suggests that a cooling event occurred at the Viséan-Serpukhovian boundary but that is was extremely short-lived.

Despite disagreements in timing, the magnitudes of isotopic shifts representative of a glacial episode around the Viséan-Serpukhovian boundary (which all the data in Fig. 6.2c show to some extent) are all in the order of ~2‰. It appears likely that not only was the glacial episode which began in the late Viséan of similar magnitude and complexity to the Pleistocene episode, but that it was also similar in development. Spectral analysis undertaken on the Tievebaun Section identified a probable influence on sedimentation of obliquity and precessional Milankovitch cycles in the early Asbian (see Section 2.5). Higher frequency (obliquity) Milankovitch forcings have been demonstrated as dominant at the beginning of the Pleistocene glaciation before "eccentricity" became more pronounced as the glacial episode matured. Rapid base-level changes were also identified in the upper Asbian and Brigantian during this work (most obviously in the rapid facies changes exhibited in the Meenymore and Bellavally Formations, but also in the palaeokarst horizon developed at the top of the Slievenaglasha Formation). Although spectral analysis could not be undertaken on the upper Asbian to Serpukhovian sediments, several studies (Miller & Eriksson, 2000; Smith & Read, 2000; Weedon & Read, 1995) have identified a dominance of the long-term eccentricity cycle later (around the middle Carboniferous) in the glacial episode (the initiation of which is identified here).

6.3 CONSIDERATIONS AND IMPLICATIONS FOR ISOTOPIC STUDIES UTILISING BIOGENIC APATITE

This project utilised the "bulk-chemical" method of biogenic apatite $\delta^{18}O$ analysis which is described in detail in Appendix C. Essentially, the PO_4^{-3} of a sufficient mass of apatite (minimum 0.5mg - usually comprising several individual ichthyolith or conodont elements) was chemically isolated and subsequently recrystallised as Ag_3PO_4 in a modified version of the procedure developed by O'Neil *et al.* (1992). Multiple small quantities (typically ~0.25mg) of the homogenised Ag_3PO_4, in conjunction with numerous standards, were analysed as CO using a TC-EA (high temperature conversion elemental analyser) connected online to a ThermoFinnigan Delta Plus mass spectrometer as described in Joachimski *et al.* (2009).

Recently, however, a new analytical method has been utilised (Wheeley *et al.*, 2009; 2010) to determine the $\delta^{18}O$ values of biogenic apatite (focusing on conodonts). This new technique uses an ion beam to ablate a small (30μm - Trotter *et al.*, 2008) area of an individual element in order to analyse the isotopic signature of the resulting gas. Given the extremely fine resolution of the new technique, it is obviously more useful (relative to the bulk apatite method) when samples sizes are especially small, or if original isotopic differences between elements, ontogenetic stages or species are being investigated. However, significant disadvantages are also associated with its use. Primarily, since the laser is indiscriminate in its ablation of material, any oxygen, regardless of its location (i.e. not only that bound in the stable PO_4^{-3}), will be analysed. Oxygen bound within inorganic molecules (e.g. carbonate) comprising part of the apatitic structure has been demonstrated to be readily isotopically adjusted during diagenesis (e.g. Iacumin *et al.*, 1996; Nelson *et al.*, 1986) and so represents a significant variable in $\delta^{18}O$ values obtained via an indiscriminate ablation method (impurities on the surface of the element represent a more obvious contaminant risk).

The ion microprobe technique is still in early stages of development and refinement and it must be capable of demonstrating (unequivocally) that the $\delta^{18}O$ values it

obtains are related only to the original isotopic composition of the apatite and not the differential contamination of elements, before it is used as a standard procedure. Wheeley *et al.* (2009; 2010), using the new technique, have claimed that substantial inter- and intra-element isotopic variation (due to a multitude of factors) exists. If this is the case, then it has very significant implications relating to "masking" of original variation that may be occurring when the bulk apatite method is utilised. The reproducibility of results obtained using the bulk method, both in previous studies (e.g. Buggisch *et al.*, 2008; Joachimski *et al.*, 2009; Žigaite *et al.*, 2010a) and this work, is significantly better than would be probable if potential variations identified by Wheeley *et al.* (2009; 2010) were universally developed. Comparisons of the results of multiple bulk ichthyolith and bulk conodont samples, run from the same bed, indicate that discrepancies between bulk samples (of either conodonts or ichthyoliths) have an average difference of 0.5‰, which is close to the combined analytical error of each individual analysis. Table 6.3 (below) outlines the results from comparing the results of multiple bulk analyses.

Bulk sample type	Maximum difference	Minimum difference	Average difference	Standard deviation	Number
Ichthyoliths	**1.30**	**0.14**	**0.49**	**0.30**	**17**
Conodonts	**1.00**	**0.02**	**0.49**	**0.35**	**11**

Table 6.3 Isotopic variation between multiple bulk samples.

All results are given in ‰. Number refers to the number of comparisons which were possible.

The compatibility of $\delta^{18}O$ values obtained from different bulk apatite samples from the same bed, argues against inter-species variation exceeding ~1‰. Whilst intra-element variation is extremely difficult to assess using the bulk method, the almost identical $\delta^{18}O$ values displayed by analyses of juvenile and mature *G. bilineatus* P_1-elements (BW4 AN1 & AN2-1, Section 5.3.3) suggests that no such differences exist because the volume ratios of the different tissues (which probably cause intra-element variation) would be distinct between the two ontogenetic element stages.

Although the isotopic values obtained from the Irish sections were largely repeatable (see above), the slight variations recorded within multiple ichthyolith or conodont analyses from the same stratigraphic horizon suggests that subtle (≤ 1‰)

variations could *potentially* be commonly masked by bulk mixed genera/species samples (a significant point raised by Wheeley *et al.*, 2009; 2010). The consistency of discrepancies towards enrichment or depletion of a specific conodont genus or species strongly supports the idea that conodonts preferentially inhabited differing palaeoenvironments or tiers within the water-column, rather than individual elements preserving hugely variable $\delta^{18}O$ values. However, given analytical error ranges, significant numbers of comparative analyses would be necessary to statistically determine the true value or significance of these, admittedly very slight (most likely palaeoecological) isotopic differences.

This study corroborates the use of the bulk apatite chemical purification method for palaeoenvironmental studies, but demonstrates that some care is required with the selection of sample apatite and data interpretation. Most importantly, this work has uncovered significant differences in the $\delta^{18}O$ values of ichthyolith and conodont apatite (Figs. 5.2.2b & 5.3.3a,c-e). It is proposed that ichthyoliths, probably due to their lack of a dense protective outer layer, commonly undergo isotopic exchange and that the degree of the isotopic shift varies predominantly (but not exclusively) due to increasing thermal grade. Through analysis of multiple ichthyolith and conodont samples from individual horizons a well-defined average "offset" can be calculated and thus ichthyolith $\delta^{18}O$ data collected from the same stratigraphic section (and therefore subjected to broadly similar diagenetic histories) can be relatively confidently returned to their original values. Optically screening ichthyolith material for alteration appears to correlate the most affected (coarse and overgrown) material with the most significantly depleted $\delta^{18}O$ values (see results of sample BW10 AN1-3, Section 5.2.2 & Fig. 4.6a - 5a-b), a result which other workers have also tentatively suggested (Žigaite *et al.*, 2010b).

6.4 STRATIGRAPHY OF THE LATE VISÉAN-SERPUKHOVIAN INTERVAL

Two principal stratigraphic problems were addressed during this study. Firstly, whether the Asbian-Brigantian boundary should remain at its position in the Bellavally Formation (as is suggested by the position of the P_{1a} and P_{1b} ammonoid Biozones - e.g. Legg *et al.*, 1998) or, alternatively, lowered to the base of the Meenymore Formation, as suggested by the microfaunal work of Cózar *et al.* (2006). Secondly, whether the FAD of the conodont *L. ziegleri* is consistent with its proposed (e.g. Nemirovskaya *et al.*, 1994; Richards & Group, 2008; Skompski *et al.*, 1995) use as defining a new Viséan-Serpukhovian boundary.

Both the traditional and newly proposed Asbian-Brigantian boundaries have their merits. The traditional model, besides the facts that it retains the original definition of the stratotype and is based on the most highly resolved biostratigraphical scheme for the interval, i.e. ammonoids, (see Fig. 1.2.1a) is additionally supported by:

- The FAD of *G. bilineatus* in the Meenymore Formation, which suggests a middle Asbian age (see Section 4.4).
- The lack of the conodont *L. mononodosa* or *L. nodosa* in the Meenymore or early Bellavally Formation (see Section 4.4).

The new model (besides the numerous biostratigraphical tools mentioned by Cózar *et al.*, 2006) is further supported by:

- The FAD of *M. bipluti* in the lower Meenymore Formation (see Section 4.4).
- The probable correlation of the regression at the base of the Meenymore Formation with the regressive phase of Ramsbottom's (1973) mesothem 5 (see Section 6.1.2).

It was decided, however, that given the conflicting evidence, it would be sensible to display *both* potential definitions on all diagrams and figures within this work, but to maintain the use of the Asbian-Brigantian boundary in its traditionally accepted sense in the text (unless stated otherwise), to prevent confusion.

Despite the discovery of unusual conodont forms, the *Lochriea* lineage was encountered in NW Ireland (Fig. 6.4) in the approximate evolutionary order described elsewhere (e.g. Nemyrovska, 2005; Nikolaeva *et al.*, 2009a; 2009b; Skompski *et al.*, 1995). Although a detailed and thorough review of the morphological variations of species within this genus is required (in order to obtain absolute consensus on definitions), the utilisation of the FAD of *L. ziegleri* to mark the Viséan-Serpukhovian boundary appears sound for the following reasons:

1. The species is particularly distinctive and typically robust.
2. *L. ziegleri* appears relatively suddenly in the late Brigantian, not exceptionally far from the current boundary definition.
3. The species is a persistent member of the conodont fauna above its FAD.
4. Other species within the *Lochriea* genus appear at a similar time to *L. ziegleri* and may be useful as proxies where *L. ziegleri* is absent for one reason or another.
5. The species is part of the *Gnathodus-Lochriea* Biofacies and thus should be relatively widely developed.

The newly defined Viséan-Serpukhovian boundary in NW Ireland would fall in the P_{2a} ammonoid biozone and the lower part of the upper Cf6δ foraminiferal Biozone between the Ardvarney and Sranagross Members of the Carraun Shale Formation (Fig. 6.4). Unfortunately, no significant lithological change occurs at this horizon although a slight isotopic excursion does appear coincident (Fig. 5.2.1d).

6.5 SUGGESTIONS FOR FUTURE WORK

Despite the significant advances in understanding which have resulted from this work, many questions remain incompletely answered and many more have been raised. Some directions for future work are provided below:

Spectral analysis of upper Asbian and Brigantian strata in Ireland should be completed to test whether Milankovitch forcings can be tracked throughout the upper Viséan, and in particular whether a shift towards the longer wavelength eccentricity orbital cycle can be detected as proposed.

Biostratigraphical investigations in the Brigantian of Co. Clare should be undertaken to determine the evolutionary lineage of the conodont genus *Lochriea* in the area and its implications for the Viséan-Serpukhovian boundary. Before the FAD of the species *L. ziegleri* can be widely adopted as marking a newly defined Viséan-Serpukhovian boundary, significant discussion is required and a clear consensus must be reached on the exact definitions of many of the complex *Lochriea* forms. Without such measures it is feared that ambiguous determinations may begin to infiltrate published works.

A detailed isotopic curve for the lower Asbian based on conodont apatite from Ireland should be constructed to unequivocally prove the validity of the cooling trend identified herein through ichthyolith $\delta^{18}O$ data.

Isotopic studies should be undertaken along a late Brigantian transect from Co. Clare to NW Ireland to investigate the isotopic offset identified between the two areas, in more detail. The study may be expanded geographically and temporally in order to investigate the variation (if any) of $\delta^{18}O$ values in the palaeo-epeiric sea, with a focus on the location of the ITCZ, significant currents and large freshwater inputs in the Carboniferous.

More research should be undertaken on the external appearance, structure, geochemistry and isotopic composition of ichthyoliths of various taxonomic affinities as well as diagenetic maturity.

Tandem analyses of ion probe and bulk chemical conodont methodologies should be used to finally address the following key areas of interest:

1. The effects of time-averaging on $\delta^{18}O$ data.
2. How $\delta^{18}O$ varies with C.A.I. (both lab induced and natural)?
3. How various lithological processing techniques (focussing on the use of standard chemicals such as Acetic acid, Formic acid, hydrogen peroxide, sodium hypochlorite, sodium polytungstate) affect $\delta^{18}O$ values?
4. How correlateable are the $\delta^{18}O$ values of biogenic apatite from palaeoenvironmentally and latitudinally separated, temporally equivalent sections?
5. Are there statistically significant and stable inter- or intra- species, genus, element (i.e. P_1 vs. P_2) or ontogenetic stage differences in $\delta^{18}O$ values amongst conodonts and ichthyoliths, and what are the implications of any differences?

Finally, isotopic data in this study suggests that future palaeoenvironmental and palaeoclimatic studies based on $\delta^{18}O$ data should focus on:

1. Conodonts as opposed to ichthyoliths (but where available they should be run in tandem).
2. Monospecific or monogeneric conodont samples.
3. Conodonts with a well understood palaeoecology.
4. As few conodont genera or species throughout a study such that definitely valid relative isotopic differences can be calculated.
5. Running multiple samples to ensure an accurate average $\delta^{18}O$ value is taken.

REFERENCES

Adlis, D.S., Grossman, E.L., Yancey, T.E., and McLerran, R.D., 1988, Isotope stratigraphy and paleodepth changes of Pennsylvanian cyclical sedimentary deposits: PALAIOS, v. 3, p. 487-506.

Agassiz, J.L.R., 1838, Reserches sur les Poissons fossiles: Neuchatel, v. 3, p. 1-87.

Aldridge, R.J., Austin, R.L., and Husri, S., 1968, Viséan conodonts from North Wales and Ireland: Nature, v. 219, p. 255-258.

Aldridge, R.J., Briggs, D.E.G., Clarkson, E.N.K., and Smith, M.P., 1986, The affinities of conodonts - new evidence from the Carboniferous of Edinburgh, Scotland: Lethaia, v. 19, p. 279-291.

Aldridge, R.J., Briggs, D.E.G., Smith, M.P., Clarkson, E.N.K., and Clark, N.D.L., 1993, The anatomy of conodonts: Philosophical Transactions of the Royal Society of London, B., v. 340, p. 405-421.

Aldridge, R.J., and Purnell, M.A., 1996, The conodont controversies: Trends in Ecology and Evolution, v. 11, p. 463-468.

Alekseev, A.S., Kononova, L.I., and Nikishin, A.M., 1996, The Devonian and Carboniferous of the Moscow Syneclise (Russian Platform): stratigraphy and sea-level changes: Tectonophysics, v. 268, p. 149-168.

Anderson, K., Ashton, J., Earls, G., Hitzman, M., and Tear, S., 1995, Irish carbonate hosted Zn/Pb deposits: Ireland, Irish Association for Economic Geology, SEG 75th anniversary guidebook series Volume 21.

Armstrong, H.A., Baldini, J., Challands, T.J., Gröcke, D.R., and Owen, A.W., 2009, Response of the Inter-tropical Convergence Zone to Southern Hemisphere cooling during Upper Ordovician glaciation: Palaeogeography, Palaeoclimatology, Palaeoecology, v. 284, p. 227-236.

Austin, R.L., 1972, Problems of Conodont Taxonomy with special reference to Upper Carboniferous forms: Geologica et Palaeontologica, v. 1, p. 115-126.

—, 1973, Phylogeny and homeomorphy of conodonts in the Lower Carboniferous, *in* Rhodes, F.H.T., ed., Conodont Paleozoology, The Geological Society of America, Special Publication 141.

—, 1974, The Biostratigraphic distribution of conodonts in Great Britain and the Republic of Ireland., *in* Bouckaert, J.a.S., M., ed., International Syposium on Belgian Micropaleontological Limits from Emsian to Viséan, Namur., Volume 3, Geological Survey of Belgium, p. 1-17.

Austin, R.L., Conil, R., and Husri, S., 1970, Correlation and age of the Dinantian rocks north and south of the Shannon, Ireland: Congrès Colloques Université de Liège, v. 55, p. 179-192.

Austin, R.L., and Davies, R.B., 1984, Problems of recognition and implications of Dinantian conodont biofacies in the British Isles: Geological Society of America, Special Paper, v. 196.

Austin, R.L., and Husri, S., 1974, Dinantian conodont faunas of County Clare, County Limerick and County Leitrim., *in* Bouckaert, J.a.S., M., ed., International Symposium on Belgian Micropaleontological Limits from Emsian to Viséan, Namur., Volume 3, Geological Survey of Belgium, p. 18-69.

Austin, R.L., and Mitchell, M., 1975, Middle Dinantian platform conodonts from County Fermanagh and County Tyrone, Northern Ireland.: Bulletin of the Geological Survey of Great Britain, v. 55, p. 43-54.

Baldwin, B., and Butler, C.O., 1985, Compaction curves: Bulletin of the American Association of Petroleum Geologists, v. 69, p. 622-626.

Balseiro, D., Rustán, J.J., Ezpeleta, M., and Vaccari, N.E., 2009, A new Serpukhovian (Mississippian) fossil flora from western Argentina: Paleoclimatic, paleobiogeographic and stratigraphic implications: Palaeogeography, Palaeoclimatology, Palaeoecology, v. 280, p. 517-531.

Bambach, R.K., Scotese, C.R., and Ziegler, A.M., 1980, Before Pangea: The geographies of the Paleozoic world: American Scientist, v. 68, p. 26-38.

Barnes, C.R., and Fahraeus, L.E., 1975, Provinces, communities and the proposed nektobenthic habit of Ordovician conodontophorids: Lethaia, v. 8, p. 133-150.

Barnett, A.J., Burgess, P.M., and Wright, V.P., 2002, Icehouse world sea-level behaviour and resulting stratal patterns in Late Viséan (Mississsippian) carbonate platforms: integration of numerical forward modelling and outcrop studies: Basin Research, v. 14, p. 417-438.

Bassett, D., Macleod, K.G., Miller, J.F., and Ethington, R.L., 2007, Oxygen isotopic composition of biogenic phosphate and the temperature of early Ordovician seawater: PALAIOS, v. 22, p. 98-103.

REFERENCES

Beck, J.W., Recy, J., Taylor, F., Edwards, R.L., and Cabioch, G., 1997, Abrupt changes in early Holocene tropical sea surface temperature derived from coral records: Nature, v. 385, p. 705-707.

Beerling, D.J., 2002, Low atmospheric CO_2 levels during the Permo-Carboniferous glaciation inferred from fossil lycopsids: Proceedings of the National Academy of Sciences, v. 99, p. 12567-12571.

Belka, Z., and Lehmann, J., 1998, Late Viséan/early Namurian conodont succession from the Esla area of the Cantabrian Mountains, Spain: Acta Palaeontologica Polonica, v. 48, p. 31-41.

Berger, A., Loutre, M.F., and Dehant, V., 1989, Pre-Quaternary Milankovitch frequencies: Nature, v. 342, p. 133.

Berner, R.A., 1990, Atmospheric carbon dioxide levels over Phanerozoic time: Science, v. 249, p. 1382-1386.

Beyrich, E., 1848, Über *Xenacanthus decheni* und *Holacanthus gracilis*, zwei Fische aus der Formation des Rothliegenden in Nord Deutschland: Monatsb. Berlin Wiss. Akad., p. 24-33.

Bischoff, G., 1957, Die conodonten-stratigraphie des rhenoherzynischen Unterkarbons mit Berücksichtigung der Wocklumeria-Stufe und der Devon/Karbon-Grenze: Abhandungen des Hessischen Landesamtes Für Bodenforschung, v. 19, p. 1-64.

Bishop, J.W., Montañez, I.P., Gulbranson, E.L., and Brenckle, P.L., 2009, The onset of mid-Carboniferous glacio-eustasy: Sedimentologic and diagenetic constraints, Arrow Canyon, Nevada: Palaeogeography, Palaeoclimatology, Palaeoecology, v. 276, p. 217-243.

Blakey, R., 2009, Global Palaeogeography, Volume 2009: Arizona.

Blake, R.E., O'Neil, J.R., and Garcia, G.A., 1997, Oxygen isotope systematics of biologically mediated reactions of phosphate: I. Microbial degradation of organophosphorus compounds: Geochimica et Cosmochimica Acta, v. 61, p. 4411-4422.

Bosscher, H., and Schlager, W., 1993, Accumulation rates of carbonate platforms: The Journal of Geology, v. 101, p. 345-355.

Braithwaite, K., 1994, Stratigraphy of a Mid-Carboniferous section at Inishcorker, Ireland: Annales de la Sociètè Gèologique de Belgique, v. 116, p. 209-219.

Brand, U., 1989, Biogeochemistry of Late Palaeozoic North American brachiopods and secular variation of seawater composition: Biogeochemistry, v. 7, p. 159-193.

—, 2004, Carbon, oxygen and strontium isotopes in Paleozoic carbonate components: an evaluation of original seawater-chemistry proxies: Chemical Geology, v. 204, p. 23-44.

Brand, U., Tazawa, J.-i., Sano, H., Azmy, K., and Lee, X., 2009, Is mid-late Paleozoic ocean-water chemistry coupled with epeiric seawater isotope records?: Geology, v. 37, p. 823-826.

Brand, U., and Veizer, J., 1981, Chemical diagenesis of a multicomponent carbonate system - 2: stable isotopes: Journal of Sedimentary Petrology, v. 51, p. 987 - 997.

Brandon, A., 1968, The Geology of Carboniferous strata (Viséan-Namurian) in parts of counties Leitrim and Cavan, Irish Republic: Southampton, University of Southampton.

—, 1972a, Clastic dykes in the Namurian shales of Co. Leitrim, Republic of Ireland: Geological Magazine, v. 109, p. 361-367.

—, 1972b, The Upper Viséan and Namurian shales of the Doagh Outlier, County Fermanagh, Northern Ireland: Irish Naturalists Journal, v. 17, p. 159-170.

—, 1973, Two fossiliferous Upper Viséan shale localities in Co. Leitrim: Irish Naturalists Journal, v. 17, p. 340-343.

—, 1977, The Meenymore Formation - an extensive intertidal evaporitic formation in the Upper Viséan (B_2) of north-west Ireland, Report of the Institute of Geological Sciences, Volume 77/23, Geological Survey of Northern Ireland, p. 14.

Brandon, A., and Hodson, F., 1984, The stratigraphy and palaeontology of the Late Viséan and Early Namurian rocks of north-east Connaught, Geological Survey of Ireland, Special Paper Number 6.

Branson, E.B., and Mehl, M.G., 1941, New and Little known Carboniferous conodont genera: Journal of Paleontology, v. 15, p. 97-106.

Bridges, P.H., Gutteridge, P., and Pickard, N.A.H., 1995, The environmental setting of Early Carboniferous mud-mounds, *in* Monty, C.L.V., Bosence, D.W.J., Bridges, P.H., and Pratt, B.R., eds., Carbonate mud-mounds their origin and evolution, Volume 23: Special Publication of the

International Association of Sedimentologists, Blackwell Science, p. 171-190.

Briggs, D., Smithson, P., Addison, K., and Atkinson, K., 1997, Denudation, weathering and mass wasting, Fundamentals of the Physical Environment: London and New York, Routledge, p. 557.

Briggs, D.E.G., and Clarkson, E.N.K., 1987, An enigmatic chordate from the Lower Carboniferous Granton "shrimp-bed" of the Edinburgh district, Scotland: Lethaia, v. 20, p. 107-116.

Briggs, D.E.G., Clarkson, E.N.K., and Aldridge, R.J., 1983, The conodont animal: Lethaia, v. 16, p. 1-14.

Brough, J., 1935, On the structure and relationships of the hybodont sharks: Memoirs of the Manchester Literary Philosophical Society, v. 79, p. 251-269.

Browne, A.N., 1981, The conodont faunas of the Lower Carboniferous Glencar and Dartry Formations of County Leitrim, and of comparable stratigraphic horizons in Northern Ireland [Masters thesis]: Belfast, Queen's University of Belfast.

Brownfield, M.E., and Weaver, J.N., 1992, Paleogeography and stratigraphy of Cretaceous coal deposits of North Africa, *in* McCabe, P.J., and Parrish, J.T., eds., Controls on the distribution and quality of Cretaceous coals, The Geological Society of America Special Paper 267, p. 369-384.

Bruckschen, P., Oesmann, S., and Veizer, J., 1999, Isotope stratigraphy of the European Carboniferous: proxy signals for ocean chemistry, climate and tectonics: Chemical Geology, v. 161, p. 127 - 163.

Brunton, C.H.C., and Mason, T.R., 1979, Palaeoenvironments and correlations of the Carboniferous rocks in west Fermanagh, Ireland: Bulletin of the British Museum of Natural History, v. 32, p. 91-108.

Buggisch, W., Joachimski, M.M., Sevastopulo, G., and Morrow, J.R., 2008, Mississippian $\delta^{13}C_{carb}$ and conodont apatite $\delta^{18}O$ records - Their relation to the Late Palaeozoic Glaciation: Palaeogeography, Palaeoclimatology, Palaeoecology, v. 268, p. 273-292.

Burrow, C.J., Long, J.A., and Trinajstic, K., 2009, Disarticulated acanthodian and chondrichthyan remains from the upper Middle Devonian Aztec Siltstone, southern Victoria Land, Antarctica: Antarctic Science, v. 21, p. 71-88.

REFERENCES

Burrow, C.J., Turner, S., and Young, G.C., 2010, Middle Palaeozoic microvertebrate assemblages and biogeography of East Gondwana (Australasia, Antarctica): Palaeoworld, v. 19, p. 37-54.

Caldwell, W.G.E., 1959, The Lower Carboniferous rocks of the Carrick-on-Shannon syncline: Quarterly Journal of the Geological Society of London, v. 115, p. 163-187.

Caldwell, W.G.E., and Charlesworth, H.A.K., 1961, Viséan Coral Reefs in the Bricklieve Mountains of Ireland: Proceedings of the Geologists Association, v. 73, p. 359-382.

Caputo, M.V., and Crowell, J.C., 1985, Migration of glacial centres across Gondwana during Paleozoic Era: Geological Society of America Bulletin, v. 96, p. 1020 - 1036.

Carpenter, S.J., and Lohmann, C.K., 1995, $\delta^{18}O$ and $\delta^{13}C$ values of modern brachiopod shells: Geochimica et Cosmochimica Acta, v. 59, p. 3749 - 3764.

Cecil, C.B., 1990, Paleoclimate controls on stratigraphic repetition of chemical and siliciclastic rocks: Geology, v. 18, p. 533-536.

Chew, D.M., and Stillman, C.J., 2009, Late Caledonian orogeny and magmatism, *in* Holland, C.H., and Sanders, I.S., eds., The Geology of Ireland: Edinburgh, Dunedin.

Clarke, W.J., 1960, Scottish Carboniferous conodonts: Transactions of the Edinburgh Geological Society, v. 18, p. 1-31.

Clarkson, E.N.K., 1979, Invertebrate palaeontology and evolution: London, George Allen & Unwin.

Clayton, G., Haughey, N., Sevastopulo, G.D., and Burnett, R., 1989, Thermal maturation levels in the Devonian and Carboniferous rocks in Ireland, Geological Survey of Ireland, 36 p.

Cleal, C.J., and Thomas, B.A., 2005, Palaeozoic tropical rainforests and their effect on global climates: is the past the key to the present?: Geobiology, v. 3, p. 13-31.

Cogné, J.-P., and Humler, E., 2008, Global scale patterns of continental fragmentation: Wilson's cycles as a constraint for long-term sea-level changes: Earth and Planetary Science Letters, v. 273, p. 251-259.

Collier, R.E.L., Leeder, M.R., and Maynard, J.R., 1990, Transgressions and regressions: a model for the influence of tectonic subsidence, deposition and eustasy, with application to Quaternary and Carboniferous examples: Geological Magazine, v. 127, p. 117-128.

Concil, R., Groessens, E., Laloux, M., Poty, E., and Tourneur, F., 1990, Carboniferous guide Foraminifera, corals and conodonts in the Franco-Belgian and Campine Basins: their potential for widespread correlation: Courier Forschungsinstitut Senckenberg, v. 13, p. 15-30.

Conway Morris, S., 1989, Conodont palaeobiology: recent progress and unsolved problems: Terra Review, v. 1, p. 135-150.

Corcoran, D.V., and Clayton, G., 2001, Interpretation of vitrinite reflectance profiles in sedimentary basins, onshore and offshore Ireland, *in* Shannon, P.M., Haughton, R.D.W., and Corcoran, D.V., eds., The petroleum exploration of Ireland's offshore basins, Volume 188, Geological Society, London, Special Publications, p. 61-90.

Cózar, P., and Somerville, I.D., 2005, Stratigraphy of upper Viséan carbonate platform rocks in the Carlow area, southeast Ireland: Geological Journal, v. 40, p. 35-64.

—, 2006, Significance of the Bradyinidae and *Parajanischewskina* N. Gen. for biostratigraphic correlations of the late Viséan (Mississippian) in Western palaeotethyan basins: Journal of Foraminiferal Research, v. 36, p. 262-272.

Cózar, P., Somerville, I.D., Aretz, M., and Herbig, H.-G., 2005, Biostratigraphical dating of Upper Viséan limestones (NW Ireland) using foraminiferans, calcareous algae and rugose corals: Irish Journal of Earth Sciences, v. 23, p. 1-23.

Cózar, P., Somerville, I.D., Mitchell, W.I., and Medina-Varea, P., 2006, Correlation of Mississippian (Upper Viséan) foraminiferan, conodont, miospore and ammonoid zonal schemes, and correlation with the Asbian-Brigantian boundary in northwest Ireland: Geological Journal, v. 41, p. 221-241.

Crowell, J.C., 1999, Pre-Mesozoic Ice Ages: Their bearing on understanding the climate system: Geological Society of America Memoir 192, p. 1-79.

Crowley, T.J., and Baum, S.K., 1991, Estimating Carboniferous sea-level fluctuations from Gondwanan ice extent: Geology, v. 19, p. 975-977.

—, 1992, Modelling late Paleozoic glaciation: Geology, v. 20, p. 507-510.

Crowley, T.J., Yip, K.-J.J., and Baum, S.K., 1993, Milankovitch cycles and Carboniferous climate: Geophysical Research Letters, v. 20, p. 1175-1178.

Davies, S.J., 2008, The record of Carboniferous sea-level change in low-latitude sedimentary successions from Britain and Ireland during the onset of the late Paleozoic ice age, *in* Fielding, C.R., Frank, T.D., and Isbell, J.L., eds., Resolving the Late Paleozoic Ice Age in Time and Space: Boulder, Colorado, The Geological Society of America Special Paper 441, p. 187-204.

Davydov, V.I., Glenister, B.F., Spinosa, C., Ritter, S.M., Chernykh, V.V., Wardlaw, B.R., and Snyder, W.S., 1998, Proposal of Aidaralash as Global Stratotype Section and Point (GSSP) for base of the Permian System: Episodes, v. 21, p. 11-18.

Deer, W.A., Howie, R.A., and Zussman, J., 1992, An introduction to the rock forming minerals: Harlow, Essex, England, Pearson Prentice Hall, 696 p.

Delsate, D., Duffin, C.J., and Weis, R., 2002, A new microvertebrate fauna from the Middle Hettangian (early Jrassic) of Fontenoille (Province of Luxembourg, south Belgium): Memoirs of the Geological Survey of Belgium, v. 48, p. 1-85.

Derycke-Khatir, C., Vachard, D., Dégardin, J.-M., Flores de Dios, A., Buitrón, B., and Hansen, M., 2005, Late Pennsylvanian and Early Permian chondrichthyan microremains from San Salvador Patlanoaya (Puebla, Mexico): Geobios, v. 38, p. 43-55.

Devuyst, F.-X., Hance, L., Hou, H., Wu, X., Tian, S., Coen, M., and Sevastopulo, G., 2003, A proposed Global Stratotype Section and Point for the base of the Viséan Stage (Carboniferous): the Pengchong section, Guangxi, South China: Episodes, v. 26, p. 105-115.

DiMichele, W.A., Pfefferkorn, H.W., and Gastaldo, R.A., 2001, Response of Late Carboniferous and Early Permian plant communities to climate change: Annual Review of Earth and Planetary Sciences, v. 29, p. 461-487.

Dixon, O.A., 1972, Lower Carboniferous rocks between the Curlew and Ox Mountains, Northwestern Ireland: Journal of the Geological Society, London, v. 128, p. 71-101.

Donoghue, P.C.J., and Purnell, M.A., 1999, Growth, function, and the conodont fossil record: Geology, v. 27, p. 251-254.

Douglas, J.A., 1909, The Carboniferous Limestone of County Clare, Ireland: Quarterly Journal of the Geological Society of London, v. 65, p. 538-586.

Druce, E.C., 1973, Upper Paleozoic and Triassic conodont distribution and the recognition of biofacies, *in* Rhodes, F.H.T., ed., Conodont Paleozoology, The Geological Society of America, Special Paper 141.

Duffin, C.J., and Ivanov, A., 2008, New chondrichthyan teeth from the Early Carboniferous of Britain and Russia: Acta Geologica Polonica, v. 58, p. 191-197.

Duncan, M., 1999, A study of some Irish lower Carboniferous fish microvertebrates [Unpublished Ph.D. thesis]: Dublin, Trinity College.

—, 2003, Early Carboniferous chondrichthyan *Thrinacodus* from Ireland, and a reconstruction of jaw apparatus: Acta Palaeontologica Polonica, v. 48, p. 113-122.

—, 2006, Various Chondrichthyan microfossil faunas from the Lower Mississippian (Carboniferous) of Ireland: Irish Journal of Earth Sciences, v. 24, p. 51-69.

Dunn, D.L., 1970, Middle Carboniferous conodonts from western United States and phylogeny of the platform group: Journal of Paleontology, v. 44, p. 312-342.

Dzik, J., 2000, The origin of the mineral skeleton in Chordates, *in* Hecht, M.K., MacIntyre, R.J., and Clegg, M.T., eds., Evolutionary Biology, Volume 31: New York, Springer, p. 230.

—, 2009, Conodont affinity of the enigmatic Carboniferous chordate Conopiscius: Lethaia, v. 42, p. 31-38.

—, 2010, Vertebrate homologies and analogies in the conodont oral apparatus, International Palaeontological Congress 3: London, England.

Elliot, T., Pulham, A.J., and Davies, S.J., 2000, Sedimentology, sequence stratigraphy and spectral gamma ray expression of turbidite, slope, and deltaic depositional systems in an Upper Carboniferous basin-fill succession, western Ireland, *in* Graham, J.R., and Ryan A., ed., Unpublished IAS Dublin September 2000. Field Trip Guidebook, The Department of Geology, Trinity College Dublin, p. 1-40.

Ellison, S., and Graves, R.W., 1941, Lower Pennsylvanian (Dimple Limestone) conodonts of the Marathon region, Texas: Missouri School of Mines and Metallurgy Bulletin, Technical Servey, v. 14, p. 1-13.

Epstein, A.G., Epstein, J.B., and Harris, L.D., 1977, Conodont colour alteration - An index to diagenesis of organic matter: U.S. Geological Survey Professional Papers, v. 995, p. 20.

Epstein, S., Buchsbaum, R., Lowenstam, H., and Urey, H.C., 1951, Carbonate-water isotopic temperature scale: Geological Society of America Bulletin, v. 62, p. 417-426.

Epstein, S., Buchsbaum, R., Lowenstam, H.A., and Urey, H.C., 1953, Revised Carbonate-water isotopic temperature scale: Geological Society of America Bulletin, v. 64, p. 1315-1326.

Epstein, A.G., Epstein, J.B., and Harris, L.D., 1976, Conodont color alteration: an index to organic metamorphism, Geological Survey Professional Paper No. 995, 31 p.

Erez, J., and Luz, B., 1983, Experimental paleotemperature equation for planktonic foraminifera: Geochimica et Cosmochimica Acta, v. 47, p. 1025-1031.

Fairbanks, R.G., 1989, A 17,000-year glacio-eustatic sea level record: influence of glacial melting rates on the Younger Dryas event and deep-ocean circulation: Nature, v. 342, p. 637-642.

Falcon-Lang, H.J., 1999a, The Early Carboniferous (Asbian-Brigantian) Seasonal Tropical Climate of Northern Britain: PALAIOS, v. 14, p. 116-126.

—, 1999b, The Early Carboniferous (Courceyan-Arundian) monsoonal climate of the British Isles; evidence from growth rings in fossil woods: Geological Magazine, v. 136, p. 177-187.

Fielding, C.R., Frank, T.D., Birgenheier, L.P., Rygel, M.C., Jones, A.T., and Roberts, J., 2008a, Stratigraphic imprint of the Late Palaeozoic Ice Age in eastern Australia: a record of alternating glacial and nonglacial climate regime: Journal of the Geological Society, London, v. 165, p. 129-140.

Fielding, C.R., Frank, T.D., and Isbell, J.L., 2008b, The Late Paleozoic ice age - A review of current understanding and synthesis of global climate patterns, *in* Fielding, C.R., Frank, T.D., and Isbell, J.L., eds., Resolving the Late Paleozoic Ice Age in Time and Space: Boulder, Colorado, The Geological Society of America Special Paper 441, p. 343-354.

Forster, P., Ramaswamy, V., Artaxo, P., Berntsen, T., Betts, R., Fahey, D.W., Haywood, J., Lean, J., Lowe, D.C., Myhre, G., Nganga, J., Prinn, R., Raga, G., Schulz, M., and Van Dorland, R., 2007, Changes in

Atmospheric Constituents and in Radiative Forcing, *in* Solomon, S., Qin, D., Manning, M., Chen, Z., Marquis, M., Averyt, K.B., Tignor, M., and Miller, H.L., eds., Climate Change 2007: The Physical Science Basis. Contribution of Working Group I to the Fourth Assessment Report of the Intergovernmental Panel on Climate Change: Cambridge and New York, Cambridge University Press.

Frakes, L.A., and Crowell, J.C., 1969, Late Paleozoic Glaciation: I, South America: Geological Society of America Bulletin, v. 80, p. 1007-1042.

Frakes, L.A., and Francis, J.E., 1988, A guide to Phanerozoic cold polar climates from high-latitude ice-rafting in the Cretaceous: Nature, v. 333, p. 547-549.

Frakes, L.A., Francis, J.E., and Syktus, J.I., 1992, Climate modes of the Phanerozoic: New York, Cambridge University Press, 274 p.

Frank, T.D., Birgenheier, L.P., Montañez, I.P., Fielding, C.R., and Rygel, M.C., 2008, Late Paleozoic climate dynamics revealed by comparison of ice-proximal stratigraphic and ice-distal isotopic records, *in* Fielding, C.R., Frank, T.D., and Isbell, J.L., eds., Resolving the Late Paleozoic Ice Age in Time and Space, Volume 441: Boulder, Colorado, Geological Society of America Special Paper, p. 331-342.

Gabbot, S.E., Aldridge, R.J., and Theron, J.N., 1995, A giant conodont with preserved muscle tissue from the Upper Ordovician of South Africa: Nature, v. 374, p. 800-803.

Gallagher, S.J., 1996, The stratigraphy and cyclicity of the late Dinantian platform carbonates in parts of southern and western Ireland, *in* Strogen, P., Somerville, I.D., and Jones, G.L., eds., Recent advances in Lower Carboniferous geology, Volume 107, Geological Society of London, Special Publication, p. 239-251.

Gallagher, S.J., MacDermot, C.V., Somerville, I.D., Pracht, M., and Sleeman, A.G., 2006, Biostratigraphy, microfacies and depositional environments of Upper Viséan limestones from the Burren region, County Clare, Ireland: Geological Journal, v. 41, p. 61-91.

Gallagher, S.J., and Somerville, I.D., 1997, Late Dinantian (Lower Carboniferous) platform carbonate stratigraphy of the Buttevant area North Co. Cork, Ireland: Geological Journal, v. 32, p. 313-335.

Galloway, W.E., and Williams, T.A., 1991, Sediment accumulation rates in time and space: Paleogene genetic stratigraphic sequences of the northwestern Gulf of Mexico basin: Geology, v. 19, p. 986-989.

Garrison, T., 2007, Oceanography - An invitation to Marine Science: Belmont, California, Thomson Brooks/Cole.

George, T.N., Johnson, G.A.L., Mitchell, M., Prentice, J.E., Ramsbottom, W.H.C., Sevastopulo, G.D., and Wilson, R.B., 1976, A correlation of Dinantian rocks in the British Isles: Geological Society of London, Special Report No.7.

Gill, W.D., 1979, Syndepositional sliding and slumping in the west Clare Namurian basin, Ireland, Geological Survey of Ireland Special Paper 4.

Ginter, M., 2009, Chondrichthyan biofacies in the late Famennian of Utah and Nevada: Journal of Vertebrate Paleontology, v. 21, p. 714-729.

Ginter, M., and Sun, Y., 2007, Chondrichthyan remains from the Lower Carboniferous of Muhua, southern China: Acta Palaeontologica Polonica, v. 52, p. 705-727.

González-Bonorino, G., and Eyles, N., 1995, Inverse relation between ice extent and the late Paleozoic glacial record of Gondwana: Geology, v. 23, p. 1015-1018.

Goodhue, R., and Clayton, G., 1999, Organic maturation levels, thermal history and hydrocarbon source rock potential of the Namurian rocks of the Clare Basin, Ireland: Marine and Petroleum Geology, v. 16, p. 667-675.

Graham, J.R., 1996, Dinantian river systems and coastal zone sedimentation in northwest Ireland: Geological Society, London, Special Publications, v. 107, p. 183-206.

—, 2009, Variscan deformation and metamorphism, *in* Holland, C.H., and Sanders, I.S., eds., The Geology of Ireland: Edinburgh, Dunedin.

Grossman, E.L., Bruckschen, P., Mii, H.-s., Chuvashov, I., Yancey, T.E., and Veizer, J., 2002, Carboniferous paleoclimate and global change: Isotopic evidence from the Russian Platform: Carboniferous stratigraphy and Paleogeography in Eurasia, p. 61 - 71.

Guilderson, T.P., Fairbanks, R.G., and Rubenstone, J.L., 1994, Tropical Temperature Variations Since 20,000 Years Ago: Modulating Interhemispheric Climate Change: Science, v. 263, p. 663-665.

Guion, P.D., Gutteridge, P., and Davies, S.J., 2000, Carboniferous sedimentation and volcanism on the Laurussian margin, *in* Woodcock, N., and Strachan, R., eds., Geological history of Britain and Ireland: Oxford, Blackwell Science Ltd.

Gunnell, F.H., 1933, Conodonts and fish remains from the Cherokee, Kansas City, and Wabaunsee Groups of Missouri and Kansas: Journal of Paleontology, v. 5, p. 244-252.

Haq, B.U., and Schutter, S.R., 2008, A chronology of Paleozoic sea-level changes: Science, v. 322, p. 64-68.

Harris, A.G., 1981, Color and alteration: an index to organic metamorphism in conodont elements, *in* Robinson, R.A., ed., Treatise on Invertebrate Paleontology, Part W, Supplement 2, Conodonta: Boulder, Colorado and Lawrence, Kansas, The Geological Society of America and the University of Kansas, p. 202.

Harris, R.W., and Hollingsworth, R.V., 1933, New Pennsylvanian conodonts from Oklahoma: American Journal of Science, v. 25, p. 193-204.

Hass, W.H., 1953, Conodonts of the Barnett Formation of Texas: U.S. Geological Survey Professional Papers, v. 243, p. 69-94.

Heckel, P.H., 1977, Origin of phosphatic black shale facies in Pennsylvanian cyclothems of mid-continent North America: AAPG Bulletin, v. 61, p. 1045-1068.

—, 1995, Glacial-eustatic base-level-climatic model for late Middle to Late Pennsylvanian coal-bed formation in the Appalachian Basin: Journal of Sedimentary Research, v. B65, p. 348-356.

—, 2002, Overview of Pennsylvanian cyclothems in midcontinent North America and brief summary of those elsewhere in the world.

—, 2004, Chairman's column: Newsletter on Carboniferous Stratigraphy, v. 22, p. 1-3.

—, 2008, Carboniferous Period: Cambridge, Cambridge University Press.

Heckel, P.H., and Clayton, G., 2006, The Carboniferous System. Use of the new official names for the subsystems, series, and stages: Geologica Acta, v. 4, p. 403-407.

Herringshaw, L.G., Thomas, A.T., and Smith, M.P., 2007, Systematics, shell structure and affinities of the Palaeozoic Problematicum Cornulites: Zoological Journal of the Linnean Society, v. 150, p. 681-699.

Heselden, R.G.W., 1991, Sedimentology and stratigraphy of the Courceyan-Asbian limestones (Dinantian, Lower Carboniferous) of the Cork Harbour area, southern Ireland [Unpublished Ph.D. thesis]: Cork, University College Cork.

Higgins, A.C., 1961, Some Namurian conodonts from north Staffordshire: Geological Magazine, v. 98, p. 210-224.

—, 1975, Conodont zonation of the Late Viséan - Early Westphalian strata of the south and central Pennines of northern England: Bulletin of the Geological Survey of Great Britain No. 53.

—, 1985, The Carboniferous System: Part 2 - Conodonts of the Silesian Subsystem from Great Britain and Ireland, *in* Higgins, A.C., and Austin, R.L., eds., A stratigraphical index of conodonts: Chichester, West Sussex, England, Ellis Horwood Ltd. and the British Micropalaeontological Society.

Higgins, A.C., and Bouckaert, J., 1968, Conodont stratigraphy and palaeontology of the Namurian of Belgium: Memoirs of the Geological Survey of Belgium, v. 10, p. 1-64.

Higgs, K., 1984, Stratigraphic palynology of the Carboniferous rocks in northwest Ireland: Geological Survey of Ireland Bulletin, v. 3, p. 171-201.

Higgs, R., 2004, Ross and Bude Formations (Carboniferous, Ireland and England): Reinterpreted as lake-shelf turbidites: Journal of Petroleum Geology, v. 27, p. 47-66.

—, 2009, Multiscale stratigraphic analysis of a structurally confined submarine fan: Carboniferous Ross Sandstone, Ireland: Discussion: AAPG Bulletin, v. 93, p. 1705-1709.

Hinde, G.J., 1900, Notes and descriptions of new species of scotch Carboniferous conodonts: Transactions of the Natural History Society of Glasgow, v. 5, p. 338-346.

Hitchings, V.H., and Ramsay, A.T.S., 1978, Conodont assemblages: A new functional model: Palaeogeography, Palaeoclimatology, Palaeoecology, v. 24, p. 137-149.

Hodson, F., 1953, The beds above the Carboniferous Limestone in North-West County Clare, Eire: Quarterly Journal of the Geological Society of London, v. 109, p. 259-283.

—, 1958, *Entogonites* CF. *Borealis*, an Alaskan Goniatite from Ireland: Palaeontology, v. 1.

Hodson, F., and Lewarne, G.C., 1961, A Mid-Carboniferous (Namurian) basin in parts of the Counties of Limerick and Clare, Ireland: Quarterly Journal of the Geological Society of London, v. 117, p. 307-333.

Hoefs, J., 2009, Stable Isotope Geochemistry: Berlin, Springer.

Holdsworth, B.K., and Collinson, J.D., 1988, Millstone Grit cyclicity revisited, *in* Besley, B.M., and Kelling, G., eds., Sedimentation in a synorogenic basin complex: The Upper Carboniferous of north-west Europe: Glasgow and London, Blackie, p. 43-52.

Horton, D.E., and Poulsen, C.J., 2009, Paradox of late Paleozoic glacioeustasy: Geology, v. 37, p. 715-718.

House, M.R., 1995, Orbital forcing timescales: an intorduction, *in* House, M.R., and Gale, A. S., ed., Orbital Forcing Timescales and Cyclostratigraphy, Volume Geological Society Special Publication No. 85, p. 1-18.

Hubbard, W.F., and Sheridan, D.J.R., 1965, The Lower Carboniferous stratigraphy of some coastal exposures in Co. Sligo, Ireland.: Scientific Proceedings of the Royal Dublin Society, v. 2, p. 189-195.

Huxley, T.H., 1880, On the application of the laws of evolution to the arrangement of the Vertebrata, and more particularly of the Mammalia: Proceedings of the Royal Society of London, v. 43, p. 649-662.

Hyde, W.T., Crowley, T.J., Tarasov, L., and Peltier, W.R., 1999, The Pangean ice age: studies with a coupled climate-ice sheet model: Climate Dynamics, v. 15, p. 619-629.

Iacumin, P., Bocherens, H., Mariotti, A., and Longinelli, A., 1996, Oxygen isotope analyses of co-existing carbonate and phosphate in biogenic apatite: a way to monitor diagenetic alteration of bone phosphate?: Earth and Planetary Science Letters, v. 142, p. 1-6.

Iannuzzi, R., and Pfefferkorn, H.W., 2002, A pre-glacial, warm-temperate floral belt in Gondwana (Late Visean, Early Carboniferous): PALAIOS, v. 17, p. 571-590.

Isbell, J.L., Lenaker, P.A., Askin, R.A., Miller, M.F., and Babcock, L.E., 2003a, Reevaluation of the timing and extent of late Paleozoic glaciation in Gondwana: Role of the Transantarctic Mountains: Geology, v. 31, p. 977 - 980.

Isbell, J.L., Miller, M.F., Wolfe, K.L., and Lenaker, P.A., 2003b, Timing of late Paleozoic glaciation in Gondwana: Was glaciation responsible for the development of northern hemisphere cyclothems?: Geological Society of America, Special Paper, v. 370, p. 5-24.

Ivanov, A., 1996, The Early Carboniferous chondrichthyans of the South Urals, Russia, *in* Strogen, P., Somerville, I.D., and Jones, G.L., eds., Recent

advances in Lower Carboniferous geology, Volume 107, Geological Society Special Publication, p. 417-425.

—, 2005, Early Permian Chondrichthyans of the the middle and south Urals: Revista Brasileira de Paleontologia, v. 8, p. 127-138.

Jaekel, O., 1921, Die Stellung der Paläontologie zur einigen Problemen der Biologie und Phylogenie. Schadelprobleme: Paläontologische Zeitschrift, v. 3, p. 213-239.

James, N.P., Bone, Y., and Kyser, T.K., 1997, Brachiopod $\delta^{18}O$ values do reflect ambient oceanography: Lacepede Shelf, southern Australia: Geology, v. 25, p. 551 - 554.

Joachimski, M.M., Breisig, S., Buggisch, W., Talent, J.A., Mawson, R., Gereke, M., Morrow, J.R., Day, J., and Weddige, K., 2009, Devonian climate and reef evolution: Insights from oxygen isotopes in apatite: Earth and Planetary Science Letters, v. 284, p. 599-609.

Joachimski, M.M., and Buggisch, W., 2002, Conodont apatite $\delta^{18}O$ signatures indicate climatic cooling as a trigger of the late Devonian mass extinction: Geology, v. 30, p. 711 - 714.

Joachimski, M.M., Horacek, M., Breisig, S., and Buggisch, W., 2003, The oxygen isotopic composition of biogenic apatite - no evidence for a secular change in seawater $\delta^{18}O$.: Geophysical Research Abstracts, v. 5.

Joachimski, M.M., van Geldern, R., Breisig, S., Buggisch, W., and Day, J., 2004, Oxygen isotope evolution of biogenic calcite and apatite during the Middle and Late Devonian: International Journal of Earth Science, v. 93, p. 542-553.

Joachimski, M.M., von Bitter, P.H., and Buggisch, W., 2006, Constraints on Pennsylvanian glacioeustatic sea-level changes using oxygen isotopes of conodont apatite: Geology, v. 34, p. 277 - 280.

Jones, A.T., and Fielding, C.R., 2004, Sedimentological record of the late Paleozoic glaciation in Queensland, Australia: Geology, v. 32, p. 153-156.

Jones, G.L., and Somerville, I.D., 1996, Irish Dinantian biostratigraphy: practical applications., *in* Strogen, P., Somerville, I.D., and Jones, G.L., eds., Recent Advances in Lower Carboniferous Geology., Volume 107, Geological Society Special Publication, p. 371-385.

Kelk, B., 1960, Studies in the Carboniferous stratigraphy of western Eire [Unpublished Ph.D. thesis]: Reading, University of Reading.

Keller, M., Bahlburg, H., Reuther, C.D., and Weh, A., 2007, Flexural to broken foreland basin evolution as a result of Variscan collisional events in northwestern Spain: Geological Society of America Memoirs, v. 200, p. 489-510.

Kelley, P.H., Raymond, A., and Lutken, C.B., 1990, Carboniferous brachiopod migration and latitudinal diversity: a new palaeoclimatic method., *in* McKerrow, W.S., and Scotese, C. R., ed., Palaeozoic Palaeogeography and Biogeography, Volume 12, Geological Society Memoir, p. 325-332.

Kelly, J.G., 1989, The Late Chadian to Brigantian Geology of The Carrick-on-Shannon and Lough Allen Synclines, North West Ireland [Unpublished Ph.D. thesis]: Dublin, University College Dublin.

—, 1996, Initiation, growth and decline of a tectonically controlled Asbian carbonate ramp: Cuilcagh Mountain area, NW Ireland., *in* Strogen, P., Somerville, I.D., and Jones, G.L., eds., Recent Advances in Lower Carboniferous Geology., Volume 107, Geological Society Special Publication, p. 253-262.

Klein, E.F., 1885, Beiträge zur Bildung des Schädels den Knochenfische, 2: Jahreshefte Vereins Vaterlandischer Naturkunde Würtenberg, v. 42, p. 205-300.

Kolodny, Y., Luz, B., and Navon, O., 1983, Oxygen isotope variations in phosphate of biogenic apatites, I. Fish bone apatite - rechecking the rules of the game: Earth and Planetary Science Letters, v. 64, p. 398-404.

Korn, D., 1990, On the Upper Viséan P_{1b} goniatite succession in north Leitrim: Irish Journal of Earth Sciences, v. 10, p. 109-114.

Korn, D., and Kaufmann, B., 2009, A high-resolution relative time scale for the Visèan Stage (Carboniferous) of the Kulm Basin (Rhenish Mountains, Germany): Geological Journal, v. 44, p. 306-321.

Kulagina, E.I., Rumiantseva, Z.S., Pazukhin, V.N., and Kotchetova, N.N., 1992, Lower/Middle Carboniferous boundary in the Southern Urals and in central Tien-Shan: Nauka, Moscow [in Russian].

Lamb, T.D., Collin, S.P., and Pugh, E.N., 2007, Evolution of the vertebrate eye: opsins, photoreceptors, retina and eye cup: Nat Rev Neurosci, v. 8, p. 960-976.

Land, L.S., and Lynch, L.F., 1996, $\delta^{18}O$ values of mudrocks: more evidence for an ^{18}O-buffered ocean: Geochimica et Cosmochimica Acta, v. 60, p. 3347-3352.

Lane, H.R., Brenckle, P.L., Baesemann, J.F., and Richards, B., 1999, The IUGS boundary in the middle of the Carboniferous: Arrow Canyon, Nevada, USA: Episodes, v. 22, p. 272-283.

Laskar, J., 1999, The limits of Earth orbital calculations for geological time-scale use: Philosophical Transactions of the Royal Society of London. Series A: Mathematical, Physical and Engineering Sciences, v. 357, p. 1735-1759.

Laskar, J., Robutel, P., Joutel, F., Gastineau, M., Correia, A.C.M., and Levrard, B., 2004, A long-term numerical solution for the insolation quantities of the Earth: Astronomy & Astrophysics, v. 428, p. 261-285.

Lebedev, O.A., 1996, Fish assemblages in the Tournasian-Viséan environments of the East European Platform, *in* Strogen, P., Somerville, I.D., and Jones, G.L., eds., Recent advances in Lower Carboniferous Geology, Volume 107, Geological Society Special Publication, p. 387-415.

Legg, I.C., Johnstone, T.P., Mitchell, W.I., and Smith, R.A., 1998, Geology of the country around Derrygonnelly and Marble Arch, Memoir of the Geological Survey of Northern Ireland.

LeGrande, A.N., and Schmidt, G.A., 2006, Global gridded data set of the oxygen isotopic composition in seawater: Geophysical Research Letters, v. 33, p. 604-608.

Lindström, M., 1973, On the affinities of conodonts, *in* Rhodes, F.H.T., ed., Conodont Paleozoology, The Geological Society of America, Special Publication 141.

—, 1974, The conodont apparatus as a food-gathering mechanism: Palaeontology, v. 17, p. 729-744.

Lisiecki, L.E., and Raymo, M.E., 2005, A Pliocene-Pleistocene stack of 57 globally distributed benthic $\delta^{18}O$ records: Paleoceanography, v. 20, p. 1-17.

Long, J.A., 1990, Late Devonian Chondrichthyans and Other Microvertebrate Remains from Northern Thailand: Journal of Vertebrate Paleontology, v. 10, p. 59-71.

Longinelli, A., and Nuti, S., 1968, Oxygen-isotope ratios in phosphate from fossil marine organisms: Science, v. 160, p. 879-882.

—, 1973, Revised phosphate-water isotopic temperature scale: Earth and Planetary Science Letters, v. 19, p. 373-376.

Luer, C.A., Blum, P.C., and Gilbert, P.W., 1990, Rate of Tooth Replacement in the Nurse Shark, Ginglymostoma cirratum: Copeia, v. 1990, p. 182-191.

Luz, B., and Kolodny, Y., 1985, Oxygen isotope variations in phosphate of biogenic apatites, IV. Mammal teeth and bones: Earth and Planetary Science Letters, v. 75, p. 29-36.

Luz, B., Kolodny, Y., and Kovach, J., 1984, Oxygen isotope variations in phosphate of biogenic apatites, III. Conodonts: Earth and Planetary Science Letters, v. 69, p. 255-262.

MacDermot, C.V., Higgs, K., Philcox, M.E., and Reilly, T.A., 1983, Volume 3. Carboniferous Stratigraphy, A Review of the Geology of Petroleum Prospecting Licence 2/80. Northwest Ireland for Marinex Petroleum Ltd., Geological Survey of Ireland Unpublished Report.

MacDermot, C.V., Long, C.B., and Harney, S.J., 1996, A geological description of Sligo, Leitrim, and adjoining parts of Cavan, Fermanagh, Mayo, and Roscommon, to accompany the Bedrock Geology 1:100,000 Scale Map Series, sheet 7, Sligo-Leitrim, with contributions by K. Claringbold, D. Daly, R. Meehan and G. Stanley, Geological Survey of Ireland, 99 p.

Martinsen, O.J., and Collinson, J.D., 2002, The Western Irish Namurian Basin reassessed - a discussion: Basin Research, v. 14, p. 523-542.

Mii, H.-s., Grossman, E.L., and Yancey, T.E., 1999, Carboniferous isotope stratigraphies of North America: Implications for Carboniferous paleoceanography and Mississippian glaciation: Geological Society of America Bulletin, v. 111, p. 960 - 973.

Mii, H.-s., Grossman, E.L., Yancey, T.E., Chuvashov, B., and Egorov, A., 2001, Isotopic records of brachiopod shells from the Russian Platform - evidence for the onset of mid-Carboniferous glaciation: Chemical Geology, v. 175, p. 133 - 147.

Mikulic, D.G., Briggs, D.E.G., and Kluessendorf, J., 1985, A Silurian soft-bodied biota: Science, v. 228, p. 715-717.

Miller, D.J., and Eriksson, K.A., 2000, Sequence Stratigraphy of Upper Mississippian Strata in the Central Appalachians: A Record of Glacioeustasy and Tectonoeustasy in a Foreland Basin Setting: AAPG Bulletin, v. 84, p. 210-233.

Miller, K.G., Kominz, M.A., Browning, J.V., Wright, J.D., Mountain, G.S., Katz, M.E., Sugarman, P.J., Cramer, B.S., Christie-Blick, N., and Pekar, S.F., 2005, The Phanerozoic Record of Global Sea-Level Change: Science, v. 310, p. 1293-1298.

Mitchell, W.I., 1992, The origin of Upper Palaeozoic sedimentary basins in Northern Ireland and relationships with the Canadian Maritime Provinces, *in* Parnell, J., ed., Basins on the Atlantic Seaboard: Petroleum Geology, Sedimentology and Basin Evolution., Volume 62, Geological Society Special Publication, p. 191-202.

—, 2004, Carboniferous, *in* Mitchell, W.I., ed., The Geology of Northern Ireland: our natural foundation: Belfast, Geological Survey of Northern Ireland, p. 79-116.

Monaghan, N.T., 1995, Fossil Insect from Carboniferous Rocks of Co Clare: The Irish Naturalists' Journal, v. 25, p. 155.

Montaňez, I.P., Tabor, N.J., Niemeier, D., DiMichele, W.A., Frank, T.D., Fielding, C.R., Isbell, J.L., Birgenheier, L.P., and Rygel, M.C., 2007, CO_2–forced climate and vegetation instability during Late Paleozoic deglaciation: Science, v. 315, p. 87-91.

Moore, E.W.J., and Hodson, F., 1958, Goniatites from the Upper Viséan shales of County Leitrim, Eire.: The Liverpool and Manchester Geological Journal, v. 2, p. 86-105.

Mora, C.I., Driese, S.G., and Colarusso, L.A., 1996, Middle to Late Paleozoic atmospheric CO_2 levels from soil carbonate and organic matter: Science, v. 271, p. 1105-1107.

Morris, R.W., and Felton, S.H., 2003, Paleoecologic Associations and Secondary Tiering of Cornulites on Crinoids and Bivalves in the Upper Ordovician (Cincinnatian) of Southwestern Ohio, Southeastern Indiana, and Northern Kentucky: PALAIOS, v. 18, p. 546-558.

Morris, R.W., and Rollins, H.B., 1971, The distribution and Palaeoecological interpretation of *Cornulites* in the Waynesville Formation (Upper Ordovician) of Southwestern Ohio: The Ohio Journal of Science, v. 71, p. 159-170.

Moss, S.A., 1972, Tooth Replacement and Body Growth Rates in the Smooth Dogfish, Mustelus canis (Mitchill): Copeia, v. 1972, p. 808-811.

Mottequin, B., and Sevastopulo, G.D., 2009, Predatory boreholes in Tournaisian (Lower Carboniferous) spiriferid brachiopods: Lethaia, v. 42, p. 274-282.

Muehlenbachs, K., 1998, The oxygen isotopic composition of the oceans, sediments and the seafloor: Chemical Geology, v. 145, p. 263-273.

Muehlenbachs, K., Furnes, H., Fonneland, H.C., and Hellevang, B., 2003, Ophiolites as faithful records of the oxygen isotope ratio of ancient

seawater: the Solund-Stavfjord Ophiolite Complex as a Late Ordovician example, *in* Dilek, Y., and Robinson, P.T., eds., Ophiolites in Earth History, Volume 218, Geological Society of London, Special Publications, p. 401-414.

Muller, D.R., Sdrolias, M., Gaina, C., Steinberger, B., and Heine, C., 2008, Long-term sea-level fluctuations driven by ocean basin dynamics: Science, v. 319, p. 1357-1362.

Müller, K.J., 1981a, Micromorphology of elements, *in* Robinson, R.A., ed., Treatise on Invertebrate Paleontology, Part W, Supplement 2, Conodonta: Boulder, Colorado and Lawrence Kansas, The Geological Society of America and the University of Kansas, p. 202.

—, 1981b, Zoological affinities of conodonts, *in* Robinson, R.A., ed., Treatise on Invertebrate Paleontology, Part W, Supplement 2, Conodonta: Boulder, Colorado and Lawrence Kansas, The Geological Society of America and the University of Kansas, p. 202.

Nelson, B.K., Deniro, M.J., Schoeninger, M.J., De Paolo, D.J., and Hare, P.E., 1986, Effects of diagenesis on strontium, carbon, nitrogen and oxygen concentration and isotopic composition of bone: Geochimica et Cosmochimica Acta, v. 50, p. 1941-1949.

Nemirovskaya, T., Perret, M.T., and Meischner, D., 1994, *Lochriea ziegleri* and *Lochriea sencenbergica* - new conodont species from the latest Visèan and Serpukhovian in Europe: Courier Forschungsinstitut Senckenberg, v. 168, p. 311-317.

Nemyrovska, T.I., 1999, Bashkirian conodonts of the Donets Basin, Ukraine: Scripta Geologica, v. 119, p. 1-115.

—, 2005, Late Visèan/early Serpukhovian conodont succession from the Triollo section, Palencia (Cantabrian Mountains, Spain): Scripta Geologica, v. 129, p. 13-89.

Nicoll, R.S., 1987, Form and function of the Pa element in the conodont animal, *in* Aldridge, R.J., ed., Palaeobiology of Conodonts: Chichester, England, British Micropalaeontological Society and Ellis Horwood Ltd., p. 180.

Nikolaeva, S.V., Akhmetshina, L.Z., Konovalova, V.A., Korobkov, V.F., and Zainakaeva, G.F., 2009a, The Carboniferous carbonates of the Dombar Hills (western Kazakhstan) and the problem of the Viséan-Serpukhovian boundary: Palaeoworld, v. 18, p. 80-93.

Nikolaeva, S.V., Kulagina, E.I., Pazukhin, V.N., Kochetova, N.N., and Konovalova, V.A., 2009b, Palaeontology and microfacies of the

Serpukhovian in the Verkhynyaya Kardailovka Section, south Urals, Russia: potential candidate for the GSSP for the Visèan -Serpukhovian boundary: Newsletters on Stratigraphy, v. 43, p. 165-193.

Nöth, S., 1998, Conodont Color (CAI) versus Microcrystalline and Textural Changes in Upper Triassic Conodonts from Northwest Germany: Facies, v. 38, p. 165-174.

O'Neil, J.R., Roe, L.J., Reinhard, E., and Blake, R.E., 1992, A rapid and precise method of oxygen isotope analysis of biogenic phosphate: Israel Journal of Earth Science, v. 43, p. 203-212.

Oswald, D.H., 1955, The Carboniferous rocks between the Ox Mountains and Donegal bay: Quarterly Journal of the Geological Society of London, v. 111, p. 167-186.

Owen, R., 1846, Comparative anatomy and physiology of the vertebrate animals, Part I. Fishes: Transactions of the Royal College of Surgeons of England, p. 1-308.

Padget, P., 1952, The geology of the Clogher-Slieve Beagh area, County Tyrone: Scientific Proceedings of the Royal Dublin Society, v. 26, p. 63-83.

Padget, P., 1953, The stratigraphy of Cuilcagh, Ireland: Geological Magazine, v. 90, p. 17-26.

Pander, C.H., 1856, Monographie der fossilen fische des Silurisehen systems der Runnisch-Baltischen gouvernements: Akademie der Wissenschaften, St. Petersburg, p. 1-91.

Paproth, E., Feist, R., and Flajs, G., 1991, Decision on the Devonian-Carboniferous boundary stratotype: Episodes, v. 14, p. 331-336.

Parrish, J.M., Parrish, J.T., and Ziegler, A.M., 1986, Permian-Triassic paleogeography and paleoclimatology and implications for Therapsid distribution, *in* Hotton, N., III, MacLean, P.D., Roth, J.J., and Roth, E.C., eds., The ecology and biology of mammal-like reptiles: Washington D.C., Smithsonian Institutional Press, p. 109-131.

Philcox, M.E., Baily, H., Clayton, G., and Sevastopulo, G.D., 1992, Evolution of the Carboniferous Lough Allen Basin, Northwest Ireland., *in* Parnell, J., ed., Basins on the Atlantic Seaboard: Petroleum Geology, Sedimentology and Basin Evolution., Volume 62, Geological Society Special Publication, p. 203-215.

Pietzner, H., Vahl, J., Werner, H., and Ziegler, W., 1968, Zur chemischen zusammensetzung und mikromorphologie der conodonten: Palaeontographica Abteilung, v. A 128, p. 115-152.

Pillans, B., Chappell, J., and Naish, T.R., 1998, A review of the Milankovitch climatic beat: template for Plio-Pleistocene sea-level changes and sequence stratigraphy: Sedimentary Geology, v. 122, p. 5-21.

Popp, B.N., Anderson, T.F., and Sandberg, P.A., 1986, Brachiopods as indicators of original isotopic compositions in some Paleozoic limestones: Geological Society of America Bulletin, v. 97, p. 1262 - 1269.

Powell, C.M., and Veevers, J.J., 1987, Namurian uplift in Australia and South America triggered the main Gondwanan glaciation: Nature, v. 326, p. 177-179.

Pracht, M., Lees, A., Leake, B., Feely, M., Long, B., Morris, J., and McConnell, B., 2004, Geology of Galway Bay: A geological description to accompany the Bedrock Geology 1:100,000 Scale Map Series, Sheet 14, Galway Bay, Geological Survey of Ireland.

Pucéat, E., Joachimski, M.M., Bouilloux, A., Monna, F., Bonin, A., Motreuil, S., Morinière, P., Hénard, S., Mourin, J., Dera, G., and Quesne, D., 2010, Revised phosphate-water fractionation equation reassessing paleotemperatures derived from biogenic apatite: Earth and Planetary Science Letters, v. 298, p. 135-142.

Pucéat, E., Reynard, B., and Lécuyer, C., 2004, Can crystallinity be used to determine the degree of chemical alteration of biogenic apatites?: Chemical Geology, v. 205, p. 83-97.

Pujana, R.R., and Cèsari, S.N., 2008, Fossil woods in interglacial sediments from the Carboniferous Hoyada Verde Formation, San Juan Province, Argentina: Palaeontology, v. 51, p. 163-171.

Purnell, M.A., 1993, Feeding mechanisms in conodonts and the function of the earliest vertebrate hard tissues: Geology, v. 21, p. 375-377.

—, 1994, Skeletal ontogeny and feeding mechanisms in conodonts: Lethaia, v. 27, p. 129-138.

—, 1995, Microwear on conodont elements and macrophagy in the first vertebrates: Nature, v. 374, p. 798-800.

Purnell, M.A., Donoghue, P.C.J., and Aldridge, R.J., 2000, Orientation and anatomical notation in conodonts.: Journal of Paleontology, v. 74, p. 113-122.

Purnell, M.A., and von Bitter, P.H., 1992, Blade-shaped conodont elements functioned as cutting teeth: Nature, v. 359, p. 629-631.

Pyles, D.R., 2009, Multiscale stratigraphic analysis of a structurally confined submarine fan: Carboniferous Ross Sandstone, Ireland: Reply: AAPG Bulletin, v. 93, p. 1710-1721.

Ramsbottom, W.H.C., 1973, Transgressions and regressions in the Dinantian: A new synthesis of British Dinantian stratigraphy: Proceedings of the Yorkshire Geological Society, v. 39, p. 567-607.

—, 1979, Rates of transgression and regression in the Carboniferous of NW Europe: Journal of the Geological Society, London, v. 136, p. 147-153.

Raup, D.M., and Stanley, S.M., 1978, Principles of paleontology: San Francisco, W. H. Freeman and Company.

Rejebian, V.A., Harris, A.G., and Stephen Huebner, J., 1987, Conodont color and textural alteration: An index to regional metamorphism, contact metamorphism, and hydrothermal alteration: Geological Society of America Bulletin, v. 99, p. 471-479.

Rexroad, C.B., 1958, Conodonts from the Glen Dean Formation (Chester) of the Illinois Basin: Report of Investigations of the Illinois State Geological Survey, v. 209, p. 1-27.

Rexroad, C.B., and Furnish, W.M., 1964, Conodonts from the Pella Formation (Mississippian) south-central Iowa: Journal of Paleontology, v. 38, p. 667-676.

Rexroad, C.B., and Varker, W.J., 1992, The new Mississippian conodont genus *Synclydognathus*: Journal of Paleontology, v. 66, p. 165-170.

Rhodes, F.H.T., Austin, R.L., and Druce, E.C., 1969, British Avonian (Carboniferous) conodont faunas and their value in local and intercontinental correlation: Bulletin of the British Museum of Natural History, Geology Supplement, v. 5, p. 4-313.

Richards, B.C., and Group, T., 2008, Report of the Task Group to establish a GSSP close to the existing Viséan-Serpukhovian boundary: Summary of progress in 2007-2008 and plans for 2009: Newsletter on Carboniferous Stratigraphy, v. 26, p. 8-9.

Rider, M.H., 1974, The Namurian of west County Clare: Proceedings of the Royal Irish Academy Section B, v. 74, p. 125-143.

Rigo, M., and Joachimski, M.M., 2010, Palaeoecology of Late Triassic conodonts: Constraints from oxygen isotopes in biogenic apatite: Acta Palaeontologica Polonica, v. 55.

Riley, N.J., 1993, Dinantian (Lower Carboniferous) biostratigraphy and chronostratigraphy in the British Isles: Journal of the Geological Society, London, v. 150, p. 427-446.

Rosman, K.J.R., and Taylor, P.D.P., 1998, Isotopic compositions of the elements 1997 (echnical report): Commission on atomic weights and isotopic abundances: Pure and Applied Chemistry, v. 70, p. 217-235.

Ross, C.A., and Ross, J.R.P., 1985, Late Paleozoic depositional sequences are synchronous and worldwide: Geology, v. 13, p. 194-197.

—, 1987, Late Paleozoic sea levels and depositional sequences: Cushman Foundation for Foraminiferal Research, Special Publication, v. 24, p. 137-149.

—, 1988, Late Paleozoic transgressive-regressive deposition, Sea-Level Changes, Volume 42, SEPM (Society for Sedimentary Geology), p. 227-247.

Rothman, D.H., 2002, Atmospheric carbon dioxide levels for the last 500 million years: Proceedings of the National Academy of Sciences, v. 99, p. 4167-4171.

Roundy, P.V., 1926, Part II. The Micro-fauna, in Mississippian formations of San Saba County, Texas: U.S. Geological Survey Professional Papers, v. 146, p. 5-23.

Royer, D.L., Berner, R.A., Montañez, I.P., Tabor, N.J., and Beerling, D.J., 2004, CO_2 as a primary driver of Phanerozoic climate: GSA Today, v. 14, p. 4-10.

Ruddiman, W.F., 2001, Earth's Climate: Past and Future: New York, W. H. Freeman, 465 p.

Rush, P.F., and Chafetz, H.S., 1990, Fabric-retentive, non-luminescent brachiopods as indicators of original $\delta^{13}C$ and $\delta^{18}O$ composition: a test: Journal of Sedimentary Petrology, v. 60, p. 968 - 981.

Rygel, M.C., Fielding, C.R., Frank, T.D., and Birgenheier, L.P., 2008, The magnitude of Late Paleozoic glacioeustatic fluctuations: A synthesis: Journal of Sedimentary Research, v. 78, p. 500-511.

Sadler, P.M., 1981, Sediment accumulation rates and the completeness of stratigraphic sections: The Journal of Geology, v. 89, p. 569-584.

Saltzman, M.R., 2002, Carbon and oxygen isotope stratigraphy of the Lower Mississippian (Kinderhookian - Lower Osagean), western United States: Implications for seawater chemistry and glaciation: Geological Society of America Bulletin, v. 114, p. 96 - 108.

—, 2003, Late Paleozoic ice age: Oceanic gateway or ρCO_2?: Geology, v. 31, p. 151 - 154.

Saltzman, M.R., González, L.A., and Lohmann, K.C., 2000, Earliest Carboniferous cooling step triggered by the Antler orogeny?: Geology, v. 28, p. 347 - 350.

Sansom, I.J., Smith, M.P., Armstrong, H.A., and Smith, M.M., 1992, Presence of the earliest Vertebrate hard tissues in Conodonts: Science, v. 256, p. 1308-1311.

Sansom, I.J., Smith, M.P., and Smith, M.M., 1994, Dentine in conodonts: Nature, v. 368, p. 591-591.

Savage, N.M., 1988, The use of sodium polytungstate for conodont separations: Journal of Micropalaeontology, v. 7, p. 39-40.

Schrag, D.P., Adkins, J.F., McIntyre, K., Alexander, J.L., Hodell, D.A., Charles, C.D., and McManus, J.F., 2002, The oxygen isotopic composition of seawater during the Last Glacial Maximum: Quaternary Science Reviews, v. 21, p. 331-342.

Schulz, M., and Mudelsee, M., 2002, REDFIT: estimating red-noise spectra directly from unevenly spaced paleoclimatic time series: Computers & Geosciences, v. 28, p. 421-426.

Schwarzacher, W., 1961, Petrology and structure of some Lower Carboniferous reefs in northwestern Ireland: Bulletin of the American Association of Petroleum Geologists, v. 45, p. 1481-1503.

—, 1964, An application of statistical time-series analysis of a limestone-shale sequence: The Journal of Geology, v. 72, p. 195-213.

—, 1989, Milankovitch type cycles in the Lower Carboniferous of NW Ireland: Terra Nova, v. 1, p. 468-473.

—, 1993, Milankovitch cycles in the pre-Pleistocene stratigraphic record: a review, *in* Hailwood, E.A., and Kidd, R. B., ed., High Resolution Stratigraphy, Geological Society Special Publication, No. 70, p. 187-194.

—, 2000, Repititions and cycles in stratigraphy: Earth-Science Reviews, v. 50, p. 51-75.

Scotese, C.R., and Barret, S.F., 1990, Gondwana's movement over the South Pole during the Palaeozoic: evidence from lithological indicators of climate., *in* McKerrow, W.S., and Scotese, C. R., ed., Palaeozoic Palaeogeography and Biogeography, Volume 12, Geological Society Memoir, p. 75-85.

Scotese, C.R., Boucot, A.J., and McKerrow, W.S., 1999, Gondwanan palaeogeography and palaeoclimatology: Journal of African Earth Sciences, v. 28, p. 99-114.

Scotese, C.R., and McKerrow, W.S., 1990, Revised World maps and introduction, *in* McKerrow, W.S., and Scotese, C. R., ed., Palaeozoic Palaeogeography and Biogeography, Volume 12, Geological Society Memoir, p. 1-21.

Scott, H.W., 1942, Conodont assemblages from the Heath Formation, Montana: Journal of Paleontology, v. 16, p. 291-301.

Sevastopulo, G.D., 2009, Carboniferous: Mississippian (Serpukhovian) and Pennsylvanian, *in* Holland, C.H., and Sanders, I.S., eds., The Geology of Ireland: Edinburgh, Dunedin Academic Press Ltd.

Sevastopulo, G.D., and Wyse Jackson, P.N., 2009, Carboniferous: Mississippian (Tournaisian and Viséan), *in* Holland, C.H., and Sanders, I.S., eds., The Geology of Ireland: Edinburgh, Dunedin, p. 215-269.

Sharp, Z.D., Atudorei, V., and Furrer, H., 2000, The effect of diagenesis on oxygen isotope ratios of biogenic phosphates: American Journal of Science, v. 300, p. 222-237.

Shaviv, N.J., and Veizer, J., 2003, Celestial driver of Phanerozoic climate?: GSA Today, v. 13, p. 4-10.

Sheridan, D.J.R., 1972, Upper Old Red Sandstone and Lower Carboniferous of the Slieve Beagh Syncline and its setting in the northwest Carboniferous basin, Ireland, Geological Survey of Ireland, Special Paper no. 2, 129 p.

Simpson, I.M., 1953, The Lower Carboniferous stratigraphy of the Omagh syncline, northern Ireland: Quarterly Journal of the Geological Society of London, v. 110, p. 391-408.

Skompski, S., Alekseev, A., Meischner, D., Nemirovskaya, T., Perret, M.-F., and Varker, W.J., 1995, Conodont distribution across the Visean/Namurian boundary: Courier Forschungsinstitut Senckenberg, v. 188, p. 177-209.

Sleeman, A.G., and Pracht, M., 1999, Geology of the Shannon Estuary. A geological description of the Shannon Estuary Region including parts of Clare, Limerick and Kerry, to accompany the Bedrock Geology 1:100,000 Scale Map Series, Sheet 17, Shannon Estuary, with contributions by K. Claringbold, and G. Stanley (minerals), J. Deakin and G. Wright (Groundwater), O. Bloetjes and R. Creighton (Quaternary), Geological Survey of Ireland, 77 p.

Smith, A.G., and Pickering, K.T., 2003, Oceanic gateways as a critical factor to initiate icehouse Earth: Journal of the Geological Society, London, v. 160, p. 337 - 340.

Smith, J., 1996, A palynofacies analysis of the Dinantian (Asbian) Glenade Sandstone Formation of the Leitrim Group, northwest Ireland., *in* Strogen, P., Somerville, I. D. and Jones, G. Ll., ed., Recent Advances in Lower Carboniferous geology., Volume 107, Geological Society Special Publication, p. 437-448.

Smith, J.S., 1995, A playnofacies analysis of the Carboniferous Leitrim Group in the Lough Allen Basin, northwest Ireland [Unpublished Ph.D. thesis]: Cork, University College Cork.

Smith, L.B., and Read, F.J., 2000, Rapid onset of late Paleozoic glaciation on Gondwana: Evidence from Upper Mississsippian strata of the Midcontinent, United States: Geology, v. 28, p. 279 - 282.

Smith, M., 1980, The Geology of the area south and east of Dowra, County Cavan, Ireland [Unpublished Master of Philosophy thesis]: Southampton, University of Southampton.

Somerville, H.E.A., 1999, Conodont Biostratigraphy and Biofacies of Upper Viséan rocks in parts of Ireland [Unpublished Ph.D. thesis]: Dublin, University College Dublin.

Somerville, H.E.A., and Somerville, I.D., 1998, Late Viséan conodont biostratigraphy and biofacies in the Kingscourt area, Ireland: Bullettino della Società Paleontologica Italiana, v. 37, p. 443-464.

Somerville, I.D., Cózar, P., Aretz, M., Herbig, H.-G., Mitchell, W.I., and Medina-Varea, P., 2009, Carbonate facies and biostromal distribution in a tectonically controlled platform in northwest Ireland during the late Viséan (Mississippian): Proceedings of the Yorkshire Geological Society, v. 57, p. 165-192.

Soreghan, G.S., and Giles, K.A., 1999, Amplitudes of Late Pennsylvanian glacioeustasy: Geology, v. 27, p. 255-258.

St. John, O., and Worthen, A.H., 1875, Part II. Palaeontology of Illinois, Section I - Description of fossil fishes: Geological Survey of Illinois, v. 6, p. 247-488.

Stone, J., 1987, Review of investigative techniques used in the study of conodonts, *in* Austin, R.L., ed., Conodonts: investigative techniques and applications: Chichester, Ellis Horwood Ltd., for The British Micropalaeontolological Society Series, p. 17-34.

Stone, J.J., and Geraghty, D. A., 1994, A predictive template for the apparatus architecture of the Carboniferous conodont *Idioprioniodus*: Lethaia, v. 27, p. 139-142.

Stow, D.A.V., 2005, Sedimentary rocks in the field - A colour guide: London, Manson Publishing, 320 p.

Strasburg, D.W., 1963, The Diet and Dentition of Isistius brasiliensis, with Remarks on Tooth Replacement in Other Sharks: Copeia, v. 1963, p. 33-40.

Strogen, P., 1988, The carboniferous lithostratigraphy of Southeast County Limerick, Ireland, and the origin of the shannon trough: Geological Journal, v. 23, p. 121-137.

Summerfield, M.A., 1993, Weathering and associated landforms, Global geomorphology: Essex, Longman Scientific and Technical, p. 537.

Sweet, W.C., 1981, Macromorphology of elements and apparatuses, *in* Robinson, R.A., ed., Treatise on Invertebrate Paleontology, Part W, Supplement 2, Conodonta: Boulder, Colorado and Lawrence, Kansas, The Geological Society of America and the university of Kansas, p. 202.

Sweet, W.C., and Donoghue, P.C.J., 2001, Conodonts: Past, present, future: Journal of Paleontology, v. 75, p. 1174-1184.

Timmerman, M.J., 2004, Timing, geodynamic setting and character of Permo-Carboniferous magmatism in the foreland of the Variscan Orogen, NW Europe, *in* Wilson, M., Neumann, E.-R., Davies, G.R., Timmerman,

M.J., Heeremans, M., and Larsen, B.T., eds., Permo-Carboniferous magmatism and rifting in Europe, Volume 223, Geological Society, London, Special Publication, p. 41-74.

Traquair, R.H., 1899, Report on fossil fishes collected by the Geological Survey of Scotland in the Silurian rocks of the south of Scotland: Transactions of the Royal Society of Edinburgh, v. 39, p. 827-864.

Trotter, J.A., and Eggins, S.M., 2006, Chemical systematics of conodont apatite determined by laser ablation ICPMS: Chemical Geology, v. 233, p. 196-216.

Trotter, J.A., Fitzgerald, J.D., Kokkonen, H., and Barnes, C.R., 2007, New insights into the ultrastructure, permeability, and integrity of conodont apatite determined by transmission electron microscopy: Lethaia, v. 40, p. 97-110.

Trotter, J.A., Williams, I.S., Barnes, C.R., Lecuyer, C., and Nicoll, R.S., 2008, Did Cooling Oceans Trigger Ordovician Biodiversification? Evidence from Conodont Thermometry: Science, v. 321, p. 550-554.

Tucker, M.E., 2001, Sedimentary Petrology: An introduction to the origin of sedimentary rocks: London, Wiley-Blackwell, 272 p.

Tucker, M.E., and Wright, P.V., 2008, Carbonate Sedimentology: Oxford, Blackwell, 482 p.

Vanstone, S., 1996, The influence of climatic change on exposure surface development: a case study from the Late Dinantian of England and Wales, *in* Strogen, P., Somerville, I.D., and Jones, G.L., eds., Recent advances in Lower Carboniferous geology, Volume 107, Geological Society of London, Special Publication, p. 281-301.

Varker, W.J., and Sevastopulo, G.D., 1985, The Carboniferous System: Part 1 - Conodonts of the Dinantian Subsystem from Great Britain and Ireland, *in* Higgins, A.C., and Austin, R.L., eds., A stratigraphical index of conodonts: Chichester, West Sussex, England, Ellis Horwood Ltd. and the British Micropalaeontological Society.

Vaughan, A., 1905, The Palaentological Sequence in the Carboniferous Limestone of the Bristol Area: Quarterly Journal of the Geological Society, v. 61, p. 181-307.

Veevers, J.J., and Powell, C.M., 1987, Late Paleozoic glacial episodes in Gondwanaland reflected in transgressive-regressive depositional sequences in Euramerica: Geological Society of America Bulletin, v. 98, p. 475 - 487.

Veizer, J., Ala, D., Azmy, K., Bruckschen, P., Buhl, D., Bruhn, F., Carden, A.F., Diener, A., Ebneth, S., Godderis, Y., Jasper, T., Korte, C., Pawellek, F., Podlaha, O.G., and Strauss, H., 1999, $^{87}Sr/^{86}Sr$, $\delta^{13}C$ and $\delta^{18}O$ evolution of Phanerozoic seawater: Chemical Geology, v. 161, p. 59 - 88.

Veizer, J., Fritz, P., and Jones, B., 1986, Geochemistry of brachiopods: Oxygen and carbon isotopic records of Paleozoic oceans: Geochimica et Cosmochimica Acta, v. 50, p. 1679 - 1696.

Vennemann, T.W., Hegner, E., Cliff, G., and Benz, G. W., 2001, Isotopic composition of recent shark teeth as a proxy for environmental conditions: Geochimica et Cosmochimica Acta, v. 65, p. 1583-1599.

Vennemann, T.W., Fricke, H. C., Blake, R. E., O'Neil, J. R., and Colman, A., 2002, Oxygen isotope analysis of phosphates: a comparison of techniques for analysis of Ag_3PO_4.: Chemical Geology, v. 185, p. 321-336.

Vinn, O., and Mutvei, H., 2005, Obervations on the morphology and affinities of cornulitids from the Ordovician of Anticosti Island and the Silurian of Gotland: Journal of Paleontology, v. 79, p. 726-737.

von Bitter, P.H., Sandberg, C.A., and Orchard, M.J., 1986, Phylogeny, Speciation, and Palaeoecology of the Early Carboniferous (Mississippian) Conodont Genus *Mestognathus*: Life Sciences Contributions, v. 143.

Wanless, H.R., and Shepard, F.P., 1936, Sea level and climate changes related to late Paleozoic cycles: Geological Society of America Bulletin, v. 47, p. 1177-1206.

Weedon, G.P., and Read, W.A., 1995, Orbital-climatic forcing of Namurian cyclic sedimentation from spectral analysis of the Limestone Coal Formation, Central Scotland, *in* House, M.R., and Gale, A. S., ed., Orbital Forcing Timescales and Cyclostratigraphy, Volume Geological Society Special Publication No. 85, p. 51-66.

Wenzel, B., Lécuyer, C., and Joachimski, M.M., 2000, Comparing oxygen isotope records of Silurian calcite and phosphate - $\delta^{18}O$ compositions of brachiopods and conodonts: Geochimica et Cosmochimica Acta, v. 64, p. 1859-1872.

West, I.M., 1965, Macrocell structure and enterolithic veins in British Purbeck gypsum and anhydrite: Proceedings of the Yorkshire Geological Society, v. 35, p. 47-58.

West, I.M., Brandon, A., and Smith, M., 1968, A tidal flat evaporitic facies in the Visean of Ireland: Journal of Sedimentary Petrology, v. 38, p. 1079-1093.

Wheeley, J.R., Smith, M.P., and Boomer, I., 2010, Conodonts as Palaeothermometers in ancient oceans: tests and limitations, 3rd International Palaeontological Congress: London.

Wheeley, J.R., Smith, P., and Boomer, I., 2009, Conodonts as palaeothermometers for ancient oceans?, The Palaeontological Association 53rd Annual Meeting: University of Birmingham.

Wignall, P.B., and Best, J.L., 2000, The Western Irish Namurian Basin reassessed: Basin Research, v. 12, p. 59-78.

Williams, M.E., 2001, Tooth Retention in Cladodont Sharks: With a Comparison between Primitive Grasping and Swallowing, and Modern Cutting and Gouging Feeding Mechanisms: Journal of Vertebrate Paleontology, v. 21, p. 214-226.

Witzke, B.J., 1990, Palaeoclimatic constraints for Palaeozoic Palaeolatitudes of Laurentia and Euramerica, *in* McKerrow, W.S., and Scotese, C. R., ed., Palaeozoic Palaeogeography and Biogeography, Volume 12, Geological Society Memoir, p. 57-73.

Woodcock, N.H., and Strachan, R.A., 2000, The Caledonian Orogeny: a multiple plate collision, *in* Woodcock, N., and Strachan, R., eds., Geological History of Britain and Ireland: Oxford, Blackwell.

Wright, V.P., 1990, Equatorial aridity and climatic oscillations during the early Carboniferous, southern Britain: Journal of the Geological Society, v. 147, p. 359-363.

Wright, V.P., and Vanstone, S.D., 2001, Onset of Late Palaeozoic glacio-eustasy and the evolving climates of low latitude areas: a synthesis of current understanding: Journal of the Geological Society, London, v. 158, p. 579-582.

Zazzo, A., Lécuyer, C., and Mariotti, A., 2004, Experimentally-controlled carbon and oxygen isotope exchange between bioapatites and water under inorganic and microbially-mediated conditions: Geochimica et Cosmochimica Acta, v. 68, p. 1-12.

Ziegler, W., 1960, Die conodonten aus den Gerdllen des Zechsteinkonglomerates von Rossensay (stidwestlich Rheinberg/Niederrhein): Fortschritte in der Geologie von Rheinland and Westfalen, Krefeld, v. 6, p. 1-15.

Žigaite, Ž., Joachimski, M.M., Lehnert, O., and Brazauskas, A., 2010a, $\delta^{18}O$ composition of conodont apatite indicates climatic cooling during the Middle Pridoli: Palaeogeography, Palaeoclimatology, Palaeoecology, v. 294, p. 242-247.

Žigaite, Ž., Pérez-Huerta, A., and Joachimski, M.M., 2010b, Palaeozoic vertebrate microfossils: stable isotope and elemental geochemistry in palaeoclimate studies, 3rd International Palaeontological Congress: London.